

# **How will projected sea-level rise affect carbon storage in floodplain fens?**

Eleanor Jane Webster

*A thesis submitted in partial fulfilment of the requirements of the  
Degree of Doctor of Philosophy.*

School of Geography, Queen Mary, University of London

2016

I, Eleanor Jane Webster, confirm that the research included within this thesis is my own work or that where it has been carried out in collaboration with, or supported by others, that this is duly acknowledged below and my contribution indicated. Previously published material is also acknowledged below.

I attest that I have exercised reasonable care to ensure that the work is original, and does not to the best of my knowledge break any UK law, infringe any third party's copyright or other Intellectual Property Right, or contain any confidential material.

I accept that the College has the right to use plagiarism detection software to check the electronic version of the thesis.

I confirm that this thesis has not been previously submitted for the award of a degree by this or any other university.

The copyright of this thesis rests with the author and no quotation from it or information derived from it may be published without the prior written consent of the author.

Signature: 

Date: 15<sup>th</sup> September 2016

Details of collaboration and publications:

Handong Yang, University College London, performed radiometric dating on three peat cores. These data are presented in section 5.3.3. All interpretation was undertaken by myself.

Professor Lisa R. Belyea, Queen Mary University of London, constructed the analytical model presented in Chapter 6. This model was based on my own conceptual knowledge, and was parameterised using field and laboratory data obtained by myself in the preceding Chapters. Interpretation of the model output was also undertaken by myself.

## **Acknowledgements**

Firstly, I would like to thank my supervisors, Professor Lisa Belyea, Dr Kate Heppell and Dr Andrea Kelly for their support, enthusiasm and wisdom over the last 4 years.

I am also grateful to the Broads Authority, Tim Strudwick, Rick Southwood, Richard Mason and David Nobbs for granting me permission to access field sites. I would also like to thank Michelle Day and Natalie Ludgate for your help and practical support in the labs and field.

Thank you to everyone from 224, Kirean Stanley, Francis O'Shea, Michelle Morris, James Holloway and Joe James, for making my time at QMUL so enjoyable. I am grateful to all of you for the support that you have given me throughout this experience; it certainly wouldn't have been the same without those many random conversations over beers, curries and coffees!

Finally, I would like to thank my mum, Helen, my sister, Loren and my dad, Martin, for your continual support, encouragement and patience. Thank you mum, for instilling in me the will to challenge myself and to always strive to achieve new things. Thank you Dad, for proofreading down to the final hours and for your words of wisdom. To Thomas Marsh – thank you for living through every moment of this experience with me, for encouraging me, for your enduring patience and for whole-heartedly supporting me through the time it has taken me to do this. Thank you for keeping me going.

In loving memory of  
Kenneth Edwin Partridge  
(1925 – 2015)

## Abstract

Floodplain fens represent an important component of the global carbon cycle through their role in carbon sequestration. Peat development depends upon rate of production exceeding rate of decomposition, yet there is little understanding of the effects of sea-level rise on these processes in lowland environments. This thesis investigates the impacts of projected sea-level rise from climate change on carbon storage in floodplain fens, using a combination of field, laboratory and simulation modelling techniques.

A gradient of saline influence was determined for the Broads, UK, based on analysis of water chemistry and published water level data, allowing for the application of a space-for-time substitution technique. Increased water level had a positive effect on above-ground production of *Phragmites australis* (cav.) Trin. Ex Steud. (1841) - perhaps because water stress limits important photosynthetic processes. An increase in salinity had a negative effect on the growth of *P. australis*, probably due in part to osmotic stress. Previous management practice significantly impacted on production – as uncut vegetation became less productive with time. There was evidence to suggest that sea-level rise may lead to faster decay rates, but this will be partially offset by litter quality.

Saline influenced sites had lower carbon accumulation potentials. Radiometric dating confirmed that these sites have lower carbon sequestration rates - probably as a result of increased mineral deposition in floodwaters. Carbon stock ranged between 33 and 144 kt C but depended greatly on peat depth and bulk density. Results from both field data and the model indicated that peat accretion in the Broads would not offset projected sea-level rise. Floodplain fen development under the influence of sea-level rise will be dependent on the majority of assimilate being allocated to above-ground vegetation.

## Contents

Acknowledgements.....	3
Abstract .....	5
Contents .....	6
List of Figures .....	11
List of Tables .....	15
List of Equations .....	18
List of Appendices .....	20
Acronyms.....	21
<b>Chapter 1: Introduction</b> .....	<b>22</b>
<b>Chapter 2: Literature Review</b> .....	<b>25</b>
2.1 Global carbon cycle .....	25
2.1.1 Accounting for peatlands as carbon sinks.....	26
2.2 Sea-level Rise.....	27
2.2.1 Sea-level rise and coastal wetlands.....	28
2.2.2 Sea-level rise in the UK .....	29
2.3 Description of floodplain fen environments.....	30
2.3.1 Hydrology .....	32
2.3.2 Vegetation .....	32
2.3.3 Chemistry .....	34
2.3.3.1 Nutrient inputs .....	34
2.3.3.2 Redox reactions .....	35
2.4 Above- and below-ground inputs to the peat carbon store .....	37
2.4.1 Water level .....	38
2.4.2 Nutrient availability .....	39
2.4.3 Salinity.....	40
2.4.4 Management practice .....	42
2.4.5 Below-ground inputs.....	42

2.5 Decay of plant litter .....	43
2.5.1 Stoichiometric control on decay rate .....	45
2.5.2 The effect of sea-level rise on decay rate .....	45
2.6 Carbon storage in peatlands .....	48
2.6.1 Quantifying carbon stock .....	48
2.6.2 Quantifying carbon sequestration rate .....	50
2.6.3 Understanding carbon dynamics using models .....	52
2.7 Summary and research questions .....	53
2.7.1 Chapter 3 .....	54
2.7.2 Chapter 4 .....	55
2.7.3 Chapter 5 .....	57
2.7.4 Chapter 6 .....	59
<b>Chapter 3: Is there an indication of a saline gradient across selected sites in the Broads? .....</b>	<b>60</b>
3.1 Introduction .....	60
3.2 Study Sites .....	62
3.2.1 Study Area .....	62
3.2.2 Site Selection .....	63
3.2.3 Site Description .....	64
3.3 Methodology .....	68
3.3.1 Field Methods .....	68
3.3.2 Laboratory Methods .....	69
3.3.3 Data Analysis .....	72
3.4 Results .....	75
3.4.1 Anion and Cation analysis .....	75
3.4.2 Relationships between water chemistry variables .....	79
3.4.3 Water level and electrical conductivity time series data for study sites .....	82
3.4.4 Response of water level and electrical conductivity to storm surge events ...	89
3.5 Discussion .....	93

3.5.1 Controls on hydrogeochemistry .....	93
3.5.2 Exploring the impact of storm surge events .....	96
3.6 Conclusions .....	98
<b>Chapter 4: Is saline influence a control on the inputs and outputs to the peat carbon stock in floodplain fens?.....</b>	<b>99</b>
4.1 Introduction .....	99
4.2 Methodology .....	102
4.2.1 Above-ground biomass and radiation use efficiency of above-ground production .....	102
4.2.2 Below-ground carbon production .....	106
4.2.3 Mass loss under native conditions .....	108
4.2.4 Mass loss of transplanted material .....	110
4.2.5 Carbon accumulation potentials .....	111
4.3 Results.....	112
4.3.1 Quantifying above-ground carbon mass .....	112
4.3.2 Testing for between site variation in the contribution of species to total biomass.....	116
4.3.3 Quantifying below-ground carbon production .....	119
4.3.4 Controls on ABCP/BGCP .....	120
4.3.5 Determining controls on rate of decay of carbon mass .....	122
4.3.6 Transplant experiment.....	131
4.3.7 Carbon accumulation potentials .....	135
4.4 Discussion .....	136
4.4.1 Controls on above-ground carbon production .....	136
4.4.2 Exploring controls on AGCP/BGCP .....	137
4.4.3 Disentangling the effects of an increasing saline influence on plant litter decomposition .....	139
4.4.4 Separating the effects of microenvironment and litter quality .....	141
4.4.5 Carbon accumulation potentials .....	141
4.4.6 Implications and future work .....	142



4.5 Conclusions .....	143
<b>Chapter 5: Carbon stock and recent peat accumulation in three floodplain fens .....</b>	<b>144</b>
5.1 Introduction .....	144
5.2 Methodology .....	147
5.2.1 Determining carbon density for different peat types .....	147
5.2.2 Carbon sequestration and peat accretion rate .....	153
5.3 Results.....	156
5.3.1 Carbon density of different peat types .....	156
5.3.2 Quantifying carbon stock .....	161
5.3.3 Recent peat dating .....	162
5.4 Discussion .....	165
5.4.1 Variation in carbon density and its components.....	165
5.4.2 Carbon stock .....	167
5.4.3 Carbon sequestration and peat accretion .....	168
5.4.4 Implications and further work .....	170
5.5 Conclusions .....	171
<b>Chapter 6: A modelling study to explore the effects of sea-level rise on peat accretion .....</b>	<b>172</b>
6.1 Introduction .....	172
6.2 Methodology .....	176
6.2.1 Model description .....	176
6.2.2 Parameter values for numerical experiments.....	181
6.3 Results.....	184
6.3.1 Mineral sedimentation rate .....	184
6.3.2 Mass flux from vegetation to peat .....	184
6.3.3 Labile and refractory components of decay .....	186
6.3.4 Relative contributions of mineral and organic matter to vertical accretion ...	187
6.3.5 Projected relative sea-level rise .....	188

6.4 Discussion .....	190
6.5 Conclusions and future research.....	193
<b>Chapter 7: Summary and Further Research .....</b>	<b>194</b>
7.1 Overview of research aims and objectives .....	194
7.2 Directions for further research.....	202
7.3 Conclusion .....	205
Reference List.....	206
Appendix 1: Field data used to calculate above-ground carbon mass.....	246
Appendix 2: Scatterplots to show goodness of fit of multiple regression models. ....	247
Appendix 3: Parameter estimates fitted to each core using the Ricker function.....	248
Appendix 4: Lambert Transect Maps .....	251
Appendix 5: The relationship between organic matter and total carbon for cores used in radiometric dating.....	254
Appendix 6: Summary statistics for the mixed-effects linear model. ....	255
Appendix 7: Raw data from radiometric dating.....	258

## List of Figures

Figure 2.1	Conceptual model outlining the distribution of redox reactions through a peat (adapted from Conrad (1996)).	35
Figure 2.2	The global carbon cycle with aerobic and anaerobic mechanisms (Adapted from Ferry (2010)).	36
Figure 2.3	Decay rate at different salinities based on a <i>P. australis</i> study (Sangiorgio et al. 2008).	46
Figure 3.1	Map of research sites and superficial geological deposits (British Geological Survey 2014)	66
Figure 3.2	Areas at risk of flooding from main rivers and the sea obtained from the Environment Agency Geostore, 2015.	67
Figure 3.3	The Broads National Park and designated SSSI obtained from the Environment Agency Geostore, 2015.	67
Figure 3.4	Na:Cl compared to distance of study site from the coast	78
Figure 3.5	Mg:Ca compared to distance of study site from the coast	78
Figure 3.6	Comparison of mean PC1 factor score $\pm$ 1 SE for porewater and surface water	79
Figure 3.7	Scatter plot to show distribution of factor scores associated with PC1 and PC2 for porewater (top) and surface water (bottom).	81
Figure 3.8	Scatter plot to show distribution of factor scores associated with PC1 and PC3 for porewater (top) and surface water (bottom).	82
Figure 3.9	Scatter plot to show distribution of factor scores associated with PC1 and PC4 for surface water.	82
Figure 3.10	Decomposed time series EC and water level at Catfield	83
Figure 3.11	Decomposed time series EC and water level at Woodbastwick	83
Figure 3.12	Decomposed time series EC and water level at Wheatfen	84
Figure 3.13	Decomposed time series EC and water level at Wheatfen	84
Figure 3.14	Decomposed time series EC and water level at How Hill	85
Figure 3.15	Summary of the trend components for EC and water level at all sites	86
Figure 3.16	Number of days water level (mAPS) is at a given height during 2012	87
Figure 3.17	Decomposed time series data during the surge event on 9 <sup>th</sup> November 2007 for water level and EC	89

Figure 3.18	Cross correlation functions for the irregular component of tide gauge data and the irregular component of water level and EC data for the 2007 surge.	90
Figure 3.19	Decomposed time series data during the surge event on 5th December 2013 for water level and EC.	91
Figure 3.20	Cross correlation functions (CCF) for the irregular component of tide gauge data and the irregular component of water level data for the 2013 surge.	92
Figure 4.1	Bar charts for above-ground carbon mass (AGCM, g C m <sup>-2</sup> ), stem density (m <sup>-2</sup> ) and stem height (cm). Interaction plots shown for a significant result.	113
Figure 4.2	Bar chart to compare of N/C of <i>P.australis</i> leaves between 2013 and 2014.	114
Figure 4.3	Scatterplots to show the relationship between significant controlling factors when radiation use efficiency (RuE) was the dependent variable.	115
Figure 4.4	Above-ground biomass for each species identified at each of the six field sites in September 2013.	116
Figure 4.5	(A) Species score bi-plots from CCA and (B) site scores (indicated by points) and constraining environmental variables.	118
Figure 4.6	Predicted model values compared to observed below-ground production (left) and comparison between standardised residuals and predicted model values (right).	119
Figure 4.7	An example of below-ground carbon density (g C m <sup>-3</sup> ) with depth (m) using the modified Ricker Function (equation 4.1).	119
Figure 4.8	Bar chart to compare below-ground carbon production between study sites (g C m <sup>-2</sup> yr <sup>-1</sup> ).	120
Figure 4.9	Bar chart to compare AGCP/BGCP between sites	120
Figure 4.10	Scatterplots to show the relationship between significant controlling factors used in multiple regression when AGCP/BGCP was the dependent variable.	121
Figure 4.11	For sites used in the litterbag experiment: water level in metres above peat surface (mAPS) recorded for the duration of the litterbag experiment (March 2014 and March 2015).	122
Figure 4.12	Bar chart to compare C/N ratio of deployment litter between sites used in the litterbag experiment.	123

Figure 4.13	Bar chart to compare mass loss (%) of original litter after one month of decay of leaves, stems and below-ground material (BG).	125
Figure 4.14	Scatterplots to show the relationship between significant controlling factors for mass loss of leaves ( $ML_L$ ) and below-ground material ( $ML_{BG}$ ).	125
Figure 4.15	Carbon mass remaining (%) relative to carbon mass at month 1.	127
Figure 4.16	Bar charts to compare decay rate coefficient, $k$ ( $yr^{-1}$ ) between sites and position of decay for leaves, stems and below-ground material (BG). Interaction plots are included for a significant result.	128
Figure 4.17	Scatterplots to show the relationship between controlling factors used in multiple regression for the decay rate of leaves ( $k_L$ ), stems ( $k_S$ ) and below-ground ( $k_{BG}$ ).	129
Figure 4.18	Bar chart to compare mass loss (%) after one month of decay for each tissue type used in the experiment.	132
Figure 4.19	Bar chart to compare mass loss of litter in the transplant experiment after 12 months.	134
Figure 4.20	Bar chart to compare above- and below-ground carbon accumulation potentials along a gradient of saline influence.	135
Figure 5.1	The relationship between organic matter derived from loss on ignition and total carbon derived from elemental analysis.	151
Figure 5.2	Stratigraphy from the deepest core from Wheatfen based on Lambert's criteria (Lambert 1960).	156
Figure 5.3	Stratigraphy from the deepest core from Woodbastwick based on Lambert's criteria (Lambert 1960).	157
Figure 5.4	Stratigraphy from the deepest core from Strumpshaw based on Lambert's criteria (Lambert 1960).	157
Figure 5.5	Scatterplots to test the assumption of homogeneity for dependent variables of mixed effects linear models.	158
Figure 5.6	Bar chart for average carbon density for each of the three sites	159
Figure 5.7	Bar chart for average carbon content (%) between peat type and site and the corresponding interaction plot	160
Figure 5.8	Scatterplots of carbon content with depth for each site.	160
Figure 5.9	Bar chart for average bulk density for all peat types at study sites.	160
Figure 5.10	Scatterplots of bulk density with depth grouped by peat type and site.	160

Figure 5.11	Bulk density and carbon content profiles used in radiometric dating.	162
Figure 5.12	Distribution of radionuclides in the dated core from each site.	163
Figure 5.13	Age-depth curves based on the results of the CRS model from radiometric dating	164
Figure 6.1	Relationship between relative net growth and salinity and water depth.	177
Figure 6.2	Relationship between relative decay and salinity and water depth.	179
Figure 6.3	Change in mineral sedimentation rate, $dP_{min}/dt$ ( $kg\ m^{-2}\ yr^{-1}$ ), when suspended sediment concentration, $\eta$ ( $kg\ m^{-3}$ ), and cumulated water depth, $W$ (m), are varied.	184
Figure 6.4	Change in the flux from vegetation to peat at steady state, $F^*$ ( $kg\ m^{-2}$ ), when salinity (ppt) and cumulated water depth, $W$ (m), are varied	185
Figure 6.5	The relationship between flux from vegetation to peat at steady state, $F^*$ ( $kg\ m^{-2}$ ) and allocation of net assimilates to below-ground organs, $\beta$ (–), when (a) salinity (ppt) and (b) cumulated water depth, $W$ (m), also varied.	185
Figure 6.6	Change in peat organic carbon and it's components ( $kg\ m^{-2}$ ) over time.	186
Figure 6.7	Change in the organic peat carbon store, $P_{org}$ ( $kg\ m^{-2}$ ), after 9000 years.	187
Figure 6.8	Change in height of a floodplain fen ( $H$ , m) under combinations of varying salinities (ppt) and cumulated water table depths ( $W$ , m).	187
Figure 6.9	Proportional contribution of organic ( $P_{org}/\rho_{org}$ ) and mineral components ( $P_{min}/\rho_{min}$ ) to the peat height ( $H$ , m) over time for varying salinity (ppt) and cumulated water table depths, $W$ (m).	188
Figure 6.10	Rate of change in peat height ( $dH/dt$ , $mm\ yr^{-1}$ ) under varying salinity, ppt, and cumulated water depth, $W$ (m).	189

## List of Tables

Table 2.1	Absolute sea-level rise (SLR) projections for 2100 based on the IPCC AR5 report (Church et al. 2013).	28
Table 2.2	Summary of above-ground biomass (AGB) and below-ground biomass (BGB) values for <i>P. australis</i> derived from the literature.	41
Table 3.1	Location and elevation of study sites	66
Table 3.2	Wavelengths selected for cation analysis on the ICP-OES	70
Table 3.3	Summary of the residual standard deviation of drift checks for analysis of porewater and surface water chemistry.	71
Table 3.4	Recording period of Environment Agency EC and water level data	73
Table 3.5	Summary statistics for analysed water chemistry variables	76
Table 3.6	Pearson's <i>r</i> correlation coefficients for water chemistry variables in porewater and surface water.	77
Table 3.7	Results of principal component analysis on water chemistry variables porewater and surface water	80
Table 3.8	Summary of water level and electrical conductivity (EC) data in 2012 obtained from the Environment Agency (EA).	88
Table 3.9	Summary of borehole data adapted from Hiscock et al. (1996)	95
Table 4.1	Recovery (%) and precision (%RSD) measurements for elemental analysis of <i>P. australis</i> .	103
Table 4.2	Summary of controlling factors used in multiple regressions in Chapter 4.	105
Table 4.3	Accuracy (%Recovery) and precision (%RSD) measurements for elemental analysis of litterbag material.	109
Table 4.4	Table outlining if a significant result from the two-way ANOVA should be interpreted as an effect of microenvironment, litter quality or both.	111
Table 4.5	Two-way ANOVA results for above-ground carbon mass.	112
Table 4.6	Stepwise multiple regression model of RuE.	115
Table 4.7	Species identified in September 2013.	116
Table 4.8	Summary of partial CCA.	117
Table 4.9	Stepwise multiple regression model of AGCP/BGCP.	121

Table 4.10	For sites used in the litterbag experiment: the proportion of the 12-month study period (March 2014 to March 2015) that the lower and upper positions of decay were either (i) submerged (Sub.) or (ii) exposed (Exp.).	122
Table 4.11	Stepwise multiple regression model of mass loss of leaves (ML <sub>L</sub> ) and below-ground material (ML <sub>BG</sub> ) after one month.	125
Table 4.12	Results of a two-way ANOVA for each tissue type where decay rate coefficient was the dependent variable and site, position and their interaction were controlling factors (IVs).	126
Table 4.13	Stepwise multiple regression model decay rate coefficient of leaves (k <sub>L</sub> ), stems (k <sub>S</sub> ) and below-ground material (k <sub>BG</sub> ).	130
Table 4.14	Results of a two-way ANOVA for the transplant experiment. Mass loss at month 1 was the DV.	131
Table 4.15	Results of a two-way ANOVA for the transplant experiment. Mass loss between month 1 and 12 was the DV.	133
Table 4.16	A summary of exponential decay constants (k) from the wider literature.	139
Table 5.1	Criteria for describing peat stratigraphy as in Lambert (1960).	149
Table 5.2	Accuracy (%Recovery) and precision (%RSD) measurements for elemental analysis of peat.	150
Table 5.3	Accuracy (%Recovery) and precision (%RSD) measurements for elemental analysis of peat samples for radiometric dating.	153
Table 5.4	Representative Concentration Pathways (RCP) scenarios used to determine sea-level projections from the IPCC AR5 report.	155
Table 5.5	Mixed-effects linear model comparing carbon content, bulk density and carbon density between site, depth and peat type.	159
Table 5.6	Components of site volume for carbon stock estimates.	161
Table 5.7	Carbon stock calculated for three floodplain fen sites.	161
Table 5.8	Recent peat accretion and carbon sequestration rate from radiometric dating.	164
Table 5.9	Comparison of bulk density values published in other studies.	166
Table 5.10	Change in carbon stock for the areal extent of lowland fens in the UK (1000 km <sup>2</sup> ) estimated by Natural England (2010) when carbon density and depth are varied according to the results in Chapter 5.	168
Table 5.11	Comparison of carbon sequestration rates in freshwater	169



	wetlands reported in the literature.	
Table 6.1	Glossary of symbols used and parameter default values.	182

## List of Equations

Equation 3.1	The conversion of water level from ACD to OCN	69
Equation 3.2	Calculation for salinity as in Shi and Yu (2014)	72
Equation 3.3	Additive procedure for Seasonal and Trend Decomposition using loess	74
Equation 4.1	Modified version of the Ricker function (Ricker 1973; Laws & Archie 1981)	107
Equation 4.2	Integration of equation 4.1 with respect to depth between $x_{\min}$ and $x_{\max}$	107
Equation 4.3	Single exponential model fit to mass loss data to determine decay rate.	110
Equation 5.1	Calculation of bulk density for peat types	150
Equation 5.2	Calculation of organic matter using loss on ignition	150
Equation 5.3	Calculation for carbon density	151
Equation 5.4	Calculation for carbon stock	152
Equation 5.5	Calculation for sub-section volume	152
Equation 5.6	Calculation to propagate errors on carbon stock	152
Equation 5.7	Calculation for cumulative carbon mass for carbon sequestration rate	154
Equation 6.1	Cosine function to integrate water level over one year.	176
Equation 6.2	Mineral deposition rate - $dP_{\min}/dt$ ( $\text{kg m}^{-2} \text{yr}^{-1}$ ).	176
Equation 6.3	Mass of mineral sediment $P_{\min}$ ( $\text{kg m}^{-2}$ ) accumulated after time T (y).	176
Equation 6.4	Stress tolerance curves to model relative net growth in response to salinity stress.	177
Equation 6.5	Stress tolerance curves to model relative net growth in response to water stress.	177
Equation 6.6	Calculation for net growth, $G$ ( $\text{kg m}^{-2} \text{y}^{-1}$ ), scaled in response to salinity and water stress.	177
Equation 6.7	Rate of change in below-ground biomass.	177
Equation 6.8	Steady-state below-ground biomass.	178
Equation 6.9	Rate of change in the standing dead stock.	178
Equation 6.10	Steady-state of standing dead mass.	178

Equation 6.11	The mass flux from vegetation to peat $F$ [ $\text{kg m}^{-2} \text{y}^{-1}$ ]	178
Equation 6.12	Steady-state of mass flux from vegetation to peat.	178
Equation 6.13	Simplified steady-state of mass flux from vegetation to peat.	178
Equation 6.14	Proportion of plant growth that enters the peat stock, $\kappa$	178
Equation 6.15	Stress tolerance curves to model relative decomposition in response to water stress.	179
Equation 6.16	Stress tolerance curves to model relative decomposition in response to salinity stress.	179
Equation 6.17	Rate of change in the labile component with time	179
Equation 6.18	Rate of change in the refractory component with time	179
Equation 6.19	Organic matter accumulated at time, $T$	180
Equation 6.20	Steady state of labile component	180
Equation 6.21	Change in peat accretion with time	180
Equation 6.22	Height of the wetland surface, $H$	180

## List of Appendices

Appendix 1	Field data used to calculate above-ground carbon mass	243
Appendix 2	Scatterplots to show goodness of fit of multiple regression models	244
Appendix 3	Parameter estimates fitted to each core using the Ricker function	245
Appendix 4	Lambert Transect Maps	248
Appendix 5	The relationship between OM (%) and total carbon (%) for cores used in radiometric dating.	251
Appendix 6	Output from mixed-effects linear models in Chapter 5.	252
Appendix 7	Raw data from radiometric dating.	255

## Acronyms

AG	Refers to above-ground pools	
AGB	Above-ground biomass	Usually expressed in $\text{g m}^{-2}$
AGCP	Above-ground carbon production	Usually expressed in $\text{g C m}^{-2} \text{ yr}^{-1}$
BG	Refers to below-ground pools	
BGB	Below-ground biomass	Usually expressed in $\text{g m}^{-2}$
BGCP	Below-ground carbon production	Usually expressed in $\text{g C m}^{-2} \text{ yr}^{-1}$
CRS	Constant Rate of Supply model	Modelling technique used to interpret the results of radiometric dating.
EC	Electrical conductivity	Common measure of salinity, units usually microsiemens ( $\mu\text{S}$ ).
Gt	Gigatonne	Unit of measurement
mAOD	Metres Above Ordnance Datum	Metres relative to mean sea level at Newlyn, Cornwall (UK).
mAPS	Metres Above Peat Surface	When a water level measurement recorded in mAOD is corrected for height of the peatland surface.
NPP	Net Primary Production	The amount of carbon dioxide absorbed during photosynthesis, minus how much carbon dioxide is lost during respiration.
OM	Organic matter	
PAR	Photosynthetically active radiation	The spectral range of solar radiation that photosynthetic organisms are able to use during photosynthesis.
ppt	Parts per thousand	Unit of measurement (salinity in this case).
RuE	Radiation Use Efficiency	Ratio between NPP and PAR
SFT	Space-for-time substitution	A field technique that assumes temporal and spatial variation are equivalent.
SRP	Soluble Reactive Phosphorous	The soluble fraction of total phosphorus

## Chapter 1: Introduction

The global carbon cycle is the flux of carbon primarily between the atmosphere, oceans and the terrestrial biosphere (Schimel 1995). Carbon dioxide and methane are greenhouse gases (GHGs) that make the earth habitable by absorbing incoming radiation. However, anthropogenic activities since the industrial revolution have increased atmospheric concentrations of these GHGs at a rate faster than natural processes can remove it, resulting in rising global temperatures (Forster et al. 2007). Northern peatlands – peat-forming wetlands above 45°N – are important natural carbon sinks owing to the accumulation of organic matter at a rate faster than it is decomposed (Bridgham et al. 1998). Covering just 3% of global land area, northern peatlands store approximately 30% of the world's soil carbon (~550 Gt C) (Blodau 2002), yet there are large uncertainties in how climate change will affect the functioning of these ecosystems. It is important to resolve these uncertainties, especially in light of pressure from recent international legislation which calls for countries to find ways to reduce or offset their GHG emissions (Bain et al. 2012). Without improved knowledge of how peatland carbon storage might be affected by climate change, our understanding of the potential for peatlands to offset anthropogenic emissions is limited (Olefeldt et al. 2012).

Peatlands can be divided into bogs and fens depending on hydrological input. A bog is an ombrotrophic peatland entirely dependent on precipitation for water and solutes, whereas fens predominantly receive water from groundwater, but also from surface water and precipitation (Diack et al. 2011). Floodplain fens are distinct because their main source of water and solutes is from surface water; therefore features of the catchment, such as geology or land-use, largely influence nutrient availability in this peatland type. Floodplain fens tend to be dominated by herbaceous species, such as sedges, reeds and grasses and occur throughout the tropical and temperate zones (van Diggelen et al. 2006; Läähteenoja et al. 2009).

Owing to their lowland location, floodplain fens throughout the world are vulnerable to a higher frequency and intensity of flooding events and saline incursion as a result sea-level rise (van Diggelen et al. 2006). Climate change predictions state that over the coming century, both the frequency and intensity of storm surges will increase, and global absolute sea-level rise is expected rise to between 4 and 6 mm yr<sup>-1</sup> (Church et al. 2013). Saline incursion has been linked to the release of carbon stored

in low-lying peatlands (Henman & Poulter 2008), due in part to a reduction in above-ground production (Hellings & Gallagher 1992) but also a change in decomposition rate (Connolly et al. 2014). However, the wider significance of sea-level rise as a driver for carbon loss remains unclear. In the UK, floodplain fens cover a relatively small area in relation to other peatland types such as ombrotrophic bogs (Natural England 2010), and their global extent remains unknown. Although only accounting for a low proportion of peatland area in the UK, floodplain fens are known to have a relatively high carbon density in comparison to bogs owing to the herbaceous character of peat (e.g. Loisel et al. 2014) and are therefore an important component of regional and probably global carbon stock estimates.

Few studies have investigated the effect of sea-level rise on carbon storage in this important peatland type and a small number have thoroughly investigated the effect of sea-level rise on the balance between rate of production and decomposition (e.g. Moore et al. 2002; Moore et al. 2011). The potential importance of sea-level rise on carbon sequestration and wetland development has been identified over the last decade, but research is limited to salt marshes and mangroves (Chmura et al. 2003; Kirwan & Mudd 2012). Studies suggest that the ability of wetlands to continue to sequester carbon depends on their rate of accretion exceeding rate of sea-level rise (Chmura et al. 2003) and there is concern that peatland development will not be able to offset rising sea-level (Whittle & Gallego-sala 2016). No study to date - neither in the UK or further afield - has quantified the carbon stock, rate of carbon sequestration or rate of peat accretion in floodplain fens differing in saline influence or provided detailed information about variation in rates of production and decomposition. Thus, the implications of sea-level rise on carbon storage for the UK and worldwide remains unclear. To this end, the overall aim of this PhD thesis is to investigate how sea-level rise will effect production and decomposition in floodplain fens, and determine the implications of these findings for carbon storage.

Specific research questions, hypothesis and rationale are identified in the following literature review (Chapter 2). The review begins with an overview of the global carbon cycle and projections for sea-level rise. Thereafter is a review of our current understanding of key processes involved in peatland carbon storage with specific emphasis on the effect of sea-level rise. Chapter 3 is an in-depth site description and investigation of water chemistry in the Broads – an area comprising of a floodplain fen located in East Anglia, UK – and aims establish whether there is a gradient of saline influence which is currently not known. Chapters 4 to 6 are self-contained research

Chapters comprising their own methods, results and discussions. Chapter 4 presents the controls on rate of above- and below-ground production and decomposition in floodplain fens differing in saline influence. The implications of findings for carbon storage are subsequently discussed. Chapter 5 quantifies carbon stock and recent peat accumulation before the key controls on these elements are discussed. An unpublished model by Belyea (2016) is used in Chapter 6 to synthesise field data from the previous two Chapters with published literature, in order to explore the effects of different components of sea-level rise (water level and salinity) on peat accretion. Finally, Chapter 7 presents a summary of the findings from this project, as well as considering possible directions for future research.



## Chapter 2: Literature Review

### 2.1 Global carbon cycle

The carbon cycle is the flux of carbon between four main reservoirs; fossil carbon, the atmosphere, the oceans and the terrestrial biosphere (Schimel 1995) which act on time scales from hours to millennia. Photosynthesis, respiration and atmosphere-ocean exchange are short-term processes, whereas the burial, incorporation into sediments, and subsequent formation of fossil fuels from organic material operate on long-term temporal scales (Berner 2003). Carbon naturally moves between these reservoirs and the atmosphere and is present primarily as carbon dioxide (CO<sub>2</sub>) but also as other less abundant gases, such as methane (CH<sub>4</sub>).

Produced naturally in the biosphere and hydrosphere, CO<sub>2</sub> and CH<sub>4</sub> are Greenhouse Gases (GHGs) which make the earth habitable by absorbing incoming radiation (Karl & Trenberth 2003). Radiative forcing is a measure of the influence of a gas in altering the balance between incoming and outgoing energy from the Earth-atmosphere system (W m<sup>-2</sup>). A positive forcing indicates a warming effect (Philipona et al. 2004; Archer & Brovkin 2008); radiative forcings for CO<sub>2</sub> and CH<sub>4</sub> are +1.791 and +0.504 W m<sup>-2</sup> respectively.

Since the industrial revolution, human activities have increased concentrations of CO<sub>2</sub> and CH<sub>4</sub> in the atmosphere at a rate faster than natural processes can remove it (Forster et al. 2007). The global atmospheric concentration of CO<sub>2</sub> has increased from 278 ppm in 1750 (Ciais et al. 2013) to over 400 ppm in January 2016 (NOAA 2016). Atmospheric concentrations of CH<sub>4</sub> have increased from 772 ppb in 1750 (Ciais et al. 2013) to over 1840 ppb in 2016 (NOAA 2016). The Intergovernmental Panel on Climate Change (IPCC) AR5 found that anthropogenic GHG emissions are extremely likely (> 95% certainty) to be the dominant cause of observed warming since the mid-20<sup>th</sup> century (Stocker et al. 2013).

Wetlands are an important sink for global carbon due to the presence of hydrological conditions that are conducive to the accumulation of organic matter (Mitch & Gosselink 2000). Peatlands are a peat producing wetland formed when, following the last glaciation approximately 12 000 years BP (Harden et al. 1992), organic matter

began to accumulate under anoxic conditions in waterlogged peat masses where rate of production exceeded rate of decomposition (Frolking et al. 2001). Globally, peatlands cover 3% of total land area and are primarily located in the Northern Hemisphere (Bridgham et al. 2006) with approximately 11% located in tropical zones (Page et al. 2011). Northern peatlands currently store an estimated 547 Gt C (around 33% of the total soil carbon pool) (Yu et al. 2010).

Peatlands are considered to be net carbon stores as CO<sub>2</sub> is removed from the atmosphere via photosynthesis, and the low decay rates in anaerobic conditions result in the rate of input exceeding the rate of decay. A change in vegetation and hydrology can result in peatlands becoming sources of carbon and thus these dense stores are at risk from global climate change, including permafrost thaw (Olefeldt et al. 2012), rising temperatures (Gorham 1991) and dissolved organic carbon export from increased run-off (Frey & Smith 2005). Peat deposits located in lowland coastal locations face additional threats such as shoreline erosion, salt intrusion, drying out due to reduced rainfall and inundation from sea-level rise (Henman & Poulter 2008). A reduction in the capacity of peatlands to sequester carbon has the potential to accelerate the greenhouse effect (Maltby & Immirzi 1993).

### **2.1.1 Accounting for peatlands as carbon sinks**

The need to curb anthropogenic GHG emissions has become increasingly apparent in recent years and options for mitigation is an expanding area of research. One option for mitigation is the sustainable management of natural carbon sequestering ecosystems, such as peatlands. Despite their ability to act as long term sinks, accounting for peatland carbon stock remains an optional part of international GHG inventories in the United Nations Framework Convention on Climate Change (UNFCCC) Kyoto Protocol. Few countries have opted to include peatlands due to difficulties in accurately accounting for GHG removal (Bain et al. 2011; Committee on Climate Change 2015). The UK Government has commissioned research to identify possible emissions savings from restoring damaged peatlands (Worrall et al. 2011). However, other threats to peatlands, such as inundation of lowland peatlands from sea-level rise have been ignored.

There is an international drive for improved monitoring of terrestrial carbon stores by the UNFCCC who have identified two measurements as 'Essential Climate Variables':

above-ground biomass and soil carbon measurements (Global Climate Observing System 2010). Thus, scientific research can help to safeguard the future of peatlands by improving the estimation of regional carbon stocks, determining recent carbon sequestration rates at a regional scale and understanding how climate change might affect carbon stores, such as increasing temperatures and sea-level rise (Dunn & Freeman 2011; Bonn et al. 2014).

## **2.2 Sea-level Rise**

The global sea-level has risen throughout the 20<sup>th</sup> century and is likely to accelerate throughout the 21<sup>st</sup> century due to climate change (Nicholls & Cazenave 2010). Global sea-level is usually the average height of the ocean surface between high and low tide and is referred to as 'absolute'. Regional sea-level change is corrected for isostatic rebound and is described as 'relative' (British Geological Survey 2015). The IPCC suggest that the rate of global sea-level rise since the mid-19<sup>th</sup> century exceeded the mean rate for the previous two millennia. Sea-level was 0.19 (0.17 to 0.21) m higher in 2010 in comparison to 1901.

The need to understand the socio-economic implications of sea-level rise and to determine adaptation strategies has driven the development of global climate models (GCMs) over the last decade. GCMs are designed to project changes in meteorological variables such as global temperature, precipitation and sea-level over various spatial and temporal scales. Projections of these variables in the IPCC AR5 report are based on four Representative Concentration Pathways (RCPs) that are defined (and named) according to their total radiative forcing in 2100 (table 2.1). Although many climate projections exist, the IPCC is the leading international body for the assessment of climate change and forms the interface between science, policy and international politics (Ford et al. 2016). Therefore, IPCC projections for sea-level rise are used in this thesis.

Table 2.1: Global absolute sea-level rise (SLR) projections for 2100 based on the IPCC AR5 report (Church et al. 2013).

RCP	Temperature (°C)	SLR (m)
2.6	1.0 (0.3 - 1.7)	0.40 (0.26 - 0.55)
4.5	1.8 (1.1 - 2.6)	0.47 (0.32 - 0.63)
6.0	1.2 (1.4 - 3.1)	0.48 (0.33 - 0.63)
8.5	3.7 (2.6 - 4.8)	0.63 (0.45 - 0.82)

Sea-level will also be affected by storm surge events, and an increase in the frequency and intensity of such events are expected as a result of climate change (Church et al. 2013). Storm surges occur when strong winds generate large waves, forcing an increased volume of water towards the coast causing sea-level extremes in coastal locations (Vermaire et al. 2013). It is expected that there will be an increase in the magnitude of storm surge events around Europe (Church et al. 2013).

Storm surge studies conducted in the North Sea indicated that both sea-level rise and meteorological changes (such as storms) are important in contributing to sea-level extremes by 2100 (Woth et al. 2006; Sterl et al. 2009). Storm surge heights will increase by 8 to 10% between 2071 and 2100 (relative to 1961 to 1990) under conservative scenarios for climate change. Increases will occur mainly over the winter season and will particularly affect the eastern North Sea and the north-western British Isles (Debernard & Røed 2008).

### 2.2.1 Sea-level rise and coastal wetlands

Sea-level rise has both biophysical and socioeconomic impacts, thereby representing a major threat to coastal landscapes and their ecosystem services (Bosello et al. 2007). Primary biophysical effects of sea-level rise include increased inundation of coastal wetlands and salt-water intrusion. Ecosystems in areas of limited human influence may be able to adapt naturally by migrating landwards where topography

allows, however, densely populated areas may render many coastal ecosystems vulnerable to rising seas (McLeod et al. 2010). Wetlands located in close proximity to the coast are important for flood defence, habitat provision and carbon storage. Research has shown that coastal wetlands across all latitudes store no less than 10 Gt C of carbon (Chmura et al. 2003) but four-fifths of these could be lost worldwide by 2100 due to sea-level rise (Nicholls 2004).

The survival of coastal wetlands is dependent on surface elevation offsetting sea-level rise (Cahoon 2006). Sea-level extremes will be an artefact of increased intensity and frequency of storm surge events (section 2.2.2) and the high energy of storm surge events can result in mass mortality of above-ground biomass resulting in the rate of input of organic matter no longer exceeding rate of decay (Cahoon et al. 2003). Inland coastal habitats, such as grazing marsh, freshwater coastal lakes and lowland peatlands are all threatened by increases in salinity due to inundation of seawater following flooding from storm surge events. Ultimately, this will result in their transformation to saltmarsh or a similar intertidal habitat (Morecroft & Speakman 2015). Whilst saltmarshes might provide some of the ecosystem services delivered by floodplain fens, they are unlikely to have such extensive above- and below-ground carbon stores and they do not support the same ecological networks (see section 2.3).

### **2.2.2 Sea-level rise in the UK**

In the UK, large areas of protected saltmarsh have already been lost since their designation due to sea-level rise (Natural England 2006). Freshwater habitats located close to the coast are also at risk (Defra 2011), with 3.5% of SSSI areas present in coastal floodplain areas, including lowland raised bogs. These areas are under direct physical threat from inundation following sea-level rise, which will affect the species and habitats present (Gillingham 2015).

Extensive records of sea-level observation exist for the British Isles (Sissons 1966; Tooley 1974; Dawson 1984; Shennan et al. 2000) and allow for empirical estimates to be made of glacial isostatic rebound or recoveries (Bradley et al. 2009). The majority of England and Wales is subsiding at a rate ranging between 0.5 and 1.1 mm yr<sup>-1</sup>, resulting in an increase in relative sea-level rise (Shennan & Horton 2002). Land is subsiding in East Anglia at an average rate of 0.5 mm yr<sup>-1</sup> (Bradley et al. 2009).

It is likely that storm surge events will increase along the North Sea coast as a result of anthropogenic climate change (Woth et al. 2006) impacting much of the east coast of England (Environment Agency 2009). East Anglia is particularly vulnerable to storm surge events as wave amplitude in this region is responsive to sea-level rise resulting in increased height and frequency of extreme waves (Chini et al. 2010). Whilst there are many documents that record surges back in time, one of the most devastating floods in recent times occurred in 1953 when water level reached 3.4 mAOD and resulted in 300 fatalities in eastern England (Sibley & Tittley 2015). More recently, the winter of 2013/2014 was the stormiest winter for the last two decades due to a series of deep Atlantic low pressure systems (Kendon & McCarthy 2015). As a result, the North Sea experienced the most significant storm-surge for 60 years on the 5<sup>th</sup> December 2013. The Met Office issued 70 flood warnings and evacuated several hundred homes in eastern England. Wave height reached 8 to 10 m and maximum gust recordings indicated that December 2013 was one of the top 10 stormiest months since the 1960s (Slingo et al. 2014). Water level during the surge event in December 2013 reached 3.3 mAOD in East Anglia. Another major surge event in this area occurred on the 9<sup>th</sup> November 2007 and reached 2.7 m above the monthly average (Met Office 2011).

## **2.3 Description of floodplain fen environments**

In wetland ecology there is much confusion about terminology. Peat producing ecosystems can be split into bogs, fens and floodplain fens (Diack et al. 2011). There is a clear distinction; bogs are dependent purely on precipitation for solutes and water whereas fens are predominantly fed by groundwater. Floodplain fens are predominantly fed by surface water (van Diggelen et al. 2006). The hydrochemistry of floodplain fens therefore depends upon their catchment, and this in turn dictates vegetation composition. Thus, floodplain fens are described by their hydrology, vegetation and chemistry in the proceeding subsections. Note that northern hemisphere peatlands is a term used broadly amongst the literature (Akumu & McLaughlin 2013). Generally, northern hemisphere peatlands refers to those at high latitudes, such as in Canada and the Arctic and does not include temperate peatlands (Gorham 1991; Loisel et al. 2014).

Floodplain fens occur throughout temperate and tropical regions (van Diggelen et al. 2006; Lahteenoja et al. 2009; Couwenberg et al. 2011). However, the global extent of floodplain fens is unclear. For example, the presence of peat in Amazonian floodplains is a recent discovery (Lahteenoja et al. 2009). Floodplain fens are located close to the coast, whilst others are further inland. As outlined in the proceeding subsections, temperate floodplain fens may be important in relation to carbon storage, due to relatively high levels of above-ground production compared to other peatlands, coupled with waterlogged conditions (Fiałkiewicz-Kozieł et al. 2014). Currently, little empirical research has been published on carbon storage in UK floodplain fens with relatively few studies globally (Bernal & Mitsch 2012). In North-America and Europe, the majority of research is associated with floodplain fen restoration as these environments are becoming increasingly rare (Mars et al. 1997) due to factors such as drainage for agriculture, which results in a reduction in above-ground biomass and compression of the peat surface (Seer & Schrautzer 2014). This has negative implications for carbon sequestration in floodplain fens (Riet et al. 2013), although there is little empirical evidence for the magnitude of the impacts of restoration on carbon sequestration (Lamers et al. 2015).

Lowland fens are thought to account for 1000 km<sup>2</sup> of the 7000 km<sup>2</sup> of deep peatlands (> 40 cm) found in the UK (Natural England 2010). In particular, the largest single proportion of floodplain fen in the UK is found in the Broads National Park, East Anglia (around 33 km<sup>2</sup>) (Giller & Wheeler 1986). Thus, the high efficiency of floodplain fens in sequestering carbon and the importance of these environments for supporting rare species makes the Broads an ideal site for studying these vulnerable ecosystems.

Floodplain fens in England are at risk from saline intrusion and increased frequency of inundation from sea-level rise (Natural England and RSPB 2014). There is a need to quantify carbon storage within floodplain fens in order to inform conservation management strategies with a view to mitigating climate change. For example, the floodplain fens of the Broads, UK is the largest area of undrained fen in Britain (Giller & Wheeler 1986) and in recent years the area has been susceptible to storm surges (section 2.2.2) (Slingo et al. 2014).

### **2.3.1 Hydrology**

Hydrology is the main control on the formation and maintenance of floodplain fens (van Diggelen et al. 2006). Although predominantly fed by surface water, ground water and precipitation also play a role (Mars et al. 1997). Due to the combination of these hydrological inputs, the water level in floodplain fens tends to be at or near the peat surface. Seasonality is an important factor in the hydrological regime, as floodplain fens tend to be flooded over the winter months when there is increased precipitation and river flow. During the summer, water levels are drawn down from evapotranspiration and plant uptake and fluctuating river water levels result in regular alternation of flooded and dry phases (Mars et al. 1997). During non-flooded periods, the floodplain can remain wet if pathways available for drainage of surface water are impeded. Fluctuation in water level causes variation between aerobic and anaerobic conditions in the peat which facilitates many chemical transformations important in determining floral composition (Mitsch & Gosselink 2000).

Surface elevation, proximity to the coast, and geomorphology influence the extent to which a floodplain fen is vulnerable to saline influence (Mitsch & Gosselink 2000). Floodplain fens located near the mouth of a river can be influenced by tides, longshore currents, and storm surges (Keough et al. 1999). In such an environment, tides, seasonal fluctuations in water level, precipitation and groundwater fluxes are high-frequency, low-magnitude stressors which exert a regular influence on ecosystem processes such as organic matter accumulation and productivity of above-ground biomass (Cahoon 2006).

With sea-level rise and the intensification of storm surge events (Church et al. 2013), floodplain fens are likely to experience more frequent inundation events which will impact on their natural functioning. It is critical to understand how alterations in this hydrological regime will impact on carbon storage in order to inform management practice aimed at minimising these effects.

### **2.3.2 Vegetation**

Floodplain fens are important environments because they provide a transitional zone between open-water and terrestrial ecosystems and the vegetation found in floodplain



fens is of a composition that provides unique habitats for endangered species (Diack et al. 2011). Furthermore, vegetation is critical for the maintenance of these environments through the production of litter (section 2.4) and subsequent decomposition (section 2.5).

Anoxia is one of the main stressors that prevent many plant species from growing in these environments and vegetation characteristic of floodplain fens have adapted to the reduced oxygen available in the root zone through the development of aerenchyma. These structures enable the transport of oxygen to the rhizosphere and protect the plant by oxidising phytotoxins in the root zone (Armstrong et al. 1999). In floodplain fens, the majority of plant growth starts in spring with peak biomass reached in September when maximum gross primary productivity occurs, followed by the onset of die-back in early October. At this point of senescence, above- and below-ground vegetation becomes litter and is available to be decomposed both aerobically and anaerobically (section 2.5) and remaining material contributes to the accumulation of peat (section 2.6).

Species found in floodplain fens range from sedges, such as *Carex* spp. and *Cladium mariscus* (L.) Pohl (1809), and reeds and grasses, including *Phragmites australis* (cav.) Trin. Ex Steud. (1841), *Glyceria maxima* (Hartm.) Holmb. (1820), *Juncus* spp. and *Calamagrostis* spp. *P. australis* (frequently termed common reed) is one of the most widely distributed species on earth (Soetaert & Herman 2008) and is believed to be one of the most ubiquitous macrophytes across temperate wetlands (Asaeda & Karunaratne 2000; González & Seastedt 2001; Windham 2001; Minchinton & Bertness 2003). For example, *P. australis* is the dominant species in floodplain fens in the Broads, UK where 75% of NVC communities recognised under the 1994 Habitats Directive are *P. australis* communities (Broads Authority 1997). Although a freshwater species, *P. australis* can tolerate fluctuating water levels and salinities up to 15 ppt (section 2.4) (Hootsmans & Wiegman 1998).

The majority of studies concerned with the growth of *P. australis* assume that all living biomass die by the start of the next growing season (Hocking et al. 1983; Asaeda & Karunaratne 2000; Soetaert et al. 2004). Dead stands of *P. australis* can remain for one to three years (termed 'standing dead') (Hocking et al. 1983; Cowie et al. 1992; Dinka et al. 2004) and are important for the transfer of gas to the rhizosphere (Armstrong et al. 1996). These dead stands tend to fall to the ground in early spring to early summer (Mason & Bryant 1975), although few studies investigate the time and

rate of standing dead collapse in detail, and this is an important consideration when understanding floodplain fen carbon cycling.

### **2.3.3 Chemistry**

Biogeochemical cycling in floodplain fens is affected by the chemistry of the peat, porewater and surface water but also by water table position, which is important for controlling redox potential. Together, biogeochemical cycling and redox potential affect plant and microbial assemblages and processes (Wassen & Joosten 1996) and have implications for plant growth (section 2.4) and decomposition (section 2.5).

#### **2.3.3.1 Nutrient inputs**

Fluvial inundation is a primary mechanism for nutrient delivery to floodplain fens. Nutrient rich water enters the system via overtopping from rivers which originated from the surrounding catchment and thus can be rich in dissolved carbonates from sedimentary rocks including elevated concentrations of calcium ( $\text{Ca}^{2+}$ ) and magnesium ions ( $\text{Mg}^{2+}$ ) (Wassen & Joosten 1996). Overtopping can also result in the delivery of anthropogenic pollutants, such as nitrate and/or phosphorous rich water from agricultural fertilizers or sewage from point-source discharge (Neal et al. 2010). Nutrient enrichment from fluvial inundation can result in the immobilisation of nutrients as microbes incorporate nutrients into their own cells for growth thus rendering them unavailable for plant growth (Sheppard et al. 2013).

Saline intrusion occurs in floodplain fens located in close proximity to the coast. This results in the delivery of water high in ionic strength in comparison to freshwater, especially the common ionic constituents of seawater; chloride ( $\text{Cl}^-$ ) and sodium ( $\text{Na}^+$ ). Storm surge events are likely to exacerbate saline intrusion due to increased volumes of seawater being transported upstream.

### 2.3.3.2 Redox reactions

The position of the water table is a critical control on biogeochemical cycling in floodplain fens and has implications for carbon storage. Under saturated conditions, oxygen is no longer the electron acceptor for chemical transformations occurring during decomposition. Instead a sequence of ions are utilised as electron acceptors as a substitute to oxygen; nitrate ( $\text{NO}_3^-$ ), manganese ( $\text{MnO}_2$ ), iron ( $\text{Fe}(\text{OH})_3$ ), sulphate ( $\text{SO}_4^{2-}$ ) and carbon dioxide ( $\text{CO}_2$ ). As stated in section 2.3.2, wetland plants such as *P. australis* adapt to waterlogged conditions by transporting oxygen to the rhizosphere via aerenchyma (Mitch & Gosselink 2000). Thus, aerobic reactions prevail around the rooting zone (figure 2.1) (Mitch & Gosselink 2000), allowing the mineralisation of carbon, nitrogen and other nutrients and  $\text{CO}_2$  is released via heterotrophic respiration or through the oxidation of  $\text{CH}_4$  by methanotrophic bacteria.

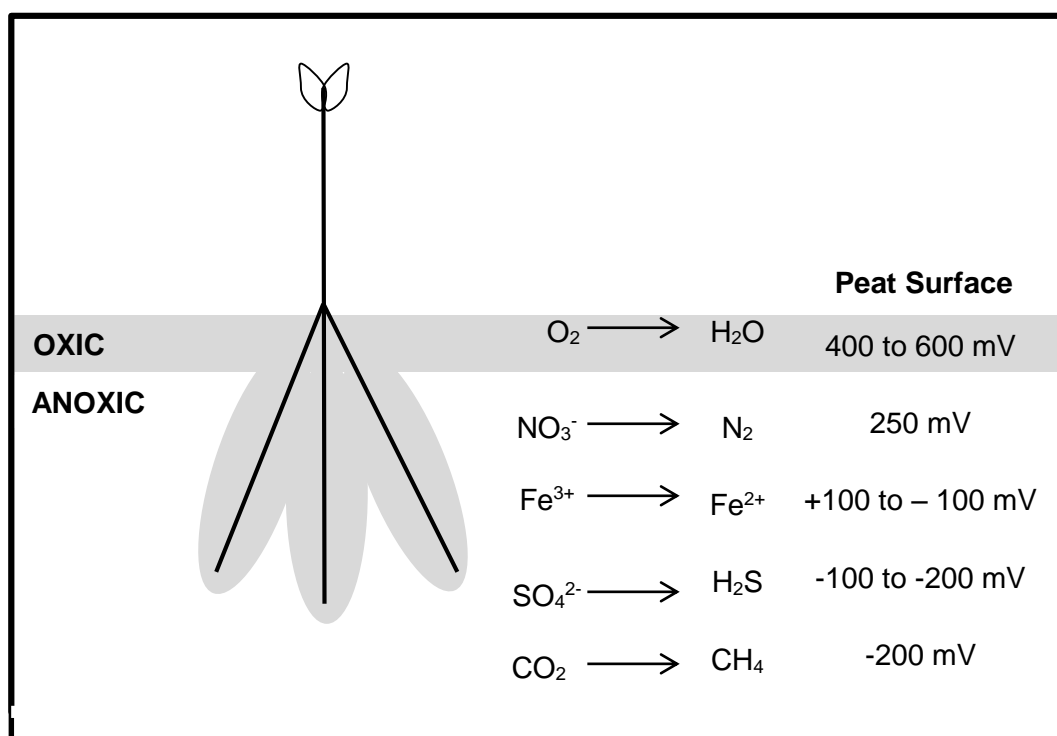


Figure 2.1: Conceptual model outlining the distribution of redox reactions through a peat profile where mV = millivolt and indicates redox potential. Shaded areas indicate oxic conditions. Adapted from Conrad (1996).

Figure 2.2 depicts the mineralisation of organic matter in wetlands (Ferry 2010). Step 1 represents the fixation of  $\text{CO}_2$  to organic matter via photosynthesis where  $\text{O}_2$  is a waste product. In step 2,  $\text{CO}_2$  is emitted as a result of heterotrophic respiration. In step 3, organic matter is deposited into the anoxic zone where water-soluble organic substances are leached. More complex biomass remains and is decomposed by anaerobic microbes producing acetate,  $\text{CO}_2$ ,  $\text{H}_2$ , and volatile fatty acids (step 4). Step 5 involves the breakdown of volatile fatty acids. Next,  $\text{CH}_4$  is produced by a reduction reaction via the acetoclastic or the hydrogenotrophic pathways (step 6) and is anaerobically oxidised to  $\text{CO}_2$  (step 7), diffused to the atmosphere (step 8) or, as depicted by step 9, aerobically oxidised to  $\text{CO}_2$ .

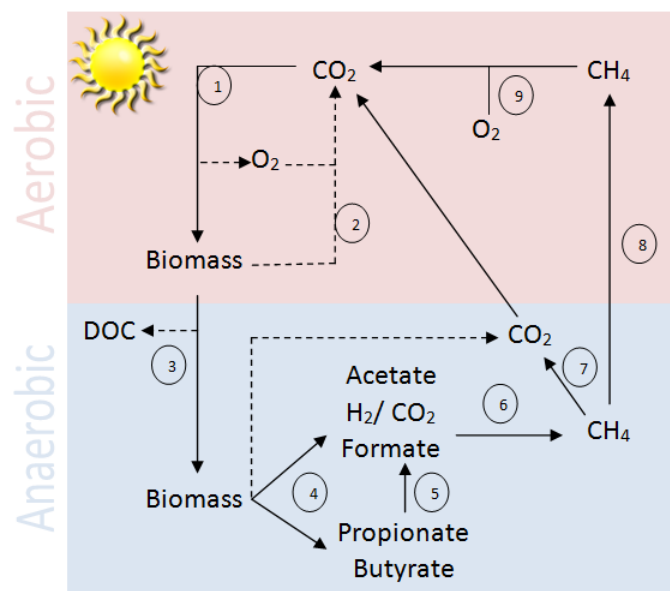


Figure 2.2: The global carbon cycle with aerobic mechanisms at the top (red) and anaerobic at the bottom (blue). Adapted from Ferry (2010).

## 2.4 Above- and below-ground inputs to the peat carbon store

Peat formation relies on organic matter input exceeding rate of decay, therefore, factors controlling the rate of organic matter input and rate of decay need to be understood to determine how an increased saline influence might affect carbon storage in floodplain fens. Above-ground biomass, and therefore the rate of organic matter input to the carbon store, is dependent on a multitude of factors including water level, nutrient availability and salinity in addition to factors such as cutting regime and trampling (Engloner 2009).

It was established in section 2.3.1 that *P. australis* is the dominant vegetation in wetlands, including floodplain fens and consequently, this section largely refers to the literature based on this species specifically. Many studies have focused on the dynamics of the growth and decay of *P. australis* (Hocking 1989; Hietz 1992; Komínková et al. 2000; Asaeda & Karunaratne 2000; Asaeda et al. 2002; Findlay et al. 2002; Scarton et al. 2002), including the effects of salinity (Hanganu et al. 1999; Lissner et al. 1999; Mauchamp & Mesleard 2001; Soetaert et al. 2004). There is, however, a lack of studies that investigate the effect of salinity on the growth and decay of *P. australis* within floodplain fens. It is important to understand how the growth of *P. australis* might be affected by increased saline influence, as the floodplain fen carbon stores are dependent on the maintenance of an input of organic material.

*P. australis* stands are highly productive with maximal above-ground biomass reported to vary between 152 (Rolletschek & Hartzendorf 2000) and 15 000 g m<sup>-2</sup> (Wheeler & Giller 1982; Eid et al. 2010) depending on a variety of environmental factors (e.g. water level and hydrogeochemistry), although biomass is typically around 1000 g m<sup>-2</sup> (Windham 2001).

Above-ground biomass can be used as a proxy for above-ground production (Soetaert et al. 2004) as maximal above-ground stocks of *P. australis* are assumed to be between 85 and 100% of net annual production (Brix et al. 2001). The limitation of this approach is that any remaining growth from the previous year is not accounted for (Linthurst & Reimoldt 1978). Other methods for determining above-ground production do account for this, such as Smalley's (Scarton et al. 2002) and the Wiegert and Evans methods (Wiegert & Evans 1964). However, these are methodologically

intensive and require an environment that does not have an erosive force, such as fluctuating water level.

#### **2.4.1 Water level**

Water level variation has been found to be more limiting to growth than nutrient loadings (Zhao et al. 2013) and Clevering (1998) suggests that water level is a stronger selective force than the availability of nutrients. Two hydrological factors can affect the growth of *P. australis*; water level and extent of fluctuation (Engloner 2009).

Periods of extended inundation, such as 100 days or more, can reduce the growth of *P. australis*, whereas growth is favoured when water level is periodically lowered over the growing season (Hudon et al. 2005). Providing water level remains stable, *P. australis* can tolerate levels up to 0.8 m before adverse effects on above-ground biomass are observed (Coops et al. 1996) and can persist when water level reduces to 1 m below the land surface (Hudon et al. 2005). Moderate water level fluctuations (within 0.23 m) do not have a pronounced effect on stem height and density (Coops & van der Velde 1996).

Timing of inundation is also an important consideration. For instance, permanent submergence in excess of 40 mm during germination can reduce shoot emergence by between 75 and 100% (Armstrong et al. 1999). When flooding level is increased over the growing season, shoot height and biomass are reduced at the end of the season in comparison to the start (Hellings & Gallagher 1992). Nevertheless, there is inconsistency as to the effect of timing of inundation on above-ground biomass in the literature: it is reported that shoot density is higher in drier environments in comparison to wetter ones (Bodensteiner & Gabriel 2003; Engloner 2009), whereas Coops et al. (1996) found an irregular pattern in shoot density along a gradient of water depth.

#### 2.4.2 Nutrient availability

The influence of nutrient availability on *P. australis* growth has been extensively researched (Engloner 2009) and is a well-known factor limiting plant growth. The underlying geology of a wetland can influence nutrient availability for example, chalk deposits can provide important nutrients, such as  $\text{Ca}^{2+}$ , to porewater via groundwater upwelling.

Nitrogen is a critical nutrient for growth, and the amount of nitrogen in leaves partly determines the rate of photosynthesis, where the more nitrogen present in the leaf the higher the rate of photosynthesis (Berendse & Aerts 1987). Both  $\text{NH}_4^+$  and  $\text{NO}_3^-$  are important sources of nitrogen with *P. australis* able to grow in a wide range of concentrations (Romero et al. 1999). Observational studies have shown that under increasing nitrogen concentrations, *P. australis* invest heavily in rhizome growth as opposed to seed production as a more efficient mechanism for dispersal (Rickey & Anderson 2004) and a significant relationship exists between nitrogen loading and the expansion of *P. australis* (Haslam 1965; Rice et al. 2000). High nitrogen availability brings about an increasing density, height, weight and diameter of shoots in comparison to non-enriched sites (Hung et al. 2007). The net result is an increased above and below-ground biomass.

Phosphorus is also an important nutrient for plant growth. Generally, peatland plants are considered to be nitrogen and phosphorus limited due to environmental conditions, with high water levels reducing mineralisation of organic matter, resulting in a deficit between the supply of bioavailable nitrogen and phosphorus and the demands of the plants and microbes (Venterink et al. 2001). Such a limitation can result in reduced plant growth but greater species diversity. It follows that increases in peat nitrogen and phosphorus content increase above-ground and below-ground biomass (Nykänen et al. 2003; Zhang et al. 2007). Greater nitrogen and phosphorus foliar contents should allow for greater uptake of carbon and nitrogen from the atmosphere and subsequent long-term storage, if prevailing conditions are conducive to peat accumulation (section 2.6). Magnesium is also an essential plant nutrient, especially its role in the photosynthesis process. Uptake by the plant from the soil is through the transpiration stream or via diffusion. Magnesium uptake can be reduced in the presence of other cations, such as potassium and ammonium.

Nutrient enrichment occurs as a result of anthropogenic activities throughout the world, such as intensive agricultural practices or sewage contamination. Growth of *P. australis* has been shown to be limited by eutrophic conditions also rich in organic matter and under anoxic conditions (Ostendorp 1989). Although wetland species tend to favour  $\text{NH}_4^+$  over  $\text{NO}_3^-$  under anoxic conditions, *P. australis* can develop  $\text{NH}_4^+$  toxicity if  $\text{NH}_4^+$  accumulates in tissues, however, the critical point of toxicity is highly dependent on other stressors (e.g. heat stress) on the plant (Tylova-Munzarova et al. 2005). Also, the amount of sclerenchyma, a specialised tissue adapted to withstand compressive and tensile stresses in stems, is reduced under eutrophic conditions (Boar 1996). Phosphate ( $\text{PO}_4^{3-}$ ) has been shown to stimulate methanogenesis (Aerts & De Caluwe 1994), as microbes are often P limited in peatlands (Basiliko et al. 2007). Therefore, nutrient enrichment from sewage works (known to be rich in phosphates, Neal et al. 2010) will accelerate organic matter mineralisation in anoxic environments.

### 2.4.3 Salinity

In relation to saline intrusion, it is hypothesised that there is a two-phase response of plant growth to salinity (Munns 2002). Initially, a decrease in osmotic potential is the result of environmental stressors outside of the plant, such as an increased concentration of NaCl and  $\text{Na}_2\text{SO}_4$  in porewater (Montero et al. 1998). During this phase, Na, S and Cl accumulate in roots, however, the accumulation of salts in *P. australis* leaves is delayed due to an efficient mechanism for exclusion (Pagter et al. 2009). Secondly, when salinity is prolonged and exceeds 15 ppt, the ability of leaf cells to inhibit the accumulation of salts is exceeded, although this takes longer to develop. As a result, energy is diverted from growth to maintaining osmotic balance. Leaf expansion and growth is inhibited and ultimately, radiation use efficiency (RuE) is reduced (Farquhar & Sharkey 1982; Pagter et al. 2009; Gorai et al. 2010).

Studies concerned with the combined effect of salinity and water level found a decline in photosynthetic efficiency with increasing salinity and soil dryness (Hellings & Gallagher 1992; Yang et al. 2014). Salinity reduces leaf area available for photosynthesis, whilst water stress induces stomatal closure to reduce water loss via evotranspiration, thereby reducing uptake of  $\text{CO}_2$  for photosynthesis. Comparing RuE gives an indication as to the relative efficiency of a plant (Yang et al. 2014). RuE is



defined as the ratio between net primary productivity (NPP) and absorbed PAR (Medlyn 1998). The use of this approach is widespread and has proved powerful for growth analysis (van Kuijk et al. 2008) despite limitations, such as the lack of inclusion of leaf inclination angles and light extinction through the canopy (Soetaert et al. 2004; Hilker et al. 2008). There have been empirical studies associated with the photosynthetic response of *P. australis* to salinity (Pater 2009) however; given the importance of above-ground carbon inputs to floodplain fens, no studies have investigated the feedback between the effect of salinity on RuE of *P. australis* and peat carbon storage.

Although RuE is affected by salinity, the proportion of total production allocated to above- and below-ground organs does not appear to change. Instead, more energy is allocated to each organ for survival, but is allocated in the same proportion (Hellings & Gallagher 1992; Lissner & Schierup 1997; Mauchamp & Mesleard 2001; Yang et al. 2014). Above- to below-ground biomass or carbon mass (biomass adjusted for carbon content) quotients can be used as an indication of above- and below-ground allocation (Bazzaz et al. 1987). These quotients vary throughout the year and typically for *P. australis*, AG/BG is around 0.25 (table 2.2), indicating that around 25% of production is allocated to above-ground organs and 75% to below-ground organs.

Table 2.2: Summary table of above-ground biomass (AGB) and below-ground biomass (BGB) values for *P. australis* derived from the literature.

Study	Location	Salinity (ppt)	Water Regime	Time of harvest	AGB (g m <sup>-2</sup> )	BGB (g m <sup>-2</sup> )	AGB/BGB
Soetaert et al. (2004)	Scheldt Estuary	4.5 to 20	15% of year inundated	-	587	2806	0.21
		0 to 6	30% of year inundated	-	1166	3346	0.35
Rolletschek et al. (1999)	Austria and Hungary	Freshwater	Permanently flooded	August	420	1500	0.28
		Freshwater	Permanently flooded	September	241	1500	0.16
Scarton et al. (2002)	Italy	6 to 25	Tidal	September	780	4087	0.19

#### 2.4.4 Management practice

Cutting is known to have an effect on the regrowth of *P. australis* (Engloner 2009) by either increasing or decreasing both stem height and stem density (Hocking et al. 1983). The response of reed beds to cutting is variable and situation specific, with some studies reporting an increased above-ground biomass the year following cutting (Warren et al. 2001; Russell & Kraaij 2008) whilst some report a reduced biomass (Asaeda et al. 2006). Growth following cutting is particularly sensitive to increasing salinity with a negative correlation observed (Asaeda et al. 2003) due to salt-stressed plants allocating more energy to maintaining an osmotic balance as opposed to growth (Hellings & Gallagher 1992).

The timing of cutting can also effect regrowth, with winter cutting resulting in increased productivity the following season as rhizome carbohydrate reserves have already been replenished (Husák 1975). Cutting during the growing season can reduce regrowth the following year (Weisner & Granéli 1989; Asaeda et al. 2006). Conversely, Ingram et al. (1980) found that in the UK, cutting at any time reduces regrowth the following year. Regardless of time, cutting below the water surface almost totally inhibits the growth of shoots as rhizome and root aeration ceases and bud growth is inhibited (Hocking et al. 1983; Mauchamp & Mesleard 2001; Engloner 2009).

It is common in wetlands for biomass to be trampled by herbivores (Hocking et al. 1983); *P. australis* stems become snapped and are therefore shorter, or entire stems are trampled to the ground and thus die prematurely (Hayball & Pearce 2004). Sites that have been recently cut are more vulnerable to trampling by herbivores as previously dense areas of *P. australis* become exposed to allow their passage.

#### 2.4.5 Below-ground inputs

Below-ground biomass is the main source of soil organic matter in fens (Sjors 1991). Carbon assimilated in above-ground tissue is translocated to roots and is distributed between root tissue, root respiration and root-released organic material. Organic matter released by roots to the rhizosphere during growth supports microbial activity

(Richert et al. 2000), which in turn influences nutrient cycling and decomposition (Van Veen et al. 1989).

Prolonged waterlogging shifts plant metabolism as more carbon is translocated to support the lignification of roots to regulate the diffusion of oxygen to the rhizosphere (Armstrong et al. 1996). Lignification of roots is also a defence against an increase of phytotoxins in the peat, such as sulphides and organic acids, which arise from inundation from saline water. Functioning aerenchyma can protect the plant by promoting the oxidation of potential phytotoxins in the rhizosphere (Saleque & Kirk 1995; Wang & Peverly 1999).

Lignification of roots deprives other plant tissues, such as stems and leaves, of assimilated carbon and results in the stunting and death of shoots (Armstrong & Armstrong 2001). Accumulation of phytotoxins in roots, such as salt ions, has also been shown to induce stomatal closure and thus reduce uptake of CO<sub>2</sub> (Pagter et al. 2009). Further, an increased concentration of phytotoxins causes the growth of calluses, which block vascular tissues (Armstrong et al. 1999). Under anoxic conditions, roots respond physiologically within 4 days following an input of phytotoxins in porewater (Armstrong & Armstrong 2001). Low concentrations of sodium and sulphur within roots in saline environments indicate that *P. australis* have an efficient mechanism to restrict uptake of these ions despite high external concentrations (Pagter et al. 2009).

## **2.5 Decay of plant litter**

As previously stated in this Chapter, *P. australis* is considered the dominant species in floodplain fens, and unless otherwise stated, references refer to studies of this species in particular. Many authors have measured the decay rate of *P. australis* in permanently saturated littoral zones (Webster & Benfield 1986; Hietz 1992; Gessner 2001; Van Dokkum et al. 2002; Dinka et al. 2004) with some studies focused on the effect of saline influence (Windham 2001; Scarton et al. 2002; Quintino et al. 2009) although these tend to be in mineral based environments such as estuaries and salt marshes. Likewise, studies have determined decomposition rate in peatlands, but these tend to be based in ombrotrophic environments (Belyea 1996; Moore et al. 2007). Few studies have measured decay rate in floodplain fens (Reynolds et al. 2007), despite the acknowledged importance of peatlands as terrestrial carbon stores.

Furthermore, few studies have examined rate of carbon mass loss (Moore et al. 2011) which is useful in determining the effect of environmental perturbations, such as saline influence, on carbon stores. Therefore, there is a distinct gap in the literature regarding the determination of carbon decay rate in floodplain fens at risk from increasing saline influence.

Decomposition is a combined result of physical breakage of tissue, leaching of dissolved components and microbial breakdown. The leaching of hydrolysable compounds (section 2.3.3.2) is known as physical decay. This happens instantaneously and is complete after a few days or weeks. These processes occur in all environments and is not as sensitive to environmental condition as microbial decay, thus many *P. australis* studies are focused on the latter processes (Hietz 1992; Komínková et al. 2000; Findlay et al. 2002; Morris & Waddington 2011; Hughes et al. 2014). After physical leaching, microbial decay begins and litter is broken down rapidly at the seasonally-saturated peat surface and decomposition slows in the deeper, permanently saturated peat (Clymo 1984). In floodplain fens, increased storm surge events will affect nutrient availability through the delivery of ion rich water and change environmental condition by disrupting hydrological regime. The position of redox boundaries associated with water level and chemical composition of plant tissues associated with nutrient status are principal controls on the decay of carbon (Smemo & Yavitt 2007; Thormann et al. 2001; Manzoni et al. 2012).

Standing dead (section 2.3.2) can be subject to air decay where shoots are colonized and decomposed by microbes in an upright and aerial position (Komínková et al. 2000). Air decay has been found to be an important component of carbon cycling in wetland ecosystems (Kuehn et al. 2004) as microbes are well adapted to not having access to nutrients that are available in the peat for below-ground decay (Gessner 2001). Fungi are known to be the primary decomposers in the aerial decay of *P. australis* and the majority of studies are concerned with the effect of aerial decay on nutrient cycling (Tanaka 1991; Kuehn et al. 2000; Komínková et al. 2000; Kuehn et al. 2004; Zhang et al. 2014) with no studies focussing on the effect of salinity.

Rate of decay is measured as the loss of mass of the original plant material over time (Hietz 1992; Thormann & Bayley 1997; Froking et al. 2001; Bradford et al. 2002; Quintino et al. 2009). The extent of mass loss by physical leaching compared to microbial decay varies due to a range of environmental and biological factors. In most cases, the proportion of mass remaining after each collection can be fit to a negative exponential model (Jenny et al. 1949; Olson 1963; Wider & Lang 1982; Bedford 2004;

Prescott 2005; Rovira & Rovira 2010). However, studies where substantially more mass is lost from physical decay than microbial decay apply a two-pool model which generates a decay rate for both of these stages (Manzoni et al. 2012).

#### 2.5.1 Stoichiometric control on decay rate

Energy for microbial processes comes from organic matter that accumulates in peat (Biasi et al. 2005). Decomposers sequester carbon and nitrogen from plant litter and favour easily decomposable compounds (Manzoni et al. 2010) therefore, peat becomes enriched with recalcitrant carbon compounds (Hilasvuori et al. 2013). Micro-organisms play a key role in inducing changes in carbon mineralization rates during periods of aeration following water table drawdown as aerobic respiration allows the build-up and maintenance of a larger microbial biomass (Blodau et al. 2004). Peat and porewater nitrogen and phosphorous concentrations greatly affect microbial populations, controlling mineralisation as increases in nutrient contents allow for microbial populations to grow, as well as increasing microbial decomposition of organic matter, as the nutrients act as reactants for the processes (Ouyang et al. 2008). Recalcitrant forms of organic matter, such as lignin, requires more energy to be broken down and therefore takes longer to be mineralised by microbes. C/N is a commonly applied indicator of how readily litter can be decomposed, and it is widely established in the literature that the higher the ratio the more energy is required to break down the litter (Janssen 1996; Moore et al. 2007; Manzoni et al. 2010; Moore et al. 2011). K-strategist microbes are specialists in mineralising recalcitrant material, whereas r-strategists specialise in the mineralisation of labile organic matter. r-strategists die or become dormant when labile material is exhausted. Conversely, K-strategists are continuously active and grow slowly due to an almost inexhaustible supply of recalcitrant material (Fontaine et al. 2003). Although labile material can be processed by K-strategists (Saiz-Jimenez 1996), in reality labile material is not available to K-strategists as r-strategists are a stronger competitor due to their ability to grow faster.

#### 2.5.2 The effect of sea-level rise on decay rate

Increasing salinity has an inhibitory effect on microbial activity and consequently, the decay of organic matter (Malik et al. 1979). The influence of salt as a stressor of microorganisms may be more potent than that of heavy metals (Sardinha et al. 2003).

A reduction in decay rate following an increase in salinity has been observed as plant growth is suppressed from saline stress and the supply of organic matter is reduced (Rietz & Haynes 2003).

Another possible cause is that salinity induces osmotic stress in microbes and reduces microbial activity (Wichern et al. 2006), however, soil microorganisms are able to adapt if this is experienced on a regular basis (Sparling & West 1989). The two main adaption strategies are the selective exclusion of  $\text{Na}^+$  and  $\text{Cl}^-$ , and the production of intracellular organic compounds to antagonise the concentration gradient between the porewater and the cell cytoplasm (Killham 1994). These adaptations result in a physiologically active microbial community but reduce substrate use efficiency and thereby a decrease in decay rate is observed (Sangiorgio et al. 2008) (figure 2.3).

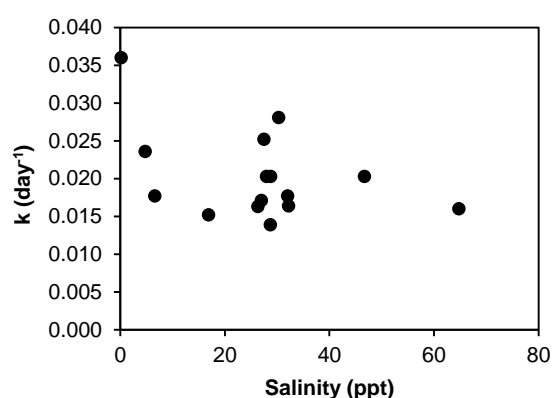


Figure 2.3: Decay rate at different salinities based on a *P. australis* study (Sangiorgio et al. 2008).

Floodplain fens are at risk from an increased frequency and intensity of storm surge events and therefore, an increase in salinity will be coupled with an increase in frequency and intensity of inundation. Impaired decay in peatlands is attributed to anoxia (Gorham 1991; McLatchey & Reddy 1998; Laiho 2006; Limpens et al. 2008) and decay is accelerated in drier conditions due to increased microbial activity (Eickenscheidt et al. 2015) which is compounded when water level is consistently below the peat surface due to the accumulation of microbial biomass (Nelson et al. 1996). However, it has been shown that re-wetting following dry periods is associated with faster decay rates than during stable dry phases (Fenner & Freeman 2011). The activity of phenol oxidase requires oxygen to degrade complex phenolic compounds, such as lignin, and therefore phenolic compounds are able to accumulate in the peat

under anoxic conditions (Brouns et al. 2014). In dry periods, phenol oxidase become active and begin breaking down phenolic compounds. On rewetting, these compounds are made available to alternative electron acceptors and are mineralized rapidly (Freeman et al. 2001).

In anoxic conditions, alternative electron acceptors are utilised by microbes to obtain energy for decay (section 2.5.1). Sulphate ( $\text{SO}_4^{2-}$ ) is an alternative electron acceptor and, being a constituent of seawater,  $\text{SO}_4^{2-}$  concentrations in porewater will increase following an inundation event. The microbial community responsible for sulphate reduction changes over a salinity gradient (Laanbroek & Pfennig 1981) and sulphate reduction rates have been found to be higher for the first week after an increase in water level, indicating that sulphate-reducing bacteria can respond rapidly to a change in condition (Lamers et al. 2001). Therefore, if the microbial community respond to an increase in storm surge events, decay of organic matter could accelerate. In addition, sulphate reduction is a more energetically efficient process than methanogenesis, thus carbon mineralization increases (Weston et al. 2011). This process is known to release hydrogen sulphide ( $\text{H}_2\text{S}$ ), an extremely potent greenhouse gas, the emission of which exacerbates global warming.

The direct effects of climate change on decomposition, such as increasing temperature, are likely to be overruled by indirect effects, such as a shift in vegetation community structure (Strakova et al. 2012). Changes in species composition and abundance could be a critical turning point for peatland carbon balance (Malmer et al. 2003) as vegetation types have varying C/N which is one of the controlling factors of decay rate (Hobbie 1996) (section 2.5.1). Generally, relatively wet conditions characteristic of floodplain fens tend to produce more readily decomposable litter (lower C/N) than drier environments (Laiho 2006). Under wetter conditions, a shift to more labile vegetation will increase decomposition rate. Conversely, rapid die off following an inundation event could result in the colonisation of increasingly recalcitrant forms of vegetation and decay rate would be reduced (Henman & Poulter 2008).

## **2.6 Carbon storage in peatlands**

Waterlogged conditions and high productivity make many freshwater wetlands important carbon sinks. Wetland carbon studies focus on quantifying carbon stock (section 2.6.1) and carbon accumulation rate (section 2.6.2) with most research focused on those located in the northern hemisphere (section 2.3) and less on other hydromorphic settings and climates (Bernal & Mitsch 2012). For example, in relation to peatlands, the majority of carbon studies are focused on ombrotrophic or boreal environments which are not susceptible to sea-level rise (Yu 2012; Loisel et al. 2014). Studies associated with carbon storage in wetlands located close to the coast are based predominantly in sediment rich and saline environments such as salt marshes (Chmura et al. 2003; Kirwan & Mudd 2012). Peatland studies of salinity focus on the effect on biodiversity of salinization from drainage for agriculture as opposed to carbon sequestration (Koch & Jurasinski 2015). Despite the known importance of peatlands in the global carbon budget, there are a lack of studies which contribute to our process based understanding of carbon storage in peatlands at risk from saline influence, such as floodplain fens. This has led to an underestimation of their importance at both regional and global scales, and probably also to the extent of their vulnerability to future threats such as climate change.

### **2.6.1 Quantifying carbon stock**

Carbon density is an important variable in assessments of local or regional peat carbon stock and, although there are subtle differences in definitions amongst the literature, carbon density can be defined as carbon content per unit volume (the product of bulk density and carbon content) whereas carbon stock is the amount of carbon contained in peat for a given depth and surface area (Bauer et al. 2006; Bernal & Mitsch 2008). This is a widely researched topic in peatland studies (Armentano & Menges 1986; Gorham 1991; Turunen et al. 2002; Yu 2012), however, few have attempted to quantify carbon stock in floodplain fens (Bernal & Mitsch 2012). *Sphagnum*-dominated peatlands are the most widely studied peatland type (Limpens et al. 2008), and regional and global studies of peatland carbon stocks commonly use estimates for their carbon content and bulk density (e.g., Yu 2012), without regard to how these parameters may differ in other peatland types. This approach may have



resulted in substantial over or underestimation of peat carbon stock. For example, Gorham (1991) estimated carbon stock of northern hemisphere peatlands as 455 Gt C when applying a bulk density of  $0.11 \text{ g cm}^{-3}$  and a carbon content of 51.7%. This estimation is lowered to 436 Gt C when a bulk density of  $0.118 \text{ g cm}^{-3}$  and carbon content 47% is applied in Loisel et al. (2014).

Carbon content has been shown to vary between peat types as a result of botanical composition (Steinmann & Shotyk 1997), for example:  $42.3 \pm 3 \%$  for *Sphagnum*,  $51.4 \pm 3.4\%$  in woody peat and  $53.2 \pm 2.6\%$  in humified peat (Loisel et al. 2014). Bulk density also varies between peat types;  $0.076 \pm 0.038 \text{ g cm}^{-3}$  in *Sphagnum* peat and  $0.192 \pm 0.082$  in humified peat (Loisel et al. 2014). Peat type can be defined by botanical composition in floodplain fens. For example in the UK, an extensive campaign to characterise peat and determine peat depth was carried out in the Broads by Joyce Lambert in the 1950s (Lambert 1951; Jennings & Lambert 1951; Lambert 1960; Buttery & Lambert 1965). Peat stratigraphy reflects the botanical composition of above-ground vegetation at the time of deposition and the stratigraphic maps produced by Joyce Lambert (appendix 4) show a range of peat types including Brushwood, that was generally deposited the earliest, and *Carex* spp. and *P. australis* peat, that usually comprise more recent stratigraphies. There is a need for research to quantify the difference in carbon content and bulk density between peat types in order to determine the importance of the inclusion of peat type in carbon stock estimates.

As described above, botanical composition is important to consider when determining the extent of uncertainty in carbon stock estimates. Frameworks have been designed with the specific intention of identifying different peat types based on botanical composition, for example both the original and modified Troels-Smith methods (Troels-Smith 1955; Kershaw 1997). Although widely applied in peatland research (Glaser 1987; Shennan et al. 2000; Chambers et al. 2010; Garneau et al. 2014), little effort is made to account for difference in peat types in carbon stock estimates with the difficulty in obtaining representative field estimates of bulk density and carbon content the most commonly cited reason (Bauer et al. 2006; Page et al. 2011; Yu 2012; Akumu & McLaughlin 2013).

Hydrological regime also has implications for carbon content and bulk density. For example, regular deposition of sediment at the peat surface during inundation results in a decreasing bulk density with depth (Castañeda-Moya et al. 2010) whereas, peatlands which are not regularly inundated are more likely to have an increasing bulk

density with depth as the weight of the peat profile compresses underlying deposits (Lindsay 2010).

The area and depth of peat used in estimates of carbon stock also gives rise to uncertainty. For example, two studies that quantified UK peatland carbon stock give varying results: 5.2 Gt (Billett et al. 2004) and 1.8 Gt (Joosten 2009). Neither study report carbon content or bulk density, however, the estimate for the former is based on an area of  $0.03 \times 10^6 \text{ km}^2$  and the latter  $0.017 \times 10^6 \text{ km}^2$ . This shows how a difference in area can alter carbon stock estimates made for the same region. Similarly with depth, some carbon stock estimates are based on the top 1 m of peat (Sjörs 1980; Armentano & Menges 1986) or the mean depth of peat for a given region (Turunen et al. 2002) which are both likely to underestimate peat depth and therefore, global carbon stock (Yu 2012). This uncertainty was acknowledged some time ago in the work of Gorham (1991), yet it appears little work has been done to improve this parameter in the estimation of peatland carbon stock, especially in relation to floodplain fens.

### **2.6.2 Quantifying carbon sequestration rate**

Many wetland studies have quantified the rate of carbon accumulation through the determination of accretion rate ( $\text{mm yr}^{-1}$ ) and carbon sequestration rate ( $\text{g C m}^{-2} \text{ yr}^{-1}$ ). It is important to consider accretion rate as the preservation of coastal wetlands is dependent on rate of accretion exceeding sea-level rise (Day et al. 1999). Carbon sequestration gives an indication as to how effective a wetland is at storing carbon.

There are many studies that consider the accretion rate of coastal marsh sediments (Morris et al. 2002; Craft et al. 2009; Mudd et al. 2009; Kirwan & Mudd 2012). Some studies related to peatlands close to the coast focus on peat accretion in freshwater and brackish environments, however, these are based in climates which are not comparable to the UK, such as Florida and North Carolina, USA (Choi & Wang 2004; Henman & Poulter 2008) or indeed mangroves (Chmura et al. 2003; Pendea & Chmura 2012; Chambers et al. 2014). Generally, peat accretion and carbon sequestration studies are limited to boreal and subarctic peatlands with little attention paid to peatlands in other climates (Chimner & Karberg 2008). Furthermore, floodplain fen studies tend to be inland (Bernal & Mitsch 2012) and are not investigating the

effect of sea-level rise. Therefore, there is a distinct gap in the literature regarding carbon sequestration and peat accretion rate in UK floodplain fens.

Due to the depositional nature of wetlands, a commonly used technique to estimate these parameters is radiometric dating using  $^{137}\text{Cs}$  and  $^{210}\text{Pb}$ . Often dates can only be calibrated to between 1963 and 1964 as this corresponds with a peak in  $^{137}\text{Cs}$  from nuclear weapons testing (Appleby 2001; Cundy et al. 2003; Bernal & Mitsch 2012). This approach is associated with a methodological error that results in a range of ages for each depth. Furthermore, both accretion and sequestration rate require an estimate of bulk density and the latter additionally requires the application of an estimate of carbon content. Therefore, uncertainty can arise in the same way outlined in section 2.6.1. Application of age-depth data can also give rise to uncertainty in accretion and carbon sequestration estimates. For example, recent rate of carbon accumulation (RERCA) simply divides the amount of carbon sequestered (or depth of peat accreted) over a given number of years (Bao et al. 2010; Petrokofsky et al. 2012). Although useful in giving an indication, this method assumes a constant rate of peat accumulation and does not consider the effects of compression or peat decomposition. This is therefore likely to give an overestimation (Kirwan et al. 2016).

Alternatives to RERCA have been developed, such as the peat development model (PDM) and other non-linear regression techniques (Turunen et al. 2002), which simulate long-term carbon sequestration and age-depth profiles whilst accounting for production and decomposition (Frolking et al. 2001; Yu et al. 2003; Belyea & Baird 2006). Although accounting for more processes than RERCA, this method is most applicable when modelling long-term rates (i.e. pre-1964) and the RERCA method is widely applied in peatland studies (Ali et al. 2008; Bao et al. 2010; Bernal & Mitsch 2012). Some salt marsh studies consider compression (Day et al. 1999; Mudd et al. 2009) but few peatland studies incorporate this into peat accretion modelling (Le Roux & Marshall 2011).

Carbon sequestration and peat accretion rate can give an indication as to how an increased saline influence might affect carbon storage. For example, increased storm surge events could result in rapid collapse of peat in coastal areas following vegetation die-off and a subsequent shift in species composition (Henman & Poulter 2008). Carbon sequestration and peat accretion could be compromised by increased surface erosion from storm surge events (van Diggelen et al. 2006). However, it is possible that following a storm surge, mineral sedimentation rate could increase

following the deposition of sediment transported by the surge (Day et al. 1999). These processes will have implications for the peat carbon stock, such as an increase in bulk density and a change in species composition will cause a shift in botanical composition of peat.

Overall, many studies have quantified carbon stock in boreal and subarctic peatlands and carbon sequestration and accretion rates have been determined in both peatlands and salt marshes. There are very few studies that have quantified carbon stock, peat accretion or carbon sequestration rate in floodplain fens and it is largely unknown how carbon storage will be affected by sea-level rise and storm surge events. Ecosystem modelling is one approach that allows published data to be combined with conceptual knowledge of a system to investigate carbon storage under varying degrees of saline influence.

### **2.6.3 Understanding carbon dynamics using models**

Peatland carbon dynamics have been widely researched due to their importance in the global carbon cycle (Chmura et al. 2003; Bridgham et al. 2006). As complex systems, peatlands exhibit both self-reinforcing and self-dampening behaviours via a network of ecological feedbacks (Morris et al. 2011). Distinct from forecasting or simulating, ecosystem modelling is a strategic method, allowing for individual processes to be linked in order to test the implications of external (e.g. climate) forces on the system as a whole. Thus, a modelling approach has been frequently used by other authors to understand the consequence of an external forcing on peatland carbon dynamics: some of these models consider peatland-atmosphere carbon exchanges (Frolking et al. 2002; Kettunen 2002; Baird et al. 2009), whereas others are focused on the effect of a change in environmental condition on peatland development (Clymo et al. 1998; Hilbert et al. 2000; Frolking et al. 2001; Morris et al. 2011).

As anthropogenic carbon emissions are likely to continue to increase, the need to understand how peatlands will respond to climate change is essential to ensure that these environments remain as carbon sinks. However, the aforementioned models are almost entirely based on ombrotrophic bogs and are concerned with altered precipitation and temperature (Clymo 1984; Belyea & Baird 2006; Baird et al. 2012;

Morris et al. 2012). A number of modelling studies in wetlands close to the coast have incorporated feedbacks between vegetation, sediment accretion and sea-level rise, but the majority of these are in salt-marshes (Mudd et al. 2009; Kirwan & Mudd 2012). To date, there is no model that specifically assesses the effect of sea-level rise on carbon storage in floodplain fens.

## **2.7 Summary and research questions**

As identified earlier in the literature review, peatlands are important stores of terrestrial carbon but also have the potential to be significant sources of atmospheric carbon. Floodplain fens are unique environments due to their vegetation, hydrology and chemistry. These same factors are key controls on the ability of floodplain fens to sequester carbon. Globally, little work has been done to quantify the carbon stock of floodplain fens with even fewer studies considering the effect of sea-level rise and storm surge events on carbon sequestration, despite the results of climate models projecting an unequivocal increase in sea-level. The Broads account for the majority of lowland fens in the UK and storm surges have been detected in water level readings throughout the area. Therefore, the Broads provide an excellent location to consider research questions outlined in the proceeding section.

An increase in saline influence combined with an increase in the frequency and intensity of storm surge events will result in the delivery of ionic rich water. Whilst an increase in nutrients may initially increase above-ground production, it is expected that the efficiency of vegetation to synthesise PAR will be compromised with increasing saline influence.

This Chapter has shown that there are many studies associated with carbon storage in peatlands and also with the growth and decay of *P. australis*. However, no single study has assessed the implications of sea-level rise on carbon storage in floodplain fens. Therefore, the overall aim of this study is to compare the ability of floodplain fens differing in saline influence to sequester carbon and to determine the main controls on carbon storage in floodplain fens under projected sea-level rise.

A combination of field studies and ecosystem modelling will be applied in order to ascertain the impacts of saline influence on carbon storage in floodplain fens. The following research questions and corresponding hypotheses (H) will be investigated. A rationale and approach for each research question are also listed below.

### 2.7.1 Chapter 3

**Research question 3.1:** What is the main environmental influence on water chemistry variables in both porewater and surface water at six floodplain fens?

H<sub>3.1.1</sub>: Salinity will be a primary environmental influence on water chemistry and the extent of influence will differ between sites

Rationale: Rivers in the Broads are influenced by tides and storm surges (section 2.2.3), which deliver chemical constituents common in seawater ( $\text{Cl}^-$  and  $\text{Na}^+$ ). Nitrate ( $\text{NO}_3^-$ ) and soluble reactive phosphorous (Birkett et al. 2002; CEH 2010) will also be detectable as a result of anthropogenic practices.

Approach: Water samples will be collected from six floodplain fens in June 2013 and the concentrations of anions and cations will be determined. Principal component analysis will be conducted on the raw data to characterise primary environmental influence(s) on water chemistry.

**Research question 3.2:** Are saline pulses following documented storm surge events evident in water level and electrical conductivity time series data at floodplain fen sites?

H<sub>3.2.1</sub>: Sites located on the River Yare will experience pulses in water level and electrical conductivity to a greater extent than other sites.

Rationale: Lowland floodplain fens are under threat from an increase in the frequency and intensity of storm surge events (section 2.2.2) with sites adjacent to rivers connected directly to the sea most vulnerable.

Approach: Environment Agency electrical conductivity and water level data for a network of floodplain fen sites will be checked for peaks in EC and water level for periods corresponding to documented storm surge events (section 2.2.2).

## 2.7.2 Chapter 4

**Research question 4.1:** What factors control above-ground carbon productivity and how do these controls vary among sites located on a gradient of saline influence?

H<sub>4.1.1</sub>: RuE will be influenced by N/C in leaves, water level, nutrient, geological and saline influences.

Rationale: Maintaining high levels of above-ground production is important in ensuring that organic inputs to the peat exceeds decomposition. Radiation use efficiency (RuE) indicates if a plant is stressed due to environmental conditions and factors associated with saline influence (i.e. salinity and water level) may invoke osmotic stress, thereby reducing RuE and the rate of organic input to the peat carbon store.

Approach: Peak above-ground biomass will be harvested over two years and for one of the years, species abundance will be determined. Carbon content will be used to determine above-ground carbon mass (AGCM, g C m<sup>-2</sup>) and PAR will be used to convert AGCM to RuE. Factor scores generated from PCA (Chapter 3) will be used as dependent variables in multiple regression analysis to determine controls on RuE.

**Research question 4.2:** What factors control below-ground carbon production and the quotient of above- to below-ground carbon production (AGCP/BGCP)? How do these controls vary between sites located on a gradient of saline influence?

H<sub>4.2.1</sub>: Nutrient availability will be a primary control on BGCP, with an increase in AGCP/BGCP observed with increasing nutrient availability.

Rationale: Below-ground biomass is the main source of soil organic matter in fens (Sjors 1991). When environmental conditions become stressful, *P. australis* invest increasingly in below-ground material, increasing below-ground production whilst also decreasing AGCP/BGCP.

Approach: In-growth cores (50 cm in depth) will be used to obtain root carbon mass, which is then integrated with depth to obtain a rate of production over 12 months. This will be compared to peak above-ground carbon mass from RQ 4.1.

**Research question 4.3:** What are the controls on the carbon decay rate of *in situ* decomposition of *P. australis* leaves, stems and below-ground material?

H<sub>4.3.1</sub>: Saline influence will be a control on the decay rate of *P. australis* leaves, stems and below-ground material, regardless of litter quality, water level and nutrient availability.

Rationale: Understanding rate of carbon decay is critical in determining the stability of peat carbon stores. Environmental factors such as salinity, nutrient availability and water level determine the activity and the size and composition of the microbial community (Weston et al. 2011). Sea-level rise is likely to alter the environment, and rate of carbon loss could be increased.

Approach: Litterbags will be deployed both *in situ* and collected periodically over a 12-month period. Carbon and nitrogen concentrations will be ascertained. A rate of carbon decay will be determined in addition to C/N.

**Research question 4.4:** Are differences in carbon decay rate due to changes in litter quality and/or microenvironment?

H<sub>4.4.1</sub>: Rate of carbon decay will be affected by both litter quality and microenvironment.

Rationale: Variation in decay rates between study sites are due to differences in both decomposition environment (e.g. moisture, oxygenation, dissolved nutrients) and inherent litter quality (litter biochemistry). Disentangling these elements gives an indication as to whether controlling factors affect decomposition rate through a change in the decomposition environment or by influencing litter biochemistry.

Approach: Litter collected from a relatively 'freshwater site' (Chapter 3) will be transplanted to a more 'saline influenced' site. Mass loss will be compared to litter buried *in situ* at each site. One-way ANOVAs will indicate significant differences between treatments.

**Research question 4.5:** Does carbon accumulation potential vary along the gradient of saline influence?

H<sub>4.5.1</sub>: AG carbon accumulation potential will decrease with increasing saline influence, whilst BG carbon accumulation potential will increase with increasing saline influence.

Rationale: Peat can only continue to accumulate if rate of production exceeds rate of decay. Studying these two processes in isolation is not sufficient in determining if a peatland will continue to accumulate carbon. Carbon accumulation potentials combine



decomposition and production to estimate the mass of peat that would be expected to accumulate if current environmental conditions remain unchanged (Clymo 1984; Thormann et al. 1999).

Approach: Rate of production (RQ 4.1 and RQ 4.2) is divided by rate of decomposition (RQ 4.3) for peat derived from above- and below-ground organic matter. This allows for the determination of differences in potentials for a gradient of floodplain fens sites.

### **2.7.3 Chapter 5**

**Research question 5.1:** Does carbon density and its components (bulk density and total carbon content) vary between different peat types found in three floodplain fen sites?

H<sub>5.1.1</sub>: Carbon density will vary between peat types

Rationale: Peat type is determined largely by botanical composition (Loisel et al. 2014). Environmental conditions, such as nutrient availability and water level, influence the composition of above-ground vegetation. Vegetation that cannot be readily broken down (i.e. contains woody components) is likely to result in peat with a higher carbon density than peat derived from vegetation that is rapidly mineralised.

Approach: Transects published by Lambert (1960) will be used to identify peat types from cores taken to the mineral layer at each of three sites. Samples will be analysed for bulk density and total carbon content to calculate carbon density. Peat types will be likened to a simplified version of the widely used Troels-Smith method to allow the application of carbon density to other floodplain fen sites.

**Research question 5.2:** What is the carbon stock for three sites varying in saline influence in a floodplain fen?

H<sub>5.2.1</sub>: Peat depth and carbon density will be the most important factors for the accurate calculation of peatland carbon stock.

Rationale: Previous studies that have quantified peatland carbon stock (primarily northern hemisphere) generally use a single value for carbon density (Zauft et al.

2010) and an average peat depth. It is likely that carbon density differs substantially between peat types, and peat depth will differ between peatlands. Therefore previous stock estimates may be underestimates, thereby undervaluing the role of peatlands in sequestering anthropogenic emissions (e.g. Yu 2012).

Approach: Carbon density from research question 4.1 will be used to calculate carbon stock based on estimates of depth and surface area for three sites. Peatland area is determined from online mapping software and peat depth is obtained from Lambert's transects.

**Research question 5.3:** What are recent carbon sequestration and peat accretion rates at three floodplain fen sites?

H<sub>5.3.1</sub>: Peat accretion will be similar between sites, whereas carbon sequestration rate will be highest at the site with the highest bulk density and/or carbon content.

Rationale: The maintenance of the peatland carbon store is essential for sequestering atmospheric carbon emissions. Little research has been conducted on carbon sequestration within floodplain fens in the UK. Floodplain fens are vulnerable to sea-level rise and it is possible that an increase in salinity and water level will reduce carbon sequestration rate in these systems.

Approach: A single core to a depth of 1 m will be extracted from three sites. Cores will be sliced into 1 cm increments and age-depth data will be determined from radiometric dating. A subsection of each increment will be sampled for bulk density and carbon content to determine peat accretion (mm yr<sup>-1</sup>) and carbon sequestration rate (g C yr<sup>-1</sup>).

## 2.7.4 Chapter 6

**Rationale:** The preceding Chapters in this thesis have looked at the various processes associated with carbon storage in floodplain fens; Chapter 4 explored the rate of carbon inputs (i.e. production) and rate of carbon outputs (i.e. decomposition), whereas Chapter 5 investigated controls on carbon density and carbon sequestration in floodplain fens. To understand how sea-level rise will affect carbon storage in floodplain fens in the future, it is necessary to understand how these processes interact with one-another, and how these interactions might be affected by an increase in salinity and/ or sea-level rise.

**Approach:** salinity and water level will be systematically varied in an unpublished model by Belyea (2016) that focuses on the link between relative sea-level rise (water level and salinity) and peatland development. The model can be parameterised by a combination of data obtained in the previous Chapters and published data.

The following research questions are answered in Chapter 6:

**Research question 6.1:** How is mineral sedimentation rate affected by a change in suspended sediment concentration and cumulated water depth?

**Research question 6.2:** To what extent is the mass flux of vegetation to peat dependent on belowground allocation, salinity and cumulated water depth?

**Research question 6.3:** How are the relative contributions of the labile and refractory components to organic matter influenced by salinity and water level? How many years does it take for the labile component to approach steady state?

**Research question 6.4:** Are the relative contributions of the mineral and organic components to vertical accretion affected by salinity and cumulated water depth?

**Research question 6.5:** What are the key controlling factors that will determine whether vertical accretion in floodplain fens can keep pace with relative sea-level rise (RSLR)?

## **Chapter 3: Is there an indication of a saline gradient across selected sites in the Broads?**

### **3.1 Introduction**

The overarching aim of this research is to assess the impact of sea-level rise on carbon storage in floodplain fens. This Chapter will establish whether there is evidence for a saline influence across a spatial gradient of sites within the Broads and if evidence of saline pulses during storm surges exists in Environment Agency time series data. Few studies have investigated the effect of a possible increase in saline influence from sea-level rise in floodplain fens, with the majority of studies focusing on salinity in salt-marshes (Bartlett et al. 1987; Craft et al. 2009), tidal freshwater marshes (Weston et al. 2011), estuaries (Chambers et al. 2003) and mangroves (Lara and Cohen, 2006). Exceptions include Giller and Wheeler (1986) who compared cation exchange capacity within peat types.

The study of the effects of environmental perturbations on ecosystems is most appropriate during real-time and direct observation thereby minimising inferences (Bakker et al. 1996). Such studies require commitment on potentially multi-decadal scales and as a result, long-term records are often spatially underrepresented and geographically limited (Fukami & Wardle 2005). These timescales often prove impractical for scientific research and this has led to the adoption of the space-for-time (SFT) substitution technique where spatial and temporal variations are assumed to be equivalent (Pickett 1989). In this well-practiced technique (Whittaker 1970; Cowles 1899; Jenny 1941; Travis & Hester 2005), multiple sites with various environmental conditions are selected as a proxy for ecological shifts which would otherwise be observed from the study of a single site over a longer time period (Fox et al. 2008). However, SFT studies can focus on a coarse scale, neglecting much spatial heterogeneity within sites (Pickett 1989). The gradient approach has been used to study varying degrees of saline influence on a variety of ecosystem functions, but without particular reference to the influence of salinity on carbon storage in floodplain fens. For instance, Quintino et al., (2009) assessed reed leaf decomposition along a salinity gradient in an estuarine environment, Yang et al., (2013) studied the influence of salinity on inundation tolerance of mangrove forests and Bartlett et al., (1987) considered methane emissions along a salt marsh salinity gradient. Chmura et al.,

(2003) explores carbon sequestration in tidal soils of mangroves and salt marshes. Where peatlands have been studied, emphasis remains on ombrotrophic bogs (Wassen et al., 1988). In this project, a gradient of saline influence was established through the application of principal component analysis (PCA) to reduce data dimensionality and thereby characterise saline influence in floodplain fens in the Broads. Other studies using this approach include Bridgham et al. (1991), where PCA was applied to explore differences in soil chemical variables between three sites, Mondal et al. (2010) who identified the influence of seawater intrusion in coastal aquifers and by Yidana et al. (2008) to determine the principal factor controlling variation in hydrogeochemistry across three different locations. Specifically, two main research questions were asked:

**Research question 3.1:** What is the main environmental influence on water chemistry variables in both porewater and surface water at six floodplain fens?

**H<sub>3.1.1</sub>:** Salinity will be a primary environmental influence on water chemistry and the extent of influence will differ between sites located on a gradient of saline influence.

To some degree the rivers in the Broads are influenced by tides and storm surges (section 2.2.3). Therefore, fluvial inputs to floodplain fens from river overtopping will include chemical constituents common in seawater ( $\text{Cl}^-$  and  $\text{Na}^+$ ). There is also likely to be an association between ions indicative of agricultural inputs and point source discharge, such as nitrate ( $\text{NO}_3^-$ ) and soluble reactive phosphorous (SRP) (Birkett 2002, CEH 2010).

**Research question 3.2:** Are saline pulses following documented storm surge events evident in water level and electrical conductivity time series data at floodplain fen sites?

**H<sub>3.2.1</sub>:** Sites located on the River Yare will experience pulses in water level and electrical conductivity to a greater extent than other sites.

The frequency and intensity of storm surges will increase with projected sea-level rise and will pose a threat to lowland floodplain fens (section 2.2.2). Therefore, it is important to ascertain the degree to which water level and/or electrical conductivity have been affected by documented storm surge events in floodplain fens.

## 3.2 Study Sites

### 3.2.1 Study Area

The floodplain fen of the Broads, UK is the largest area of undrained fen in Britain (around 3300 ha) (Giller & Wheeler 1986). A unique feature of this wetland is the expanse of broads (lakes) interconnected by navigable rivers and drainage ditches (known as dykes). As evidenced by extensive stratigraphic analysis, dykes and broads are artificially derived from the extraction of peat for fuel in the twelfth century (Lambert 1960).

The Broads are a mosaic of wetland habitats including open water, floodplain fen, carr woodland and grazing marsh. This combination is able to support unique wildlife attracting highly specialised species such as nationally rare invertebrates, butterflies, flora, and birds. Consequently, the Broads is the largest protected wetland in Britain and is designated a National Park with 55 km<sup>2</sup> protected under Ramsar designations (Joint Nature Conservation Committee 2014), such as Sites of Special Scientific Interest (SSSI), Special Areas of Conservation (SAC) and Special Protected Areas (SPAs) under the European Commission Habitats Directive and Birds Directive (Figure 3.3) (Council Directive 1992; Gilbert et al. 2007).

The Broads are located in a chalk valley overlain by Breydon formation sediment and peat of freshwater or brackish origin. The Breydon formation results from a large sedimentary deposition event during the Flandrian Age consisting of a combination of unconsolidated silt and clay derived from shallow marine environments (Figure 3.1) (British Geological Survey 2014). Boundaries in stratigraphy between clay and peat may be derived from marine transgressions and retreats throughout the post-glacial era (Ellis 1965; Godwin & Tallantire 1951). The peat deposits have a basal age of between 9000 and 9200 <sup>14</sup>C BP (Cooper et al. 2008), around 2000 years after the retreat of the last ice age (Blodau 2002). Following glacial retreat, flooding of the East Anglian plateau was relatively rapid at around 20 mm yr<sup>-1</sup> (Cooper et al. 2008) which would have driven the accumulation of organic deposits. This post-glacial accumulation was restricted to narrow channels which cut through the wider floors of east Norfolk and are now deeply alluviated (Jennings 1955; British Geological Survey 2014). It is thought that the majority of organic matter was accumulated at mean sea-

level, and that the formation of freshwater fen was permitted by a fall in eustatic sea-level over parts of the Bronze and Iron Ages (Godwin 1945; Jennings 1955).

The Broads are highly segregated in terms of land ownership with no clear demarcation between boundaries. Some areas of the National Park remain under private ownership; others have been donated to, leased to or purchased by conservation bodies or non-government organisations (NGOs) such as the RSPB, Natural England and the Norfolk Wildlife Trust. To co-ordinate land management practices, the Broads Authority was established in 1989 to manage the Broads National Park and liaise with private owners over the effective management of their land for conservation and sustainability purposes (Broads Authority 2013).

### **3.2.2 Site Selection**

This study focuses on *P. australis* reed beds to ensure observed variations in water chemistry could not be attributed to species composition. *P. australis* communities are estimated to account for 615 of a total 805 ha of National Vegetation Classification (NVC) communities recognised under the 1994 Habitats Directive in the Broads (Broads Authority 1997). *P. australis* is believed to be one of the most ubiquitous macrophytes across temperate wetlands (Asaeda & Karunaratne 2000) and, in the wider literature, its role in carbon cycling has been studied more extensively than other wetland species (Clevering & Lissner 1999; Brix et al. 2001).

Management practice was a key consideration for site selection, and sites under conservation cutting were chosen. Sites cut for commercial purposes (e.g. for thatch) can be difficult to access due to the high economic value of reed. Additionally, reed is cut every 2-4 years, which would conflict with the timescale required for this project. Conservation cutting, however, tends to be more informal and conducted in response to other factors, such as to encourage nesting birds following a season of absence (Tanneberger et al. 2009). Whilst access can be limited to conservation sites during certain months, the timing of this is not expected to conflict with the fieldwork requirements of this study. The informal nature of conservation management meant that the requirement for an area of reed to remain uncut for three years was possible. As a result, sites under conservation management where *P. australis* was last cut in the summer of 2012 and not before the autumn of 2014 were selected.

For research question 3.2, it was necessary to obtain electrical conductivity and water level time series data for selected sites. Sites identified as dominant in *P. australis* and under conservation management were cross-referenced with sites on an Environment Agency master list that outlined locations where *in situ* data loggers actively monitored electrical conductivity and water level. One of the sites, Sutton, is not actively monitored by the Environment Agency, however, research was conducted at this site from spring 2011 to spring 2014 and existing electrical conductivity and water table data for porewater (<5m adjacent to the ditch) was used (Stanley 2015). An electrical conductivity and water level logger (Solinst) was deployed in the closest dyke in February 2014.

### 3.2.3 Site Description

Following the application of the above criteria, six suitable sites were located within an area of 150 km<sup>2</sup> with a minimum and maximum distance from the North Sea coast of 11 and 21 km respectively (table 3.1). All sites are within the Broads National Park and are designated Ramsar sites. They contain species under the Priority Habitats Index (PHI) and are SSSIs (figure 3.3). Study sites are managed by NGOs with the exception of Wheatfen, which is privately managed by the Ted Ellis Trust. All sites aside from Sutton allow public access, commonly for recreational activities related to wildlife education.

Sites are located on three river catchments of similar geology, specifically, Norwich chalk overlain by the Breydon formation (figure 3.2). Average rainfall in the area is 435 mm yr<sup>-1</sup> (Shand et al. 2007). The source of the River Bure on which Woodbastwick is located, lies to the north east of East Anglia and flows southward to the Yare. Problems of eutrophication in recent years have resulted in the monitoring of invertebrates and a programme of phosphate stripping at a sewage treatment works located on the Bure (CEH 2010).

The River Ant is a tributary to the Bure and How Hill, Sutton and Catfield are located here. Land use tends to be arable with grazing meadows. The quality of the water is considered moderate (Johnes et al., 1996) with some areas susceptible to phosphorus loading as a result of proximity to waste water treatment centres,



however, stripping regimes implemented in recent years have helped to reduce nutrient loading (Surridge 2004).

Wheatfen and Strumpshaw were located directly opposite each other on the River Yare, the southernmost river used in this study. It flows eastwards towards the sea and is joined by the River Waveney further downstream. The catchment is more influenced by underlying chalk deposits than the Bure or Ant and has very different hydrochemistry due primarily to land-use. For example, the Yare is perhaps one of the most urban of the rivers studied and agriculture involves intensive cropping and pesticide application. Although now controlled, historic point source discharge from Whitlingham Sewage Treatment Works has resulted in Hg, Cd and Cu contamination in the Yare (Birkett et al. 2002). The Yare is subject to relatively strong tidal flows with tidal currents detectable through to Norwich. Since approximately 1900, the floodplain around Strumpshaw has been embanked and secondary channels connected to the River Yare were blocked to allow the area to drain for low intensity grazing (Ellis 1965). Management of Strumpshaw was transferred to the RSPB in 1978 who, following improvement of water quality within the Yare, have attempted to restore the pre-disturbance hydrological regime (Surridge et al. 2012). Water table position is now managed through a ditch and sluice network (Self 2005) with managed draw down occurring in response to tidal surges. Raised banks on the Yare are continuously managed by the Environment Agency as a means of flood defence (Environment Agency 2009). Banks are not raised at Wheatfen and tidal currents frequently inundate the site. Open dykes conduct river water into and beneath the peats within the site. During the summer, areas not subject to lateral flooding from dykes can become dry, however, generally Wheatfen has become increasingly wet due to higher tides in the Yare (Wheeler & Shaw 2000).

Table 3.1: Site locations (based on British National Grid reference) and site elevation (metres above Ordnance datum, mAOD) is presented as mean  $\pm$  1 SE where  $n = 50$ . Surface elevation was obtained from geospatial techniques (section 3.2.1). Distance to coast measured using Digimap® software (available at <http://digimap.edina.ac.uk>).

Site	Easting	Northing	mAOD	Distance to coast (km)	River	Management
Catfield Fen	637170	321079	0.41 $\pm$ 0.006	12	Ant	Butterfly Conservation
How Hill	636725	319483	0.37 $\pm$ 0.004	13	Ant	Broads Authority
Strumpshaw Fen	633665	306916	0.40 $\pm$ 0.006	20	Yare	RSPB
Sutton Fen	636687	323079	0.40 $\pm$ 0.005	11	Ant	RSPB
Wheatfen	632563	306417	0.59 $\pm$ 0.004	21	Yare	Ted Ellis Trust
Woodbastwick Fen	633707	316598	0.79 $\pm$ 0.006	17	Bure	Natural England

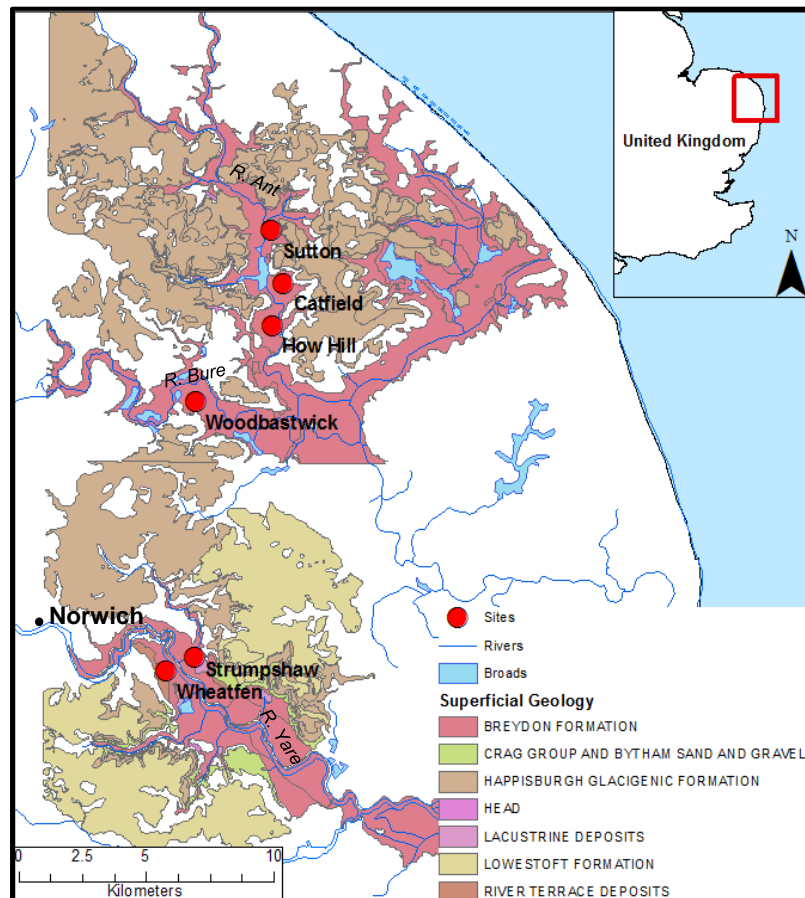


Figure 3.1: Map showing the location of research sites and superficial geological deposits (British Geological Survey 2014).

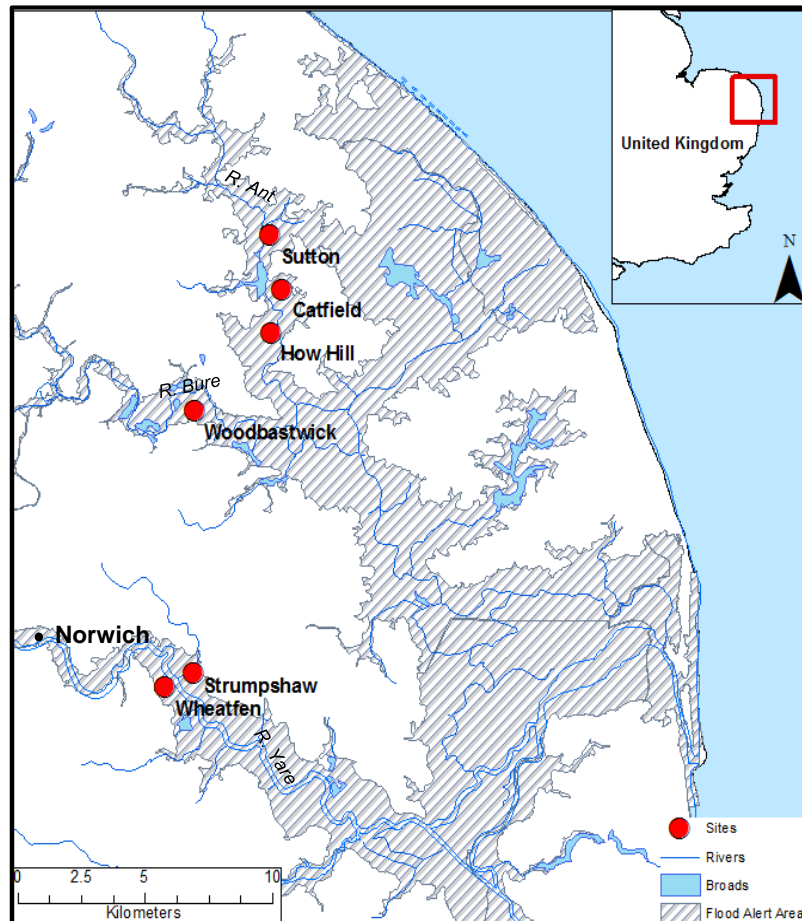


Figure 3.2: Areas at risk of flooding from main rivers and the sea obtained from the Environment Agency Geostore, 2015.

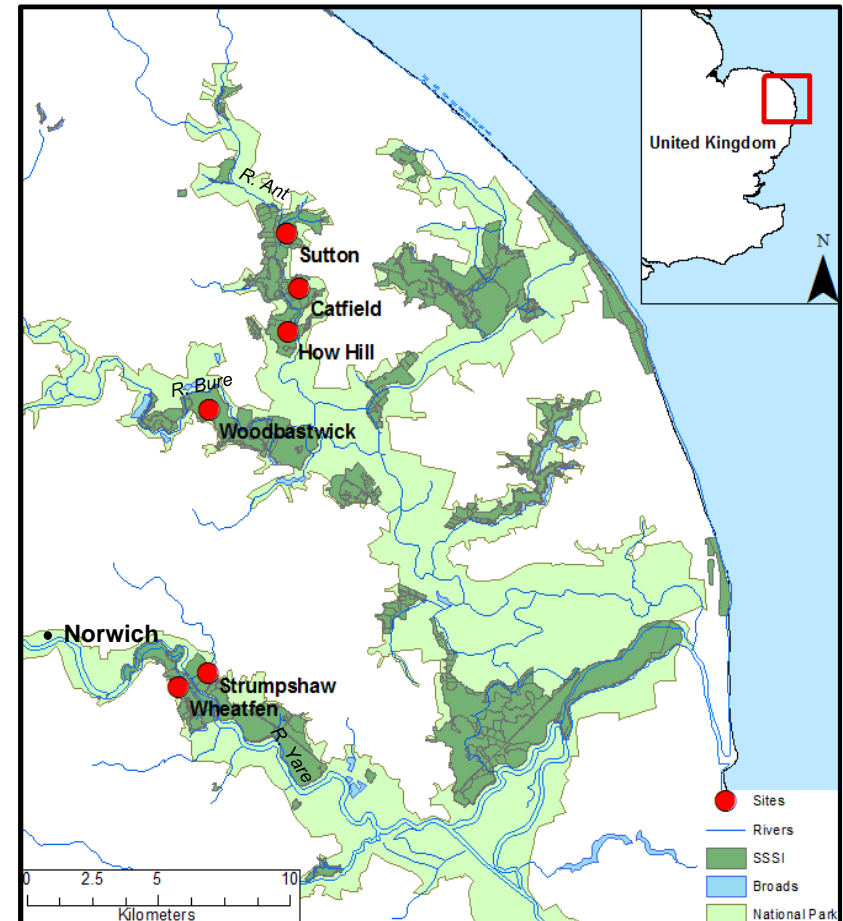


Figure 3.3: The Broads National Park and designated SSSI obtained from the Environment Agency Geostore, 2015.

### 3.3 Methodology

#### 3.3.1 Field Methods

For porewater extraction, steel porewater probes were inserted 30 cm below the surface at five randomly selected locations within a 20 x 20 m area adjacent to an *in situ* Environment Agency logger. A 60 ml luer-slip syringe was attached to the top of the probe with a spacer to allow the syringe to fill with water. Occasionally dry conditions meant that a sample could not be obtained; these occurrences are marked as 'no sample' in the water chemistry data table included in the appendices. For surface water, samples were collected with a bailer from five randomly selected locations in the ditch 25 m either side of the logger. A 60 ml luer-slip syringe was filled from the bailer and the water samples were then processed as below for both porewater and surface water:

1.  $\text{Fe}^{2+}$  analysis:

For porewater only, the filter attached to the luer-slip syringe was flushed with sample before 3 ml was inserted into a polypropylene vial containing 3 ml of pre-prepared buffered phenanthroline solution. Samples were placed in a rack and stored in a cool box before being returned to the laboratory.

2. pH:

The filter was removed from the end of the syringe and replaced with a three-way valve. A 10 ml container was half filled with sample and the probe inserted. pH was recorded when the probe had stabilized and the pH meter was calibrated every five samples.

3. Anion and cation analysis:

A new 0.45  $\mu\text{m}$  filter was attached and flushed with sample before a 10 ml screw-top polypropylene vial was filled with porewater or surface water. Samples were stored in a rack within a cool box containing ice packs until return to the laboratory where they were frozen prior to analysis.

Water level in metres above ordnance datum (mAOD) and electrical conductivity data ( $\mu\text{S cm}^{-1}$ ) were obtained from the Environment Agency periodically over the duration of the project. A quality flag that indicated whether each data point was unchecked, suspect or good accompanied all data where, if data was unchecked or suspect, missing values would be removed. Data was also inspected visually to observe any offsetting or flat lining which was taken as an indication of change of logger setting, such as the switch from  $\mu\text{S}$  to S for EC, with data corrected accordingly (Environment Agency 2003). Time series for EC and water level data were plotted to highlight gaps in data that usually arose from an expired battery or faulty equipment and were subsequently removed (personal communication, Liz Klotz of the Environment Agency, January 2015).

To calculate water level compared to peat surface, it was necessary to correct Environment Agency water level data given in mAOD to metres above peat surface (mAPS). A Global Navigation Satellite System (GNSS) was used with the base station (Leica Viva GS10) erected in an uncovered area within 100 m from the site. Fifty points were recorded within 20 x 20 m of the Environment Agency logger to map the surface elevation of the peat using a rover (Leica Viva GS14). Data was post-processed in Leica Geo Office using Ordnance Survey RINEX data from three stations located within a 40 km radius of the central point of the experimental area.

Tide gauge data from the Lowestoft recording station ( $52^{\circ} 28' 23.2''$  N,  $01^{\circ} 45' 00.4''$  E) for the period 2006 to 2014 was obtained from the British Oceanographic Data Centre as part of the UK Coastal Monitoring and Forecasting programme. Data derived from a full-tide and mid-tide bubbler gauge are to Admiralty Chart Datum (ACD). The conversion of ACD to OCN for the Lowestoft station is given as (McGarrigle et al. 2014):

$$\text{ODN} = \text{ACD} + 1.5 \text{ meters} \quad \text{Equation 3.1}$$

### 3.3.2 Laboratory Methods

Cations ( $\text{Ca}^{2+}$ ,  $\text{Mg}^{2+}$ , Fe and  $\text{K}^{+}$ ) were analysed using inductively coupled plasma/optical emission spectrometry (ICP-OES). All glassware was acid washed in 10% HCl and rinsed in deionised water prior to use. Standards and samples were acidified to 2 % with  $\text{HNO}_3$  to stabilize elements prior to analysis. An eight-point

calibration was created using individual 1000 ppm calibration solutions (Fisher Scientific) of Ca, Mg, Fe and K diluted with UHQ (filtered to 18 MΩ cm<sup>-1</sup> at 25 °C). The 10 ppm standard was used as the drift control. All samples and standards were spiked with 100 000 mg l<sup>-1</sup> Cs to suppress easily ionisable elements (Todolí et al. 2002).

A linear regression was used to calculate a calibration curve. Table 3.2 outlines the wavelengths selected to optimize analysis and samples flagged as <LOD (limit of detection) by the instrument were rejected. Analysis showed that the vast majority of results for Fe were <LOD and therefore this element was removed from the dataset. A drift control was analyzed every 10 samples and a correction factor was applied if drift occurred. As a measure of relative precision of the instrument, relative standard deviation (%RSD) was calculated and samples were re-run if RSD > 10% (Taverniers et al. 2004).

Table 3.2: Wavelengths selected for cation analysis on the ICP-OES.

Ion	Wavelength (nm)
Ca <sup>2+</sup>	315.88
Fe (withdrawn)	261.187
K <sup>+</sup>	766.491
Mg <sup>2+</sup>	285.213

A spectrophotometer was used to measure Fe<sup>2+</sup>. To make the stock solution, hydroxyl ammonium chloride was added to a 50 ppm Fe standard and eventually mixed with a phenanthroline buffer acidified to pH 4 with analytical glacial acetic acid (Fisher Scientific). The phenanthroline buffer was made by combining a phenanthroline solution (0.1 g 1-10 o-phenanthroline monohydrate powder in 100 ml of UHQ, Fisher Scientific) with an acetate buffer. The acetate buffer comprised of 16.59 g of anhydrous sodium acetate powder and 350 ml of UHQ. A linear regression was used to calculate a calibration curve and drift checks undertaken intermittently using a combination of standards to calculate %RSD (table 3.3). The %RSD for the drift checks at 0.05 and 0.1 ppm were > 10% and therefore the LOD was defined as < 0.1 ppm. As for Fe, the majority of results fell <LOD and Fe<sup>2+</sup> was withdrawn from further analysis.

An automated colorimetric continuous flow analyser (Skalar San++ continuous flow analyser) was used to analyse soluble reactive phosphorus (SRP). Stock solution for SRP was made up of potassium dihydrogen phosphate (Fisher Scientific) and a seven-point calibration was made from the stock solution diluted with UHQ. Samples were diluted by a factor of 0.5 and results were corrected accordingly post analysis. Drift checks were analyzed throughout the run and were rejected if > 10% (table 2.rsd).

Finally, anions ( $\text{Cl}^-$ ,  $\text{SO}_4^{2-}$  and  $\text{NO}_3^-$ ) and  $\text{Na}^+$  were analysed using ion chromatography (Dionex ICS-2500 chromatographic system).  $\text{Na}^+$  was analysed at the University of Essex and % RSD was found to be > 10%. Sensitivity analysis was conducted on this data where principal components analysis (section 3.3.3) run with  $\text{Na}^+$  samples adjusted for % RSD (+/- 26.33%, table 3.3). No difference in the statistical output was observed and the results for  $\text{Na}^+$  from the Dionex were retained. A five point calibration was made up independently for both anion and cation analysis using the corresponding stock solutions diluted with UHQ. In both cases drift checks were made up of the 5 ppm standard.

Table 3.3: Summary of the residual standard deviation (%) of drift checks and  $R^2$  value for calibration curves from the instrumental analysis of water chemistry data. Sutton\* refers to data obtained from another project (Stanley 2015) where samples were extracted from Sutton at the same time as other sample sites for this project (June 2013).

Ion	%RSD
$\text{Na}^+$	26.33
$\text{Ca}^{2+}$	3.18
$\text{K}^+$	2.12
$\text{Mg}^{2+}$	1.36
Fe	2.22
$\text{Fe}^{2+}$ (0.25 ppm)	8.68
$\text{Fe}^{2+}$ (0.5 ppm)	3.47
$\text{Fe}^{2+}$ (1 ppm)	2.60
$\text{Cl}^-$	3.77
$\text{SO}_4^{2-}$	6.45
$\text{NO}_3^-$	3.88
SRP	7.34
$\text{Fe}^{2+}$ Sutton*	1.91
SRP Sutton*	8.03

### 3.3.3 Data Analysis

Porewater and surface water datasets were treated separately. Each dataset was interrogated to discern the form of the frequency distribution in order to choose appropriate statistical tests (Dytham 2011). Normality was tested; numerically through the observation of skewness and kurtosis, visually through the inspection of histograms and statistically through the application of the Shapiro-Wilk (S-W) test. Where data was not normally distributed, Box-Cox transformations were applied until lambda ( $\lambda$ ) was as close as possible to 1 (Nakagawa & Cuthill 2007). Porewater and surface water datasets were not normally distributed and were transformed successfully with the exception of SRP in the surface water dataset. Despite this, the majority of data could be transformed and parametric tests were conducted. Descriptive statistics were carried out on untransformed data. Transformed data was used for Pearson's  $r$  and ANOVA. For correlation analysis, coefficients  $< 0.5$  were considered as a weak relationship and removed from analysis (Taylor 1990). Following ANOVA, Tukey HSD *post hoc* analysis was applied to identify the groups statistically different from one another.

Correlation analysis indicated an intercorrelation between variables with the exception of  $\text{Ca}^{2+}$  in surface water, however,  $\text{Ca}^{2+}$  was retained given its conceptual importance within floodplain fen systems, specifically the Broads (Giller and Wheeler, 1986). Principal components analysis (PCA) was used to ascertain related chemical variables (Dytham 2011; Reid & Spencer 2009). PCA was conducted on transformed and standardised data. Criteria for analysis were based on the Kaiser principle where components with eigenvalues  $> 1$  and contributing  $> 10\%$  to the total variance of each dataset were retained (Arambarri et al. 2003). Within each component, factor loadings  $> 0.4$  or  $< -0.4$  were considered significant (Field, 2013). Factor scores for each component were normally distributed and therefore treated parametrically.

To compare saline influence with studies from the wider literature, salinity (ppt) was calculated as in Shi and Yu (2014) (equation 3.2) using raw  $\text{Cl}^-$  ( $\text{mg l}^{-1}$ ). Salinity was not normally distributed and a Box-Cox transformation was applied.

$$\text{Salinity (ppt)} = \text{Cl}^- \left( \text{mg l}^{-1} \right) \times 0.0018066 \quad \text{Equation 3.2}$$

Missing values arose from an inability to extract the full spectrum of replicates in the field (as outlined in section 3.2.1) and from results lying outside the bounds of instrumental limit of detection (LOD). A total of 270 samples were analysed for each of



the porewater and surface water datasets (five replicates for nine variables within each of the six sites), with 39 and 7 samples missing respectively. To minimise the information lost through the removal of a sample, pairwise deletion (Marsh 1998) was applied in the calculation of descriptive statistics, correlation analysis and testing for differences. PCA was conducted in R studio (version 3.1.3) where the NIPALS algorithm (Grung & Manne 1998) was applied within the ade4 package (Dray & Dufour 2007).

Environment Agency electrical conductivity and water level data were corrected for instrumentation errors and water level was adjusted to account for peat surface elevation (section 3.2.1.2). Sites were monitored periodically between 2006 and 2014 where 2012 had the most complete record (table 3.4). To assess flooding duration at each site, stage-duration graphs were constructed to summarise water level for 2012 only (USEPA 2008). Sites were ranked according to duration of flooding throughout 2012.

Table 3.4: Summary of water level (WL) and electrical conductivity (EC) data obtained from the Environment Agency (EA). Data for Sutton (\*) was not available from the EA and was obtained from a logger deployed as part of this research.

Site	Logger ID	Record Period (WL)	Record Period (EC)
Catfield	TG32711	2006 - 2013	2006 - 2014
How Hill	TG31697C	2008 - 2012	2007 - 2014
Wheatfen	TG30265	2006 - 2014	2006 - 2014
Sutton*	Own logger	2012 - 2015	2014 - 2015
Strumpshaw	TG30366e	2006 - 2014	2006 - 2014
Woodbastwick	TG31367d	2007 - 2012	2007 - 2014

Long-term trends and seasonality in water level and electrical conductivity (EC) time series data were modelled using STL (Seasonal and Trend Decomposition using loess) (Cleveland et al. 1990). This procedure uses nonparametric smoothing to decompose a time series into seasonal (systematic, calendar related movements), trend (long term direction) and irregular components (unsystematic, short term fluctuations). Visual inspection of the data indicated that the magnitude of seasonal fluctuations did not vary with the overall trend of the data for both EC and water level across all sites. Accordingly, an additive procedure was used as described by equation 3.3:

$$Y_t = T_t + S_t + I_t$$

Equation 3.3

where  $Y_t$  is the water level at time  $t$ ,  $T_t$  is the trend component,  $S_t$  is the seasonal component and  $I_t$  is the irregular component (Cleveland et al. 1990). Seasonal effects were assumed to be the same for each year apart from random differences, which are reflected in the irregular component. STL supports robust estimation of seasonal and trend components to limit the effect of outliers (Chaloupka 2001) and has been used in ecological (Marcovaldi & Chaloupka 2007; Chaloupka 2001) and hydrological (Shamsudduha et al. 2009) contexts. The STL procedure requires time series data without gaps for a minimum of two seasonal cycles. Accordingly, the precise period analysed varies for each site. The longest consistent record at Sutton was 12 months; therefore STL could not be applied at this site. Time series data was recorded in 15-minute intervals and was averaged for each 24-hour period to give daily time series data. Trend and seasonality of tide-gauge data obtained from the Lowestoft recording station for the period 2006 to 2014 was also modelled using STL. Grey bars to the right of STL plots indicate the relative scale of the component. Thus, the longer the bar the smaller the contribution (Hyndman & Athanasopoulos 2014).

The STL procedure was applied to water level, EC and tide gauge time series data for two documented storm surge events (9<sup>th</sup> November and 5<sup>th</sup> December). Cross correlation was used to measure the similarity between tide gauge data in the present (lag 0) with water level or EC at various lags (Heyman et al. 2000). In this research, the time period represented by each lag is one day, where a negative lag indicates that the leading variable (tide) significantly effects water level and/ or EC at each site after  $n$  days (lags). The significance of correlation coefficients are reported as 95% confidence intervals (Kettunen et al. 1996). The aim of this procedure is to test for a significant correlation between surge peaks in tide gauge and corresponding site water level and/ or EC. Accordingly, each time series must be 'prewhitened' prior to cross correlation (Chaloupka 2001; Kettunen et al. 1996) to avoid misleading results from autocorrelations arising from seasonal and trend components, thus, the irregular components from the STL procedure was used (Paradis et al. 1999; Bjørnstad et al. 1999). The irregular components for each time series were log transformed to meet the assumption of normality for confidence intervals. Trend analysis and cross correlation were conducted in R studio (version 3.1.2) using the STL and CCF functions respectively (R Core Development Team 2014).

### 3.4 Results

#### 3.4.1 Anion and Cation analysis

As shown in table 3.5,  $\text{Cl}^-$  was found in the highest concentrations in porewater, however,  $\text{Ca}^{2+}$  was particularly high at Sutton, Woodbastwick and Wheatfen (table 3.5), whereas How Hill and Strumpshaw had elevated concentrations of  $\text{Mg}^{2+}$ . Interestingly,  $\text{SO}_4^{2-}$  concentration at Wheatfen was found to be at least ten times higher than other sites, whereas Soluble Reactive Phosphorus (SRP) and  $\text{NO}_3^-$  tended to be found in the lowest concentrations.

Generally,  $\text{Ca}^{2+}$  was found in the highest concentration in surface water. Notably,  $\text{Cl}^-$  and  $\text{Na}^{2+}$  in surface water at Strumpshaw was three times that of other sites. Generally,  $\text{NO}_3^-$  and SRP were found in the lowest concentrations and pH was higher than in porewater (table 3.5).

.

Table 3.5: Summary statistics for analysed water chemistry variables (mg l<sup>-1</sup>) presented as count (n), mean ( $\mu$ )  $\pm$  1 SE. Site abbreviations: Ca = Catfield, HH = How Hill, St = Strumpshaw, Su = Sutton, Wh = Wheatfen, Wo = Woodbastwick. Dash (-) is where no sample was collected. All data is in mg l<sup>-1</sup> with the exception of pH and salinity, where the latter is in ppt and calculated as a proportion of Cl<sup>-</sup> as in equation 3.1 (Shi & Yu 2014).

Site		Na <sup>+</sup>		Ca <sup>2+</sup>		K <sup>+</sup>		Mg <sup>2+</sup>		Cl <sup>-</sup>		SO <sub>4</sub> <sup>2-</sup>		NO <sub>3</sub> <sup>-</sup>		SRP		pH		Salinity*		Mg <sup>2+</sup> : Ca <sup>2+</sup>		Na+:Cl <sup>-</sup>	
		pw	sw	pw	sw	pw	sw	pw	sw	pw	sw	pw	sw	pw	sw	pw	sw	pw	sw	pw	sw	pw	sw	pw	sw
Ca	n	5	5	4	5	3	5	4	5	5	5	5	5	5	5	5	5	3	5	5	5	4	5	5	5
	$\mu$	18	11	32	44	0.31	3.6	12	12	38	27	1.3	13	0.07	0.54	0.02	0.06	6.1	8.1	0.07	0.05	0.39	0.27	0.51	0.45
	SE	2.8	1.00	2.2	3.01	0.15	0.60	0.68	1.6	8.3	4.9	0.46	1.9	0.01	0.45	0.00	0.04	0.06	0.09	0.01	0.01	0.02	0.03	0.06	0.07
HH	n	3	5	5	5	5	5	5	5	5	5	5	5	5	5	5	5	5	5	5	5	5	5	5	5
	$\mu$	21	4.5	64	51	3.4	7.3	28	12	97	43	3.8	20	0.12	0.21	0.04	0.02	6.70	7.9	0.18	0.08	0.42	0.23	0.24	0.11
	SE	9.09	0.48	3.09	4.6	1.12	0.73	2.9	0.91	9.4	6.07	0.55	2.9	0.02	0.04	0.01	0.00	0.14	0.22	0.02	0.01	0.03	0.02	0.12	0.01
St	n	4	4	5	5	5	5	5	5	3	4	4	5	1	5	4	5	5	5	3	4	5	5	3	4
	$\mu$	66	32	63	45	13	19	34	31	133	121	1.00	11	0.08	0.19	0.56	0.13	7.10	7.58	0.24	0.18	0.55	0.68	0.36	0.28
	SE	19	7.5	6.7	3.3	1.5	2.3	2.4	4.05	23	34	0.28	3.3	-	0.10	0.47	0.01	0.24	0.05	0.04	0.06	0.05	0.05	0.03	0.03
Su	n	5	5	5	5	5	5	5	5	5	5	5	5	4	0	5	5	5	5	5	5	5	5	5	5
	$\mu$	4.9	2.2	119	64	5.03	4.2	9.3	8.5	9.02	5.2	0.24	0.69	0.07	-	0.05	0.01	6.41	8.09	0.02	0.01	0.08	0.13	0.66	0.48
	SE	0.95	0.06	21	7.27	1.17	0.45	1.49	0.96	2.51	0.77	0.05	0.11	0.06	-	0.00	0.00	0.00	0.08	0.00	0.00	0.01	0.01	0.15	0.09
Wh	n	5	5	4	5	4	5	4	5	5	5	5	5	5	5	5	5	5	5	5	5	4	5	5	5
	$\mu$	14	9.4	90	89	2.5	6.7	9.2	9.70	49	40	23	26	0.35	0.41	0.13	0.18	6.8	7.6	0.09	0.07	0.10	0.11	0.30	0.25
	SE	1.6	1.9	17	8.2	1.3	0.54	2.40	0.51	10	10	1.8	6.2	0.08	0.12	0.04	0.02	0.22	0.06	0.02	0.02	0.01	0.01	0.03	0.02
Wo	n	3	5	3	5	3	5	3	5	3	5	3	5	3	5	3	5	3	5	3	5	3	5	3	5
	$\mu$	3.4	2.7	48	43	1.7	2.6	7.6	8.8	15	10	2.09	2.6	0.40	0.06	0.14	0.09	6.66	7.22	0.03	0.02	0.16	0.20	0.22	0.41
	SE	1.09	0.37	4.02	4.4	0.64	0.60	1.05	1.6	4.3	3.06	0.76	0.78	0.20	0.03	0.08	0.02	0.16	0.10	0.01	0.01	0.01	0.02	0.04	0.16

Pearson's r correlation analysis (table 3.6) indicated that the strongest correlation was between Na<sup>+</sup> and Cl<sup>-</sup> in both porewater and surface water. pH and SRP in surface water was the only observed negative correlation. EC was found to correlate with Mg<sup>2+</sup> and K<sup>+</sup> in surface water and only K<sup>+</sup> in porewater.

Table 3.6: Correlations between water chemistry variables for porewater (below diagonal line) and surface water (above diagonal line). Only significant coefficients ( $p < 0.05$ ) are shown. Coefficients significant to  $p < 0.0001$  are in italic. Coefficients  $> 0.5$  are highlighted in bold. Electrical conductivity (EC) is obtained from the Environment Agency (section 3.2.3.2)

Variables	Na <sup>+</sup>	Ca <sup>2+</sup>	K <sup>+</sup>	Mg <sup>2+</sup>	Cl <sup>-</sup>	SO <sub>4</sub> <sup>2-</sup>	NO <sub>3</sub> <sup>-</sup>	SRP	pH	EC
Na <sup>+</sup>			0.499	<b>0.520</b>	<b>0.865</b>	<b>0.621</b>				0.448
Ca <sup>2+</sup>										
K <sup>+</sup>		0.452		<b>0.841</b>	<b>0.563</b>					<b>0.728</b>
Mg <sup>2+</sup>	<b>0.669</b>		<b>0.545</b>		0.439					<b>0.625</b>
Cl <sup>-</sup>	<b>0.747</b>			<b>0.642</b>		<b>0.737</b>				
SO <sub>4</sub> <sup>2-</sup>							<b>0.566</b>			
NO <sub>3</sub> <sup>-</sup>						<b>0.539</b>				
SRP		0.437	0.460						<b>-0.617</b>	
pH			0.403		0.457			0.439		
EC	0.466		<b>0.715</b>	0.455				0.497	0.447	

Na:Cl is higher in porewater than surface water (figure 3.4). Generally, Na:Cl decreased with increasing distance from the coast, although Wheatfen and Strumpshaw had slightly higher ratios than sites located closer to the coast.

There are two clear groups of sites with a similar Mg:Ca for both porewater and surface (figure 3.5). Catfield and How Hill are the two sites where Mg:Ca in porewater exceeds that of surface water.

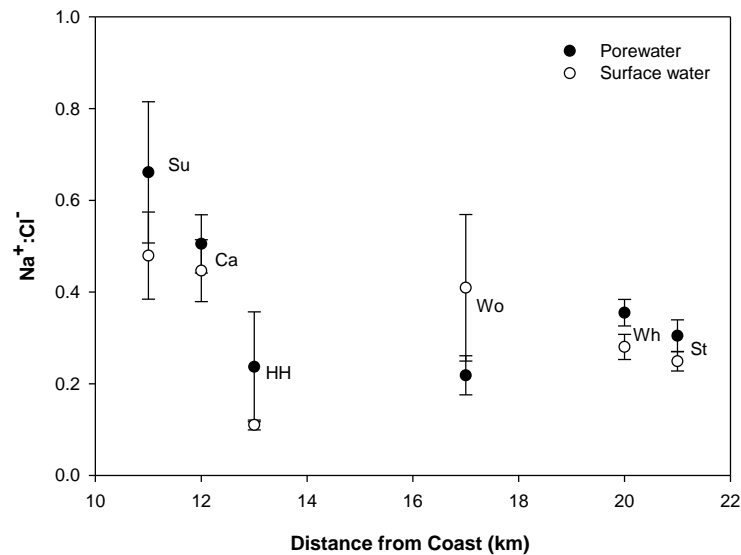


Figure 3.4: Na:Cl compared to distance of site from the coast. Ratios are Na/ Cl. Points are means and error bars are  $\pm 1$  SE. Site abbreviations: Ca = Catfield, HH = How Hill, St = Strumpshaw, Su = Sutton, Wh = Wheatfen, Wo = Woodbastwick.

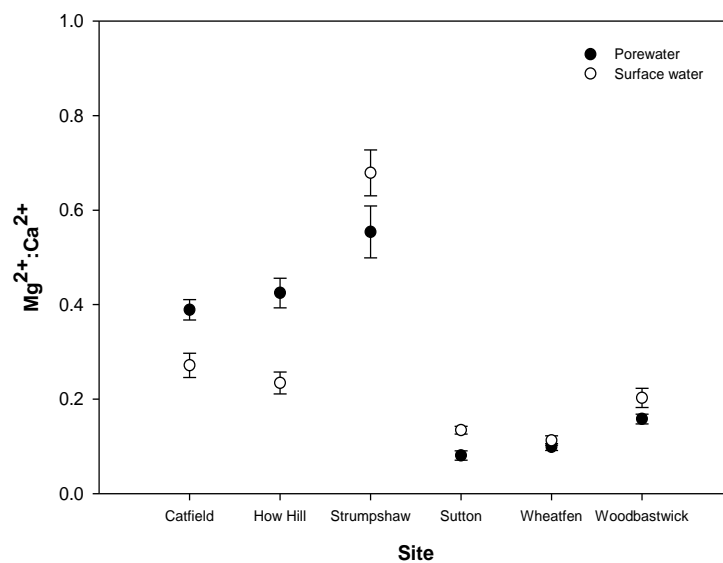


Figure 3.5: Mg:Ca for each site using porewater and surface water data. Ratios are Mg/ Ca. Points are means and error bars are  $\pm 1$  SE.

### 3.4.2 Relationships between water chemistry variables

Three principal components (PCs) were retained for porewater and four for surface water (table 3.7).  $\text{Na}^+$  and  $\text{Cl}^-$  were the only variables to significantly load onto the first principal component (PC) for both porewater and surface water. Figure 3.6 indicates that factor scores were significantly different between sites and Tukey HSD *post hoc* indicated that Strumpshaw had the significantly highest score for PC1 ( $p < 0.05$ ). For porewater, figure 3.7 shows a separation of sites along PC1, with factor scores from Sutton at Woodbastwick at the negative end and Strumpshaw at the positive end.

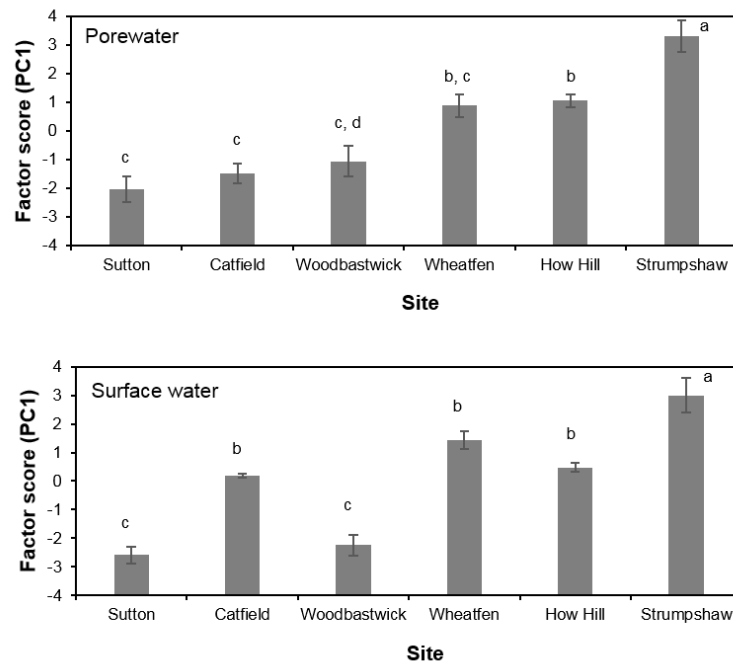


Figure 3.6: Comparison of factor scores for PC1 for porewater and surface water. Bars represent means and error bars are  $\pm 1$  SE. Sites are ordered according to increasing mean factor score for porewater. One-way ANOVA indicated significant differences were found between sites for both porewater ( $F_{5,22} = 24$ ,  $p < 0.001$ ) and surface water ( $F_{5,24} = 49$ ,  $p < 0.001$ ). Letters represent grouping of Tukey HSD *post hoc* analysis following ANOVA.

Table 3.7: Eigenvalue, variable loadings and percentage explained for porewater (left) and surface water (right). Only components contributing >10 % to the total variance were retained and loadings > 0.4 or < -0.4 are presented.

<b>Porewater</b>				<b>Surface water</b>			
Principal Component Loadings	1	2	3	1	2	3	4
Eigenvalue	4.352	2.278	1.846	4.348	1.765	1.615	1.23
Variance Explained	43	23	18	46	18	17	13
<b>Principal Component Loadings</b>				<b>Principal Component Loadings</b>			
Na <sup>+</sup>	0.409			0.479			
Ca <sup>2+</sup>		-0.582					-0.869
K <sup>+</sup>						-0.406	
Mg <sup>2+</sup>			0.406			-0.479	
Cl <sup>-</sup>	0.508			0.492			
SO <sub>4</sub> <sup>2-</sup>			-0.558				
NO <sub>3</sub> <sup>-</sup>			-0.542		0.417	0.436	
SRP		-0.467			-0.538		
pH					0.617	-0.409	



$\text{Ca}^{2+}$  and SRP were the only two variables loading onto PC2 for porewater (table 3.7). A clear separation of sites was apparent (figure 3.7), and factor scores were significantly different between sites according to a one-way ANOVA ( $F_{5, 22} = 42$ ,  $p < 0.001$ ). Tukey HSD *post hoc* analysis indicated that Catfield had the highest score and Sutton had the lowest.

Nitrate and pH loaded positively onto PC2 for surface water (table 3.7), whereas SRP loaded negatively. Factor scores were not so clearly separated as for porewater (figure 3.7), but were significantly different between sites ( $F_{5, 24} = 7.6$ ,  $p < 0.001$ ). *Post hoc* analysis showed Catfield to be the highest and Woodbastwick to be the lowest.

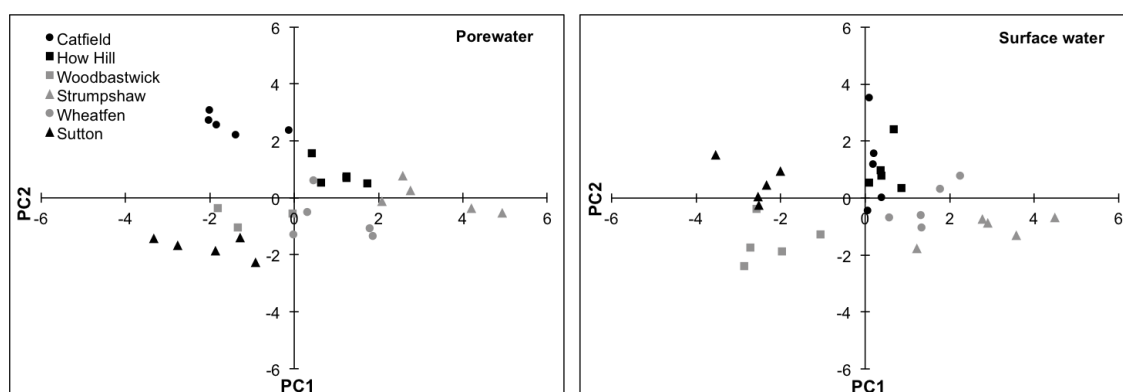


Figure 3.7: Scatter plot to show distribution of factor scores associated with PC1 (x-axis) and PC2 (y-axis) for porewater and surface water.

$\text{Mg}^{2+}$  loaded positively onto PC3 for porewater, whereas  $\text{SO}_4^{2-}$  and  $\text{NO}_3^-$  loaded negatively (table 3.7) – and most sites had negative scores (figure 3.8). Factor scores are significantly different between sites ( $F_{5, 22} = 14$ ,  $p < 0.001$ ) and *post hoc* analysis identified Woodbastwick and Wheatfen to be significantly lower than the other sites.

For surface water,  $\text{NO}_3^-$  loaded positively and pH,  $\text{K}^+$  and  $\text{Mg}^{2+}$  loaded negatively (table 3.7). Sites appear to overlap more along PC3 in comparison to other principal components (figure 3.8).

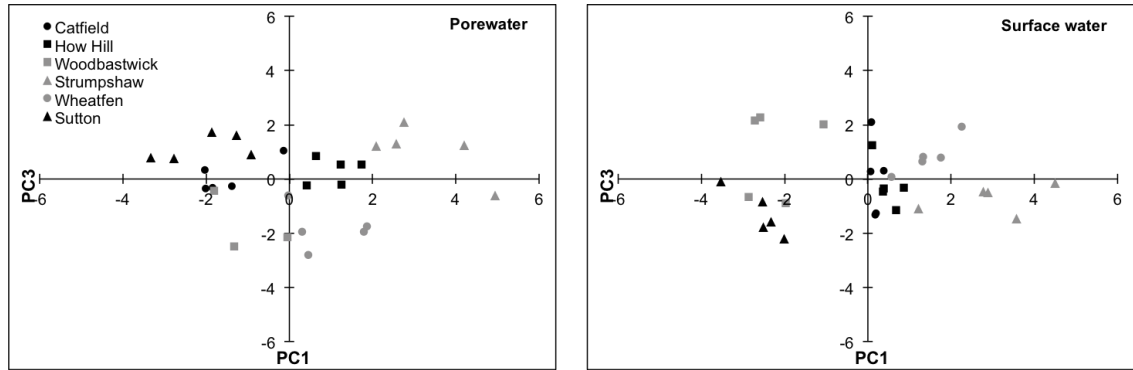


Figure 3.8: Scatter plot to show distribution of factor scores associated with PC1 and PC3 for porewater and surface water.

A fourth PC was extracted for surface water and only  $\text{Ca}^{2+}$  loaded strongly onto this component (table 3.7). As apparent from the scatterplot (figure 3.9), Wheatfen had the significantly lowest factor score ( $F_{5, 24} = 13, p < 0.0001$ ).

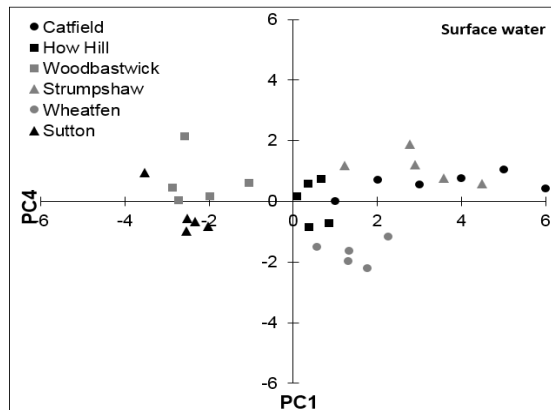


Figure 3.9: Scatter plot to show distribution of factor scores associated with PC1 and PC4 for surface water.

### 3.4.3 Water level and electrical conductivity time series data for study sites

Irregularities appeared to be most influential in time series data (figures 3.10 to 3.14), whereas the trend component contributed the least to observed water level at all sites. Strumpshaw, Woodbastwick and How Hill appeared to have a water level most influenced by seasonal cycles relative to other sites. Although documented storm surge events are discussed further in section 3.3.5, the surge event on 9<sup>th</sup> November

2007 is evident in the EC time series at Catfield and the December 2013 event is evident in the EC time series at Strumpshaw (peaks are indicated by arrows).

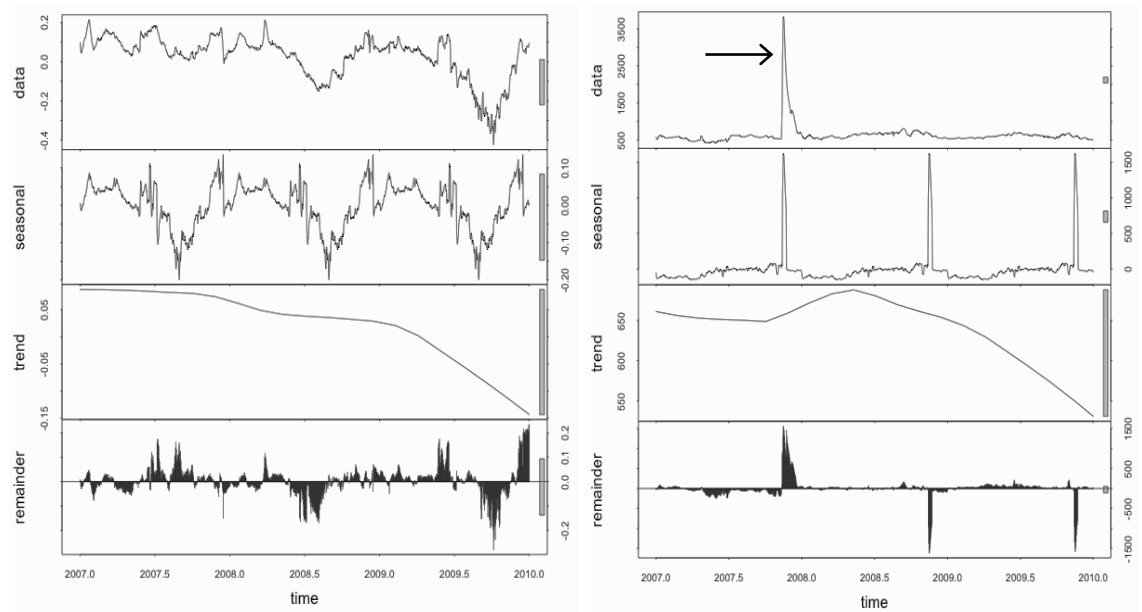


Figure 3.10: Decomposed time series data for water level (mAPS) (left) and electrical conductivity ( $\mu\text{S cm}^{-1}$ ) (right) at **Catfield** for the period January 2007 to January 2010. Data (top box) indicates observed data. Seasonal, trend and remainder are relative fluctuations from observed data obtained from robust additive STL decomposition. The grey bar indicates the relative contribution of each time series component to overall variability (the smaller the bar the higher the contribution).

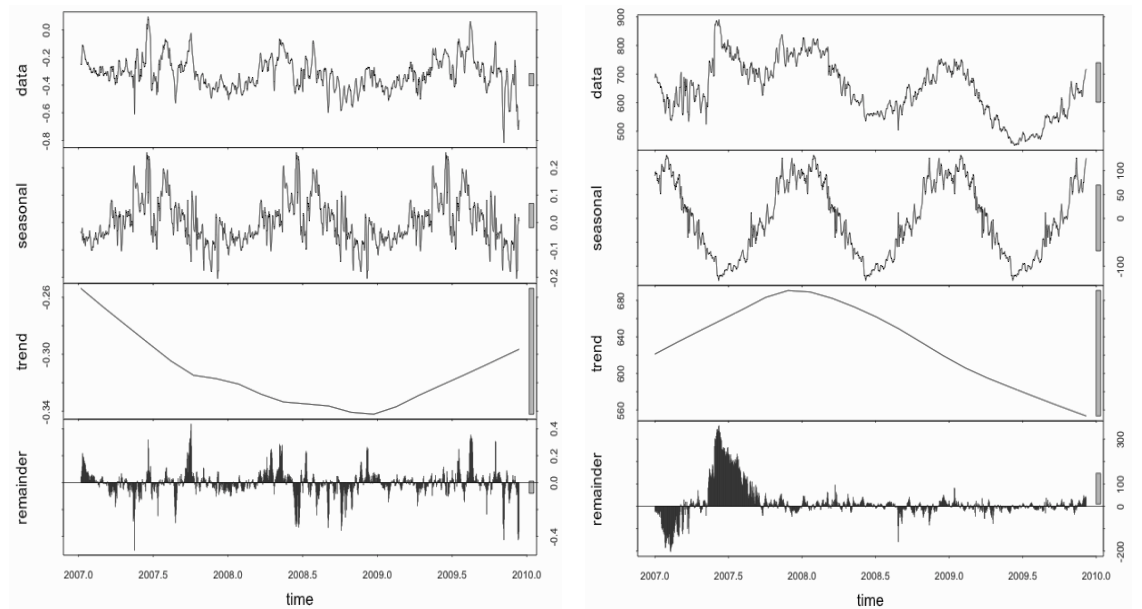


Figure 3.11: Decomposed time series data for water level (mAPS) (left) and electrical conductivity ( $\mu\text{S cm}^{-1}$ ) (right) at **Woodbastwick** for the period July 2007 to July 2010. Data (top box) indicates observed data. Seasonal, trend and remainder are relative fluctuations from observed data obtained from robust additive STL decomposition. The grey bar indicates the relative contribution of each time series component to overall variability (the smaller the bar the higher the contribution).

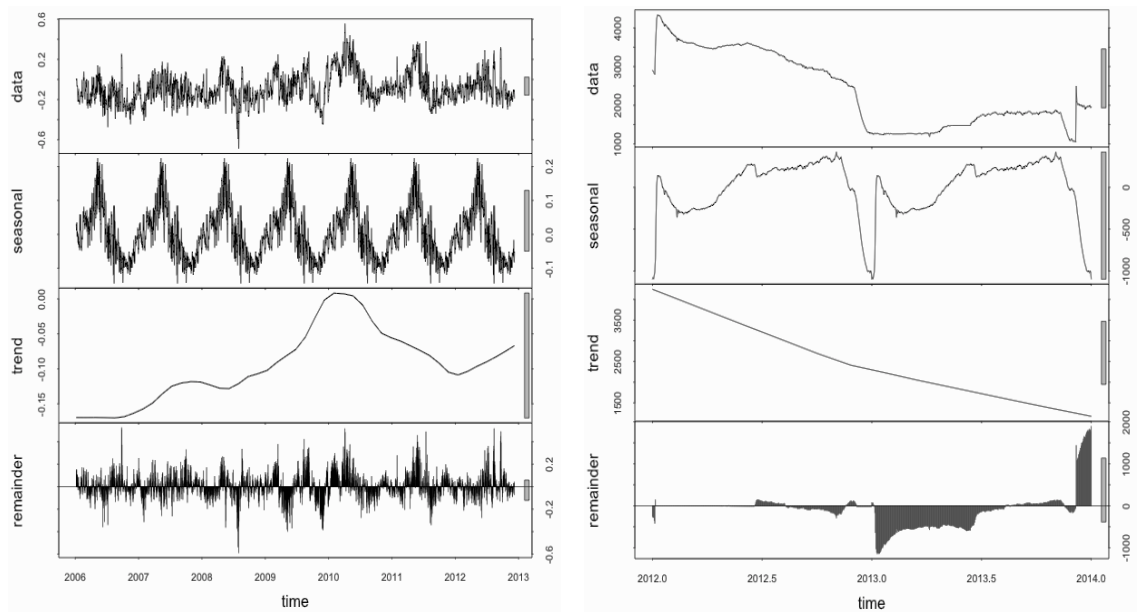


Figure 3.12: Decomposed time series data for water level (mAPS) (left) and electrical conductivity ( $\mu\text{S cm}^{-1}$ ) (right) at **Wheatfen**. The former covers the period July 2006 to July 2013 and the latter covers the period January 2012 to January 2014. Data (top box) indicates observed data. Seasonal, trend and remainder are relative fluctuations from observed data obtained from robust additive STL decomposition. The grey bar indicates the relative contribution of each time series component to overall variability (the smaller the bar the higher the contribution).

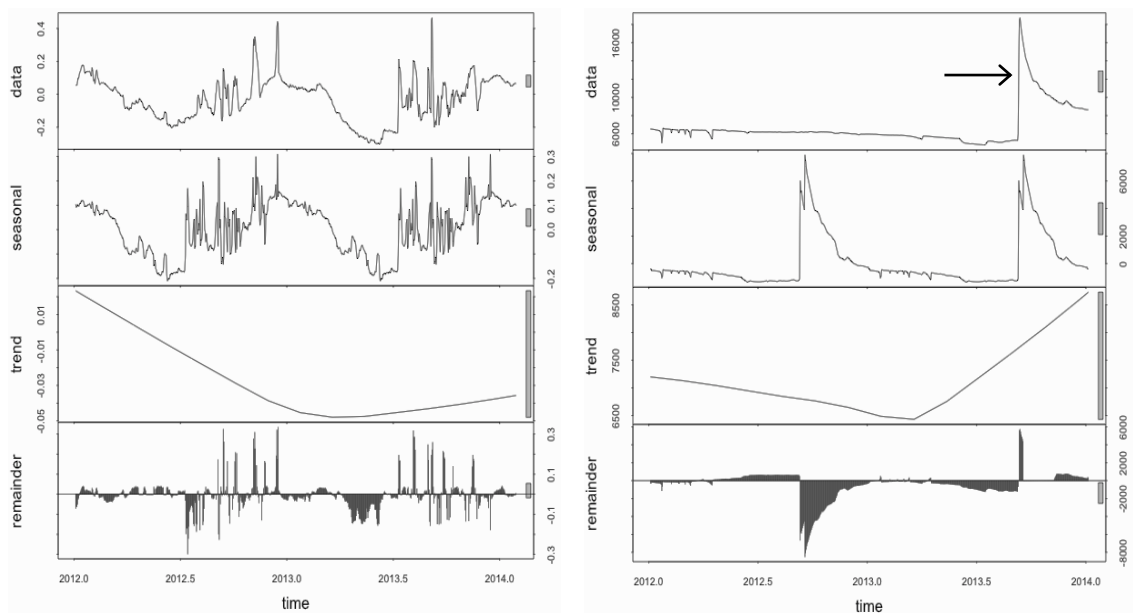


Figure 3.13: Decomposed time series data for water level (mAPS) (left) and electrical conductivity ( $\mu\text{S cm}^{-1}$ ) (right) at **Strumpshaw** for the period April 2012 to April 2014. Data (top box) indicates observed data. Seasonal, trend and remainder are relative fluctuations from observed data obtained from robust additive STL decomposition. The grey bar indicates the relative contribution of each time series component to overall variability (the smaller the bar the higher the contribution).

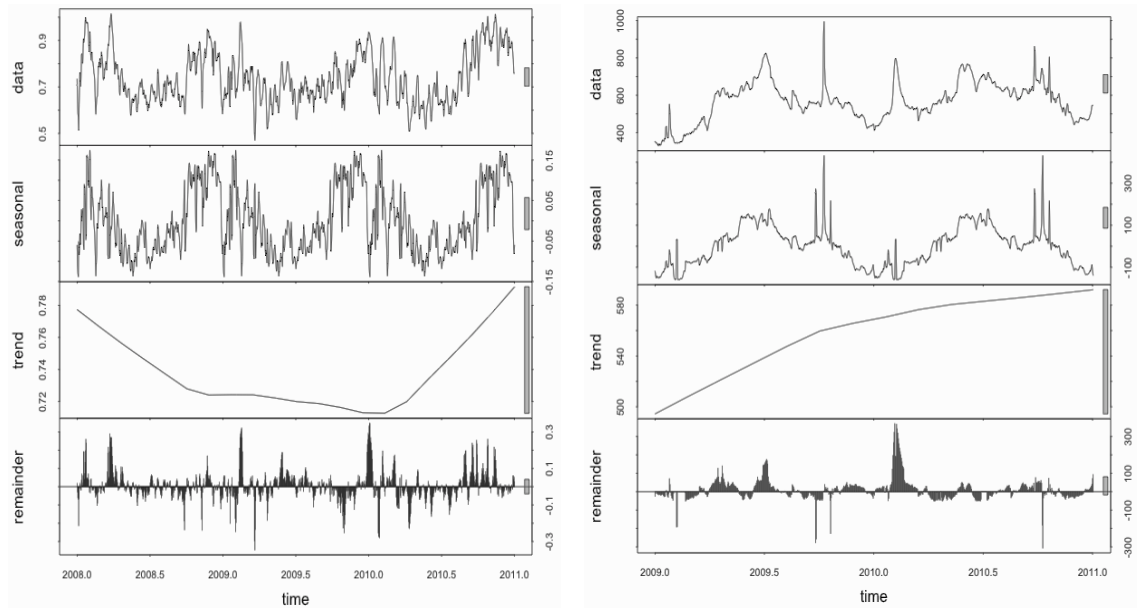


Figure 3.14: Decomposed time series data for water level (mAPS) (left) and electrical conductivity ( $\mu\text{S cm}^{-1}$ ) (right) at **How Hill** for the period January 2009 to January 2011. Data (top box) indicates observed data. Seasonal, trend and remainder are relative fluctuations from observed data obtained from robust additive STL decomposition. The grey bar indicates the relative contribution of each time series component to overall variability (the smaller the bar the higher the contribution).

As shown in figure 3.15, water level generally decreases over respective monitoring periods with the exception of Wheatfen, where water level is at a similar level at the start and the end of the trend. The small fluctuation at this site during 2010 corresponded with a particularly wet year in 2010, however, this fluctuation is not apparent at any other site. EC appeared to decrease abruptly at Wheatfen and Strumpshaw.

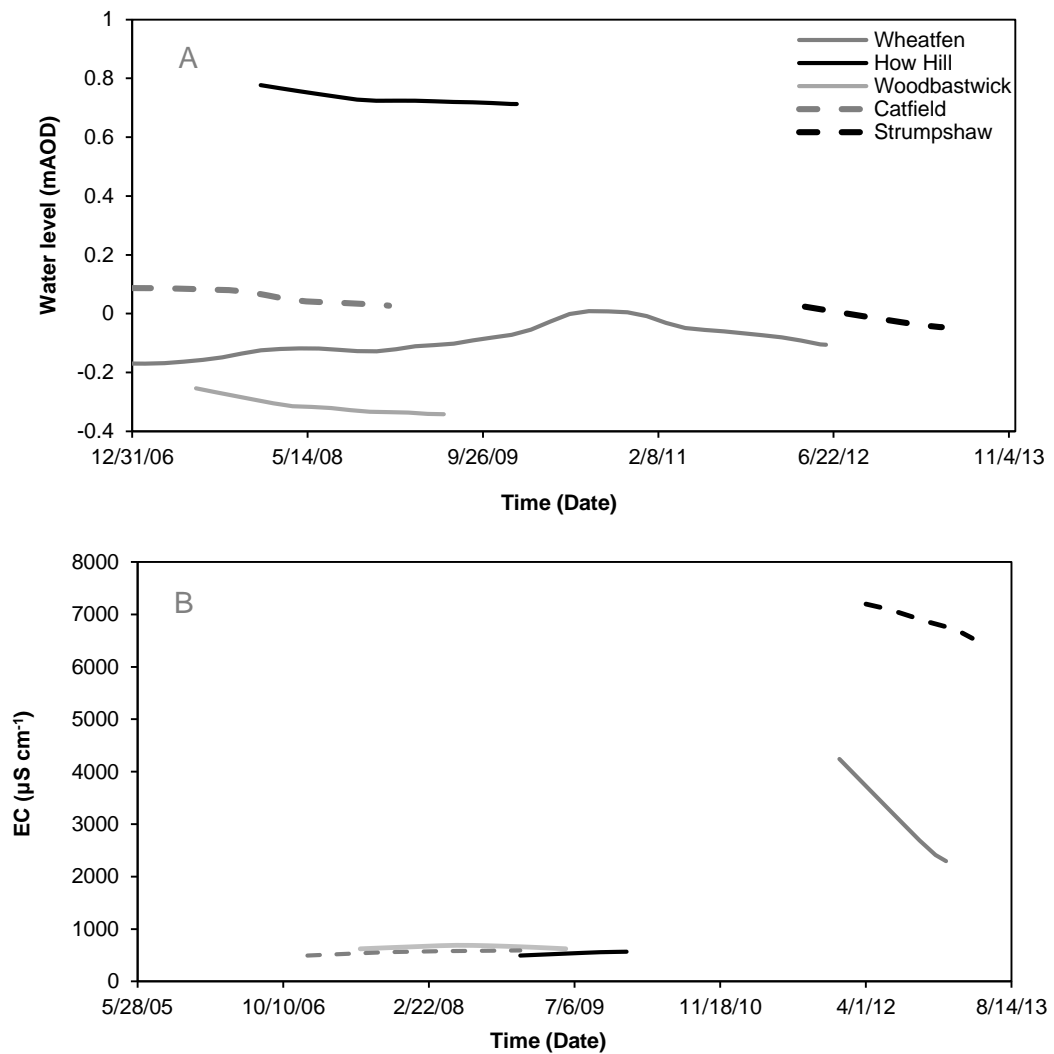


Figure 3.15: Summary of trends for water level (A) and electrical conductivity (EC) (B) derived from decomposing raw time series data. Note the conversion of water level from mAPS back to mAOD to allow for comparison between sites (section 3.2.1.2).

Figure 3.16 shows How Hill to be the only site where water level remained above the peat surface, and Woodbastwick the only site where the water level was at or below the peat surface throughout 2012. Generally, water level was most frequently between -0.25 and 0.5 mAPS across all sites over the year (table 3.8).

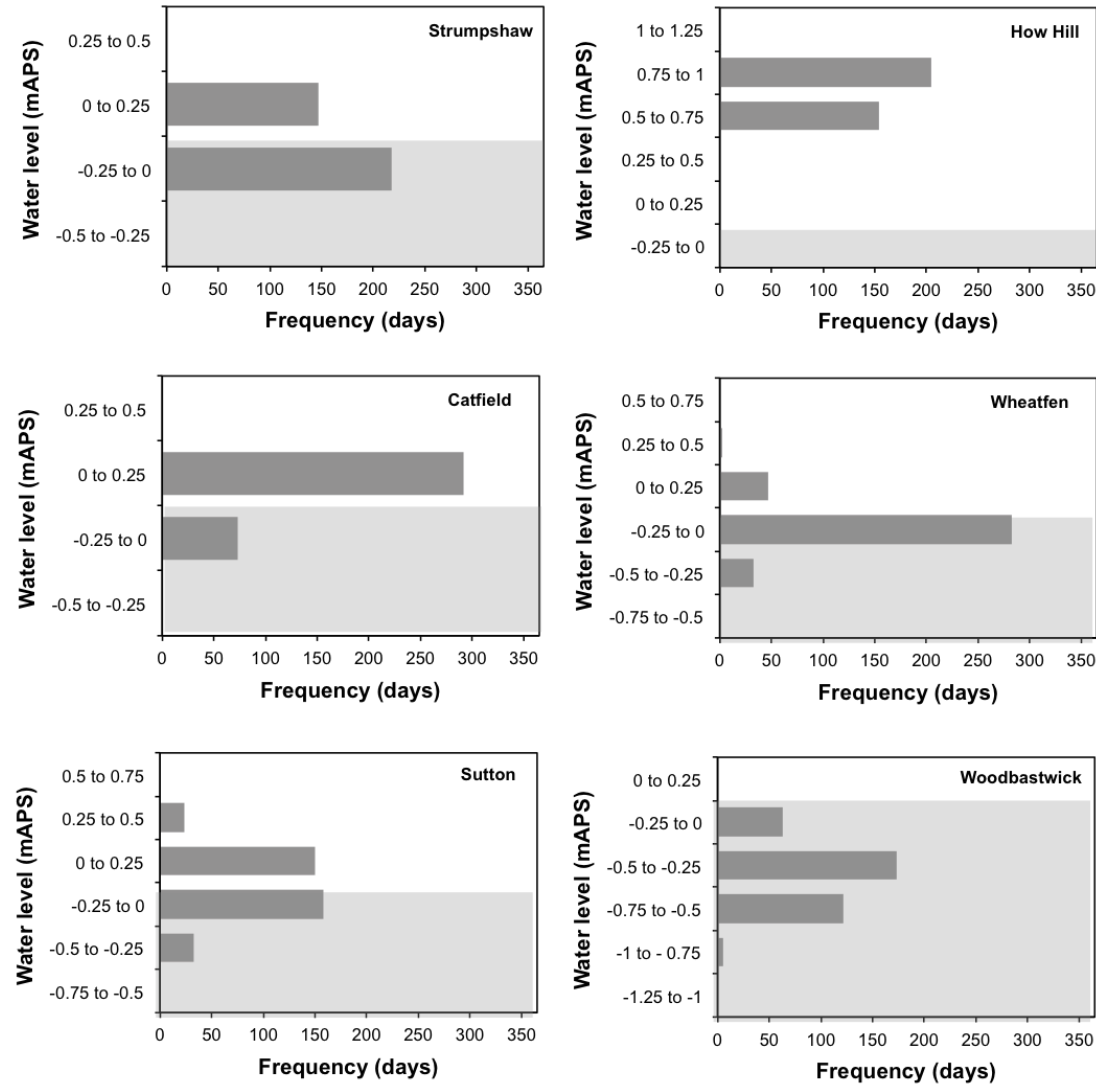


Figure 3.16: Number of days water level (mAPS) is at a given height during 2012. Water level is grouped into increments of 0.25 metres. The grey shaded area indicates when water level is below the peat surface.

Table 3.8: Summary of water level and electrical conductivity (EC) data in 2012 obtained from the Environment Agency (EA). Data for Sutton (\*) was not available from the EA and was obtained from a logger deployed as part of this research throughout 2014. Peat elevation was obtained from a geospatial survey using a Leica GNSS as in section 3.2.1. Water level was recorded in mAOD and corrected for ground level to give metres above peat surface (mAPS). Sites are ordered based on the proportion of the year that water level is above the peat surface.

Site	Water Level (mAPS)					Electrical Conductivity ( $\mu\text{S cm}^{-1}$ )					Above peat surface (days)	Proportion of year	Below peat surface (days)	Proportion of year
	<i>n</i>	Mean	SE	Min	Max	<i>n</i>	Mean	SE	Min	Max				
How Hill	8544	0.7752	0.0020	0.43	2.21	8544	631.2	3.6	380	5670	365	1.00	0	0.00
Catfield	35134	0.02884	0.00027	-0.11	0.14	35136	673.26	0.53	530	980	292	0.80	73	0.20
Sutton	8675	-0.0125	0.0019	-1.27	0.52	8711	2832	23	484	8679	174	0.48	191	0.52
Strumpshaw	35173	-0.02538	0.00054	-0.21	0.31	35179	6371.4	1.6	4780	7180	147	0.40	218	0.60
Wheatfen	35131	-0.10973	0.00074	-0.35	0.55	35131	3201.3	3.3	1040	4390	49	0.13	316	0.87
Woodbastwick	35177	-0.4066	0.0010	-0.84	0.72	35177	566.53	0.35	420	750	2	0.01	363	0.99



### 3.4.4 Response of water level and electrical conductivity to storm surge events

The surge event on 9<sup>th</sup> November 2007 was observed in the time series data at three sites, however the response times appeared to vary (figure 3.17). The cross correlation functions for the surge event on 9<sup>th</sup> November 2007 indicated that the peak in tide gauge data was significantly correlated ( $p < 0.05$ ) with peaks observed in water level at Woodbastwick and Strumpshaw and EC at Catfield after the event (figure 3.18). Water level at Strumpshaw was the quickest to respond to the surge in sea-level (4 days), whereas water level at Woodbastwick responded after 5 days. EC at Catfield took the longest to respond to the surge event (14 days).

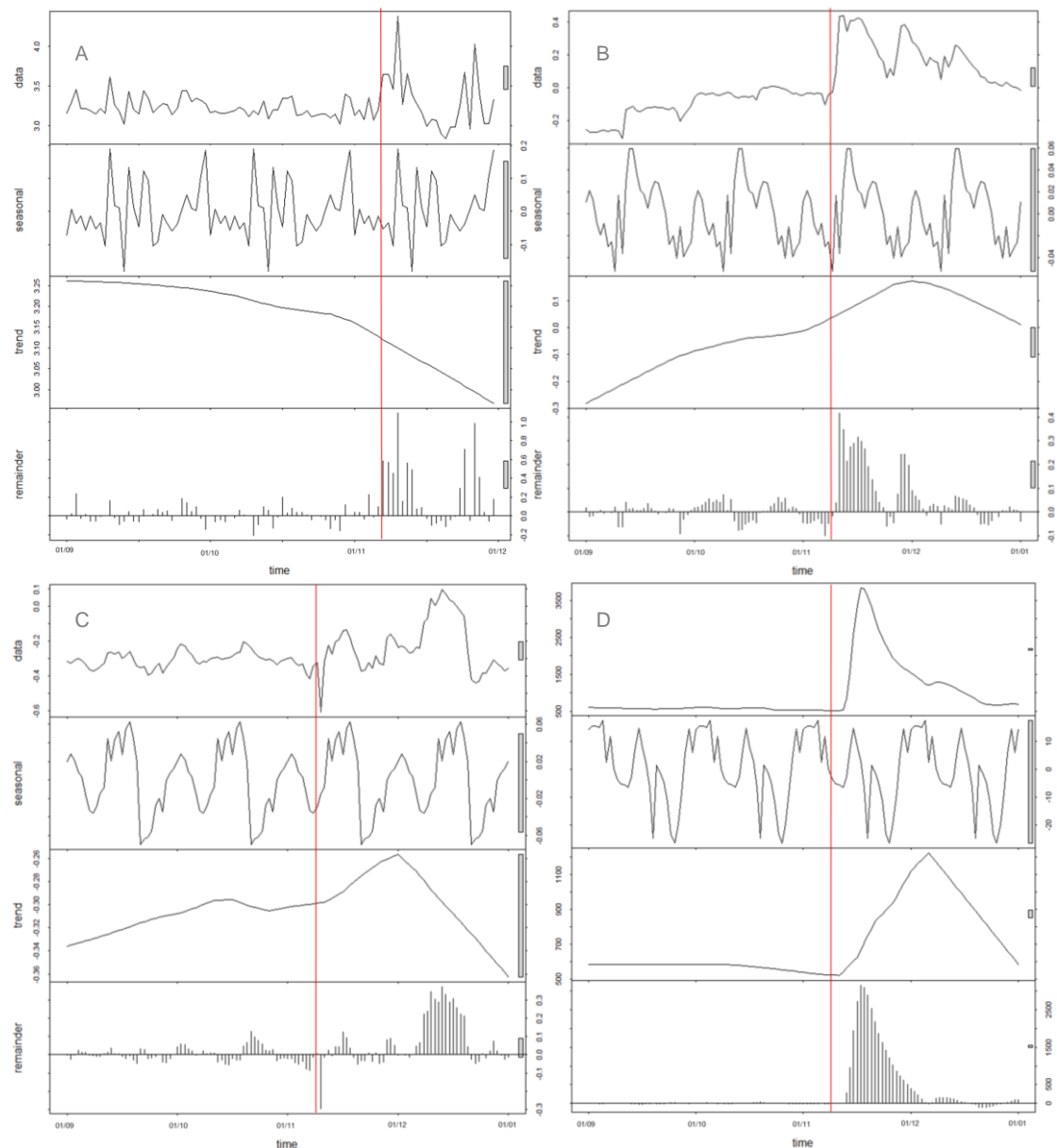


Figure 3.17: Decomposed time series data during event on 9<sup>th</sup> November 2007 (indicated by red line). (A) Tide gauge, (B), Strumpshaw water level, (C) Woodbastwick water level, (D) Catfield EC.

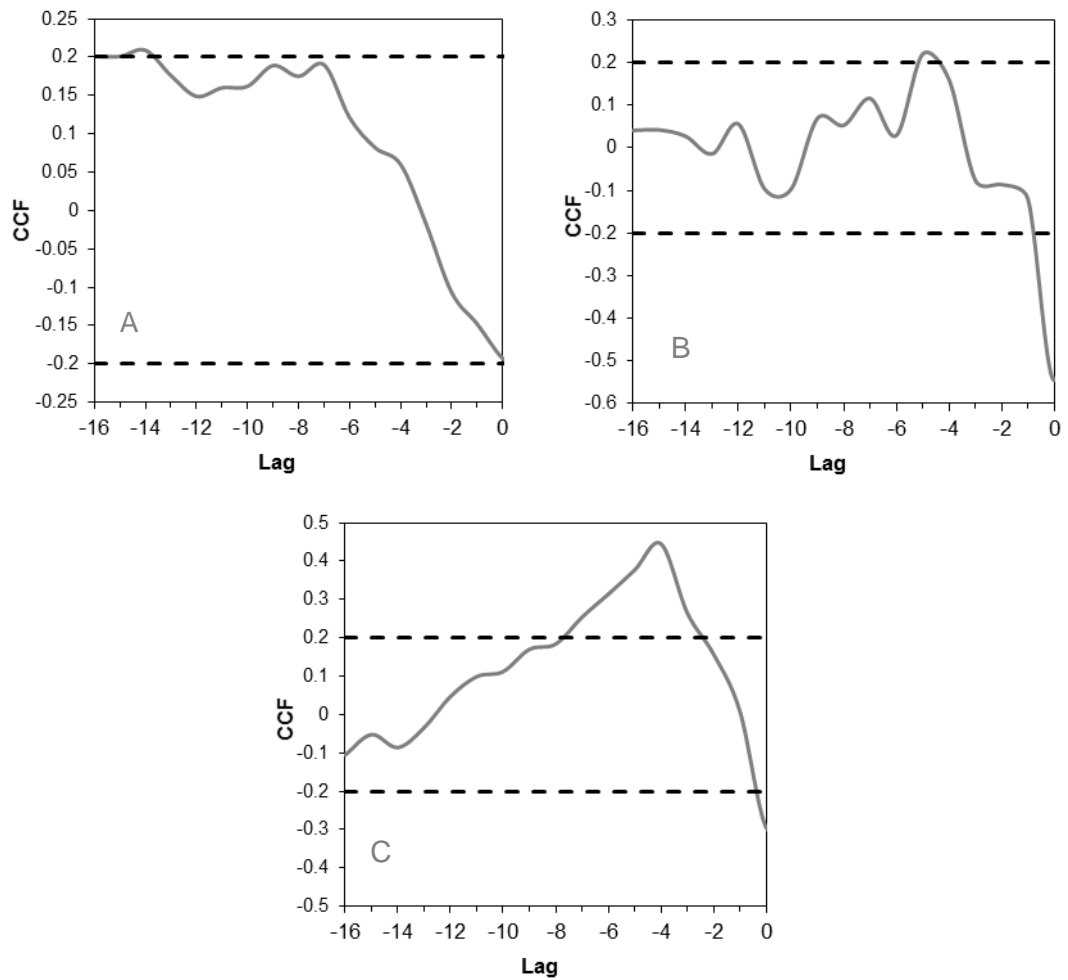


Figure 3.18: Cross correlation functions (CCF) for the irregular component of tide gauge data and the irregular component of water level and EC data. Cross correlation between tide and EC at Catfield (A), water level at Woodbastwick (B) and Strumpshaw (C). Dashed line indicates 95% confidence intervals and only significant cross correlations are shown. All data was log transformed prior to analysis.

The storm surge event on 5<sup>th</sup> December 2013 was evident in EC and water level at Strumpshaw and water level at Woodbastwick and Wheatfen (figure 3.19). The irregular component for Strumpshaw suggests that water level quickly returned to the pre-event level. Water level at Woodbastwick recovered after 1 to 2 days and the peak in water level at Wheatfen appeared to return to levels expected from seasonal and trend components after 2 to 3 days. Figure 3.20 indicates that observed peaks in water level following the event at Strumpshaw, Woodbastwick and Wheatfen, were significantly correlated ( $p < 0.05$ ) to the surge in tide gauge data after a lag time of one day.

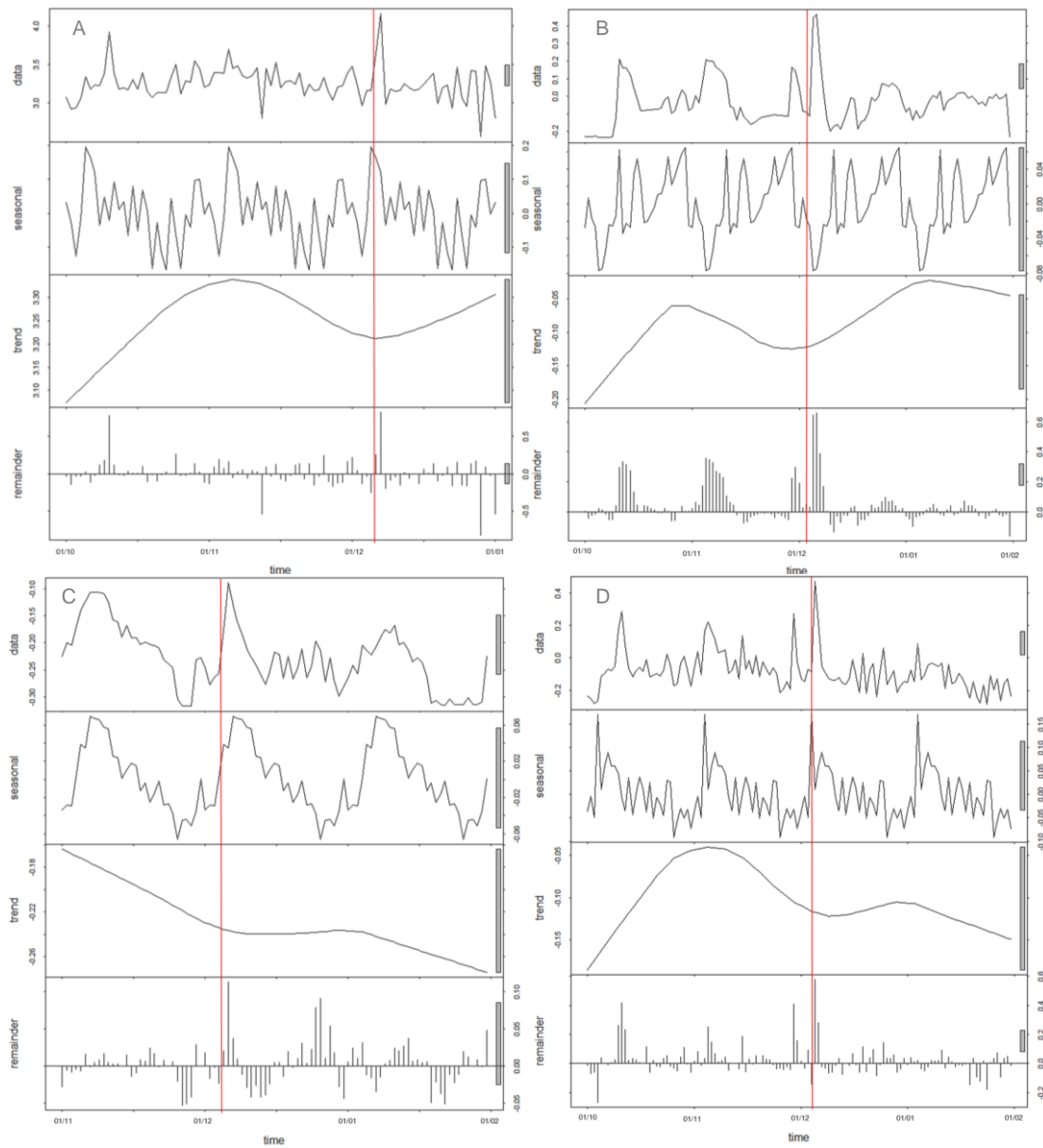


Figure 3.19: Decomposed time series data during the surge event on 5<sup>th</sup> December 2013 (indicated by red line). (A) Tide gauge, (B) Strumpshaw water level, (C) Woodbastwick water level, (D) Wheatfen water level.

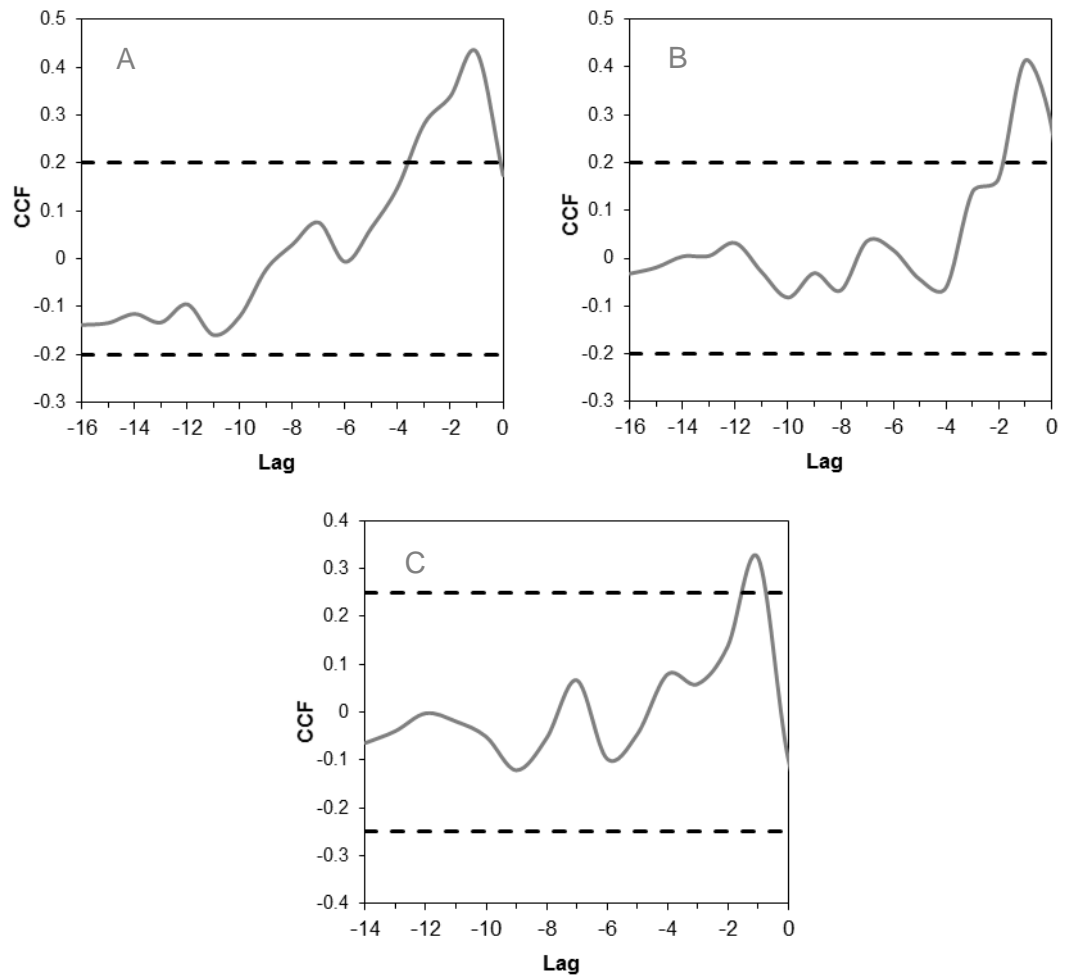


Figure 3.20: Cross correlation functions (CCF) for the irregular component of tide gauge data and the irregular component of water level data. Cross correlation between tide and water level at Strumpshaw (A), Wheatfen (B) and Woodbastwick (C). Only sites with statistically significant lags are shown ( $p < 0.05$ ). Dotted lines indicate 95% confidence levels. All data is log transformed prior to analysis.

## 3.5 Discussion

### 3.5.1 Controls on hydrogeochemistry

The principal components and what they represent are discussed before examining temporal trends in water level and electrical conductivity. Principal component 1 (PC1) explains the majority of variation in water chemistry with ions indicative of saline influence loading onto this component for both porewater and surface water ( $\text{Cl}^-$  and  $\text{Na}^+$ ) (Neal & Kirchner 2000; El Moujabber et al. 2006). Significantly different factor scores between sites implied a spatial gradient of saline influence where, according to mean factor score, Sutton was the least saline influenced site and Strumpshaw the most (section 3.3.2). Overall,  $\text{Cl}^-$  concentration at Strumpshaw in both porewater and surface water are similar to other coastal lowland studies discussed in the literature:  $30 - 150 \text{ mg l}^{-1}$  (Mollema et al. 2013) and  $172 \pm 190 \text{ mg l}^{-1}$  (Helton et al. 2014).  $\text{Cl}^-$  concentration at all sites exceeded that found in rainfall in coastal locations ( $3.3 \pm 0.5 \text{ mg l}^{-1}$  and  $2.6 \pm 0.37 \text{ mg l}^{-1}$ , DEFRA 2014), indicating an additional source of  $\text{Cl}^-$  ions such as inundation from surface water.

Analysis of  $\text{Na}^+:\text{Cl}^-$  helps to distinguish the predominant source of  $\text{Na}^+$  and  $\text{Cl}^-$  at each site (Thimonier et al. 2008). Sutton is located closest to the coast and has the highest  $\text{Na}^+:\text{Cl}^-$  for both surface water and porewater.  $\text{Na}^+:\text{Cl}^-$  at this site was similar to  $\text{Na}^+:\text{Cl}^-$  of precipitation detected in the Broads ( $0.62 \pm 0.013$ , DEFRA 2014) and to precipitation over the North Sea: 0.44 (Möller, 1990) and 0.57 (Shand et al. 2007). Based on this evidence, it is possible that  $\text{Na}^+:\text{Cl}^-$  is primarily controlled by precipitation at Sutton. Furthermore, this site has the lowest score for PC1, suggesting that precipitation alone is not enough to explain the higher factor scores at other sites, thus supporting the argument that PC1 indicates the delivery of  $\text{Na}^+$  and  $\text{Cl}^-$  from an additional source.

Although located furthest from the coast, Wheatfen and Strumpshaw do not have the lowest  $\text{Na}^+:\text{Cl}^-$  as would be expected. These sites are located on the River Yare, the only river in this study to be directly connected to the sea and with a known tidal influence (section 3.2.3). As the river flows eastwards to the coast there is a westward flow of seawater with tidal currents reaching Strumpshaw and Wheatfen, acting as the predominant mechanism for the delivery of  $\text{Na}^+$  and  $\text{Cl}^-$  to these sites.

The influence of geology is the second most important control on the chemical composition of porewater (i.e. PC2) and was the least important control for surface water (i.e. PC4).  $\text{Ca}^{2+}$  loaded onto PC2 for porewater and PC4 for surface water and is likely a result of dissolution of calcite ( $\text{CaCO}_3$ ) in the extensive chalk aquifer underlying unconsolidated glacial deposits in East Anglia (Shand et al. 2007). The aquifer has been extensively studied (e.g. Allen et al. 1997; Outram & Hiscock 2012) and is known to influence the hydraulic conditions and hydrochemistry of groundwater (Song & Atkinson 1985). A knowledge of the movement of groundwater is essential to develop an understanding of the biogeochemistry of any wetland system (Hemond 1980) and Hiscock et al., (1996) found that groundwater in the Broads principally  $\text{Ca}^{2+}$  in nature, with concentrations of  $\text{Ca}^{2+}$  decreasing with increasing distance from the groundwater store, indicating the vertical movement of ions towards the surface (table 3.9).

Analysis of  $\text{Mg}^{2+}:\text{Ca}^{2+}$  provides more information in relation to the influence of geology on hydrochemistry (Mondal et al. 2010) and the ratio for the Broads was between that of a continental (0.26; Vitt and Chee, 1990) and maritime peatland (1.25; Wind-Mulder et al., 1996) – which is unsurprising considering the location of the Broads at the terrestrial/ open water interface.  $\text{Mg}^{2+}:\text{Ca}^{2+}$  was lowest at Woodbastwick, Wheatfen and Sutton and  $\text{Ca}^{2+}$  was notably higher in porewater compared to the other three sites, indicating the presence of groundwater upwelling (Hiscock et al. 1996). The additional loading of soluble reactive phosphorous (SRP) onto PC2 for porewater could be a result of SRP introduction from point source discharge into groundwater (Neal et al. 2002). However, as SRP does not load onto PC4 for surface water, it is more likely that the desorption of P from calcite driven by relatively acidic conditions in the porewater compared to the alkaline conditions in the chalk groundwater is the dominant mechanism here (Shand et al. 2007).

Table 3.9: Summary of borehole data adapted from Hiscock et al. (1996). Surface samples (\*) are derived from this study.

Site	Depth (m below chalk surface)	Major ion analysis (mg l <sup>-1</sup> )						pH	Salinity (ppt)
		Ca <sup>2+</sup>	Mg <sup>2+</sup>	Na <sup>+</sup>	K <sup>+</sup>	SO <sub>4</sub> <sup>2-</sup>	Cl <sup>-</sup>		
Wo	Ground level	48	7.6	3.4	1.7	2.09	16	6.7	0.028
	9.3	55	1.2	25	6.1	14	42	8.4	0.076
	27.3	109	4.9	58	6.7	36	184	7.7	0.332
	31.3	118	13	108	8.9	43	325	7.8	0.587
St	Ground level	63	34	66	13	1.0	133	7.1	0.241
	48	125	3.1	23	1.9	32	38	7.1	0.041
	55	121	3.3	24	1.7	26	44	7.1	0.079
	65	122	5.7	33	2.3	33	54	7.2	0.098

The influence of anthropogenic sources was attributed to PC3 for both porewater (Mg<sup>2+</sup>, SO<sub>4</sub><sup>2-</sup>, NO<sub>3</sub><sup>-</sup>) and surface water (K<sup>+</sup>, Mg<sup>2+</sup>, NO<sub>3</sub><sup>-</sup>, pH) and represents the third most important influence on water chemistry. Common constituents of agricultural fertilizers (Mg<sup>2+</sup>, NO<sub>3</sub><sup>-</sup>) loaded onto PC3 which suggests agriculture is an important influence (Feast et al. 1998; urtola & Yli-Halla 1999; Neal et al. 2010). NO<sub>3</sub><sup>-</sup> was found in relatively high concentrations at Wheatfen in both porewater and surface water – probably representing the residual effect of historic point source discharge from Whitlingham Sewage Treatment Works (Birkett et al. 2002) in addition to run-off from fertilizers. Although Mg<sup>2+</sup> in porewater could be the result of incongruent dissolution of calcite (Shand et al. 2007), table 3.9 indicates that Mg<sup>2+</sup> concentrations in surface water far exceed those in the chalk aquifer and indicates a surface input of Mg<sup>2+</sup>. K<sup>+</sup> only loaded onto PC3 for surface water and was generally present in higher concentrations in surface water than porewater, indicating an anthropogenic source. It is likely that the uptake of K<sup>+</sup> by plants in the root zone compounds the absence of K<sup>+</sup> from porewater (Shand et al. 2007). The loading of SO<sub>4</sub><sup>2-</sup> is probably the result of the oxidation localised pyrite deposits known to exist in the area (Ander et al. 2006). However, SO<sub>4</sub><sup>2-</sup> concentrations were particularly elevated at Wheatfen in both porewater and surface water, indicating an additional isolated source of SO<sub>4</sub><sup>2-</sup>, probably anthropogenic inputs from the Whitlingham Sewage Treatment Works, or from overtopping of the River Yare during flood events.

In relation to surface water, the influence of PC2 was difficult to separate from PC3 as ions loading onto this component also indicated an anthropogenic influence (SRP, NO<sub>3</sub><sup>-</sup> and pH). Lamers et al. (2015) suggested that floodplain fens, due to their direct

connection to groundwater and surface water, are particularly vulnerable to large-scale land-use changes, namely  $\text{NO}_3^-$  run off from fertilizers and P from manure. It is not possible that SRP,  $\text{NO}_3^-$  and pH could be related by redox conditions due to the aerated nature of surface water; therefore, it is probable that these constituents arise from anthropogenic sources, with specific reference to agricultural inputs (Shand et al. 2007).

The aim of this Chapter was to determine a possible influence of salinity in the Broads. Analysis of factor scores and ion ratios indicates that PC1 explains the most variation in water chemistry and significantly different factor scores suggests that PC1 is representative of a gradient of saline influence. Generally in the literature, salinity is discussed in parts per thousand (ppt) (e.g. Craft et al. 2009; Ciais et al. 2013). In this study, the highest salinity was found at Strumpshaw, but was an order of magnitude lower than sites in other saline gradient studies, for example: mangrove sites ranging between 10 and 28 ppt (Yang et al. 2013) and salt marshes with salinity ranging between 5 to 17 ppt (Bartlett et al. 1987). Craft et al., (2009) defined salt marshes as 20 to 35 ppt, brackish marshes as 5 to 20 ppt and freshwater marshes as < 0.5 ppt. Therefore, sites in this study are considered freshwater in the breadth of wetland research.

### **3.5.2 Exploring the impact of storm surge events**

Although sea-levels are known to have been rising over the last century (Church et al. 2013), decomposed time series data showed no overall trend for an increase or decrease in water level and EC. Distinct differences in the general position of water level relative to peat surface was found (figure 3.15), with How Hill consistently above the peat surface and Woodbastwick primarily below the peat surface, although between-site variation is a common occurrence in fens (Thormann & Bayley 1997).

Storm surge events are likely to be the primary cause for sea-level rise in low-lying coastal areas (Woth et al. 2006). An increased saline influence in lowland wetlands as a result of storm surge events could be manifested in two ways (Henman & Poulter 2008): via an increase in volume of water following a surge event or from an increase in ionic concentration of porewater and surface water. Thus, Environment Agency time series data was used to determine if electrical conductivity (EC) and water level at study sites was influenced by documented storm surge events. Water level was



quicker to respond after the surge on 5<sup>th</sup> December 2012 in comparison to the event on 9<sup>th</sup> November 2007. The maximum height of the surge on 5<sup>th</sup> December 2012 was 0.4 m higher than on 9<sup>th</sup> November 2007, indicating that the higher the surge the faster an increased volume of water travels through the river network within the Broads. In terms of distance travelled upstream, it appears that an increase in water level was not detectable past Woodbastwick after either event. Catfield is located further upstream than Woodbastwick, indicating that a pulse in EC as a result of a surge is able to travel further upstream than an increased volume of water.

The results indicate that increased water level is likely to be the primary cause for increased saline intrusion as a result of sea-level rise in the Broads. A space-for-time (SFT) substitution can be used to explore the possible effect of sea-level rise on carbon storage in floodplain fens. When coupled with published data, the application of a SFT approach can provide a convenient means of studying the effect of an environmental perturbation on an ecosystem without the need to make real-time direct observations over an extended period of time (Chmura et al. 2003). Gaps in published data is a limitation of the SFT approach (Bartlett et al. 1987) and in this study, long-term trends in water level could not be compared due to the inconsistent recording of Environment Agency data. Water level data was recorded at the majority of sites for 2012, and so proportional inundation over a year could be determined.

### 3.6 Conclusions

With respect to specific questions outlined in section 3.1, the following conclusions can be made in relation to water chemistry and hydrologic regime of the Broads:

1. A gradient of saline influence has been shown to exist in the Broads and accounts for the majority of variation in hydrogeochemistry with geology and anthropogenic inputs (including agricultural fertilizers) contributing to a lesser extent. Strumpshaw was found to be the most saline influenced site and is located on the River Yare, which has a known tidal influence.
2. Documented storm surge events were found to result in elevated water levels and EC. Physical characteristics of the surge, specifically peak height and the period sea-level was elevated as a result of the surge, were found to effect the travel time and geographical extent reached by the increased volume of water. An increase in water level was not detected any further upstream than Woodbastwick after both events, whereas EC was found to travel further upstream. Therefore, it is probable that saline intrusion will be primarily a result of salt-intrusion in sites located upstream, as opposed to an increase in water level at sites located further downstream.

## Chapter 4: Is saline influence a control on the inputs and outputs to the peat carbon stock in floodplain fens?

### 4.1 Introduction

The maintenance of peatland carbon accumulation is dependent on rate of above-ground production exceeding rate of decay, and sea-level rise has the potential to disrupt this balance in floodplain fens. Sea-level rise will result in an increase in salinity and/or an increase in water level. This Chapter reports measurements of inputs to, and outputs from, the carbon store at floodplain fen sites located along a gradient of saline influence (Chapter 3). Measured inputs are above- and below-ground carbon production; measured outputs are above- and below-ground decomposition. The primary control(s) for each are explored by answering the following research questions:

**Research question 4.1:** What factors control above-ground carbon productivity and how do these controls vary among sites located on a gradient of saline influence?

Radiation Use Efficiency (RuE) is a measure of the efficiency of a plant to synthesise photosynthetically active radiation (PAR), hence, stress caused to the plant via environmental conditions (such as nutrient availability, water level and salinity) are reflected in RuE (Yang et al. 2014). An increase in available nutrients is expected to increase productivity as the higher the concentration of nitrogen in leaves, the higher the rate of photosynthesis (Berendse & Aerts 1987). Productivity may be inhibited when salinity exceeds 10 ppt as this will induce stomatal closure. This response mechanism regulates the supply of oxygen to the rhizosphere as a defence against the uptake of phytotoxins (Armstrong et al. 1996), but also reduces CO<sub>2</sub> uptake for photosynthesis in *Phragmites australis* (Cav.) Trin. Ex Steud (Pagter et al. 2009). The aggressive growth of *P. australis* below 10 ppt (Mauchamp & Mesleard 2001) is likely to inhibit the growth of other species common in floodplain fens (Meyerson et al. 2000). Growth of *P. australis* will be limited when water level is 0.8 m above the peat surface during the growing season due to increased investment in below-ground organs (Coops et al. 1996; Coops & van der Velde 1996). Cutting of *P. australis* followed by an inundation event that submerges the shoots will reduce productivity (Hocking et al. 1983; Mauchamp & Mesleard 2001), and regular trampling will cause damage to above-ground tissue (Engloner 2009).

**H4.1.1:** RuE will be influenced by N/C in leaves, water level, nutrient, geological and saline influences.

**Research question 4.2:** What factors control below-ground carbon production (BGCP) and the quotient of above- to below-ground carbon production (AGCP/BGCP)? How do these controls vary between sites located on a gradient of saline influence?

AGCP/BGCP will reduce in nutrient poor conditions as plants invest heavily in BGCP to ensure resources continue to be obtained (Rydin & Jeglum 2013). An increase in salinity may decrease AGCP/BGCP as water high in ionic strength (such as seawater) can reach toxic levels and plants respond by reallocating assimilates from growth to the lignification of roots to reduce the uptake of phytotoxins (Saleque & Kirk 1995; Wang & Peverly 1999). However, other studies suggest that proportional allocation to above- and below-ground organs is the same, just reduced under stressful conditions (e.g. Hellings & Gallagher 1992; Yang et al. 2014). Cutting and trampling may induce stress on the plant, resulting in a shift in the allocation of assimilates between AG and BG organs to facilitate the repair of damaged tissues or regrowth following cutting (Hocking et al. 1983).

**H4.2.1:** Nutrient availability will be a primary control on BGCP, with an increase in AGCP/BGCP observed with increasing nutrient availability.

**Research question 4.3:** What are the controls on the carbon decay rate of *in situ* decomposition of *P. australis* leaves, stems and below-ground (BG) material?

Litter quality explains much of the variation in decomposition rate as recalcitrant forms of organic matter require more energy to break down, therefore decomposers favour easily decomposable compounds (Manzoni et al. 2010). Waterlogged conditions impair microbial activity, and thus the mineralisation of organic matter (e.g. Limpens et al. 2008). Nutrient availability is an important factor in determining the size of the microbial population and the extent of their activity. Salinity induces osmotic stress in microbes, hence reducing their activity (Wichern et al. 2006), although it is possible for microbes to adapt through selective exclusion of Na<sup>+</sup> and Cl<sup>-</sup> (Killham 1994). Other studies have shown that decomposition is not affected when salinity is < 5 ppt, probably because microbes are not yet stressed (Sangiorgio et al. 2008). Decomposition in the first month is largely driven by the physical leaching of hydrolysable compounds, whereas decay after this point is driven by microbial activity (e.g. Morris & Waddington 2011; Hughes et al. 2014).

**H<sub>4.3.1</sub>:** Saline influence will be a control on the decay rate of *P. australis* leaves, stems and BG material, regardless of litter quality, water level and nutrient availability.

**Research question 4.4:** Are differences in carbon decay rate due to changes in litter quality and/or microenvironment?

Differences in decay rates among sites (as in RQ 4.3) are due to differences in both decomposition environment (e.g. moisture, oxygenation, dissolved nutrients) and inherent litter quality (litter biochemistry). Litter biochemistry may vary within species due to growth environment (e.g., nutrient availability, salinity), and hence the inherent litter quality of *P. australis* may vary along the site gradient. The disentanglement of microenvironment and litter quality can be achieved through the execution of a transplant experiment (Belyea 1996).

**H<sub>4.4.1</sub>:** Rate of carbon decay will be affected by both litter quality and microenvironment.

**Research question 4.5:** Does carbon accumulation potential vary along the gradient of saline influence?

Carbon accumulation potentials allow for the difference between carbon lost via decomposition and gained through production to be evaluated (Clymo 1984; Thormann et al. 1999). Carbon derived from above-ground (AG) material will decrease with increasing saline influence; given that decomposition is likely to remain unchanged when salinity is < 5 ppt (H<sub>4.3.1</sub>) and AG production may decrease (H<sub>4.1.1</sub>). Conversely, *P. australis* increasingly invest in below-ground organs under stressful conditions (e.g. increased water level and salinity, RQ 4.2), therefore, the carbon accumulation potential from below-ground material is likely to increase.

**H<sub>4.5.1</sub>:** AG carbon accumulation potential will decrease with increasing saline influence, whilst BG carbon accumulation potential will increase with increasing saline influence.

## 4.2 Methodology

### 4.2.1 Above-ground biomass and radiation use efficiency of above-ground production

Above-ground biomass (AGB) was collected in September 2013 and September 2014 from seven replicate quadrats (0.5 m<sup>2</sup>), randomly placed within a 25 m<sup>2</sup> area around the Environment Agency data logger at each site (Chapter 3). Within each quadrat, stem height was recorded for six randomly selected stems of all species. Stem density was also recorded for all species. All species whose stem lay inside the quadrat were identified when collecting AGB in September 2013. In 2014, AGB was harvested without accounting for different species. Vegetation was cut from the peat surface and, because living AGB was required, only 'green' plant material was retained (Gonzalez-Alcaraz et al. 2012). Growth in the Broads is thought to be maximal in September (Minchinton & Bertness 2003), thus the harvested material represented peak above-ground biomass which is correlated with net production (Brix et al. 2001; Soetaert et al. 2004). To ascertain the percentage contribution of different species to total AGB, biomass was separated according to species and weighed separately (2013 only).

On return to the laboratory, AGB (g m<sup>-2</sup>) was air dried to a constant weight. AGB was converted to above-ground carbon mass (AGCM, g C m<sup>-2</sup>) using the carbon content of *P. australis*, the dominant species at these sites. A subsample of *P. australis* was removed from three of the seven quadrats and leaves were separated from stems and ground to a fine powder before being weighed into tin boats for analysis on the Flash Elemental Analyser 1112 Series. Weights were recorded to 6 decimal places (mg) and all glassware and handling equipment was acid washed in 10% HCl. A certified reference material (CRM) was used to measure accuracy: IPE 176 (*P. australis*; 332 g kg<sup>-1</sup> C and 8.08 g kg<sup>-1</sup> N; Wageningen University, The Netherlands) and average recoveries < 90% or > 110% were rejected. Sulphanilamide (16.23% N and 41.81% C; Thermo Scientific) was used as a drift check and average relative standard deviation (%RSD) was calculated to determine the precision of the instrument (table 4.1) with deviations > 10% rejected. A three-way ANOVA showed that carbon content did not differ among sites, years, tissue types (leaf and stem) or their interaction (appendix 1). Therefore, AGCM was obtained by multiplying AGB by average carbon content (42 ± 0.45%).

Table 4.1: Recovery (%) and precision (%RSD) measurements for elemental analysis of *P. australis*.

CRM	Check	N	C
Wepal IPE 176 ( <i>P. australis</i> )	%Recovery	107	109
Sulphanilamide ( <i>P. australis</i> )	%RSD	3	1

Radiation use efficiency (RuE) of above-ground production was calculated as AGCM, divided by photosynthetically active radiation (PAR) accumulated over the growing season. Hourly global solar radiation (GSR) for Norwich Airport weather station (UK grid reference TG 217140; BADC 2016) was summed for daylight hours from the start of the growing season to vegetation harvest (10<sup>th</sup> April 2013 to 20<sup>th</sup> September 2013 and 2014) as in Piao et al. (2007). The result was multiplied by 0.45 to give the photosynthetically available proportion (Dykyjova 1971; Soetaert & Herman 2008).

Two-way ANOVAs were used to test for significant differences in AGCM (g C m<sup>-2</sup>), stem height (cm) and stem density (m<sup>-2</sup>) among sites, years and their interaction. Tukey HSD *post hoc* analysis was conducted where a significant result was found.

The influence on RuE of several controlling factors (table 4.2) was analysed using multiple regression. Both dependent variables (DV) and continuous controlling factors were standardised and centred prior to analysis, hence, the coefficients indicate relative effect sizes. As nitrogen availability in leaves is known to be a controlling factor of photosynthetic efficiency, a foliar N/C coefficient (average N/C for each quadrat determined from elemental analysis of leaves) was also included. The significance of controlling factors was determined using stepwise regression selecting variables in both directions. If by inspection of scatterplots the relationship between a controlling factor and DV was suspected to be non-linear, the square of the controlling factor was included in the model as an additional variable. The model with the best fit for each DV was selected using maximum likelihood ratios (Field et al. 2012; Winter 2013). Multicollinearity was tested using Spearman's rank correlation for continuous variables and Pearson's Chi-squared test for categorical variables. Where multicollinearity was found, the controlling factors resulting in the best model fit were retained (Field 2013).

Canonical Correspondence Analysis (CCA) was used to relate the biomass contribution of different species to environmental variables. The contribution of each identified species to total AGB was expressed as a relative proportion (%) of total

biomass in each quadrat ( $n = 7$  per site). Species occurring in a single quadrat and contributing <10% were removed from the data set prior to analysis (Mitchell & Gilbert 2004; Gilbert & Lechowicz 2004). Intercorrelation of environmental variables was tested using Spearman's Rank correlation for continuous variables and Pearson's Chi-squared test for categorical variables. The significance of the CCA was assessed using permutation tests (permutation  $n = 9,999$ ,  $p < 0.05$ ) (Gilbert & Lechowicz 2004; Lindo & Winchester 2009). The variation explained by each environmental variable was determined by partial CCA, in which the effects of all other significant environmental variables are removed (Gilbert & Lechowicz 2004). Unexplained variation could arise as an artefact of CCA or from unmeasured environmental variables (Ter Braak & Prentice 1988). CCA was carried out using the 'vegan' package (Oksanen et al. 2015).



Table 4.2: Summary of controlling factors used in multiple regressions in this chapter. Not all IVs are used for all analysis and this is clarified in the text. Proportion inundated refers to the proportion of a year water level is above the peat surface based on Environment Agency data from chapter 3. Two categorical variables were also included; cutting regime and extent of trampling. Cutting regime had four levels, which refer to the number of years between cutting and harvest. Trampling had three levels: 1 = no trampling, 2 = animals were present but there was no evidence of trampling, and 3 = explicit evidence of trampling e.g. crushed vegetation. The derivation of N/C is described in section 4.2.1. PCA scores were derived in chapter 3. Saline, geological and nutrient influences are average PCA scores for each site from chapter 3.

Year	Site	Proportion of year submerged	Trampling	Cutting	Saline influence (PCA socres)	Geological influence (PCA scores)	Nutrient influence (PCA scores)	N/C
2013	Catfield	0.80	1	1	-1.485	-2.602	-0.086	0.053
2013	HowHill	1.00	3	3	1.055	-0.815	-0.299	0.046
2013	Strumpshaw	0.40	3	1	3.306	-0.010	-1.051	0.051
2013	Sutton	0.48	1	1	-2.033	1.714	-1.162	0.058
2013	Wheatfen	0.13	2	1	0.879	0.720	1.807	0.061
2013	Woodbastwick	0.01	2	3	-1.062	0.655	1.684	0.063
2014	Catfield	0.80	3	1	-1.485	-2.602	-0.086	0.027
2014	HowHill	1.00	3	>3	1.055	-0.815	-0.299	0.040
2014	Strumpshaw	0.40	1	2	3.306	-0.010	-1.051	0.055
2014	Sutton	0.48	2	2	-2.033	1.714	-1.162	0.057
2014	Wheatfen	0.13	3	2	0.879	0.720	1.807	0.054
2014	Woodbastwick	0.01	1	>3	-1.062	0.655	1.684	0.055

#### 4.2.2 Below-ground carbon production

To estimate belowground production, root ingrowth cores (seven replicates per site) were incubated from October 2013 to October 2014, in the same area where AGB was harvested. The material captured is referred to as 'below-ground production', although it is likely to have consisted mainly of fine roots and to have excluded ingrowth of rhizomes, introducing a bias to the estimate (Maria do Rosário et al. 2000). Each root ingrowth core was constructed by forming hessian fabric into a cylinder (diameter, 10 cm; length, 50 cm), sealing it with duct tape, and then filling it with a 50:50 mixture of inorganic material (perlite and sand). The average dry bulk density of the cores ( $0.13 \pm 0.042 \text{ g cm}^{-3}$ ) was similar to bulk density values for peat reported in literature (Yu 2012) but slightly higher than for peat collected from these sites ( $\sim 0.8 \text{ g cm}^{-3}$ ). Ingrowth cores were deployed by inserting them into holes of 10 cm diameter created with a gouge corer. When collecting the cores, protruding roots were cut with scissors to minimise disturbance. A few cores could not be located or disintegrated when they were removed from the peat matrix (1 from Strumpshaw, How Hill and Woodbastwick; 2 from Catfield and 3 from Wheatfen).

Upon return to the laboratory, ingrowth cores were frozen and sliced into 10 cm subsections using a hacksaw. The hessian casing was removed and the contents emptied into pre-weighed metal trays. Samples were oven dried at  $50^{\circ}\text{C}$  to a constant weight before being placed into a muffle furnace at  $550^{\circ}\text{C}$  for 4 hours and then re-weighed. The inorganic matrix used to construct the cores contained negligible organic matter ( $0.7 \pm 0.1$ ). Hence, the density of below-ground inputs ( $\text{g m}^{-3}$ ) in a subsection was estimated as the difference between oven dry mass and mass after ignition, divided by subsection volume. Root carbon density ( $\text{g C m}^{-3}$ ) was obtained by multiplying root density by 43%, the average carbon content of *P. australis* leaves and stems. Carbon content of roots and rhizomes was not measured in this thesis, but other studies indicate little variation in carbon content among *Phragmites* tissue types (42.5% for leaves versus 44% for rhizomes; Romero et al. 1999).

Net annual BG production ( $\text{g C m}^{-2} \text{ yr}^{-1}$ ) was obtained by fitting a non-linear model to BG carbon density measurements at different depths, before integrating the function analytically. The non-linear model selected was a modified version of the Ricker function (Ricker 1973; Laws & Archie 1981):

$$y = \alpha x e^{-bx} + c \quad \text{Equation 4.1}$$

where  $y$  is the dependent variable (BG carbon density in this example,  $\text{g C m}^{-3}$ ),  $x$  is the controlling factors (depth, m),  $\alpha$  describes the initial rate of increase in BG carbon density,  $b$  describes the subsequent non-linear decrease in BG carbon density and  $c$  is a baseline value. Equation 4.1 was fitted to each core individually. The depths,  $x_{\min}$  and  $x_{\max}$ , at which equation 4.1 reaches zero were found numerically using the 'uniroot' function in package 'rootSolve' (Soetaert 2015). The fitted parameters ( $a$ ,  $b$ ,  $c$ ) were used to obtain an estimate of below-ground carbon production (BGCP, in  $\text{g C m}^{-2} \text{ yr}^{-1}$ ) by analytically integrating equation 4.1 with respect to depth between  $x_{\min}$  and  $x_{\max}$ :

$$BGCP = \frac{\alpha}{b^2} \left( e^{-bx_{\min}} (bx_{\min} + 1) - e^{-bx_{\max}} (bx_{\max} + 1) \right) + c(x_{\min} - x_{\max}) \quad \text{Equation 4.2}$$

The quotient of above-ground to below-ground carbon production (AGCP/BGCP) was also calculated, using AGCM as a proxy for above-ground carbon production (Chapter 2). Below-ground carbon production and AGCP/BGCP were tested for differences among sites using one-way ANOVA. Influence of the controlling factors in table 4.1 (2014 only) was analysed using multiple regression. Inter-correlations, the significance of controlling factors and model fit were tested as in section 4.2.1. Six of the seven controlling factors and their interactions were included in multiple regression analysis as geological influence showed inter-correlation with N/C and was therefore removed from analysis.

### 4.2.3 Mass loss under native conditions

Litter-bag mass loss was measured at three sites representative of the gradient of saline influence; Woodbastwick represented the least saline influenced site, Strumpshaw the most saline influenced site and Wheatfen the intermediate site. These three sites had a similar hydroperiod, and as discussed in Chapter 3, all experienced increased water level following documented storm surge events. The number of sites included in this study was limited by available time for constructing the litterbags and processing samples.

Three tissue types were used: *P. australis* leaves, *P. australis* stems, and mixed below-ground tissues (roots and rhizomes of unidentified species). 'Standing dead' material (i.e., recently dead AGB) was collected from Woodbastwick, Wheatfen and Strumpshaw at the end of the growing season (October 2013), air-dried, and then separated into stems and leaves. Below-ground material was extracted manually from peat cores (length 0.5 m) after they were oven dried at 40°C; peat residue was removed by lightly spraying with UHQ (filtered to 18 MΩ cm<sup>-1</sup>). Litterbags (10 cm x 10 cm) were constructed of polyethylene mesh (aperture 1350 μm) and each bag was filled with approximately 1 g of material. An aperture of 1350 μm was used to allow access to microorganisms but excluded macro fauna and preclude the incorporation of fresh litter or peat material.

Litterbags were returned to the site of their source material, and incubated in three positions of decay (more detailed description of positions in paragraph below); air (leaves and stems only), upper and lower (all tissue types). To simulate decay of standing dead material, the litterbag in the air position was at the height of the surrounding vegetation and was never submerged by surface water. The litterbag in the upper position was at the peat surface and was submerged periodically. Lastly, the lower position was 30 cm below the peat surface and was submerged for at least 80% of the 12-month experimental period. Litterbags were deployed in March 2014 and in total, the experiment lasted for 12 months. Five replicates of each tissue type in each position at each site were collected after one, three, six and 12 months.

Water level (relative to peat surface) was recorded hourly at each site for the duration of the litterbag deployment using a Solinst Junior Levellogger (model 3001) corrected for barometric pressure. The proportion of time each litterbag was submerged between March 2014 and March 2015 was determined by calculating the number of days that water level exceeded the depth at which the litterbag was incubated. For

example, in relation to the upper position, the number of days where water level was above the peat surface (i.e. the litterbag was submerged) was determined in addition to the number of days water level was below the peat surface (i.e. the litterbag was exposed). Similarly for the lower position, the number of days water level was more than 0.3 m below the peat surface (i.e. the litterbag was exposed) was calculated in addition to the number of days water level was higher than 0.3 m below the peat surface (i.e. the litterbag was submerged).

Once litterbags were retrieved and returned to the laboratory, bags were gently sprayed with distilled water to remove peat residue and roots that had grown through the mesh were removed with tweezers. Bags were frozen for 24 hours and freeze-dried to a constant weight before being weighed to 6 decimal places (mg). A correction factor was applied to initial mass to account for relative humidity (Pouyat & Carreiro 2003). Once freeze-dried and weighed, tissue from three of the five retrieved bags was ground and weighed into tin boats and carbon and nitrogen contents (%) were determined using a Flash Elemental Analyser 1112 Series. The method follows that described in section 4.2.1.2. The C/N quotient was calculated as total carbon content (%) / total nitrogen content (%). Mass remaining (g) was multiplied by carbon content (%) to determine carbon mass remaining (g) after each collection as in Moore et al. 2011.

Table 4.3: Accuracy (%Recovery) and precision (%RSD) measurements for elemental analysis of litterbag material.

CRM	Check	N	C
Wepal IPE 176	%Recovery	104	102
Sulphanilamide	%RSD	6	4

Data for each tissue type were analysed separately and mass loss data were analysed over two different time periods, assuming that mass lost in the first month of incubation is indicative of physical leaching, whereas mass lost from one to 12 months of incubation is indicative mainly of microbial decomposition (Hietz 1992; Morris & Hughes et al. 2014). Differences in litter quality were assessed for each tissue type by ANOVA on initial C/N (one-way ANOVA across sites) and C/N at month one (two-way ANOVA across sites, positions and their interaction).

For mass loss in the first month (physical leaching only), a two-way ANOVA was used to test for differences among sites, positions and their interaction. For mass loss from

one to 12 months (microbial decomposition), a single exponential model (equation 4.3; Olson, 1963; Henman and Poulter, 2008; Quintino et al., 2009) was fit to the data using the 'nmle' package (Pinheiro et al., 2015):

$$X_t = X_0 e^{-kt} \quad \text{Equation 4.3}$$

where  $X_t$  is the proportion of initial mass ( $X_0$ ) remaining at time  $t$ , and the parameter  $k$  is a decay rate coefficient ( $\text{yr}^{-1}$ ). A two-way ANOVA was used to test for differences in decay rate coefficients among sites, positions and their interaction. For mass loss over both time periods, the influence of putative controlling factors (initial/one month C/N, proportion of year submerged, saline influence, geological influence and nutrient influence) and their interactions were analysed using multiple regression.

Spearman's rank was used to test for inter-correlations between controlling factors and where a significant result was found, the controlling factor resulting in the best model fit was retained. For leaves and BG material, saline influence and C/N were inter-correlated ( $r_s = .79$ ,  $p < 0.0001$  and  $r_s = -.96$ ,  $p < 0.0001$ , respectively). Saline influence was retained for leaves and C/N was retained for BG. For stems, submergence and C/N were significantly correlated ( $r_s = .79$ ,  $p < 0.0001$ ) and submergence was retained. Geological and nutrient influences were inter-correlated for leaves, stems and BG material ( $r_s = .99$ ,  $p < 0.0001$ ). Geological influence was retained for leaves, and nutrient influence was retained for stems and BG.

#### 4.2.4 Mass loss of transplanted material

To provide further insight on the sources of variation in mass loss across the gradient, a one-directional litterbag transplant experiment was carried out, in which tissue collected from the least saline site (Woodbastwick) was incubated at the most saline site (Strumpshaw). Together with data for *in situ* mass loss at these sites (from 4.2.3, above), three treatments were considered: Strumpshaw litter incubated at Strumpshaw (st:st), Woodbastwick litter incubated at Strumpshaw (wo:st), and Woodbastwick litter incubated at Woodbastwick (wo:wo). The transplant experiment allows separation of the effects of litter quality, i.e., the difference between (st:st) and (wo:st), and decomposition environment, i.e., the difference between (wo:st) and (wo:wo). The difference between (st:st) and (wo:wo), as in the *in situ* study (4.2.3,

above), reflects the combined effect of both litter quality and decomposition environment.

The majority of the methodology for the collection of above-ground biomass and extraction of root material follows that in section 4.2.3, however, there were two differences for the transplant experiment: (i) only two collections were made, after one month and 12 months and (ii) *Calamagrostis canescens* L. (Weber) and *Juncus subnodulosus* Schrank (1789) were also dominant at Woodbastwick in addition to *P. australis* (section 4.3.1.2) and were included in the experiment. Laboratory methods followed the procedures outlined in section 4.2.3. A two-way ANOVA was used to determine the differences among treatments, positions and their interaction for mass loss after the first month and from one to 12 months, as well as for initial C/N and C/N at month 1.

Table 4.4: Table outlining if a significant result from the two-way ANOVA should be interpreted as an effect of microenvironment, litter quality or both.

Difference	Effect
st:st minus wo:st	Litter quality
wo:st minus wo:wo	Environment
st:st minus wo:wo	Litter quality + environment

#### 4.2.5 Carbon accumulation potentials

Production to decomposition quotients were determined by dividing average production for 2014 ( $\text{g C m}^{-2} \text{ yr}^{-1}$ ) by decay rate,  $k$  ( $\text{yr}^{-1}$ ), where  $p/k$  is the asymptote for peat accumulation under the assumption of constant  $p$  and first-order decay constant,  $k$  (Clymo 1984; Thormann et al. 1999). Potentials were calculated for both the above- and below-ground components. For above-ground, production ( $P_{\text{AG}}$ ) refers to above-ground carbon mass (i.e. leaves and stems) in 2014 (RQ 4.1), which in this case is used as a proxy for annual production.  $k_{\text{AG}}$  is the average of the decay rate coefficient for leaves and stems for the lower and upper positions (determined in RQ 4.3). Below-ground production ( $P_{\text{BG}}$ ) is determined from in-growth cores (RQ 4.2), and below-ground decay ( $k_{\text{BG}}$ ) is simply the decay rate coefficient for below-ground material averages for the upper and lower positions of decay (derived in RQ 4.3).

## 4.3 Results

### 4.3.1 Quantifying above-ground carbon mass

As shown in figure 4.1, AGCM ranged between 300 and 500 g C m<sup>-2</sup> in 2013 and 200 to 400 g C m<sup>-2</sup> in 2014. Sutton was the only site not to exhibit a decrease between years and instead showed very little variation (figure 4.1). It seemed that most sites lost around 100 g C m<sup>-2</sup> between the two years. Stem density decreased between years at all sites, reducing from approximately 400 m<sup>-2</sup> in 2013 to 150 m<sup>-2</sup> by 2014. Contrary to the general pattern, stem density at Wheatfen did not decrease. Stem height ranged between 100 to 200 cm, and there was no obvious pattern between stem height and year. Notably, stem height decreased by two-thirds at Sutton between 2013 and 2014.

Table 4.5: Two-way ANOVA results.

<b>Factors</b>	<b>Df</b>	<b>F</b>	<b>p - value</b>
<i>AGCM</i>			
Site	5, 72	27	< 0.0001
Year	1, 72	60	< 0.0001
Interaction	5, 72	5	< 0.0001
<i>N/C</i>			
Site	5, 24	6	< 0.01
Year	1, 24	5	< 0.05
Interaction	ns	ns	ns
<i>Stem height</i>			
Site	5, 72	7.5	< 0.0001
Year	1, 72	6	< 0.05
Interaction	5, 72	19	< 0.0001
<i>Stem density</i>			
Site	5, 72	25	< 0.0001
Year	ns	ns	ns
Interaction	5, 72	8	< 0.0001



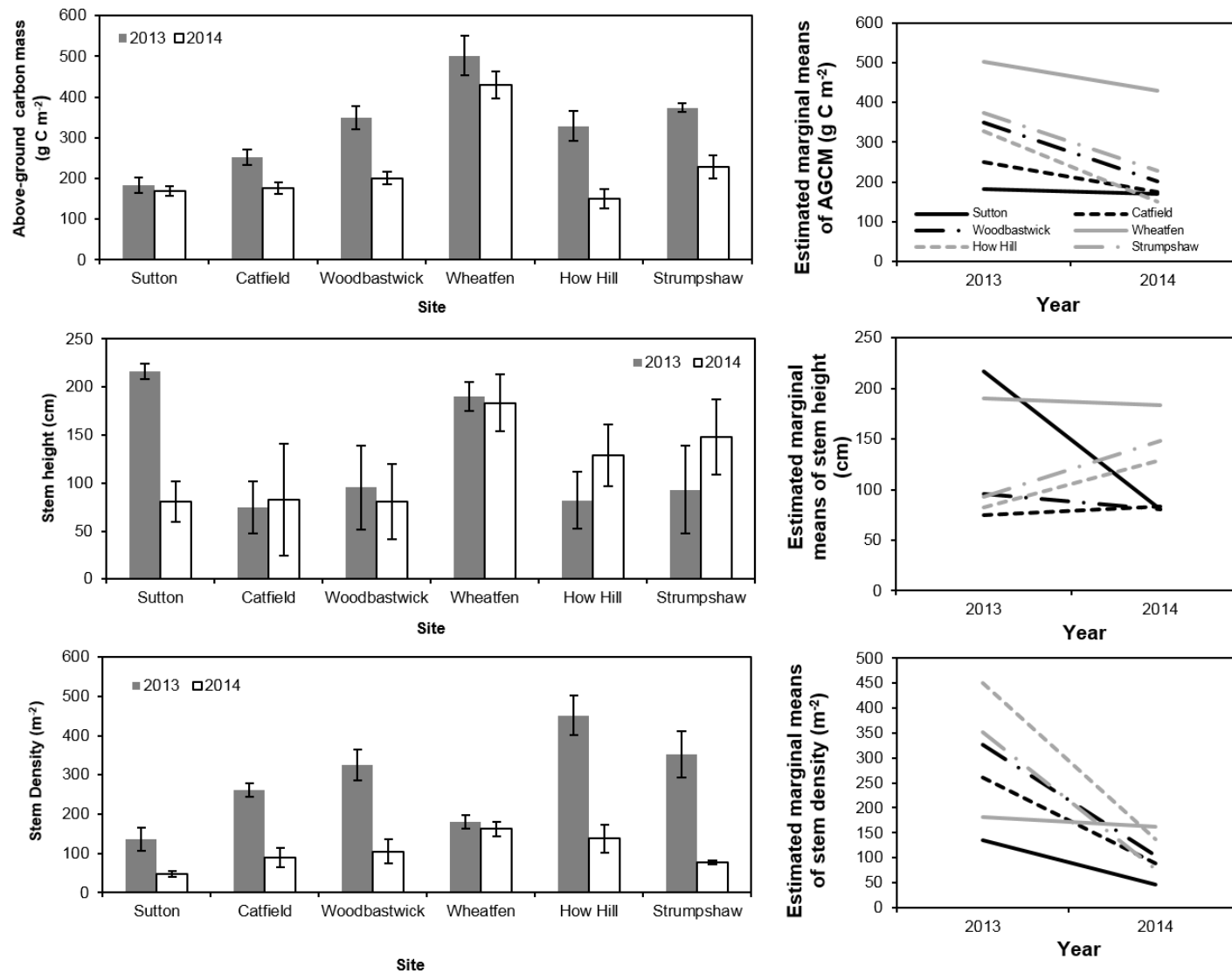


Figure 4.1: Bar charts for above-ground carbon mass (AGCM, g C m<sup>-2</sup>), stem density (m<sup>-2</sup>) and stem height (cm). Bars indicate means ( $n = 7$ ) from each site. Error bars indicate  $\pm 1$  SE. See table 4.5 for results of two-way ANOVAs. Interaction plots are also shown.

With regard to figure 4.2, sites are ordered along the x-axis according to saline influence (increasing left to right) and generally, no increase or decrease in N/C along the gradient of saline influence was apparent. A two-way ANOVA confirmed this, showing that N/C in 2014 was significantly higher than in 2013.

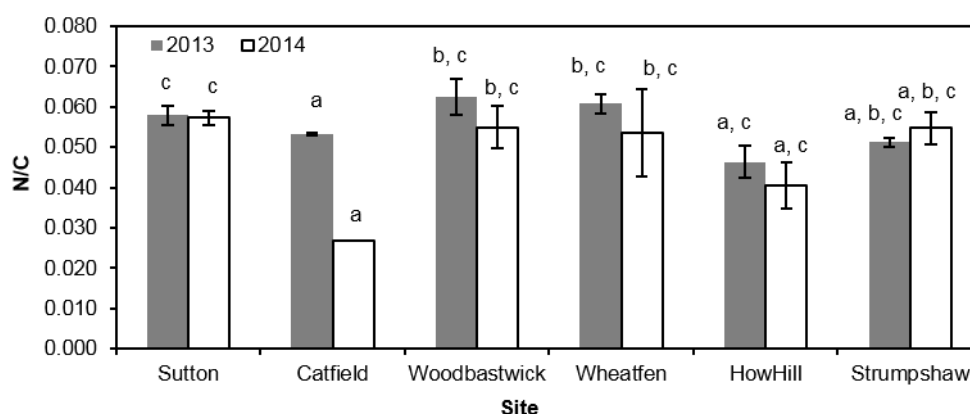


Figure 4.2: Comparison of N/C of *P. australis* leaves between 2013 and 2014. Bars indicate mean values and errors are  $\pm 1$  SE. Letters indicate groupings from Tukey HSD *post hoc* analysis. Results from a two-way ANOVA can be found in table 4.5.

PAR summed over the growing season differed little between years ( $1.25 \times 10^6$  kJ m<sup>-2</sup> yr<sup>-1</sup> in 2013 and  $1.26 \times 10^6$  kJ m<sup>-2</sup> yr<sup>-1</sup> in 2014), so variation in radiation use efficiency (RuE, g C kJ<sup>-1</sup>) largely reflects variation in AGCM. Seven independent variables and their interactions were included in the multiple regression analysis (table 4.6). RuE increased with increasing nutrient influence (figure 4.3) and cutting regime. The magnitude of the effect of cutting >3 years before harvest was almost double that of cutting 2 years before harvest. The interaction between N/C and submergence increased RuE. Scatterplots to assess model fit can be found in appendix 2.

Table 4.6: Stepwise multiple regression model of RuE. ns indicates a non-significant result. Dependent and controlling factors were standardised prior to analysis.

$\text{RuE} = b_0 + b_1.\text{Saline} + b_2.\text{N/C} + b_3.\text{Submerged} + b_4.\text{Not trampled} + b_5.\text{Trampled} + b_6.\text{Cut 2} + b_7.\text{Cut 3} + b_8.\text{Cut >3} + b_9.\text{Nutrients} + b_{10}.(\text{N/C.submerged})$				
$r^2$	<b>Df</b>	<b>F</b>	<b>p-value</b>	
0.75	10, 73	22	< 0.0001	
Predictors	Estimate	SE	t-test	p-value
(Intercept)	0.96	0.30	3.15	< 0.01
Salinity	0.384	0.072	5.292	< 0.0001
N/C	-0.05	0.21	-0.26	ns
Submerged	0.01	0.12	0.08	< 0.05
Not trampled	-0.58	0.24	-2.39	< 0.05
Trampled	-0.11	0.31	-0.36	ns
Cut 2 years before harvest	-0.65	0.17	-3.88	< 0.01
Cut 3 years before harvest	0.11	0.24	0.48	ns
Cut > 3 years before harvest	-1.17	0.19	-6.05	< 0.0001
Nutrients	0.65	0.10	6.60	< 0.0001
N/C.submerged	0.56	0.20	2.85	< 0.01

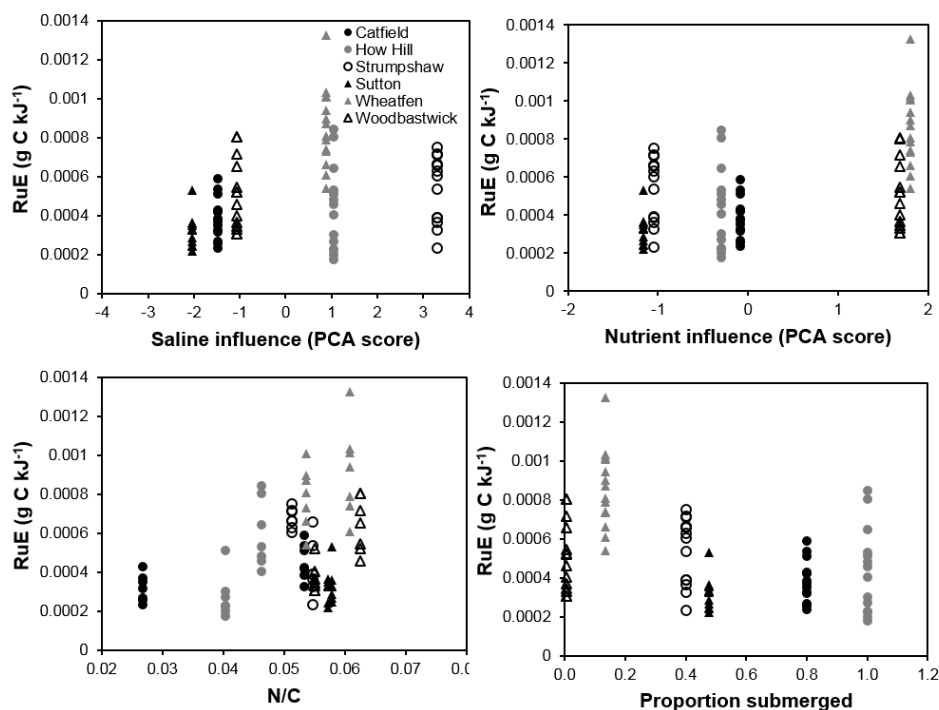


Figure 4.3: Scatterplots to show the relationship between significant controlling factors when radiation use efficiency (RuE) was the dependent variable. Points are grouped by site.

#### 4.3.2 Testing for between site variation in the contribution of species to total biomass

*P. australis* contributed the highest proportion to above-ground biomass at all sites, confirming that this species is dominant at the study sites (figure 4.4). Other species identified are outlined in table 4.7.

Table 4.7: Identified species at all sites measured in September 2013.

Species Identified
<i>Myrica gale</i> (L.) Haeckel (1866)
<i>Calamagrostis canescens</i> L. (Weber)
<i>Carex acutiformis</i> Ehrh. (1789)
<i>Cladium mariscus</i> (L.) Pohl (1809)
<i>Eupatorium cannabinum</i> L. (1753)
<i>Juncus subnodulosus</i> Schrank (1789)
<i>P. australis</i> (Cav.) Trin. ex Steud. (1841)
<i>Lythrum salicaria</i> L. (1753)
<i>Thelypteris palustris</i> Schott (1834)

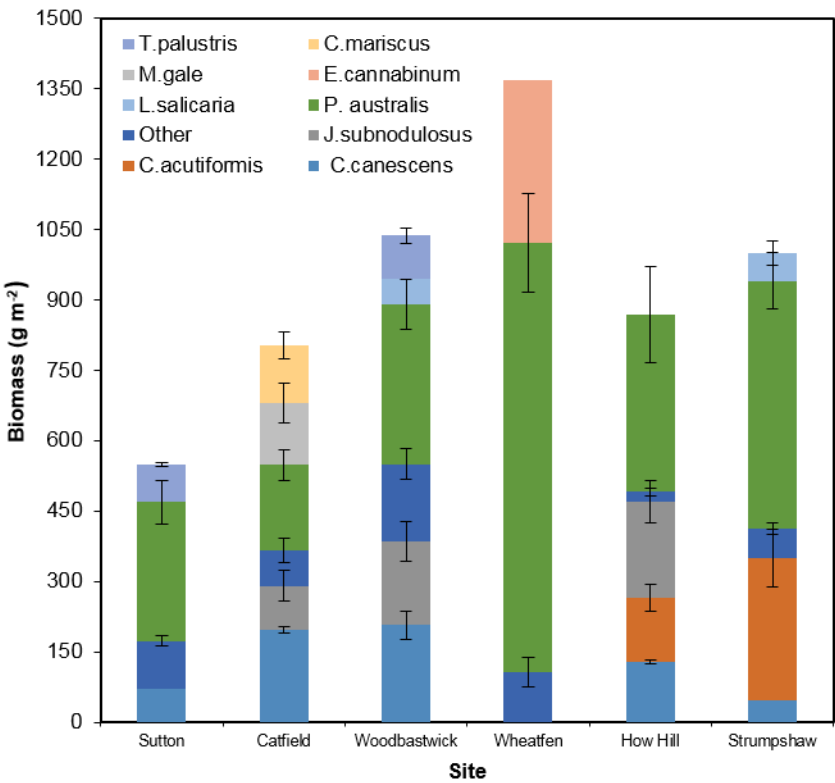


Figure 4.4: Above-ground biomass for each species identified at each of the six field sites. Data collected in September 2013. Bars indicate mean value of seven quadrats from each site. Error bars indicate  $\pm 1$  SE.

Canonical Correspondence Analysis (CCA) was used to explore the relationship between environmental variables and the proportional contribution of identified species to total biomass. As shown in table 4.8, CCA 1 explained 39% of total variance, whereas CCA 2 explained 25% and CCA 3 explained 16%. As CCA 1 and CCA 2 explain 64% of variation, only these axes were retained (Ter Braak & Verdonschot 1995). All variables apart from nutrient influence significantly explained variation in biomass when partitioned out ( $p < 0.05$ ) (table 4.8), with geological influence and trampling explaining the most variation. With reference to figure 4.5, species points, site points and arrows of the environmental variables jointly reflect the species and site distributions along each environmental variable. *L. salicaria* occurs at the higher end of the salinity gradient (figure 4.5), whereas *M. gale*, *C. canescens* and *C. mariscus* occur at high saturation. Within-site variation was low at Strumpshaw, with quadrats clustered closely together. Conversely, within-site variation was high at Woodbastwick and Catfield. *P. australis* lies at the centre of the ordination plot, indicating that it occurs everywhere.

Table 4.8: Summary of partial CCA. Proportion of total variance explained by each environmental variable when partitioned out (constrained) and variance explained by combining remaining variables (conditional). ns indicated a non-significant result.

Variable	% Constrained	% Conditional	% Unexplained	Df	F	p-value
Saline	1	42	57	1, 34	3.2	< 0.01
Saturation	5	38	57	1, 34	3.2	< 0.01
Nutrient	3	39	57	1, 34	2.0	ns
Geological	9	34	57	1, 34	5.6	< 0.01
Trampled	9	34	57	2, 34	2.7	< 0.01
Cut	4	39	57	1, 34	2.5	< 0.05

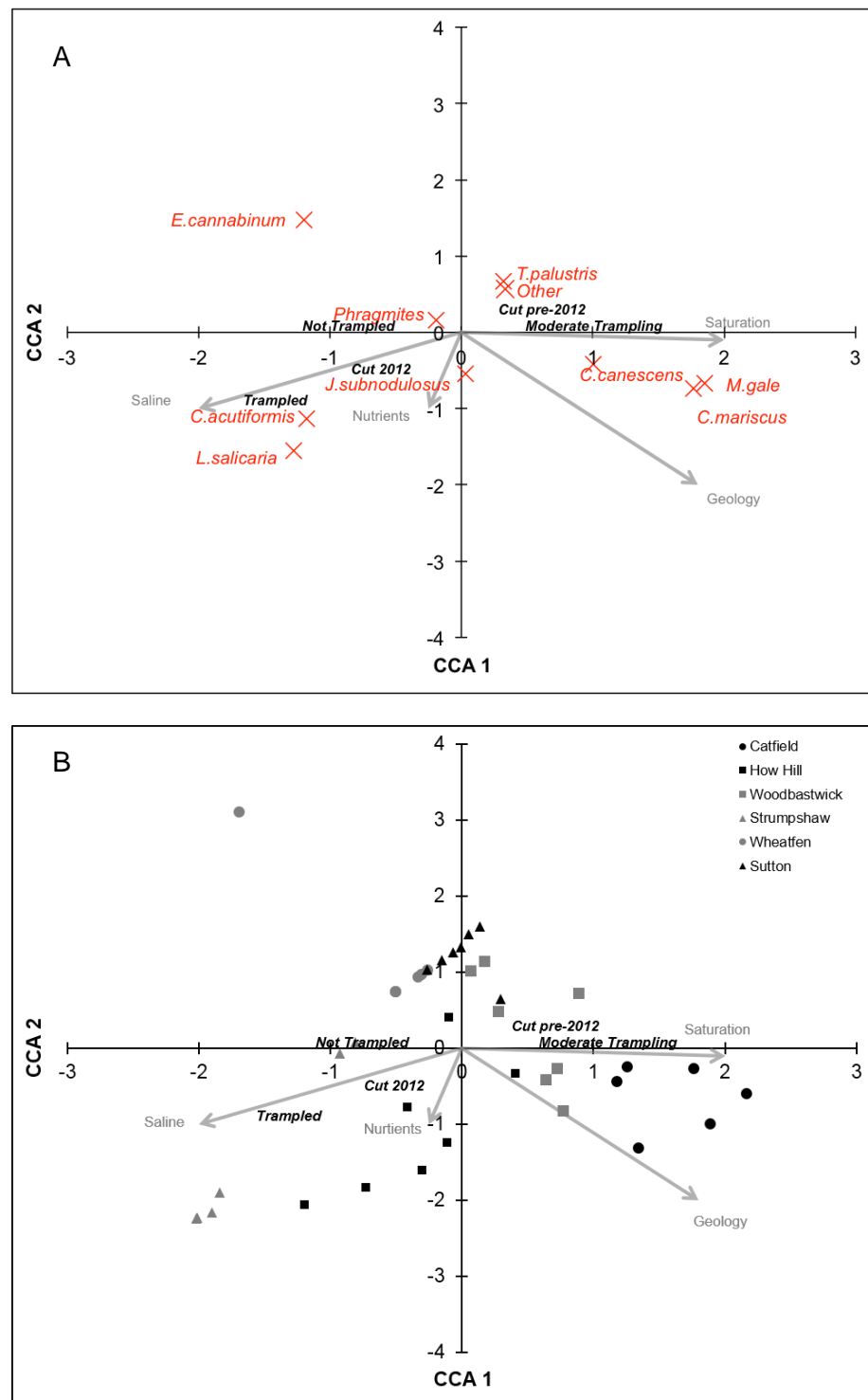


Figure 4.5: (A) species score bi-plots from CCA. Constraining environmental variables are indicated by arrows and are in grey. Centroids of categorical variables indicated by bold and italic font. (B) Site scores (indicated by points) and constraining environmental variables.

### 4.3.3 Quantifying below-ground carbon production

This section presents results related to research question 4.2. The modified Ricker function gave a good fit to the data for all cores (figure 4.6) and an example of the change in BG carbon density ( $\text{g C m}^{-3}$ ) with depth for observed and modelled data is shown in figure 4.7. There was no significant difference in net below-ground carbon production (BGCP) between sites (figure 4.8). Scatter plots (see appendix 2) indicated that none of the controlling variables affected net BGCP and this was confirmed by a non-significant multiple regression.

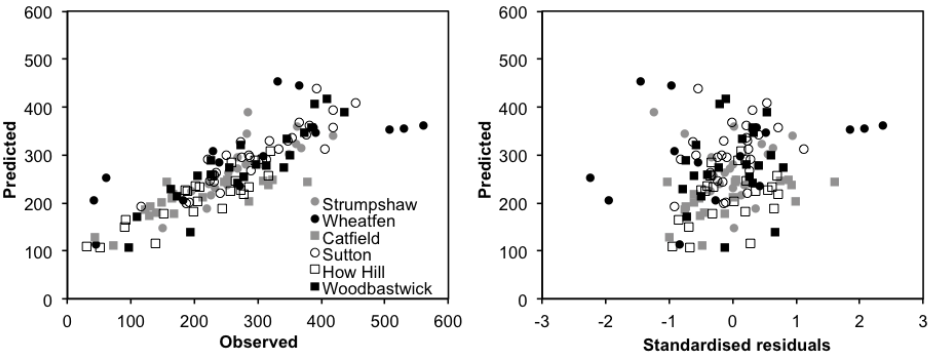


Figure 4.6: Predicted model values compared to observed data (left). Standardised residuals compares to predicted model values (right).

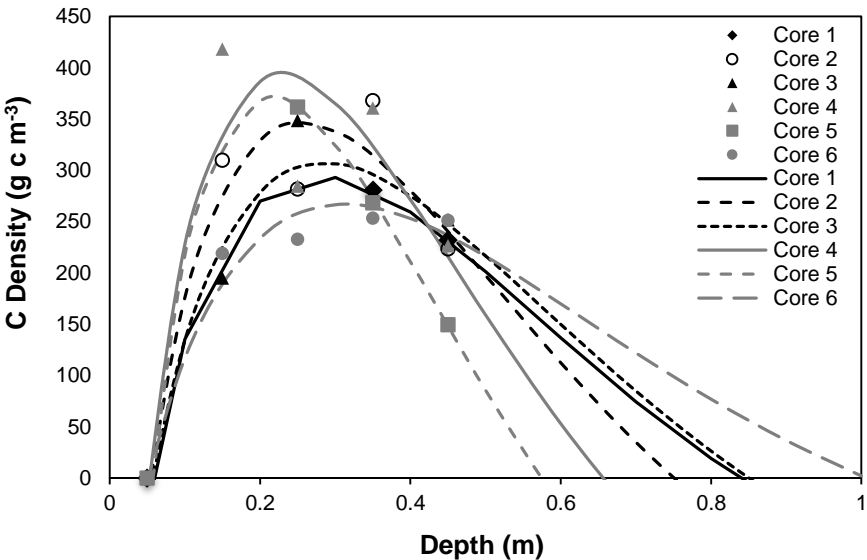


Figure 4.7: An example of below-ground carbon density ( $\text{g C m}^{-3}$ ) with depth (m). Points indicate mean observed value and error bars are  $\pm 1$  SE. Lines indicate the fitted Ricker function. Output for all cores can be found in appendix 3.

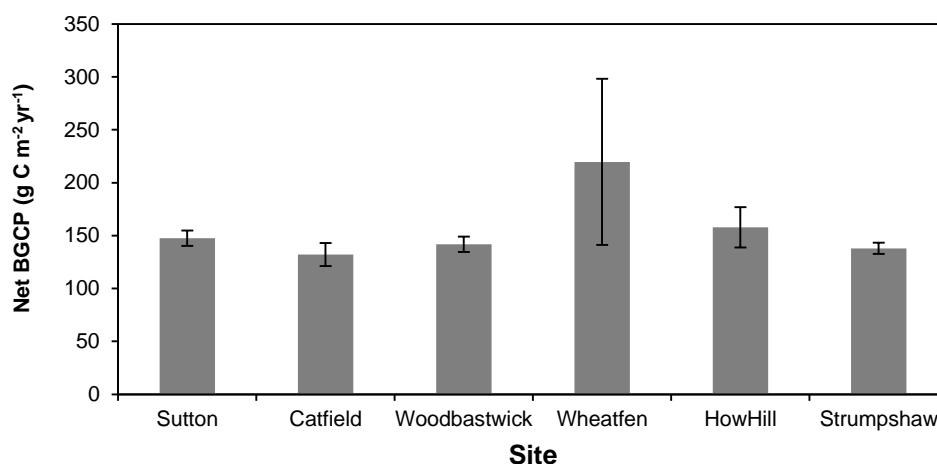


Figure 4.8: Net below-ground carbon production ( $\text{g C m}^{-2} \text{yr}^{-1}$ ). Bars indicate mean value of all cores at each site and errors are  $\pm 1$  SE. A one-way ANOVA indicated no significant difference between sites.

#### 4.3.4 Controls on ABCP/BGCP

A one-way ANOVA indicated little variation between sites, with the exception of Wheatfen where AGCP/BGCP was significantly higher (figure 4.9). Cutting tended to increase AGCP/BGCP, with cutting 2 years before harvest being the most important controlling factor overall (table 4.9). An increase in submergence and N/C both had a reducing effect (figure 4.10). It should be noted that there is no 'cut 3 years before harvest level' as this did not occur in 2014.

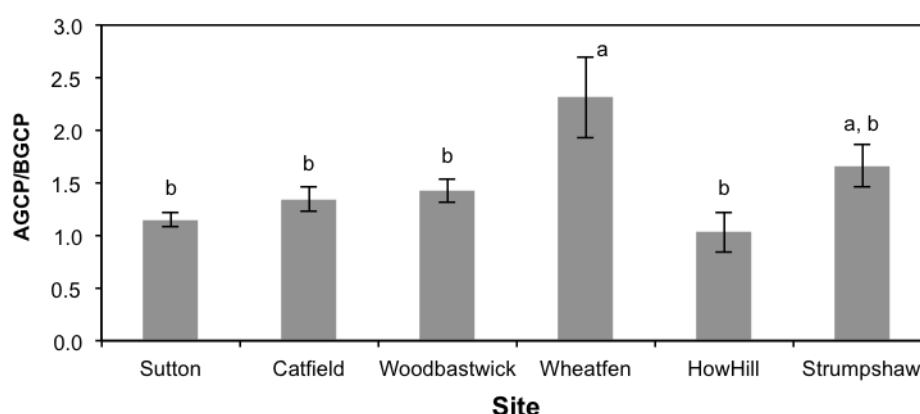


Figure 4.9: Comparison of AGCP/BGCP between sites. Bars indicate mean values ( $n = 7$ ) and errors are  $\pm 1$  SE. Results from a one-way ANOVA indicated a significant difference between site ( $F_{5, 36} = 5.0$ ,  $p < 0.05$ ). Letters indicate site groupings from Tukey HSD *post hoc* analysis.



Table 4.9: Stepwise multiple regression model of AGCP/BGCP. ns indicates a non-significant result. DVs and controlling factors were standardised prior to analysis.

AGCP/BGCP = $b_0$ . $b_1$ .Salinity + $b_2$ .Submerged + $b_3$ .Cutting <sub>2yrs</sub> + $b_4$ .Cutting <sub>&gt;3yrs</sub>				
$r^2$	<b>Df</b>	<b>F</b>	<b>p-value</b>	
0.41	4, 37	6.0	< 0.001	
Predictors	Estimate	SE	t-test	p-value
(Intercept)	-2.89	0.96	-3.00	< 0.01
N/C	-1.95	0.58	-3.36	< 0.01
Submerged	-1.12	0.26	-4.26	< 0.01
Cut 2 years before harvest	4.1	1.3	3.2	< 0.01
Cut > 3 years before harvest	2.56	0.99	2.59	< 0.05

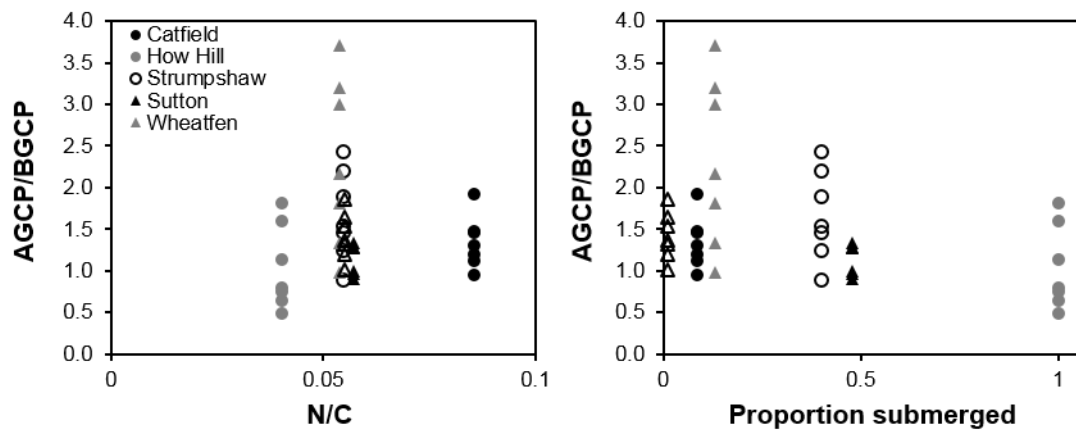


Figure 4.10: Scatterplots to show the relationship between significant controlling factors used in multiple regression when AGCP/BGCP was the dependent variable. Points are grouped by site.

#### 4.3.5 Determining controls on rate of decay of carbon mass

Mean water level was approximately 10 to 20 cm below the peat surface and was lowest at Wheatfen and highest at Woodbastwick (table 4.10). Litterbags in the lower position of decay were permanently submerged at Woodbastwick (figure 4.11) and were submerged for at least 80% of the year at Wheatfen and Strumpshaw. The litterbag in the upper position was submerged longest at Woodbastwick and least at Wheatfen. Water level fluctuated less at Woodbastwick than at Wheatfen or Strumpshaw.

Table 4.10: The proportion of the 12-month study period (March 2014 to March 2015) that the lower and upper positions of decay were either (i) submerged (Sub.) or (ii) exposed (Exp.). Water level reported in metres above peat surface (mAPS) where a minus value indicates that water level is below the peat surface. Data is presented as mean  $\pm$  1 SE.

Site	Water Level (mAPS)			Upper Position		Lower Position	
	<i>n</i>	Mean	SE	Sub.	Exp.	Sub.	Exp.
Strumpshaw	8761	-0.18	1.61E-03	0.20	0.80	0.87	0.13
Wheatfen	8761	-0.24	1.26E-03	0.06	0.94	0.81	0.19
Woodbastwick	8760	-0.10	8.27E-04	0.31	0.69	1.00	0.00

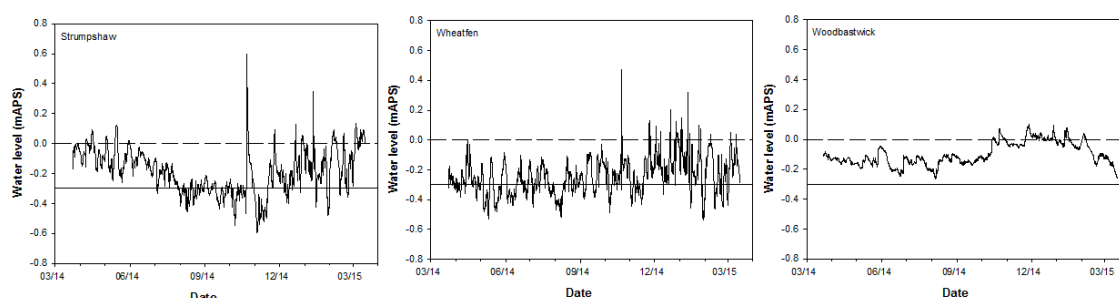


Figure 4.11: Water level in metres above peat surface (mAPS) recorded for the duration of the litterbag experiment (March 2014 and March 2015). Dashed line represents the peat surface and the solid line represents the position of the anoxic litterbag. Date is in the format MM/YY.

C/N of deployment litter (i.e. initial C/N) was used as a controlling factor in multiple regression models. As shown in figure 4.12, on average, C/N of leaves was similar to BG (around 30), and stems were slightly higher (around 50). A one-way ANOVA indicated that initial C/N of leaves was highest at Strumpshaw, and C/N of BG was lowest at Wheatfen. No significant difference was found for stems.

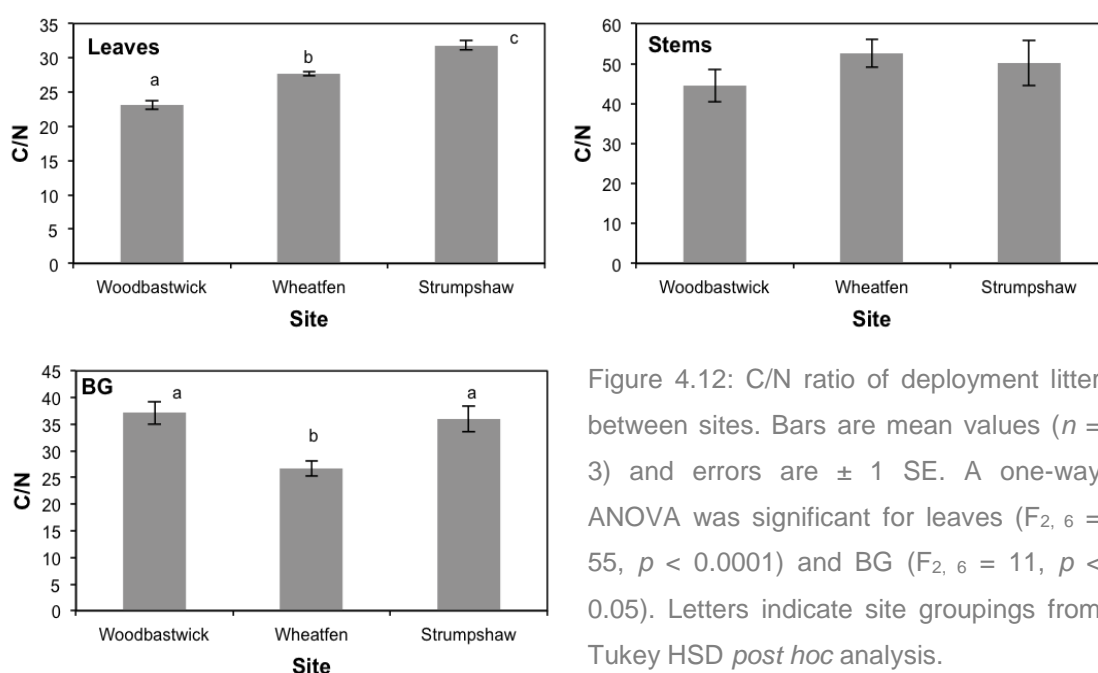


Figure 4.12: C/N ratio of deployment litter between sites. Bars are mean values ( $n = 3$ ) and errors are  $\pm 1$  SE. A one-way ANOVA was significant for leaves ( $F_{2, 6} = 55$ ,  $p < 0.0001$ ) and BG ( $F_{2, 6} = 11$ ,  $p < 0.05$ ). Letters indicate site groupings from Tukey HSD *post hoc* analysis.

#### 4.3.5.1 Mass loss after one month

Several of the litterbags collected after one month showed mass gains ( $n = 7$  at Strumpshaw,  $n = 10$  at Woodbastwick and  $n = 15$  at Wheatfen) and were removed from further analysis. Fungal growth was noticed on the majority of litterbags returned from Wheatfen and Strumpshaw in the air decay position and may explain the mass gains at these sites. Mass loss in the first month ranged between 5 and 20%. There was little difference in mass loss between the upper and lower positions for leaves, whereas substantially more mass was lost in the upper position of decay for BG material. On average stems lost the least mass (between 2 and 10%) and no significant difference was found between site, position or their interaction.

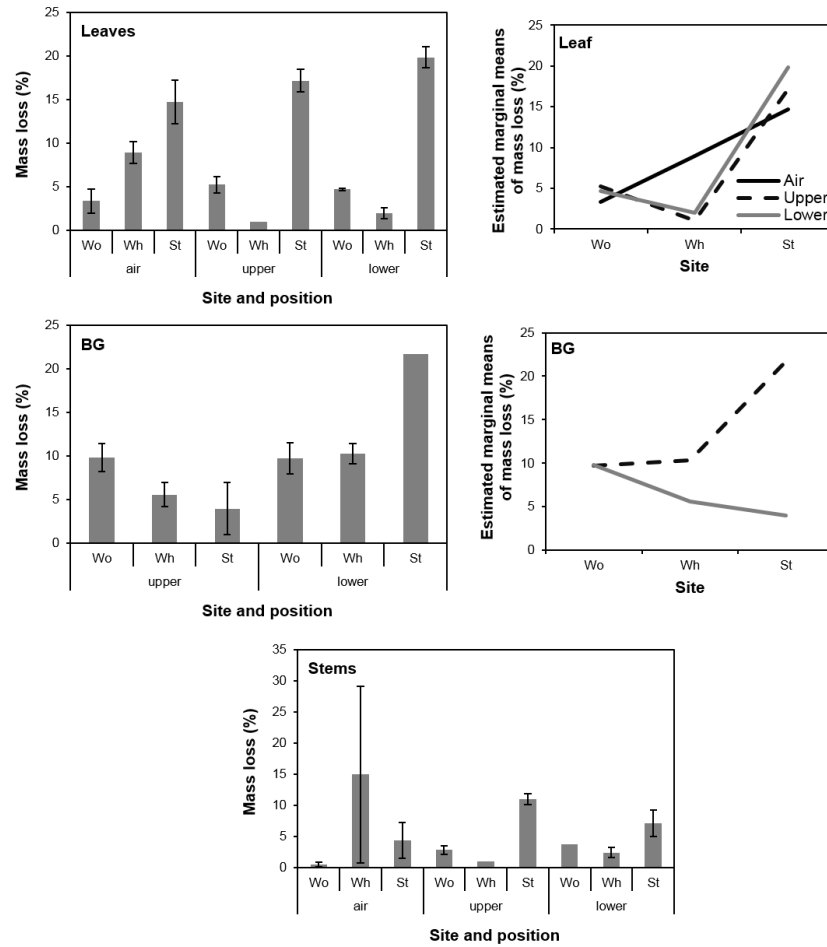


Figure 4.13: Mass loss (%) of original litter after one month of decay of leaves, stems and below-ground material (BG). Bars indicate mean values ( $n = \sim 5$ ) and errors are  $\pm 1$  SE. Results from a two-way ANOVA indicated a significant interaction between site and position for leaves ( $F_{2, 17} = 5.3$ ,  $p < 0.05$ ) and BG ( $F_{2, 26} = 7.0$ ,  $p < 0.001$ ). Interaction plots are shown to summarise significant interactions. The two-way ANOVA was non-significant for stems.

Multiple regression analysis (table 4.11) showed that submergence was the most important control for both leaves and BG material, where an increase in submergence increased mass loss for both tissue types (figure 4.14). Salinity was also an important control for leaves and BG, where an increase in salinity increased mass loss (figure 4.14). The inspection of scatter plots (appendix 2) and  $r^2$  indicated that the model fit the data reasonably well. None of the controlling factors included in the model were significant for stems.

Table 4.11: Stepwise multiple regression model of mass loss of leaves (ML<sub>L</sub>) and below-ground material (ML<sub>BG</sub>) after one month. DVs and IVs were standardised prior to analysis.

$ML_L = b_0 + b_1.Salinity + b_2.C/N + b_3.submerged + b_4.(Salinity.submerged) + b_5.(C/N.submerged)$				
<b>r<sup>2</sup></b>	<b>Df</b>	<b>F</b>	<b>p-value</b>	
0.82	5, 29	27	< 0.0001	
Predictors	Estimate	SE	t-test	p-value
(Intercept)	38.3	7.6	5.0	< 0.0001
Salinity	5.8	1.0	5.8	< 0.0001
C/N	-1.4	0.3	-5.0	< 0.0001
Submerged	21.7	7.7	2.8	< 0.01
Salinity.submerged	3.0	1.0	2.9	< 0.01
C/N.submerged	-0.8	0.3	-2.8	< 0.01

$ML_{BG} = b_0 + b_1.Salinity + b_2.Submerged + b_3.(Salinity.submerged)$				
<b>r<sup>2</sup></b>	<b>Df</b>	<b>F</b>	<b>p-value</b>	
0.5	3, 19	6.3	< 0.01	
Predictors	Estimate	SE	t-test	p-value
(Intercept)	-0.06	0.18	-0.33	ns
Salinity	-0.21	0.21	-0.98	ns
Submerged	0.81	0.20	4.02	< 0.001
Salinity. Submerged	0.74	0.23	3.16	< 0.001

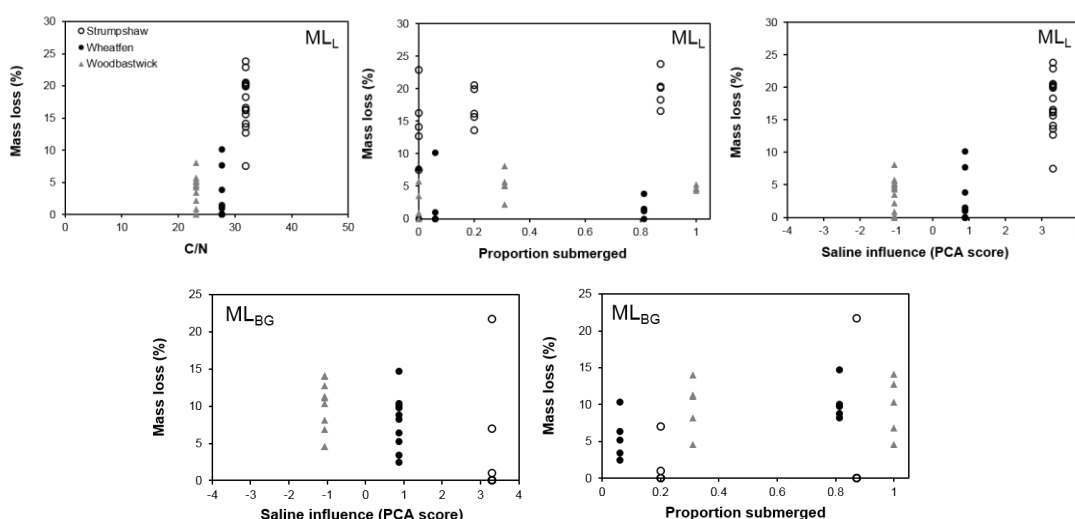


Figure 4.14: Scatterplots to show the relationship between significant controlling factors for mass loss of leaves (ML<sub>L</sub>) and below-ground material (ML<sub>BG</sub>). Points are grouped by site.

#### 4.3.5.2 Determining a decay rate coefficient for mass loss between month 1 and month 12

Several of the litterbags collected between month 1 and month 12 showed mass gains ( $n = 6$  at Strumpshaw,  $n = 11$  at Woodbastwick and  $n = 8$  at Wheatfen) and were removed from further analysis. Fungal growth was not observed on replicates after month 1 and mass gains are attributed to both the incorporation of peat material into the bag fine root growth.

A decay rate coefficient ( $k$ ) was determined for each position of decay at the three study sites for each tissue type between month 1 and month 12 (figure 4.15). The decay rate coefficient ranged between 0.05 and 0.1  $\text{yr}^{-1}$  and was highest for leaves. Leaves and stems decayed fastest at Strumpshaw (figure 4.16). The interaction plot shows that decomposition in the upper position was most variable between sites. The decay rate coefficient of BG material was not affected by position of decay.

Table 4.12: Results of a two-way ANOVA for each tissue type where decay rate coefficient was the dependent variable and site, position and their interaction were controlling factors (IVs). ns indicates a non-significant difference.

IV	Df	F	p-value
<i>Leaves</i>			
Site	2, 18	206	< 0.0001
Position	2, 18	121	< 0.0001
Site.position	4, 18	23	< 0.0001
<i>Stems</i>			
Site	2, 18	147	< 0.0001
Position	2, 18	71	< 0.0001
Site.position	4, 18	7.8	< 0.0001
<i>BG</i>			
Site	2, 12	62	< 0.0001
Position	1, 12	0.11	ns
Site.position	2, 12	0.74	ns

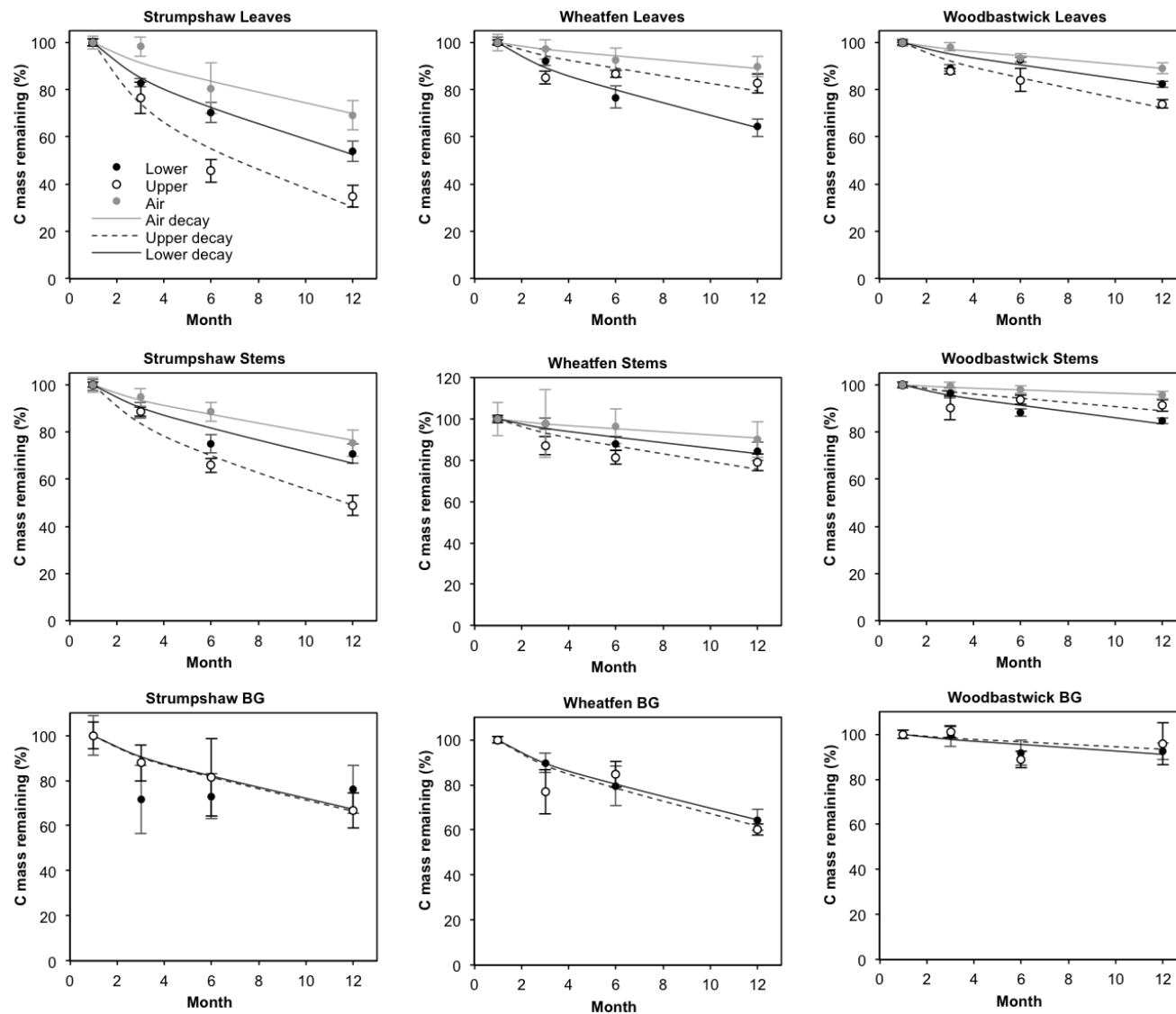


Figure 4.15: Carbon mass remaining (%) relative to carbon mass at month 1. Four collections were made over a 12 month period: 1 month, 3 month, 6 months and 12 months. Points are means and error bars are  $\pm 1$  SE (n=5). Lines are modelled decay rates derived from a single exponential model.

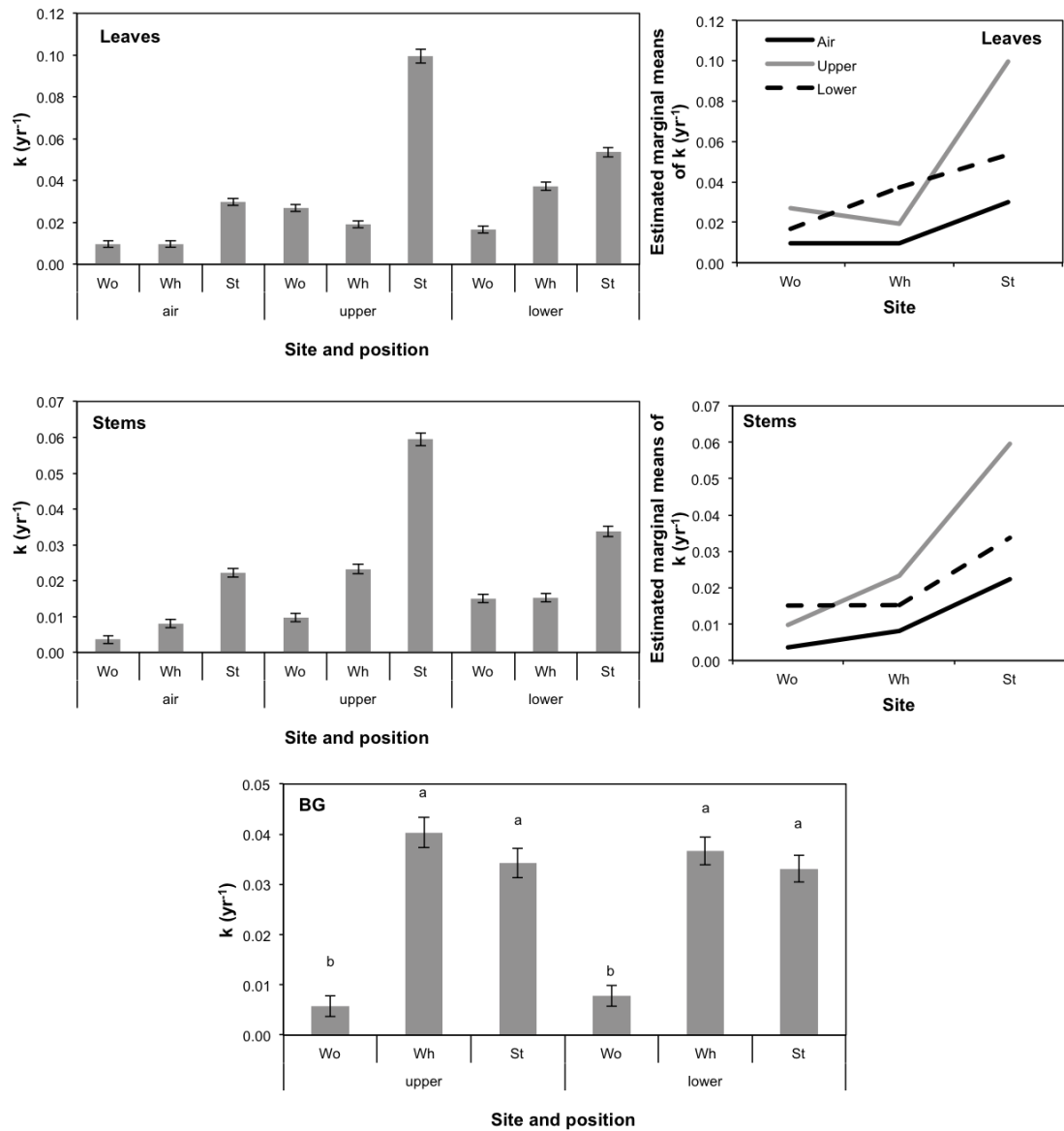


Figure 4.16: Comparison of decay rate coefficient,  $k$  ( $\text{yr}^{-1}$ ) between sites and position of decay for leaves, stems and below-ground material (BG). Coefficients were derived from a single exponential model (equation 5.6). Bars indicate the mean value and error bars indicate standard error. Letters indicate site groupings from Tukey HSD *post hoc* analysis and interaction plots are shown for those tissue types where a significant interaction was found.



Multiple regression models were found to be a good fit to the data for all tissue types through the inspection of  $r^2$  values and residual plots (appendix 2). Submergence was an important control for all tissue types (table 4.13), decreasing decomposition for leaves and BG (figure 4.17). Decay of BG material increased with nutrient influence, whereas decay of leaves increased with geological influence. C/N was not as important as other controlling variables and saline influence was an important controlling factor for stems.

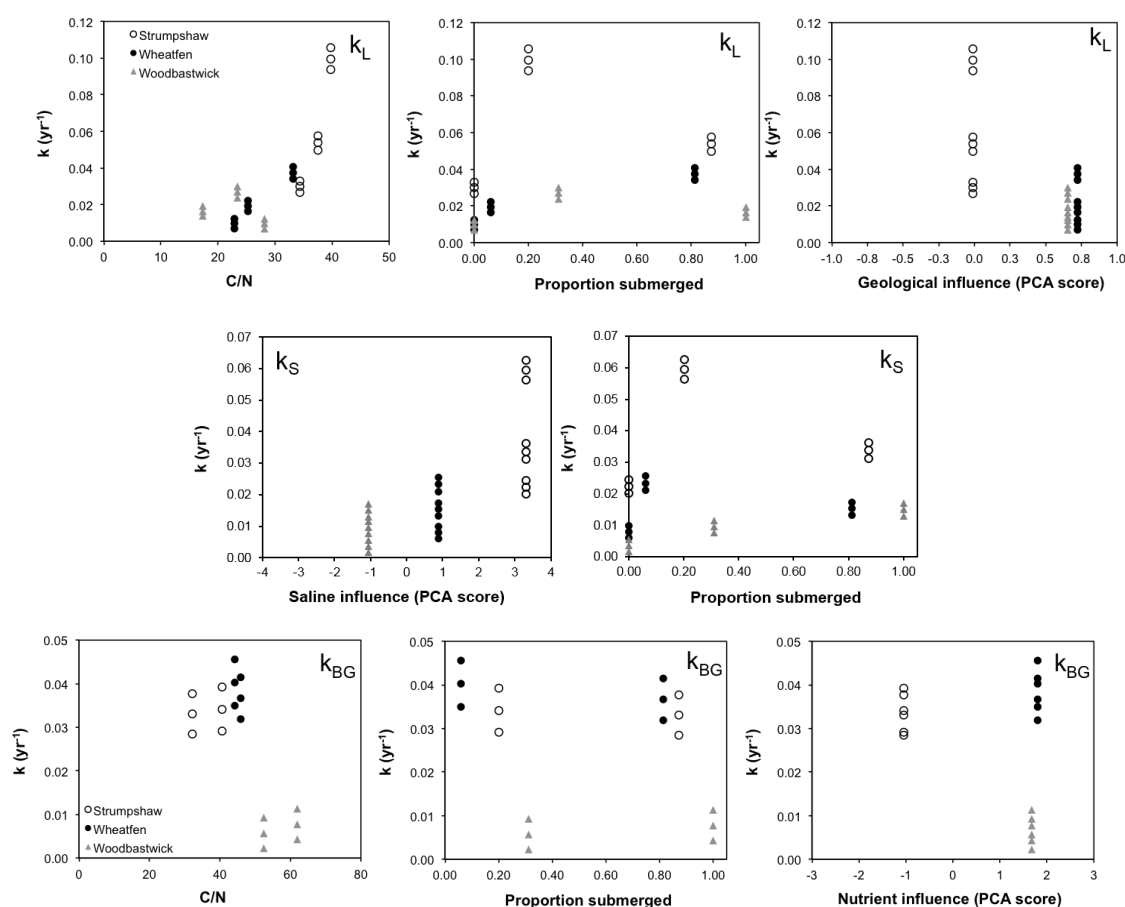


Figure 4.17: Scatterplots to show the relationship between controlling factors used in multiple regression for the decay rate of leaves ( $k_L$ ), stems ( $k_S$ ) and below-ground ( $k_{BG}$ ). Points are grouped by site.

Table 4.13: Stepwise multiple regression model decay rate coefficient of leaves ( $k_L$ ), stems ( $k_S$ ) and below-ground material ( $k_{BG}$ ) DVs and IVs were standardised prior to analysis.

$k_L = b_0 + b_1.C/N + b_2.Submerged + b_3.Geology + b_4.(C/N.submerged) + b_5.(C/N.geology) + b_6.(Submerged.geology) + b_7.(C/N.submerged.geology)$				
<b>r<sup>2</sup></b>	<b>Df</b>	<b>F</b>	<b>p-value</b>	
0.95	7, 19	54	< 0.0001	
<b>Predictors</b>	<b>Estimate</b>	<b>SE</b>	<b>t-test</b>	<b>p-value</b>
(Intercept)	-98	17	-6	< 0.0001
C/N	2.42	0.43	5.66	< 0.0001
Submerged	-127	23	-5	< 0.0001
Geology	180	32	6	< 0.0001
C/N.submerged	3.38	0.62	5.46	< 0.0001
C/N.geology	-4.86	0.87	-5.58	< 0.0001
Submerged.geology	208	38	5	< 0.0001
C/N.submerged.geology	-5.61	1.04	-5.39	< 0.0001
$k_S = b_0 + b_1.Salinity + b_2.Submerged + b_3.(Salinity.submerged)$				
<b>r<sup>2</sup></b>	<b>Df</b>	<b>F</b>	<b>p-value</b>	
0.74	3, 23	22	< 0.0001	
<b>Predictors</b>	<b>Estimate</b>	<b>SE</b>	<b>t-test</b>	<b>p-value</b>
(Intercept)	0.01	0.10	0.13	ns
Salinity	0.79	0.10	7.56	< 0.0001
Submerged	0.25	0.11	2.38	< 0.05
Salinity.submerged	-0.21	0.10	-2.01	ns
$k_{BG} = b_0 + b_1.C/N + b_2.Submerged + b_3.Nutrients + b_4.(C/N.submerged) + b_5.(C/N.Nutrients) + b_6.(Submerged.Nutrients) + b_7.(C/N.submerged.Nutrients)$				
<b>r<sup>2</sup></b>	<b>Df</b>	<b>F</b>	<b>p-value</b>	
0.94	7, 10	23	< 0.0001	
<b>Predictors</b>	<b>Estimate</b>	<b>SE</b>	<b>t-test</b>	<b>p-value</b>
(Intercept)	7.4	1.2	6.1	< 0.001
C/N	-0.149	0.028	-5.306	< 0.001
Submerged	-2.27	0.93	-2.45	< 0.05
Nutrients	6.6	1.5	4.5	< 0.01
C/N.submerged	0.051	0.021	2.405	< 0.05
C/N.nutrients	-0.151	0.036	-4.239	< 0.01
Submerged.nutrients	-2.7	1.2	-2.3	< 0.05
C/N.submerged.nutrients	0.062	0.028	2.233	< 0.05

### 4.3.6 Transplant experiment

#### 4.3.6.1 Mass loss after one month

Some litterbags collected at month 1 showed weight gains and were removed from analysis ( $n = 12$  at Woodbastwick,  $n = 11$  for litter from Woodbastwick transplanted to Strumpshaw and  $n = 7$  at Strumpshaw). C/N of *C. canescens* and *J. subnodulosus* was around 30 and C/N of other tissue types are reported in figure 4.12. Treatment was significant for leaves, stems and *J. subnodulosus* (table 4.14). An increase in mass loss of stems and leaves (for both the upper and lower positions) was seen along the gradient from wo:wo to st:st (figure 4.18). This is due to a more favourable decomposition environment, the effect of which increased mass loss between 7 and 16% (derived from figure 4.18). However, the poorer litter quality of transplanted material offsets this increase by between 1 and 3%. The result is a net increase in mass loss along the gradient of around 3% for stems and 15% for leaves. Conditions along the gradient were not favourable for the decomposition of *J. subnodulosus*, as transplanting resulted in a decrease in mass loss of between 3 and 11%.

Table 4.14: Results of a two-way ANOVA for the transplant experiment. Mass loss at month 1 was the DV. ns indicates no significant difference.

IV	Df	F	p-value
<b>Leaves</b>			
Treatment	2, 30	41	< 0.0001
Position	2, 30	6.0	< 0.05
Treatment.position	4, 30	2.5	ns
<b>Stems</b>			
Treatment	2, 23	11	< 0.001
Position	2, 23	4.9	< 0.05
Treatment.position	3, 23	0.45	ns
<b>BG</b>			
Treatment	2, 17	3.6	ns
Position	1, 17	0.90	ns
Treatment.position	2, 17	2.4	ns
<b><i>C. canescens</i></b>			
Treatment	1, 23	1.4	ns
Position	2, 23	10	< 0.05
Treatment.position	2,	2.0	ns
<b><i>J. subnodulosus</i></b>			
Treatment	1, 22	7.1	< 0.05
Position	2, 22	6.3	< 0.05
Treatment.position	2, 22	1.0	ns

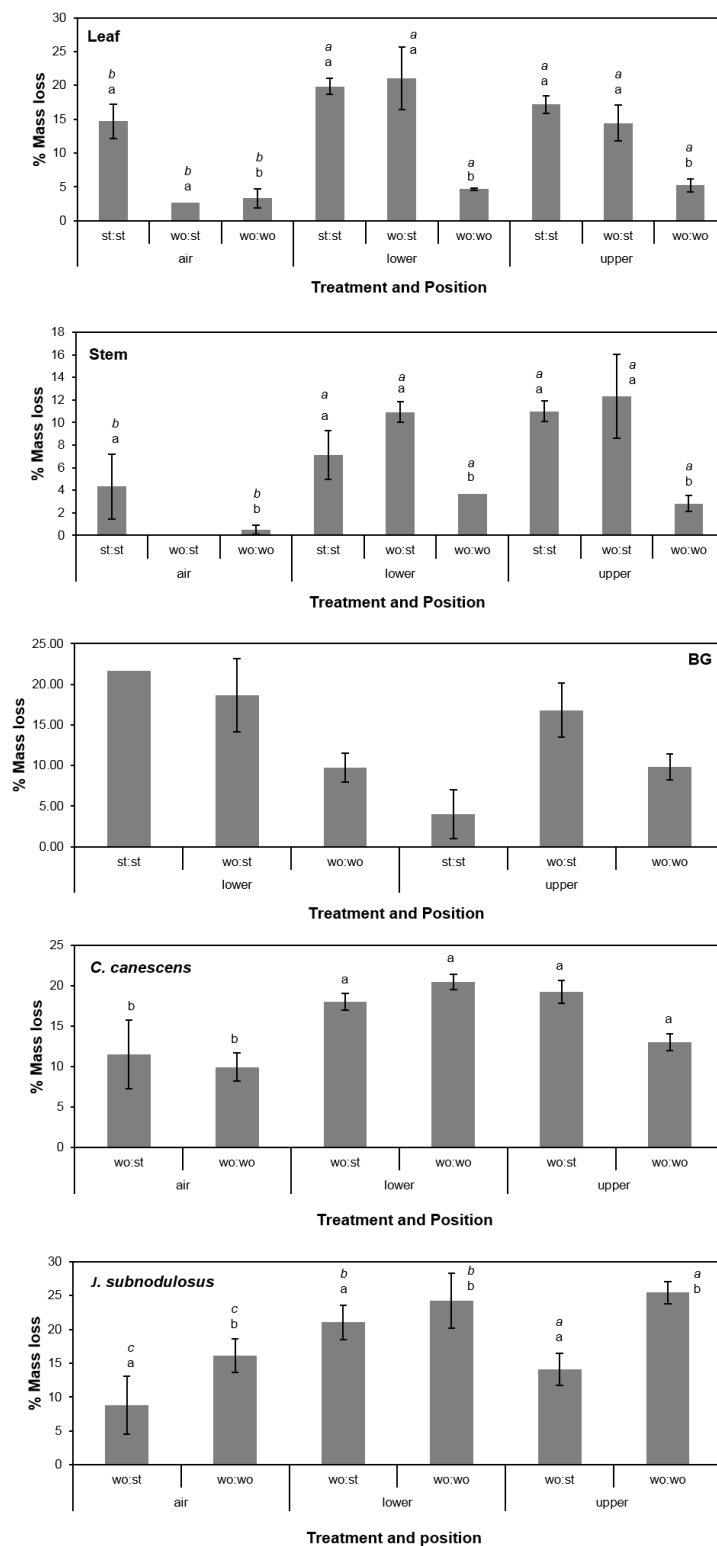


Figure 4.18: Mass loss (%) after one month of decay for each tissue type used in the experiment. Bars indicate mean ( $n = 5$ ) and errors are  $\pm 1$  SE. See table 4.1 for abbreviations of treatments. Letters indicate the output from Tukey HSD *post hoc* analysis: When significant, letters in italics are significant groupings for position and other letters indicate significant site groupings.

#### 4.3.6.2 Mass loss between month 1 and month 12

Mass gains found after collections made between 1 and 12 months were removed from analysis ( $n = 5$  at Woodbastwick,  $n = 3$  for litter from Woodbastwick transplanted to Strumpshaw and  $n = 6$  at Strumpshaw). Treatment was only a significant effect for leaves and stems (table 4.15), and patterns of mass loss were complicated by position of decay. As shown in figure 4.19, a more favourable decomposition environment along the gradient led to a 10% increase in mass loss for stems compared to 15 to 60% for leaves. In the lower position, this increase was offset to a relatively large degree by the poorer litter quality of transplanted material (36% for leaves and 1% for stems). However, in the upper position of decay, the quality of transplanted litter increased mass loss by 40% for leaves and 12% for stems.

Table 4.15: Results of a two-way ANOVA for the transplant experiment. Mass loss between month 1 and 12 was the DV. ns indicates no significant difference.

DV	Df	F	p-value
<b>Leaves</b>			
Treatment	2, 36	107	< 0.0001
Position	2, 36	82	< 0.0001
Treatment.position	4, 36	4.8	< 0.05
<b>Stems</b>			
Treatment	2, 33	33	< 0.001
Position	2, 33	27	< 0.001
Treatment.position	4, 33	5.9	< 0.05
<b>BG</b>			
Treatment	2, 14	0.56	ns
Position	1, 14	0.47	ns
Treatment.position	2, 14	0.42	ns
<b><i>C. canescens</i></b>			
Treatment	1, 24	4.0	ns
Position	2, 24	38	< 0.001
Treatment.position	2, 24	1.6	ns
<b><i>J. subnodulosus</i></b>			
Treatment	1, 23	1.1	ns
Position	1, 23	15	< 0.001
Treatment.position	2, 23	2.0	ns

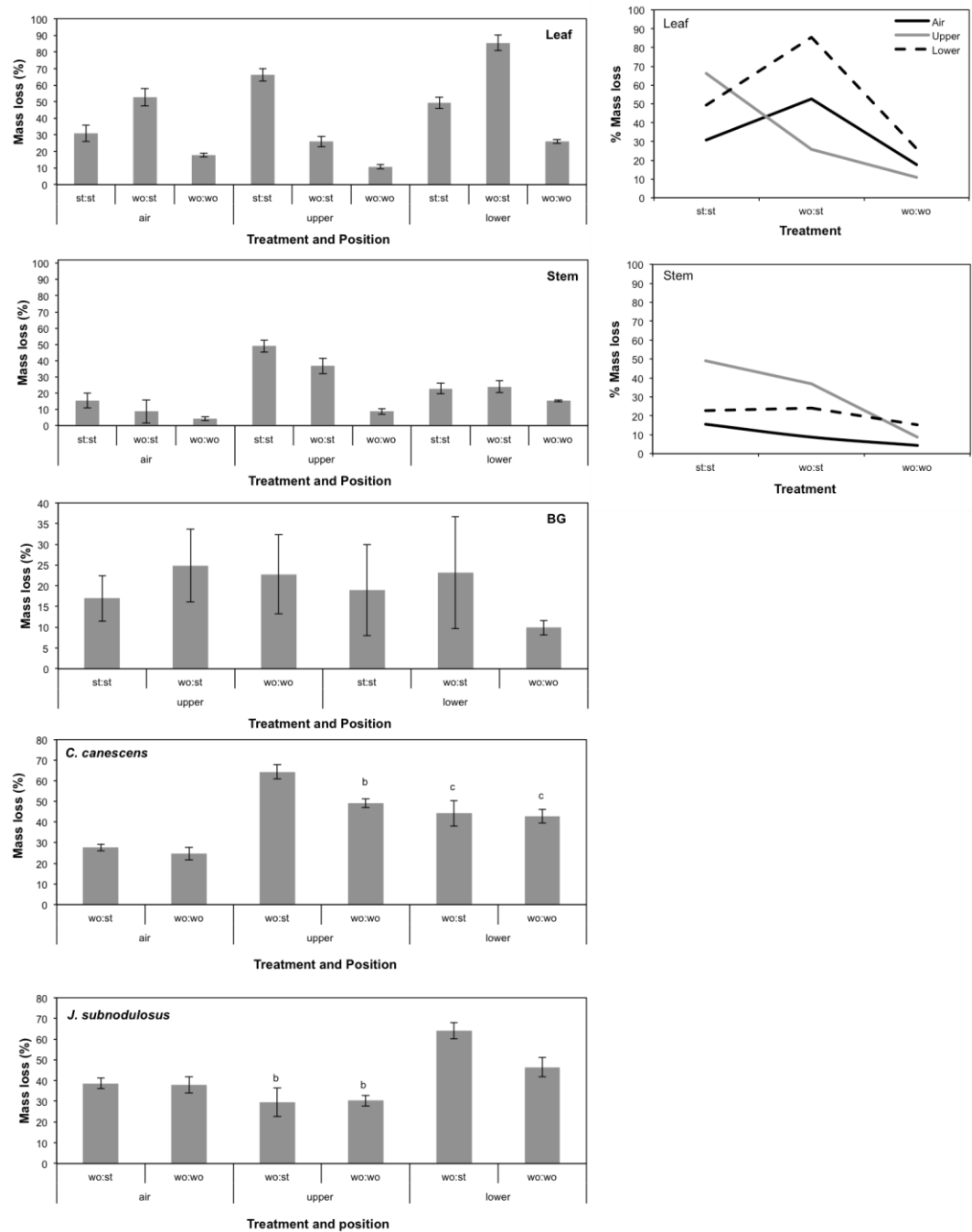


Figure 4.19: Mass loss of litter after 12 months. Bars indicate means ( $n = 3$ ) and bars are  $\pm 1$  SE. A separate two-way ANOVA was carried out for each tissue type with site, position of decay and their interaction as dependent variables. See table 4.15 for a summary of results. Letters indicate significant groupings according to Tukey HSD *post hoc* analysis. An interaction plot is shown for leaves only as this term was significant according to a two-way ANOVA.

#### 4.3.7 Carbon accumulation potentials

Carbon accumulation potentials roughly indicate that above- and below-ground components contribute equally to peatland carbon storage (i.e. figure A + figure B = total carbon storage potential). Since  $P_{BG}$  was comparable between sites (section 4.3.3), the substantially higher  $P_{BG}/k_{BG}$  at Woodbastwick must be due to a slower rate of decomposition ( $k_{BG} = 0.007 \text{ yr}^{-1}$ , versus  $0.03$  at Strumpshaw and  $0.04 \text{ yr}^{-1}$  at Wheatfen). Above-ground carbon accumulation potential showed a similar trend to  $P_{AG}$ , where Wheatfen was the most productive site (section 4.3.1). There is a large difference in  $P_{AG}/k_{AG}$  at either end of the gradient, and this corresponds with a slower rate of decomposition at Woodbastwick ( $k_{AG} = 0.02 \text{ yr}^{-1}$  versus  $0.06 \text{ yr}^{-1}$  at Strumpshaw).

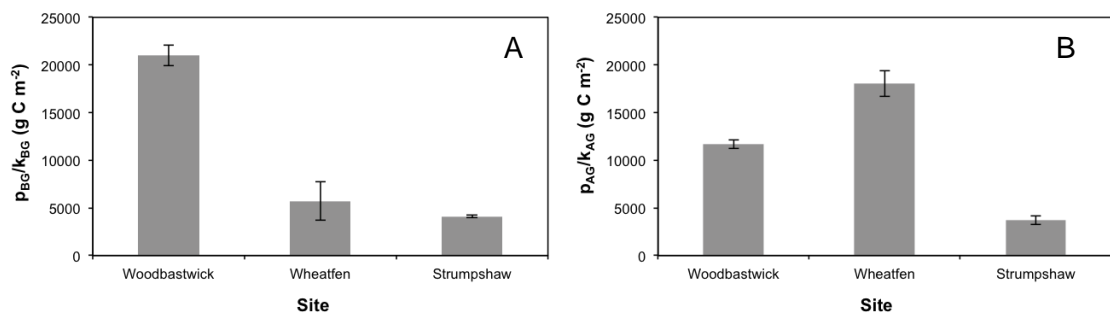


Figure 4.20: A comparison of below- (figure A) and above-ground (figure B) carbon accumulation potentials along a gradient of saline influence. Above-ground carbon production,  $P_{AG}$  (g C m<sup>-2</sup> yr<sup>-1</sup>), is from section 4.3.1 and above-ground decay rate coefficient,  $k_{AG}$  (yr<sup>-1</sup>), is the combined exponential decay rate for leaves and stems for all positions (section 4.3.5.2). Below-ground production,  $P_{BG}$  (g C m<sup>-2</sup> yr<sup>-1</sup>), is from section 4.3.3 and below-ground production,  $k_{BG}$  (yr<sup>-1</sup>), is the exponential decay rate for below-ground material combined for all positions (section 4.3.5.2).

## 4.4 Discussion

This Chapter investigated the main carbon inputs and carbon outputs to a floodplain fen, with a view to hypothesise how projected sea-level rise as a result of climate change will affect carbon storage. Measured inputs were above- and below-ground carbon production; measured outputs were above- and below-ground decomposition.

### 4.4.1 Controls on above-ground carbon production

The results in the Chapter suggest RuE is principally controlled by nutrient influence and cutting regime. Note that RuE may be an overestimate, as results in this Chapter do not account for canopy light extinction (Hilker et al. 2008), plus a bias is introduced as pre-harvest mortality is not accounted for. The decline in above-ground biomass between years is probably due to a reduction in stem density. The flood event of December 2013 is likely to have been extremely important and perhaps cleared some stems from the summer of 2013, allowing remaining stems to grow taller. Nevertheless, above-ground biomass for both years was in good agreement with other studies conducted in the Broads ( $600 \pm 120$  to  $1000 \text{ g m}^{-2}$ , Buttery & Lambert 1965, Giller & Wheeler 1986 and Boar 1996), and carbon content of *P. australis* reflected published values (Romero et al. 1999). Overall, the multiple regression model was a good fit to the data and  $H_{4.1.1}$  is partially accepted.

Cutting reed during spring or autumn has been shown in other studies to increase growth rate in the following year (Warren et al. 2001; Russell & Kraaij 2008) and this may explain why RuE in this Chapter decreased with each additional year that the reed remained uncut. The increase in RuE three years after cutting is probably an artefact of the difference in biomass between years, as this categorical level only occurred in 2013 when biomass was higher. A lack of interaction between cutting and hydrochemical variables indicates that porewater chemistry does not either exacerbate or alleviate the effect of cutting. It is therefore reasonable to assume that RuE and period between cutting and harvest will have a negative relationship.

Nutrients form important constituents of amino acids and help facilitate the formation of chlorophyll, therefore RuE is likely to be affected by nutrient availability (Engloner 2009). Nitrogen in particular is known to be important for growth (e.g. Romero et al.



1999), and this explains the positive relationship between RuE and nutrient influence. Photosynthetic capacity is related to foliar nitrogen content because proteins used in the light-dependent and independent reactions of photosynthesis represent the majority of leaf nitrogen content (Evans 1989). Water stress limits light independent reactions (Calvin cycle), as the production of glucose is the product of the reaction between water CO<sub>2</sub>, which explains why the interaction between submergence and leaf N/C have a positive effect on RuE. Nitrogen concentrations are highest in leaves that receive the highest PAR (i.e. at the top of the canopy) (Field 1983). This may bias the result if leaves are not sampled from a consistent position below the canopy. While the pooling of leaves for each quadrat may have mitigated this to some degree, there is still the potential for this to have led to a bias in the estimation of foliar nitrogen content.

Saline influence had a relatively small effect on RuE. Other studies have suggested that RuE would increase with increasing saline influence up to around 5 ppt (e.g. Mauchamp & Mesleard 2001), however, the range of salinity in the Broads is perhaps too narrow for such an effect to be noticed (0 to 0.2 ppt). Nonetheless, the results of CCA indicated that *P. australis* became increasingly dominant along the gradient of saline influence. This might suggest that in the Broads, increasing salinity is advantageous to this species, allowing it to outcompete other fen species. This trend is supported by other *P. australis* studies in environments ranging between 0 and 5 ppt (Hellings & Gallagher 1992; Yang et al. 2014).

#### **4.4.2 Exploring controls on AGCP/BGCP**

Results presented here suggest that there was no difference in below-ground carbon production (BGCP) between sites, however, the hypothesis made a priori was: nutrient availability will be a primary control on BGCP, with an increase in AGCP/BGCP observed with increasing nutrient availability. The lack of difference in BGCP between sites should be treated tentatively, as data presented here is likely an underestimate for several reasons: maximum rooting depth was inferred using the Ricker function, thus below-ground biomass may have penetrated much lower than assumed here. Ingrowth cores only capture fine root growth (Giardina & Ryan 2002), and the hessian bags become a physical barrier (Maria do Rosário et al. 2000; Scarton et al. 2002), especially as bulk density of the infill mixture was around 15% higher than bulk density found in this study (Chapter 5). Nonetheless, the results are a

good relative measure between sites, but are not necessarily comparable to the wider literature.

In comparison to other dependent variables, AGCP/BGCP was not well explained by the controlling factors used in this Chapter and results should be interpreted tentatively. It is possible that the inclusion of rhizomes may have resulted in a better model fit. The hypothesis made *a priori* was based on *P. australis* studies that look at both root and rhizome growth, albeit to varying depths (e.g. Moore et al. 2012). Nevertheless, scatterplots show that submergence and leaf N/C clearly had a reducing effect on the quotient and therefore  $H_{4.2.1}$  is rejected.

AGCP/BGCP indicates patterns in allocation between above- and below-ground organs, and cutting regime may disrupt this balance by inducing stress on the plant (Hocking et al. 1983). Since there was no significant difference in BGCP, the notable increase in the quotient two years after cutting is probably weighted by the significantly higher AGCP at Wheatfen. Since RuE decreases with increasing time since cutting (section 4.4.1), the trend toward increasing AGCP/BGCP with time since cutting is probably related to an increase in the translocation of assimilate from BG to AG organs as photosynthesis becomes less efficient (Soetaert et al. 2004; Russell & Kraaij 2008). Note that the result for RuE was based on AGCP from 2013 and 2014, whereas only 2014 was used here. In 2014, the site cut one year before harvest was also cut in 2013 (Catfield), thus the results may be showing that cutting in two consecutive years reduces AGCP to a greater extent than sites uncut for two or more years, although further research should investigate this finding further.

Since nitrogen availability plays a critical role in photosynthesis (Evans 1989), it was expected that N/C and AGCP/BGCP would have a positive relationship. N/C at Catfield biased the data, and perhaps the lower N/C at Catfield suggests that cutting over two consecutive years reduces nitrogen content in leaves, thereby reducing RuE. Submergence also showed a strong negative relationship. This is probably because increasing submergence results in the use of assimilates for lignification as opposed to growth to regulate diffusion of oxygen to the rhizosphere (Armstrong et al. 1996).

#### 4.4.3 Disentangling the effects of an increasing saline influence on plant litter decomposition

The use of litterbags and subsequent fitting of a negative exponential model is an inexpensive, simple and frequently used technique to quantify decay rate (Yu et al. 2001). Indeed, it has been exceptionally useful in this case as results from *P. australis* litter across three sites and three positions of decay confirm the slow rates of carbon decomposition in peatlands and are generally comparable to other studies (table 4.16).

Table 4.16: A summary of exponential decay constants (k) from the wider literature. Examples are drawn from peatlands and *P. australis* studies. Duration of experiments ranges between 8 months and 5 years and mesh sizes are similar to those used in this study.

Surface	Location	Country	k	Source
Tree leaves	Bog and swamp	USA	0.07 - 0.38	Moore et al. (2007)
<i>P. australis</i> shoot	Norfolk Broads	UK	0.0029	Mason & Bryant (1975)
<i>P. australis</i> leaves	Littoral reed stand	Germany	0.0045	Gessner (2000)
Shrub roots (BG)	Temperate bog & fen	USA	0.00 - 0.21	Moore et al. (2007)
<i>P. australis</i> leaves	Floodplain fen	UK	0.01 – 0.1	This study
<i>P. australis</i> stem	Floodplain fen	UK	0.005 – 0.06	This study

The sequential pattern of decay is largely determined by fiber structure, with compounds of lower molecular weight rapidly leached, whereas hemicellulose structures tend to require microbial breakdown (Berg & McClaugherty 2008). Submergence and salinity were important controlling factors of mass loss of both leaves and BG material after one month. Since the majority of mass loss in this early stage of decay can be explained by the leaching of low molecular weight compounds, it is unsurprising that submergence is a controlling factor. Other studies have shown that an increase in strong inorganic salts (such as NaCl) decreases the surface tension of organic compounds, thereby increasing the solubility of phenols (Sahu et al. 2010). This probably explains why salinity, and the interaction of salinity with submergence had an increasing effect on mass loss. The high C/N of stems gives a rough indication that this tissue is comprised of less soluble compounds than leaves

and BG material, and this perhaps explains the lower mass loss in the first month and the absence of controlling factors to some degree.

Submergence was an important controlling variable on decay rate (between month 1 and 12) for all tissue types, which is unsurprising as decomposition is retarded when oxygen is limited (e.g. Smemo & Yavitt 2007). It is well established that P and N are key macronutrients for decomposition due to their importance in sustaining microbial populations (Berg & McClaugherty 2008; Ouyang et al. 2008) - hence an increase in porewater SRP and  $\text{NO}_3^-$  accelerated decomposition for leaves and BG material respectively. The significant interaction between submergence and nutrient influence for leaves is probably related to the increase in SRP mobilisation with increasing submergence (Loeb et al. 2008). Consequently, H<sub>4.3.1</sub> is partially accepted.

Despite similar decay rates between BG and stems, only the latter was controlled by salinity. It was surprising that salinity increased decay rate due to its inhibitory effect on microbial activity from osmotic stress (e.g. Wichern et al. 2006). However, the majority of studies to support this are usually laboratory based (e.g. Malik et al. 1979; Sardinha et al. 2003). Supporting the findings here, *in situ* *P. australis* studies either show little change in decomposition at < 5 ppt (as in the Broads) (Sangiorgio et al. 2008), or remain inconclusive (Quintino et al. 2009; Connolly et al. 2014). No study has yet to compare tissue types along a gradient of saline influence, thus it remains unclear why salinity is only significant for stems. Decay rate was twice that for leaves than BG material and this difference is likely due to decomposer community, as leaf associated microbial biomass in wetlands has been shown to consist primarily (63-99%) of fungi (Hieber & Gessner 2002). Fungal activity is stimulated under elevated  $\text{Ca}^{2+}$  concentrations due to increase activity of pectin lyase, the enzyme commonly used by aquatic fungi to macerate leaves (Jenkins & Suberkropp 1995). This supports the results here, as  $\text{Ca}^{2+}$  (a component of geological influence) was shown to increase decay rate of leaves. C/N of BG was higher than leaves, and the importance of  $\text{Ca}^{2+}$  decreases with increasing lignification, suggesting that activity of pectin lyase is more limited for the decay of BG material (Berg & McClaugherty 2008). However, this is a broad conclusion as C/N alone gives a limited view of litter quality. Nevertheless, decomposition studies tend to focus on litter quality and macronutrients (Garcia-Palacios et al. 2016); here the importance of micronutrients is highlighted, as  $\text{Ca}^{2+}$  enrichment has the potential to lead to greater carbon mineralisation rates in floodplain fens.

#### **4.4.4 Separating the effects of microenvironment and litter quality**

Strumpshaw was a more favourable environment for both physical leaching and microbial decomposition. During each stage of decay, litter quality negated the effect of decomposition environment. Only stems and leaves were affected, thus H<sub>4.4.1</sub> is partially accepted. Whilst the transplant experiment aids the interpretation of litter quality and microenvironment on decomposition in natural situations, it is not possible to attribute differences in mass loss to a specific environmental parameter, for example a higher saline influence. Rather the environmental conditions of each site are taken collectively, and it should be noted that some important processes for decomposition are not included, such as peat temperature or microbial community.

It is likely that Strumpshaw is a more favourable decomposition environment due in part to a more variable water level. Other studies have shown that complex phenolic compounds of litter are broken down during dry phases, which are rapidly consumed by alternative electron acceptors following re-wetting (Freeman et al. 2001). As shown in section 4.4.3, a higher saline influence is also likely to contribute to faster decay rates, although the reason for this remains inconclusive. Higher porewater concentrations of NO<sub>3</sub><sup>-</sup> at Woodbastwick may explain the lower foliar C/N at this site and thus the poorer (i.e. more readily decomposed) litter quality (Garcia-Palacios et al. 2016). The increased period of submergence in the lower position might be the reason why transplanted litter resisted decay to a greater degree than in the upper position (e.g. Limpens et al. 2008). This indicated that regardless of litter quality, the maintenance of saturated conditions mitigates the effect of a sudden change in porewater chemistry. In the short-term, saline conditions or more frequent inundation events (i.e. a greater degree of water level fluctuation) may initially lead to faster decay rates, but longer-term changes in litter quality would partially offset these changes.

#### **4.4.5 Carbon accumulation potentials**

The most saline influenced site had the lowest carbon accumulation rates for both the above- and below-ground components and H<sub>4.5.1</sub> is rejected. Note that the derived potentials represent a crude measure of carbon accumulation as parameters are measured over a short time frame and longer-term estimations would be required to

achieve a more accurate measure. The high  $P_{AG}/K_{AG}$  at Wheatfen is maintained by high rates of production, in agreement with other studies that suggest fens are maintained by higher rates of production (Vitt 1990). However, this does not give the full picture, as the relative contribution of the below-ground component has been shown both in this study and by other authors to be important in peatland carbon accumulation (e.g. Lissner et al. 1999; Lamers et al. 2015). Since  $P_{BG}$  was similar between sites, the high  $P_{BG}/K_{BG}$  is maintained by slow rates of decomposition. Peatlands are only carbon sinks if rate of production exceeds rate of decay (van Diggelen et al. 2006), and the most saline influenced site appears to be closest to becoming a carbon source. It is estimated that approximately 30% of the global peatland carbon pool ( $20.2 \pm 2.5$  Gt C) is stored less than 5 m above sea-level (Whittle & Gallego-Sala 2016) and will therefore be vulnerable to projected sea-level rise and an increase in intensity and frequency of storm surge events (Church et al. 2013). Under these circumstances, the findings here suggest that carbon accumulation will decrease and may ultimately cease altogether - resulting in severe consequences for the global carbon balance (Yu et al. 2010).

#### **4.4.6 Implications and future work**

This Chapter has looked in detail at the controlling factors on inputs (carbon production) and outputs (rate of decomposition) to the peat carbon store. Multiple regression analysis allowed for the most important controlling variables (in terms of effect size) to be isolated. Regular cutting has been shown to be important for maintaining high RuE, however, future studies should determine whether cutting over consecutive years would eventually have a detrimental effect. Uncertainties in BGCP estimates limited the scope of the interpretation of AGCP/BGCP. It is recommended that future work use longer ingrowth cores that would ideally be filled with peat cleared of fresh organic matter residue to ensure bulk density is reflective of the specific environment. This study has provided a valuable overview of decomposition dynamics in floodplain fens, in particular confirming saline influence as a significant control on the decomposition of stems, but also that in the short term, poorer litter quality will offset an increase in mass loss due to an increase in salinity and/or water level. Indeed, both of these findings represent areas for this research to be developed in the future through the quantification of litter quality (i.e. relative contributions of fibers) and microbial community.

## 4.5 Conclusions

With respect to specific research questions in section 4.1, the following conclusions can be made from observations made in the Broads, UK:

1. RuE decreases with period since cutting, but increases with increasing nitrogen availability. The interaction between increased submergence and foliar N/C also had a positive effect on RuE. Overall,  $H_{4.1.1}$  is partially accepted.
2. AGCP/BGCP increases with time since cutting and is probably related to the translocation of assimilate from BG to AG organs as photosynthesis becomes less efficient. Although, the results could also be showing the detrimental effect on RuE of over two consecutive years. N/C had a relatively negligible effect and  $H_{4.2.1}$  is rejected.
3. Physical leaching controlled mass loss in the first month. The importance of geological influence is probably related to available  $Ca^{2+}$  stimulating microbial decay of leaves, whereas nitrogen availability was most important for BG decay. Saline influence controlled the decay rate of stems. Overall,  $H_{4.3.1}$  is partially accepted.
4. Microenvironment significantly affected mass loss, although this was partially offset by litter quality.  $H_{4.4.1}$  is partially accepted since only stems and leaves were affected.
5. Saline influenced sites have a lower carbon accumulation rate, and thus have the potential to become carbon sources under projected sea-level rise. Since both AG and BG potentials were lowest,  $H_{4.5.1}$  is rejected

## Chapter 5: Carbon stock and recent peat accumulation in three floodplain fens

### 5.1 Introduction

This Chapter reports carbon density for three sites representative of a gradient of saline influence within the Broads, UK. Peat types identified according to the criteria in Lambert (1960) are matched to a simplified version of the widely applied Troels-Smith criteria (section 2.4.2). Carbon stock for each site is quantified in addition to peat accretion and carbon sequestration rate using results from radiometric dating. The controls on carbon density are explored and recent rates of peat accretion are compared to projections for relative sea-level rise. The following research questions will be answered and hypotheses (H) tested:

**Research question 5.1:** Does carbon density and its components (bulk density and total carbon content) vary between different peat types found in three floodplain fen sites?

The components of carbon density will primarily be influenced by peat type which is generally described on the basis of botanical composition (Loisel et al. 2014). Botanical composition of peat can be affected by a variety of factors, such as nutrient availability and water level. A higher nutrient availability will result in the growth of vegetation that can be more readily decomposed, and therefore, peat will contain fewer woody components and is more likely to be homogeneous in nature (Cahoon et al. 2003). Increasing saline influence is expected to give rise to above-ground biomass more resistant to decay, which is eventually reflected in the botanical composition of the peat (Henman & Poulter 2008). Carbon content and bulk density of the peat increases with increasing recalcitrance of material (and, therefore, higher carbon density).

This study purposefully selected sites dominant in *Phragmites australis* (Cav.) Trin. Ex Steud, therefore, the range of peat types identified is not expected to differ substantially between sites. Nonetheless, bulk density and carbon content of peat types may well vary between sites due to localised factors, such as the deposition of



sediment during inundation events (that has been shown to occur in the Broads, Chapter 3) which increases compression of surface peat (Day et al. 1999). The occurrence of this process will be evident in a reduced organic matter content (or loss on ignition). Also, differences in nutrient status between sites (Chapter 3) might affect carbon content between sites, as a higher nutrient status could result in an increase in carbon decay rate (Chapter 4). The results of this section will highlight the need to account for peat type and/or local variation in peat type when determining carbon density that, in turn, is used to calculate carbon stock.

Determining parameters such as carbon content and bulk density for different peat types can be a laborious process, often resulting in the disregard of this variation in carbon stock estimates. As described in Chapter 2, Lambert (1960) extensively surveyed both peat type and depth of deposits in the Broads and created numerous stratigraphic transects. These published transects provide a unique opportunity to assign a carbon density value to peat types, and if carbon density is found to be significantly different between peat types, then the stratigraphic maps can be used to determine carbon stock without the need to make tenuous estimations of depth. However, peat types described by Lambert are specific to the Broads, therefore her descriptions are likened to a simplified version of the more widely used Troels-Smith criteria to make these findings transferable to other wetland studies so that they could apply the data in the present Chapter to their own peat types, thereby improving carbon stock estimates.

H<sub>5.1</sub>: Carbon density will vary between peat types

**Research question 5.2:** What is the carbon stock for three sites varying in saline influence in a floodplain fen?

Carbon stock estimates generally use one value for carbon density without regard for peat type (Zauft et al. 2010), and this has probably led to inaccurate estimations at a regional scale (e.g. Yu 2012). Research question 5.1 suggested that carbon density will differ between peat types and therefore, it is expected that carbon stock estimations will be improved by accounting for carbon densities of different peat types. Since estimates of peatland area are reasonably easy to obtain through digital mapping software (Jaenicke et al. 2008), uncertainties related to volume estimates are likely to be due to unrepresentative measurements of peat depth. It is intended that the results of this Chapter will improve carbon stock estimates by highlighting the

importance of obtaining accurate measurements (e.g. depth, m, and carbon density, g C m<sup>-3</sup>). Not only are the variables used in previous studies likely be too general, estimates of 'northern hemisphere' peat carbon stock have often ignored floodplain fens with a tendency to focus on ombrotrophic peatlands (Bernal & Mitsch 2012). In a broader sense, this has implications for policy makers who are probably underestimating the increasingly important role of peatlands in helping to offset anthropogenic carbon emissions.

H<sub>5.2</sub>: Peat depth and carbon density will be the most important factors for the accurate calculation of peatland carbon stock.

**Research question 5.3:** What are recent carbon sequestration and peat accretion rates at three floodplain fen sites?

Peat accretion is partly affected by rate of mass flux from vegetation to the peat, therefore the most productive sites may have a higher peat accretion rate (Vitt 1990). Although, hydrological regime is likely to affect peat accretion, since fluctuations in water level can erode surface material in lowland wetlands (Mudd et al. 2009), but also affect decomposition rate (e.g. Limpens et al. 2008). Suspended sediment concentration increases with water level, and the deposition of this material might compress underlying peat (Kirwan & Mudd 2012). Study sites in this Chapter are located within the same region and have probably experienced a similar flooding history with periods of erosion and deposition of mineral material (Lindsay 2010) – therefore, peat accretion rate is unlikely to differ between sites. It is not known if peat accretion in floodplain fens will keep pace with sea-level rise and, given projections range between 5 – 6 mm yr<sup>-1</sup> (Church et al. 2013) and accretion rates in other lowland wetland studies suggest an accretion rate of ~2 mm yr<sup>-1</sup> (Armentano & Menges 1986), it is unlikely that floodplain fen development will offset sea-level rise. Rate of carbon sequestration depends on carbon content and bulk density (i.e. carbon density) of accumulated peat (Loisel et al. 2014). Therefore, carbon sequestration rate will be highest at sites with a higher bulk density and/or carbon content of peat.

H<sub>5.3</sub>: Peat accretion will be similar between sites, whereas carbon sequestration rate will be highest at the site with the highest bulk density and/or carbon content.

## **5.2 Methodology**

Three sites representative of the gradient of saline influence determined in Chapter 3 are used in this Chapter. Woodbastwick represents the site of least saline influence, Strumpshaw the most saline influenced and Wheatfen as the intermediate site. All three sites experienced an increase in water level following documented storm surge events (Chapter 3). The extraction of cores for the identification of peat types and the extraction of cores for radiometric dating followed different field, laboratory and statistical methodologies and will be discussed separately in this section.

In relation to data analysis (summarised here for simplicity), throughout this Chapter the distribution of data was checked using the Shapiro-Wilk test in addition to the inspection of histograms, QQ plots and skewness and kurtosis. Box-cox transformations were applied when data did not conform to a normal distribution (Field 2013). All averages are presented as mean  $\pm$  1 standard error unless stated otherwise. Analysis was conducted in XLSTAT and R 3.4.1 (R Core Development Team 2014).

### **5.2.1 Determining carbon density for different peat types**

This section outlines field, laboratory and statistical methodologies to answer research questions 5.1 and 5.2.

Peat stratigraphy was characterised at Woodbastwick, Wheatfen and Strumpshaw using transects published by Lambert (1960). Five cores were extracted from each site using a 5 cm gouge corer until the mineral base was reached. The use of a gouge corer can disturb the peat profile and introduce a bias to bulk density measurements. The limitation of this method is discussed in section 5.4.1. Cores were extracted at evenly spaced intervals to cover as much of the transect as possible. Occasionally, the exact location of Lambert's transect could not be used due to access restrictions. Where this occurred, a parallel transect as close as possible to Lambert's was used. Changes in stratigraphy were identified according to categories recorded on Lambert's transect maps. Each of Lamberts categories was related to descriptions according to a simplified version of the Troels-Smith method (table 5.1) (Kershaw 1997; Troels-Smith 1955). For the latter method, the proportion of each component

(woody detritus, herb detritus, fine detritus, humus and clay) was recorded as 1%, 25%, 50%, 75% or 100% of the peat matrix. Mineral particles were recorded (<0.002 mm = clay, 0.002 - 0.06 mm = silt, 0.06 - 2mm = sand and > 2mm = gravel). Structure was also described as: fibrous, sub-fibrous, granular, heterogeneous, coarse or very coarse. Degree of humification was assessed using the von Post method and peat colour was noted using a Munsell chart (Chambers et al. 2010).

The top of each horizon was subsampled for bulk density and elemental analysis. A subsample was also extracted for pH and one for electrical conductivity (EC) and each was placed into separate containers and homogenised with UHQ (filtered to 18 MΩ cm<sup>-1</sup> at 25 °C). A pH probe was inserted into one container and an EC probe into the other. Readings were recorded when stabilised.

Table 5.1: Criteria for describing peat stratigraphy as in Lambert (1960).

Lambert Peat Type	Abbreviation	Lambert Description	von Post	Colour	Corresponding Troels - Smith
Phragmites Communis	PC	Tough, fibrous, cohesive, amorphous Massive intertwined roots, rhizomes and stems	2 to 9	Straw Yellow to grey-black with increasing humification	Fibrous: Predominantly fine detritus with some herb and woody detritus
Brushwood 'typical'	B	Incoherent with granular ground mass Including twigs and wood fragments of a mixture of sizes	6	Red-brown	Fibrous: Generally even mixture of fine and herb detritus.
Brushwood 'soft'	BS	Incoherent with granular ground mass including twigs and smaller wood fragments than BF	7	chocolate-brown	Fibrous: More herb than fine detritus in BS than B
Brushwood 'fibrous'	BF	Incoherent with granular ground mass including twigs and large wood fragments	9	black-brown	Fibrous: Woody detritus dominates in BF
Highly Humified Surface Peat	HHS	Incoherent Occasional root stock	8 to 10	black-brown to black	Heterogeneous: Predominantly humus with some fine detritus
Nekron Mud	NM	Partial decay of peat which pools at bottom of core with a gel-like texture	10	Black	
Clay	C	Dense, solid and incoherent	NA	Grey	Heterogeneous: Clay, very little woody or herb detritus incorporated into matrix

A Flash Elemental Analyser 1112 Series was used to obtain total carbon (TC) and total nitrogen (TN). Peat was ground to a fine powder before being weighed into tin boats prior to analysis. Weights were recorded to 6 decimal places (mg) and all equipment was acid washed in 10% HCl. A certified reference material (CRM) was used to measure accuracy: Wepal ISE 865 (loam soil; 40 g kg<sup>-1</sup> C and 3.31 g kg<sup>-1</sup> N; Wageningen University, The Netherlands) and average recoveries < 90% or > 110% were rejected. Sulphanilamide (16.23% N and 41.81% C; Thermo Scientific) was used as a drift check and average relative standard deviation (%RSD) was calculated to determine the precision of the instrument (Table 5.2) and deviations > 10% were rejected.

Table 5.2: Accuracy (%Recovery) and precision (%RSD) measurements for elemental analysis of peat.

CRM	Check	N	C
Wepal IPE 176 (peat)	%Recovery	98	110
Sulphanilamide (peat)	%RSD	4	2

For bulk density of peat types, samples of known volume were weighed and oven dried at 100°C for 12 hours (Chambers et al. 2010). Sample volume was calculated from the diameter of the corer (5 cm) and the length of the sample (4 cm). Bulk density was calculated as:

$$\rho_d = \frac{M_{dry}}{V} \quad \text{Equation 5.1}$$

where  $\rho_d$  is dry bulk density (g cm<sup>-3</sup>),  $M_{dry}$  is the mass of dry peat (g) and  $V$  is the volume of the sample (cm<sup>3</sup>). To obtain percentage organic matter (%OM), samples were weighed and placed in the muffle furnace at 550°C for 4 hours (Chambers et al. 2010) before being cooled in a desiccator. Samples were re-weighed and %OM was calculated as:

$$OM = \frac{M_{dry} - M_{ash}}{M_{dry}} \cdot 100 \quad \text{Equation 5.2}$$

where  $M_{dry}$  is the mass of dry peat (g) and  $M_{ash}$  is the mass remaining after ignition of the peat sample (g).

Total carbon derived from elemental analysis includes organic and inorganic components. Organic matter is high in peat accumulating ecosystems and is assumed to account for the majority of carbon (Chambers et al. 2010). Therefore, a linear

regression was applied to total carbon data derived from the elemental analyser and organic matter data derived from loss on ignition (Olefeldt et al. 2012). The distribution of the data followed a normal distribution and model fit was checked through inspection of residuals and  $r^2$ . A significant relationship was found (figure 5.1) therefore, it was concluded that total carbon was an appropriate estimate of organic carbon in peat samples used in this Chapter. The y-intercept indicates the inorganic C component, which in this case is around 7%.

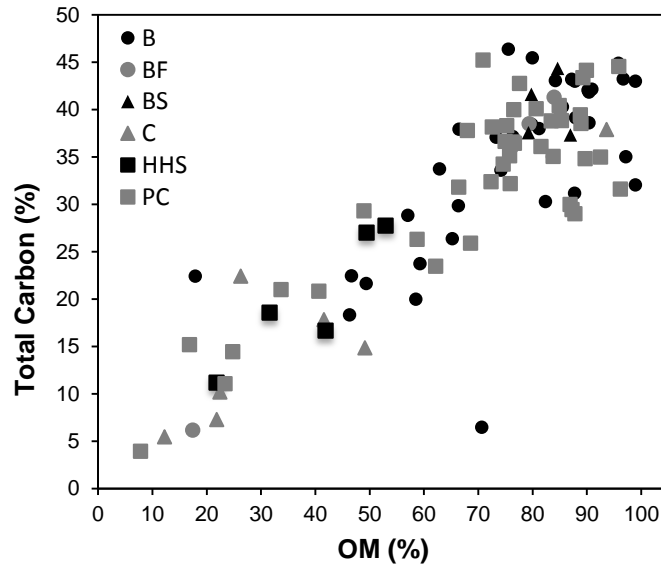


Figure 5.1: The relationship between organic matter derived from loss on ignition and total carbon derived from elemental analysis. Solid line indicates a significant linear regression result ( $F_{1, 96} = 259$ ,  $p < 0.0001$ ) where  $r^2 = 0.73$ . Linear regression equation: Total carbon (%) =  $0.36 \cdot (\%OM) + 7$ .

In this study, carbon density is defined as carbon content per unit volume of peat (i.e.  $\text{g C cm}^{-3}$ ) as in Bauer et al. (2006) and Bernal & Mitsch (2008). Carbon density was calculated as:

$$\rho_{cd} = \rho_{bd} \cdot C \quad \text{Equation 5.3}$$

where  $\rho_{cd}$  is carbon density ( $\text{g C cm}^{-3}$ ),  $\rho_{bd}$  is bulk density ( $\text{g cm}^{-3}$ ) and  $C$  is proportion of carbon determined from elemental analysis (section 5.2.1.2).

Carbon content (%), bulk density ( $\text{g cm}^{-3}$ ) and carbon density ( $\text{g C cm}^{-3}$ ) were compared using linear mixed effect models, which allow for variation in response

variables to be accounted for using fixed and random effects. Depth below the surface, site and peat type (based on Lambert's criteria, table 5.1) were fixed effects and core was a random effect. The interactions between fixed effects were also included in the model. Pairwise comparisons were conducted for significant results. The dependent variables were normalised and standardised prior to analysis. The lmer function was used from the package lme4 (Bates 2010). As  $r^2$  values cannot be calculated for mixed-effects models, Nash Sutcliffe model efficiency (NSE) coefficients were used to compare observed and predicted data (Nash & Sutcliffe 1970; Kandel et al. 2013; Eickenscheidt et al. 2015). Measures of model efficiency determine the predictive power for a given model, where a value of 1 indicates that the modelled data is a perfect fit to observed data. The significance of fixed effects was determined using maximum likelihood estimation as  $p$ -values for individual model coefficients are not estimated in the 'lmer' function (Bates et al. 2014). Note, for the interpretation of categorical variables, the lmer function takes the level of the categorical variable that is first alphabetically as the reference level (Brushwood peat, in this case).

Carbon stock for each site was calculated by multiplying carbon density by volume of peat, with the latter inferred from Lambert's published stratigraphic transects (appendix 4):

$$C_{stock} = \frac{\sum V_{sub} \cdot \rho_{cd}}{1 \cdot 10^{-12}} \quad \text{Equation 5.4}$$

where  $C_{stock}$  is carbon stock for each site (Mt C),  $V_{sub}$  is the volume of each subsection ( $m^3$ ),  $\rho_{cd}$  is carbon density ( $g \text{ C } m^{-3}$ ) (equation 5.3) and  $1 \cdot 10^{-12}$  is a conversion factor from g C to Mt C.  $V_{sub}$  is calculated as:

$$V_{sub} = W \cdot D_{sub} \cdot L_{sub} \quad \text{Equation 5.5}$$

where  $W$  is site width (m), measured using Digimap® (2015),  $L_{sub} = 50$  m and refers to the length of the subsection of Lambert's transect (m) and  $D_{sub}$  is the depth of each subsection (m). As there was no associated statistical error associated with these measurements, logical estimates to account for methodological error were made. The fractional uncertainty ( $\sigma_{cs}$ ) of the carbon stock estimate ( $C_{stock}$ ) was determined as:

$$\frac{\sigma_{cs}}{C_{stock}} = \sqrt{\left(\frac{\sigma_v}{v}\right)^2 + \left(\frac{\sigma_{cd}}{\rho_{cd}}\right)^2} \quad \text{Equation 5.6}$$

Where  $v$  is site volume ( $m^3$ ) and  $\sigma_v$  is the associated error.  $\rho_{cd}$  and  $\sigma_{cd}$  are the mean and associated error of carbon density, respectively.



### 5.2.2 Carbon sequestration and peat accretion rate

This section outlines field, laboratory and statistical methodologies to answer research question 5.3.

One core (50 to 70 cm in length) in a randomly selected location along Lambert's transect as used for research question 1 was extracted from Woodbastwick, Wheatfen and Strumpshaw in August 2014 using a polyvinyl chloride (PVC) pipe of 20 cm in diameter. To avoid compaction, peat was sliced with a knife around the edge of the pipe to cut through roots. The pipe containing the peat was lifted out and capped with PVC lids.

On return to the laboratory, cores were frozen and sliced into 1 cm increments using a bandsaw. Five subsamples were removed from each disk using a hole-saw of 3 cm in diameter. For each core individually, bulk density was analysed in triplicate for each disk as in section 5.2.1.2 and was calculated using equation 5.1. The fourth subsample from each disk was freeze-dried and ground for elemental analysis and follows the method outlined in section 5.2.1.2. Elemental analysis was not conducted in triplicate for total carbon and total nitrogen because %RSD of triplicates from stratigraphic analysis (section 5.2.1.2) was < 10% for the majority of samples. The CRM used to measure accuracy was Wepal ISE 865 (loam soil; 40 g kg<sup>-1</sup> C and 3.31 g kg<sup>-1</sup> N; Wageningen University, The Netherlands) (table 5.3). As in section 5.2.1.2, the relationship between total carbon derived from the elemental analyser and organic matter was significant (appendix 5). Data was transformed prior to analysis to ensure conformation with a normal distribution and the quality of the model fit was checked through inspection of residuals. In comparison to the long cores (section 5.2.1.2), the slope was steeper but the y intercept was lower (Total carbon (%) = 0.47.(%OM) + 2), indicating the presence of less inorganic material in the dated cores.

Table 5.3: Accuracy (%Recovery) and precision (%RSD) measurements for elemental analysis of peat samples for radiometric dating.

CRM	Check	N	C
Wepal ISE 865	%Recovery	96	104
Sulphanilamide	%RSD	2	0

Once freeze-dried, the fifth and final subsample was used to determine carbon sequestration and peat accretion rate through the measurement of  $^{210}\text{Pb}$  ( $T_{1/2} = 22.6$  years), a naturally occurring isotope which is originally derived from  $^{238}\text{U}$  and is a member of the  $^{226}\text{Ra}$  decay chain (Álvarez-Iglesias et al. 2007).  $^{210}\text{Pb}$  was measured in peat samples through both  $^{210}\text{Pb}_{\text{supported}}$ , a product of natural *in situ*  $^{238}\text{U}$  degradation, and  $^{210}\text{Pb}_{\text{unsupported}}$  from the decay of  $^{210}\text{Pb}$  deposited from the atmosphere.  $^{210}\text{Pb}_{\text{unsupported}}$  is calculated by subtracting  $^{210}\text{Pb}_{\text{supported}}$  from  $^{210}\text{Pb}_{\text{total}}$ . Chronology is calculated through the application of the constant rate of supply (CRS) model (Appleby & Oldfield 1978; Cundy et al. 2003) which assumes that the rate of supply of  $^{210}\text{Pb}_{\text{unsupported}}$  is constant. The constant initial concentration (CIC) model is another approach, which suggests a constant initial concentration regardless of accumulation rate (Appleby & Oldfield 1978).

The anthropogenic radionuclide  $^{137}\text{Cs}$  ( $T_{1/2} = 30$  years), which is produced from nuclear weapons testing and nuclear plant accidents, had a peak fallout in 1964 from nuclear weapons testing and in 1986 following the Chernobyl nuclear accident (Appleby 2008). Marked maxima in  $^{137}\text{Cs}$  can be corroborated with  $^{210}\text{Pb}$  as an independent validation of chronological estimates (Appleby 2001; Cundy et al. 2003).

Samples were counted by direct gamma assay in the Environmental Radiometric Facility at University College London, using an ORTEC HPGe GWL series well-type coaxial low background intrinsic germanium detector. Absolute efficiencies of the detector were determined using sediment samples of known activity and calibrated sources.

The methodology outlined in this section was applied to each core individually (one core collected from each of three sites). To determine cumulative carbon mass ( $\text{g C cm}^{-2}$ ) as opposed to peat mass ( $\text{g cm}^{-2}$ ), carbon density was calculated for each increment as in equation 5.3. Cumulative carbon mass was then calculated as in Appleby (2001):

$$C_n = C_{n-1} + S_n (x_n - x_{n-1}) \quad \text{Equation 5.7}$$

where  $C_n$  is cumulative carbon mass ( $\text{g C cm}^{-2}$ ) above  $X_n$  (lower surface of consecutive sections) and  $S_n$  is carbon density of consecutive sections. Peat accretion and carbon sequestration rate were determined using the Recent Rate of Carbon Accumulation (RERCA) method: total peat accreted and cumulative carbon density is divided by the number of years taken to accumulate (as in Turunen et al. 2004; Bao et al. 2010). This method does not account for losses of carbon by decay

(Rydin & Jeglum 2013). Bulk density was analysed in triplicate, therefore there is an associated uncertainty with carbon density measurements. The fractional uncertainty for each dated section was determined before errors were accumulated to give the total uncertainty of cumulative carbon density. A one-way ANOVA was used to test for a significant difference in carbon accumulation rate.

Peat accretion was compared to the projected rate of relative sea-level rise. Two representative concentration pathways (RCPs) were chosen to evaluate a range in sea-level projections; RCP 2.6 and RCP 6.0 for the year 2100 (table 5.4). Scenarios were adjusted for regional post-glacial isostatic rebound responsible for a rate of subsidence of  $0.5 \text{ mm yr}^{-1}$  (Bradley et al. 2009). Relative sea-level rise projections were also corrected for porosity of peat which is cited in the literature as around 0.95 (Baldwin & Mendelssohn 1998; Pagter et al. 2005; Saltmarsh et al. 2006; Stanley 2015).

Table 5.4: Representative Concentration Pathways (RCP) scenarios used to determine sea-level projections by 2100 from the IPCC AR5 report. Sea-level projections are corrected for isostatic rebound and porosity.

Scenario	Projection (m)	Isostatic rebound (m yr <sup>-1</sup> )	Years (2016 to 2100)	Isostatic rebound over 85 years (m)	Isostatic + projection (m)	Relative SLR (accounting for porosity) (m)	Relative SLR to 2100 (mm yr <sup>-1</sup> )
RCP 2.6	0.4	0.0005	84	0.042	0.442	0.46	5.5
RCP 6.0	0.48	0.0005	84	0.042	0.522	0.55	6.5

## 5.3 Results

### 5.3.1 Carbon density of different peat types

Carbon and nitrogen followed a similar pattern with depth at each of the three sites (figures 5.2, 5.3 and 5.4). Bulk density tended to be highest in the top third of the profile and, generally, pH and electrical conductivity (EC) declined with depth. A clay pan was identified at a depth of between 1 and 1.5 m, this can also be seen in Lambert's transects (appendix 4). Generally, brushwood peat (typical, soft and fibrous, for a full description of peat types see table 5.1) was found below the clay pan. Herb and fine detritus were generally found in the top half of the cores, whereas woody detritus was isolated to the bottom half of the cores. A layer of humus was found directly below the clay pan at Wheatfen.

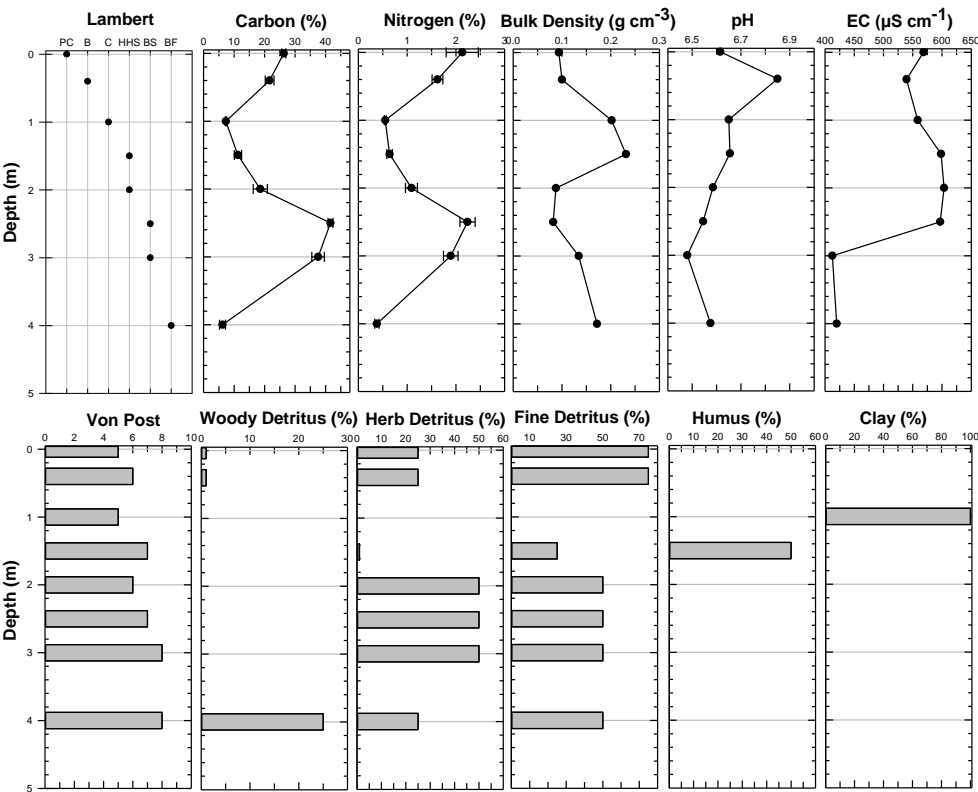


Figure 5.2: Stratigraphy from the deepest core from Wheatfen based on Lambert's criteria (Lambert 1960). Points in the Lambert plot indicate the top of each identified horizon.

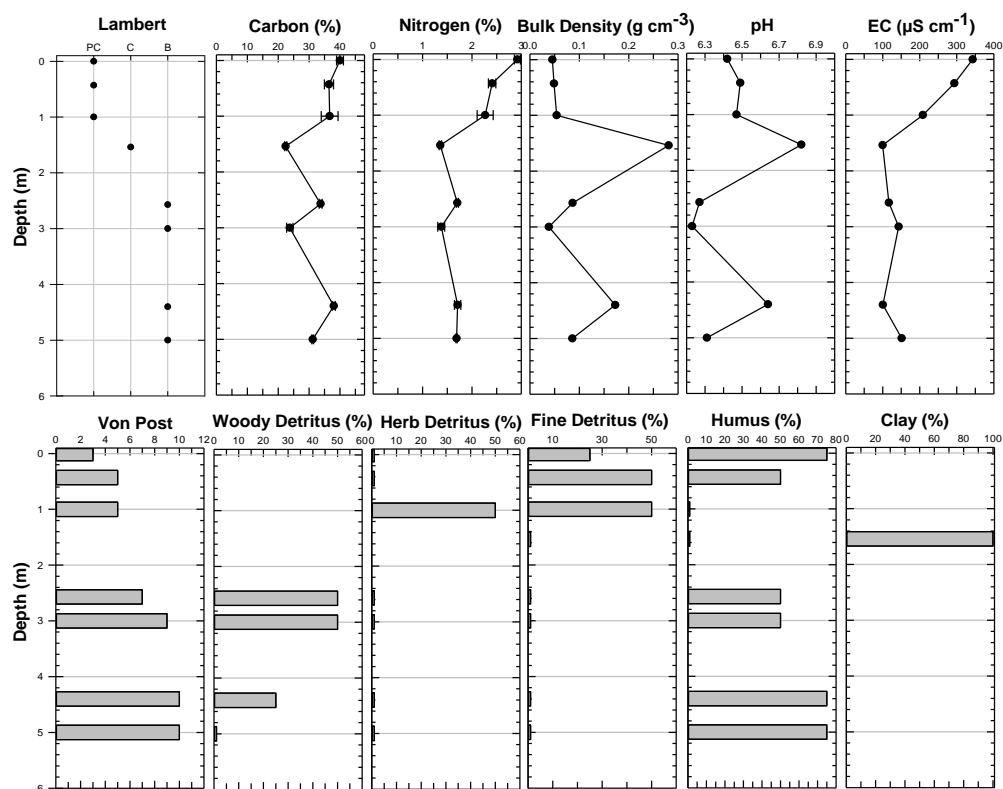


Figure 5.3: Stratigraphy from the deepest core from Woodbastwick based on Lambert's criteria (Lambert 1960). Points in the Lambert plot indicate the top of each identified horizon.

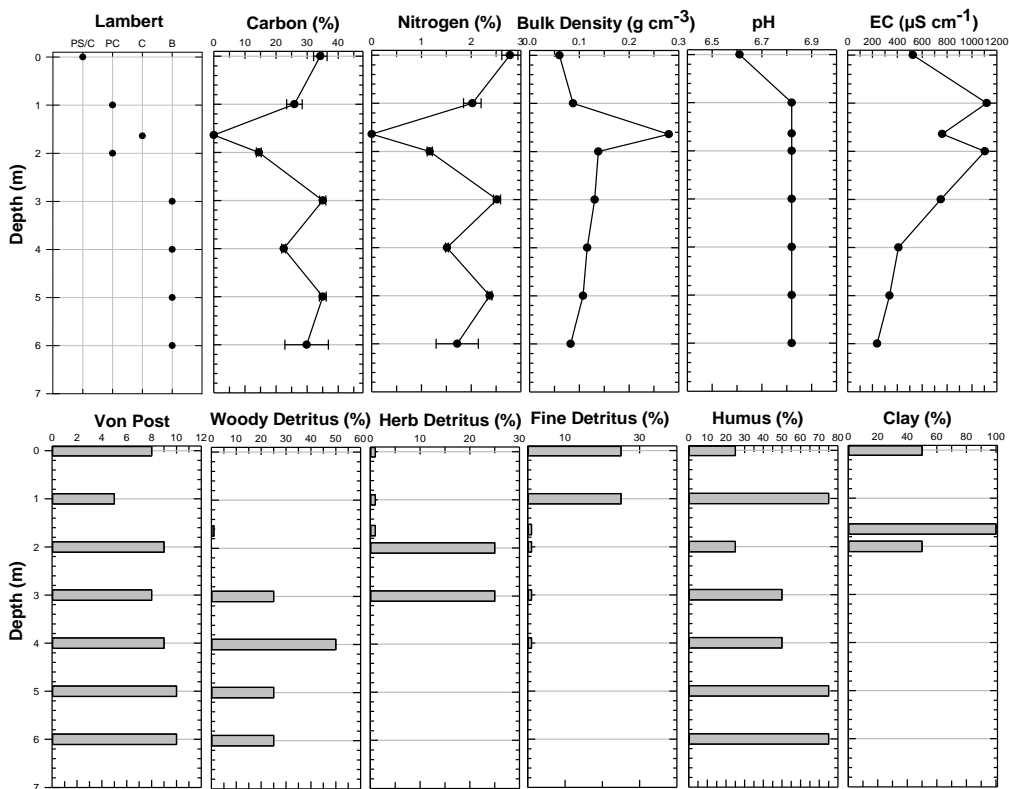


Figure 5.4: Stratigraphy from the deepest core from Strumpshaw based on Lambert's criteria (Lambert 1960). Points in the Lambert plot indicate the top of each identified horizon.

Mixed-effects linear models were used to test the effects of site, peat type, depth and their interaction on peat carbon content, bulk density and carbon density whilst controlling for variation between cores. The model output can be found in table 5.5. Scatterplots indicated that predicted values fitted the data reasonably well for all models (figure 5.5) and acceptable Nash-Sutcliffe measures of efficiency were achieved (0.5 for carbon content and 0.4 for both bulk and carbon densities). The full output from the models can be found in appendix 6.

As shown in table 5.5 and figure 5.6, carbon density varied by site only, and was significantly highest at Strumpshaw. Carbon content, however, varied between sites, and the interactions of site with peat type and with depth (table 5.5). Carbon content was highest in brushwood peat and lowest in highly homogenised surface peat (figure 5.7) and appeared to decrease with depth at Woodbastwick, which does not follow the trend of the other two sites (figure 5.8). Bulk density was significantly different between site, depth and their interactions (table 5.5). On the whole, bulk density increased with depth for all sites, but this relationship was weak at Wheatfen (figure 5.9). Bulk density of *Phragmites* peat increased to a greatest extent with depth at Woodbastwick (figure 5.10).

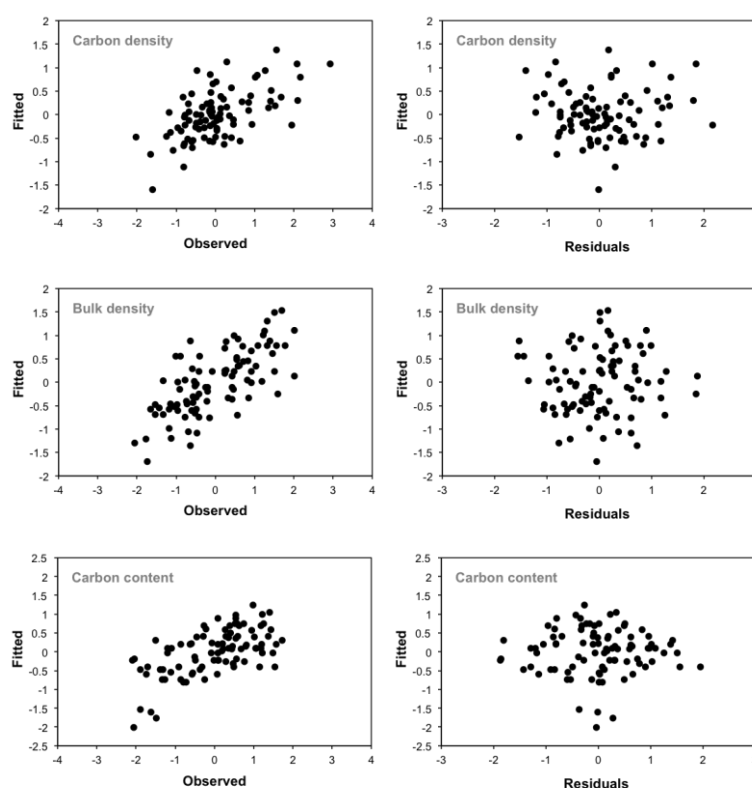


Figure 5.5: Scatterplots of observed vs. fitted and fitted vs. residuals to test the assumption of homogeneity for dependent variables of mixed effects linear models.

Table 5.5: Mixed-effects linear model comparing carbon content, bulk density and carbon density between site, depth ( $d$ ), peat type ( $P_t$ ) and their interaction. ns indicates a non-significant result for maximum likelihood estimation.

Fixed Effect	Df	F	<i>p</i> -value
<b>Carbon density (<math>\text{g C cm}^{-3}</math>)</b>			
$P_t$	4, 68	1.5	ns
Site	2, 68	3.3	< 0.05
$d$	1, 68	1.2	ns
$P_t$ .Site	3, 68	0.87	ns
$P_t$ . $d$	4, 68	0.95	ns
Site. $d$	2, 68	1.9	ns
$P_t$ .Site. $d$	2, 68	1.7	ns
<b>Bulk density (<math>\text{g m}^{-3}</math>)</b>			
$P_t$	4, 68	0.42	ns
Site	2, 68	11	< 0.0001
$d$	1, 68	8.7	< 0.01
$P_t$ .Site	3, 68	1.1	ns
$P_t$ . $d$	4, 68	0.95	ns
Site. $d$	2, 68	3.5	< 0.05
$P_t$ .Site. $d$	2, 68	3.8	< 0.05
<b>Carbon (%)</b>			
$P_t$	4, 68	3.4	< 0.05
Site	2, 68	1.8	ns
$d$	1, 68	2.5	ns
$P_t$ .Site	3, 68	3.0	< 0.05
$P_t$ . $d$	4, 68	1.0	ns
Site. $d$	2, 68	3.9	< 0.05
$P_t$ .Site. $d$	2, 68	0.19	ns

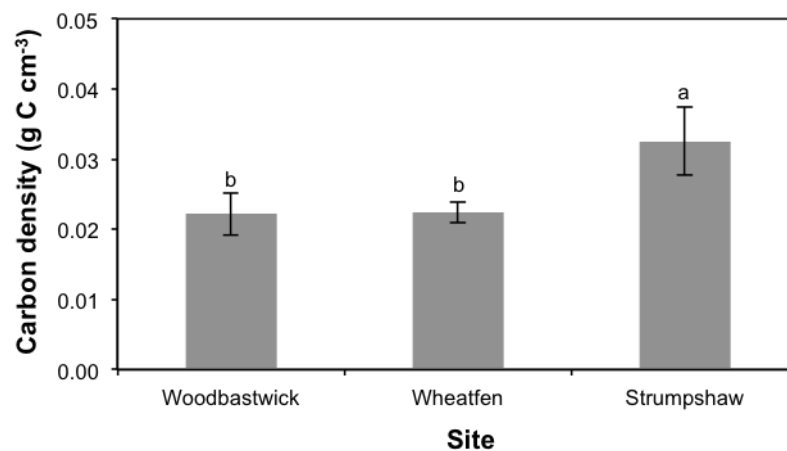


Figure 5.6: Average carbon density for each of the three sites. Bars are  $1 \pm \text{SE}$ . Letters indicate significant groupings from pairwise comparisons.

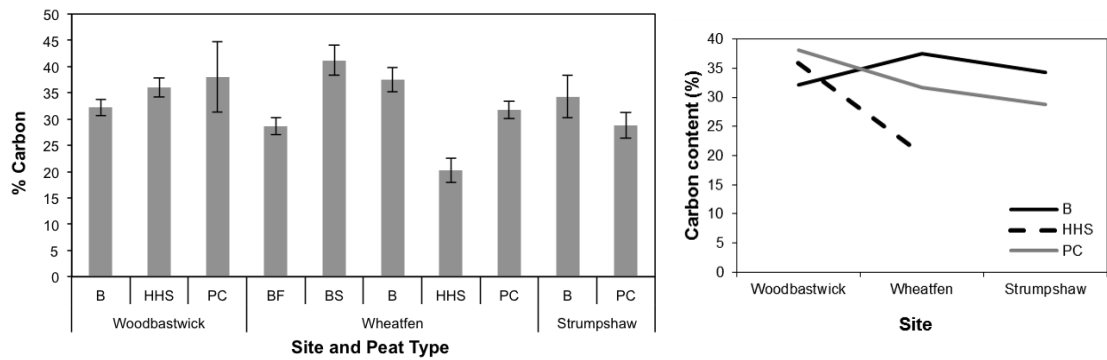


Figure 5.7: Carbon content (%) between peat type and site (left) and an interaction plot to show significant differences from (right). Bars indicate mean and error bars are  $\pm 1$  SE. See table 5.1 for peat type abbreviations

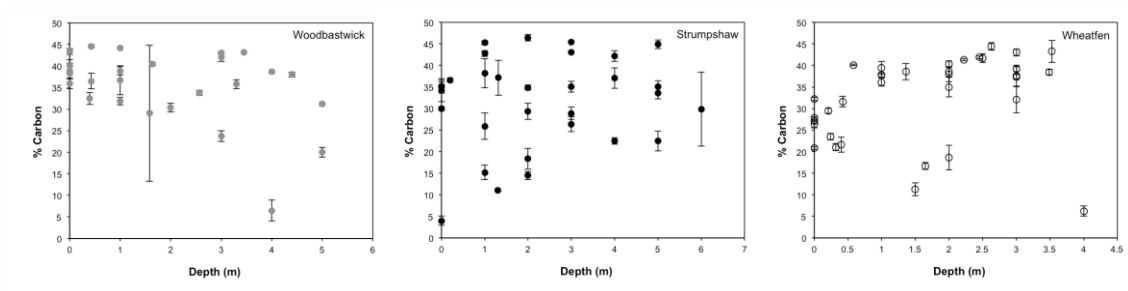


Figure 5.8: Scatterplots of carbon content with depth for each site.

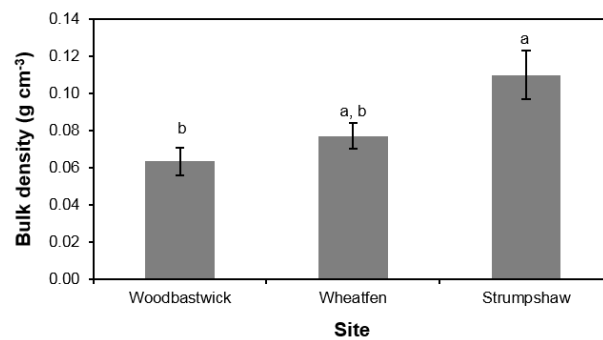


Figure 5.9: Bulk density for all peat types at study sites. Bars indicate mean and error bars are  $\pm 1$  SE and letters indicate significant differences.

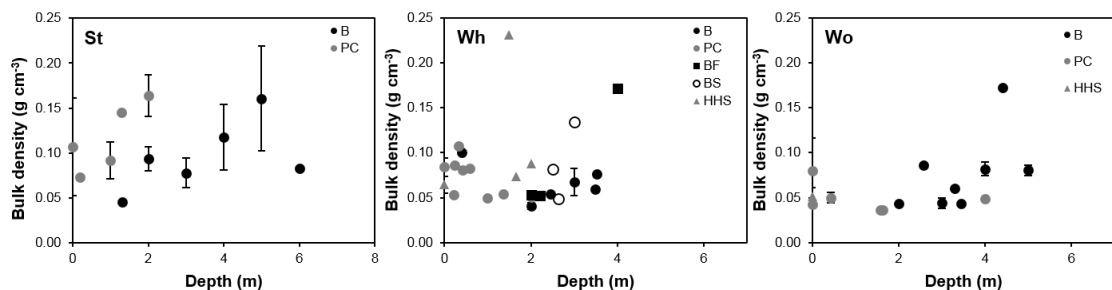


Figure 5.10: Scatterplots of bulk density with depth grouped by peat type and site. Points are averages and bars are  $\pm 1$  SE. St = Strumpshaw, Wh = Wheatfen and Wo = Woodbastwick.



### 5.3.2 Quantifying carbon stock

In section 5.3.1, carbon density did not differ significantly between peat type or depth, but did differ significantly between site therefore, carbon stock will be calculated without regard for peat type. A one-way ANOVA on coring data indicated that peat depth was significantly different between sites ( $F_{2, 48} = 12$ ,  $p < 0.0001$ ), with peat at Strumpshaw significantly deeper than Wheatfen and Woodbastwick ( $p < 0.05$ ). Strumpshaw had the largest carbon stock (table 5.7), although this difference was not significant. It is likely that this site had the largest carbon stock due to a significantly higher carbon density and significantly deeper peat in comparison to the other sites. Woodbastwick had the smallest carbon stock owing to a smaller volume of peat.

Table 5.6: Site width determined from Digimap® (2015). Length and depth refer to the dimensions of published stratigraphic transects (appendix 4). Depth (mean  $\pm$  1 SE) was averaged from values recorded at 50 m intervals along published transects.

Site	Site width (m)	Length of Lambert's transect (m)	Depth (m)
Wheatfen	1060	800	3.6 $\pm$ 0.63
Woodbastwick	760	800	2.5 $\pm$ 0.00
Strumpshaw	1000	850	5.5 $\pm$ 0.39

Table 5.7: The volume of each site was determined from site width multiplied by transect depth at 50 m intervals. Carbon density was determined in section 4.3.1. Values for carbon density are reported as mean  $\pm$  1 SD. The error for carbon stock was propagated as in equation 5.6.

Site	Volume of site (m <sup>3</sup> )	Carbon density (g C cm <sup>-3</sup> )	Carbon stock (kt C)
Wheatfen	3 x 10 <sup>6</sup>	0.02238 $\pm$ 0.0085	68 $\pm$ 8.2
Woodbastwick	1.5 x 10 <sup>6</sup>	0.022 $\pm$ 0.015	33 $\pm$ 5.8
Strumpshaw	4.5 x 10 <sup>6</sup>	0.033 $\pm$ 0.027	144 $\pm$ 31

### 5.3.3 Recent peat dating

Bulk density did not follow the same pattern with depth at all sites (figure 5.11). An overall decrease in carbon content was evident at Strumpshaw whereas at Wheatfen, carbon content increased to a depth of 15 cm before decreasing to 35 cm. Carbon content remains constant at Woodbastwick for depths below 13 cm. It appears as though there was some degree of compaction at Woodbastwick, since bulk density of surface peat from the coring survey is slightly lower than found here (see figure 5.3 for comparison).

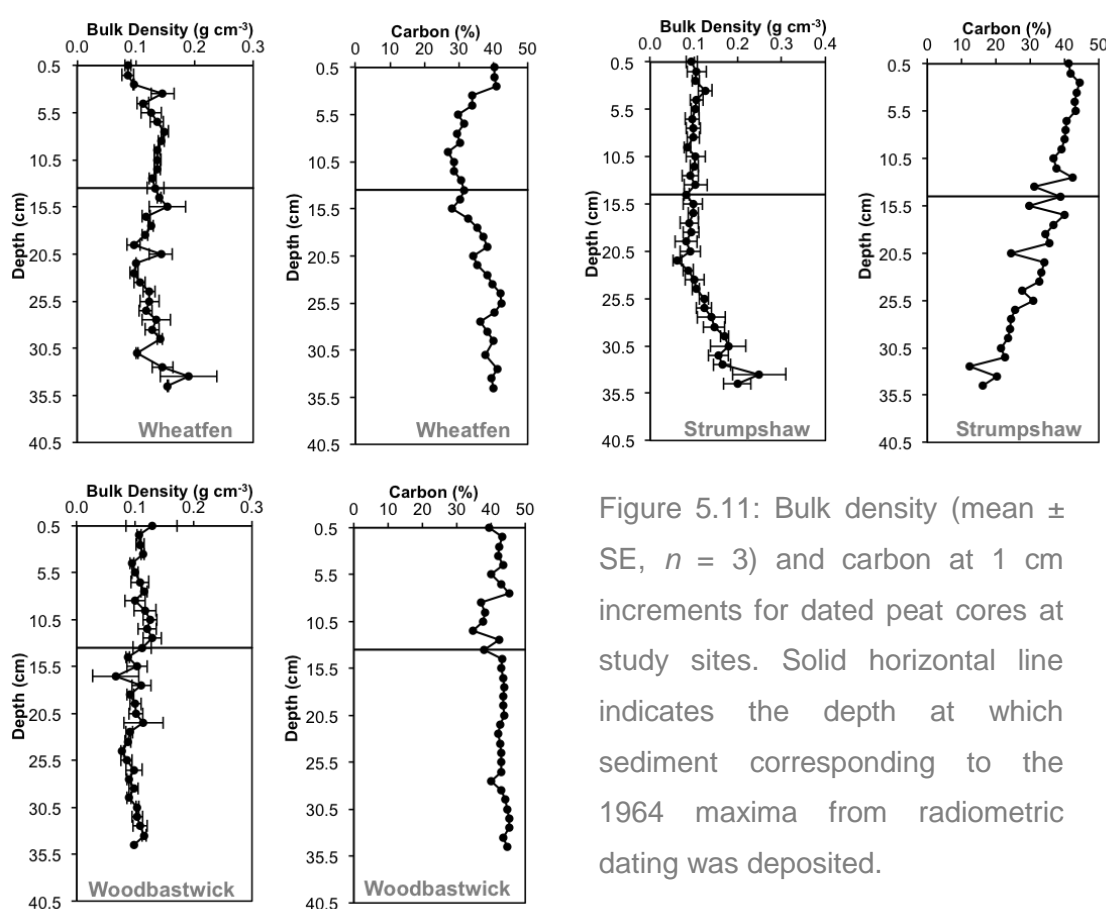


Figure 5.11: Bulk density (mean ± SE,  $n = 3$ ) and carbon at 1 cm increments for dated peat cores at study sites. Solid horizontal line indicates the depth at which sediment corresponding to the 1964 maxima from radiometric dating was deposited.

A peak in <sup>137</sup>Cs activity was observed at 13.5 cm at Wheatfen. There were two broad peaks at Strumpshaw and Woodbastwick and it is likely that the first peaks are a result of fallout from the Chernobyl accident in 1986 and the second peaks were from nuclear weapons testing in 1964 (figure 5.12). However, evidence of the Chernobyl accident have not been found in previous radiometric dating studies in the Broad, therefore the 1986 peak should be interpreted with caution (Personal communication, Carl Sayer, UCL, December 2016). The irregular activity in <sup>210</sup>Pb<sub>unsupported</sub> precluded

the use of the constant initial concentration model (CIC) and chronologies were obtained using the constant rate of supply model (CRS). The CRS model placed 1964 at 9.5 cm at Wheatfen, 10 cm at Woodbastwick and 7.5 cm at Strumpshaw. Not all modelled estimates agreed with the  $^{137}\text{Cs}$  record and the final chronology was corrected assuming sediment at a depth of 13.5 cm was formed in 1964. The resulting age-depth curve is shown in figure 5.13.

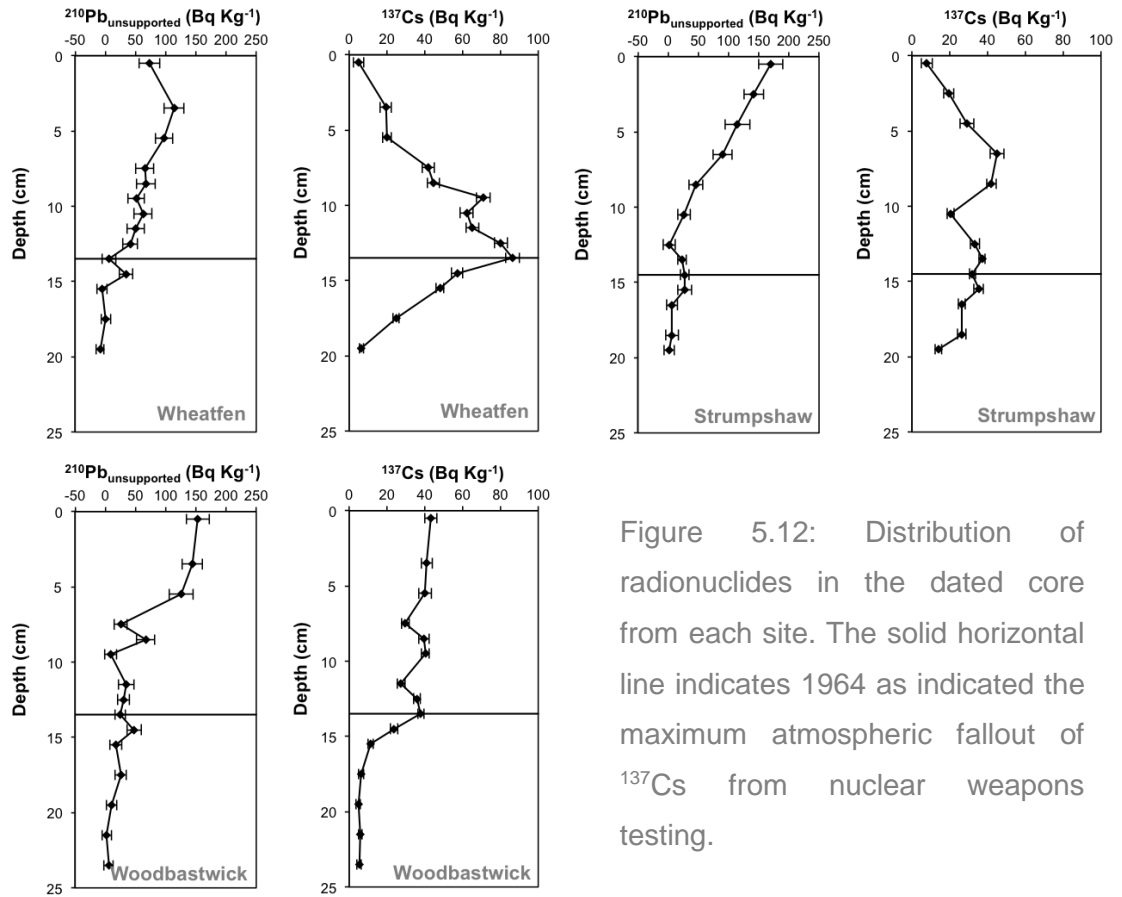


Figure 5.12: Distribution of radionuclides in the dated core from each site. The solid horizontal line indicates 1964 as indicated the maximum atmospheric fallout of  $^{137}\text{Cs}$  from nuclear weapons testing.

Generally, a similar amount of peat has accreted at each of the three sites since 1964 (between 13.5 and 14.5 cm) (figure 5.13) and therefore, recent peat accumulation rate is very similar between sites (table 5.8). The average accretion rate of  $\sim 2.7 \text{ mm yr}^{-1}$  is smaller than projected sea-level rise. The relatively large errors on dated samples below 8 cm at Strumpshaw indicate that peat accretion rate could have fluctuated substantially more than the mean value suggests. However, even when considering the upper estimates, peat accretion would still have been more rapid between 35 and 50 years ago in comparison to more recent deposits. Since 1964, Woodbastwick has sequestered the most carbon in comparison to the other two sites, whereas Wheatfen

has accumulated the least. Recent carbon accumulation rate (RERCA) is very similar at Wheatfen and Strumpshaw (table 5.8).

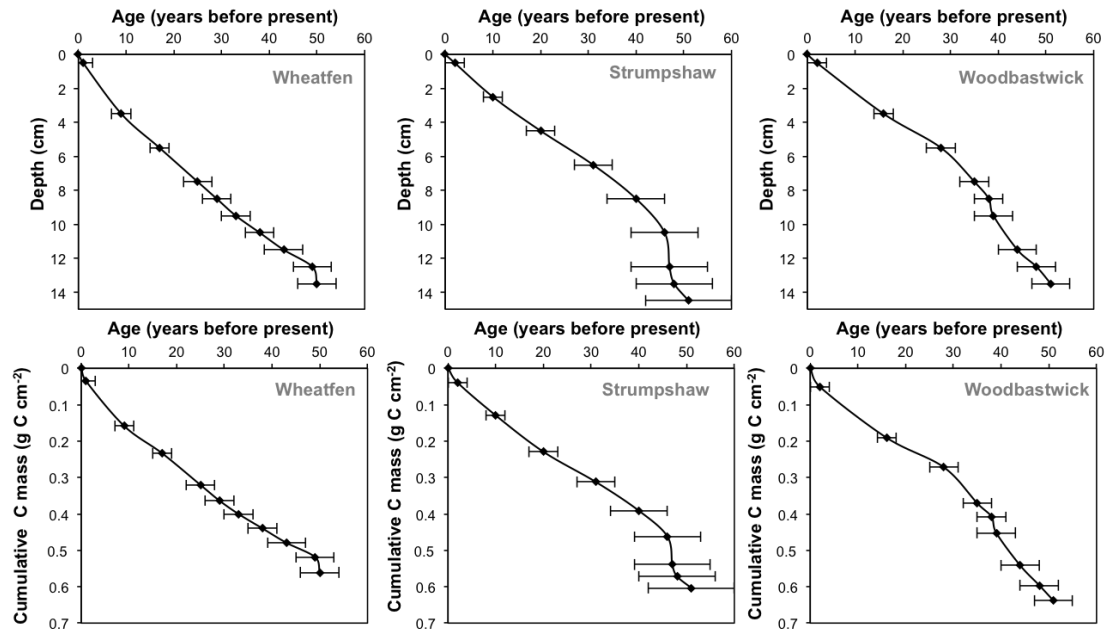


Figure 5.13: Age-depth curves based on the results of the CRS model from radiometric dating corrected for maximum atmospheric fallout of <sup>137</sup>Cs in 1964 from nuclear weapons testing. Error bars are based on the uncertainty on the counted <sup>210</sup>Pb values (personal communication, Handong Yang, UCL, October 2015).

Table 5.8: Recent peat accretion and carbon sequestration rate. Peat accretion rate determined from radiometric dating. Carbon sequestration rate was calculated from age-depth data and the calculation of cumulative carbon density using carbon content and bulk density determined in this chapter (see section 5.2.2.2 for methods).

Site	Peat Accretion (mm yr <sup>-1</sup> )	RERCA (g C m <sup>-2</sup> yr <sup>-1</sup> )
Wheatfen	2.7	112 ± 10
Woodbastwick	2.6	125 ± 12
Strumpshaw	2.8	112 ± 21

## 5.4 Discussion

The present study sought to identify relationships between carbon density (i.e. carbon content and bulk density), depth, peat type and site with the intention of determining how this relates to the estimation of carbon stock. Additionally, this Chapter quantified recent peat accretion and carbon sequestration rates at three floodplain fen sites varying in degree of saline influence.

### 5.4.1 Variation in carbon density and its components

Carbon content was significantly different between peat types. In particular, brushwood and brushwood soft peat (more fibrous peats containing wood and herb detritus mixed with wood fragments) had higher carbon contents than highly homogenised surface peat. As speculated in the introduction of this Chapter, the difference in peat type is probably due to botanical composition, which has been shown by other studies to be an important control on peat carbon content (Zauft et al. 2010). For example, brushwood peat is indicative of a period when the peatland was dominated by small woody shrubs, which are more resistant to decay than *P. australis* (Chambers et al. 2010). Highly homogenised surface peat is comprised predominantly of humus (table 5.1) and is therefore probably derived from decayed leaves of *P. australis*. It is apparent from other lowland peatland studies that carbon content can range between 5% and 60% depending on the botanical composition of peat, with peat types more resistant to decay having a higher carbon content (e.g. Bernal & Mitsch 2008; Henman & Poulter 2008).

Bulk density measurements obtained via different field methods (i.e. gouge corer for the peat survey and wide-diameter pipe for radiometric dating) compared favourably to one another, indicating that compaction of peat samples was largely avoided for all sites. Since the wide-diameter corer was only used to a depth of ~50 cm, it is not possible to tell if compaction occurred beyond this depth. However, bulk density values reflected those of other studies (table 5.9).

Table 5.9: Comparison of bulk density values published in other studies.

Study	Bulk density (g cm <sup>-3</sup> )	Location	Site
Bernal & Mitsch 2008	0.1 - 0.2	Costa Rica and Ohio, USA	<i>P. australis</i> dominated floodplain fen
Castañeda-Moya et al. 2010	0.15 - 0.18	Florida, USA	Tidal floodplain fen
Yu 2006	0.088	Western Canada	Ombrotrophic bog
Yu 2006	0.068	Western Canada	Nutrient poor fen
Callaway et al. 1996	0.33 - 0.75	Stiffkey Marshes, UK	Influenced by North Sea storm surges
This study	0.04 – 0.3	Norfolk, UK	Floodplain fen

Site was the most significant control on bulk density, suggesting a large degree of spatial variation. This could be due a range of factors, such as water level, frequency of inundation and carbon content of peat (since the higher the organic matter, the lower the bulk density) (Chaudhari et al. 2013). The significant interaction between site, peat type and depth helps to interpret this spatial variation. It is unsurprising that bulk density increased depth, as this has been frequently demonstrated in other peatland studies (Clymo et al. 1998; Bridgham & Richardson 1993; Froking et al. 2002; Lindsay 2010; Pendea & Chmura 2012). Bulk density of surface peat increased with depth to a greater extent at the two sites located on the tidally influenced River Yare. This is probably due to the deposition of mineral sediment at the peat surface following an inundation event which compresses existing surface peat (Castañeda-Moya et al. 2010) – especially since other studies have shown a positive relationship between water level and suspended sediment concentration (e.g. Kirwan et al. 2016). Indeed, surface peat at these two sites had lower carbon contents than Woodbastwick, indicating a greater degree of mineral influence. A clay pan was identified between 1.5 and 2 m at all study sites, which corresponds with the Romano-British marine transgression around 1600 BP (Giller & Wheeler 1986). Brushwood is generally the only peat type found beneath this deposit, and therefore it is likely that the relationship between peat type and depth beyond 2 m is due to the compression of brushwood peats under the clay pan.

The overarching aim of this section was to determine the controls on carbon density by examining the controls on its components (i.e. carbon content and bulk density). It was expected that carbon density would vary between peat types; however, the linear mixed effects model indicated that carbon density differed between sites. Therefore, H<sub>5.1.1</sub> is rejected. Since site is the most significant control on bulk density, it is likely that processes driving variation in carbon density reflect those of bulk density, such as

compression. Organic matter content is probably important to a lesser degree, as this was not significantly different between sites. Carbon density in this Chapter was comparable to other floodplain fen studies (e.g. 0.02 to 0.06 g C cm<sup>-3</sup>, Bernal & Mitsch 2008), however, the results of this section have shown that carbon density is highly spatially variable, which is likely to have implications for regional carbon stock estimates.

#### **5.4.2 Carbon stock**

It is clear from the linear mixed effect model that carbon density is significantly different between sites and therefore, carbon stocks in this Chapter were calculated irrespective of peat type, applying the average carbon density from each site. The results indicate that peat depth is an important element of volume calculation and is recorded in many locations in the Broads, which makes for accurate estimates of peat stock. The difficulty in obtaining accurate peat depth measurements (Tarnocai et al. 2009) means that a single value for peat depth (usually between 1 and 3 m) is often applied to regional carbon stock estimates (e.g. Gorham 1991; Beilman et al. 2008). Other studies have shown peat depth to be extremely variable, with some large areas of peat being relatively shallow (0.5 m, Weissert & Disney (2013)), whilst other peatlands located in basins, for example, can be more than 5 m deep (Ingram & Otte 1981). Therefore, it is likely that estimations of carbon stocks globally have previously been underestimated. Indeed, peat depth in the UK is variable, with depths obtained in this study at the higher end of estimates reported for UK peatlands (0.4 to 8 m - Natural England 2010). Thus, it is likely that the proportional contribution of the Broads to the total peat carbon stock of the UK has been under-estimated.

The results in this Chapter also suggest that it is important to have a measure of bulk density for each site/location to calculate carbon density. Lowland fens are especially important in carbon stock estimates, as despite accounting for approximately 1000 km<sup>2</sup> of the 7000 km<sup>2</sup> of England's deep peatland (>40 cm), they store 25% of total peatland carbon (144 of 590 Mt C) (Natural England 2010) (note that the peat depth and carbon density used were undisclosed). This is probably because lowland peats tend to have a herbaceous botanical composition in comparison to bogs which are generally sphagnum dominated (Natural England and RSPB 2014); and herbaceous peats have been shown by other authors to have a higher bulk density than

sphagnum peat ( $\sim 0.12 \text{ g cm}^{-3}$  and  $< 1 \text{ g cm}^{-3}$  respectively) (Frolking et al. 2002 and Loisel et al. 2014).

Applying depth and carbon density values obtained in this Chapter to the area of lowland fen given by Natural England (2010) indicates that site level variation can have a large effect on carbon stock, decreasing the estimate by almost two-thirds in some cases (table 5.10). Previous studies have acknowledged the need to obtain more representative depth and carbon density data in order to improve regional stock estimates, but a lack of primary data is often the limitation to achieving this (e.g. Yu 2012). The magnitude of change in carbon stock presented here could be used by future studies to understand the potential variability in regional carbon stock estimates, especially those where it is perhaps not practical to obtain depth and bulk density data at a relatively small spatial scale (i.e. spatial variation in this study was observed within  $25 \text{ km}^2$ ).

Table 5.10: Change in carbon stock for the areal extent of lowland fens in the UK ( $1000 \text{ km}^2$ ) estimated by Natural England (2010) when carbon density and depth are varied according to the results in this chapter (section 5.3.2).

Site	Carbon density ( $\text{g C cm}^{-3}$ )	Depth (m)	Mt C
Strumpshaw	0.033	5.3	175
Wheatfen	0.022	3.6	80
Woodbastwick	0.022	2.5	55

### 5.4.3 Carbon sequestration and peat accretion

Chronology derived from radiometric dating has frequently been used to determine recent carbon sequestration and peat accretion rate in peatlands (e.g. Bernal & Mitsch 2012; Garneau et al. 2014). Peat accretion rate and recent rate of carbon accumulation (RERCA) were determined by dividing the number of years since 1964 to 2014 by the total amount of peat accreted (Ali et al. 2008) or carbon sequestered (Bao et al. 2010). The vertical peaks of  $^{137}\text{Cs}$  were well defined, allowing reliable inferences about peat accretion and carbon sequestration rate to be made for each of the study sites.

As speculated in the introduction to this Chapter, recent rate of peat accretion was similar across all study sites, probably because these sites have experienced a similar



climate and erosion and deposition history (Lindsay 2010). The age-depth model indicates that peat accreted relatively quickly at Wheatfen over the last decade, possibly due to the higher rate of above-ground production at this site (Chapter 4). The method used to calculate recent peat accretion in this Chapter does not account for such variation in rate of production and decomposition, and has been shown by other studies to be an overestimation (e.g. Turetsky et al. 2004). However, this method is widely applied in the literature (Turunen et al. 2002; Wang et al. 2014) and since there is a lack of studies quantifying peat accretion rate in temperate floodplain fens, results were found to be comparable to accretion rate in wetlands with a surface water influence, for example; a UK saltmarsh susceptible to North Sea storm surges (2.6 to 2.7 mm yr<sup>-1</sup>, Callaway et al. 1996) and sub-tropical histosols (2.0 mm yr<sup>-1</sup>, Armentano & Menges 1986). The results of this Chapter indicate that peat accretion will not keep pace with relative sea-level rise even under a conservative scenario and when accounting for peat porosity. How this will affect carbon storage in lowland peatlands remains relatively unknown, with other studies suggesting that peat stocks will gradually erode due to increased DOC export and a reduction in organic inputs due to vegetation die-off (Henman & Poulter 2008; Reichstein et al. 2013).

To put the carbon sequestration rates obtained in this study into perspective, rates are compared with those from other freshwater wetlands (table 5.11) and estimates in this Chapter fell within the published range. As outlined in the introduction to this Chapter, it is likely that the relatively high carbon content at Woodbastwick is the reason this site had the highest sequestration rate and H<sub>5.3.1</sub> is accepted. As in section 5.4.1, carbon content in dated peat (i.e. the top 50 cm) is probably higher due to the higher rate of mineral deposition at the other two sites.

Table 5.11: Comparison of carbon sequestration rates in freshwater wetlands reported in the literature. All studies used radiometric dating with <sup>210</sup>Pb and <sup>137</sup>Cs.

Study	Carbon accumulation (g C m <sup>-2</sup> yr <sup>-1</sup> )	Site
Bernal & Mitsch 2012	140 ± 16	<i>Phragmites</i> dominated floodplain fen, Ohio, USA
Poulter et al. 2006	102 ± 2	Lowland peatland with surfacewater inputs, North Carolina, USA
Reddy et al. 1993	104 - 167	Cattail-sawgrass marsh, Florida
This study	112 - 125	<i>Phragmites</i> dominated floodplain fen, UK

It should be noted that this Chapter refers to recent carbon accumulation rate since peat deposits could only be dated to the marked  $^{137}\text{Cs}$  maxima of 1964, and long-term accumulation rates are often much different (Turunen et al. 2004). Data from the coring survey can be used to give an indication of long-term sequestration rate in the Broads as the clay pan observed at a depth of approximately 2 m probably corresponds with the last marine transgression around 1600 BP (Giller & Wheeler 1986) – approximately 7400 years after the Broads began forming (Cooper et al. 2008). Using Strumpshaw as an example, it is possible that carbon was sequestered at a rate of  $28 \text{ g C m}^{-2} \text{ yr}^{-1}$  between 9000 BP and 1600 BP, which is very similar to the long term carbon sequestration rate that encompasses all northern peatlands ( $23 \pm 2.0 \text{ g C m}^{-2} \text{ yr}^{-1}$ ) (Loisel et al. 2014). Although a rough estimate, this example is useful in giving an insight into the differences in carbon sequestration under different climatic, edaphic and autogenic factors (temperature, ground-water flow and water level), but also perhaps under different vegetation types, since brushwood peat is derived from vegetation more woody in composition than *P. australis*.

#### **5.4.4 Implications and further work**

Peatland carbon stock estimates have been calculated using a regionally averaged value for bulk density and carbon content for several decades. This study has shown that peat depth is important in volume calculations and that bulk density measurements should be obtained for each 'location', since both of these elements are found to vary in the Broads over a spatial scale of approximately 25 km<sup>2</sup>. Floodplain fen sites are unique to other peatland studies since mineral deposition is likely to be important, especially under the influence of sea-level rise (Kirwan et al. 2016). This issue has been raised in the wider literature, but is currently limited to marsh accretion studies (Neubauer 2008). Therefore, the results in this Chapter could form the basis of future work on the relative contributions of mineral and organic components to floodplain fen carbon stock and carbon sequestration rate. This Chapter has shown that rate of peat accretion will not keep pace with sea-level rise, however, the implications of this on carbon storage in floodplains fens is likely to become apparent on timescales exceeding those of field experiments. A modelling approach is therefore recommended with data derived from field studies combined with a conceptual understanding of carbon cycling in floodplain fens, enabling the change in carbon storage as a result of sea-level rise in the future to be determined.

## 5.5 Conclusions

With respect to the specific questions outlined in section 5.1, the following conclusions can be made from radiometric dating and the analysis of peat carbon density in the Broads:

1. Carbon density differed between the three floodplain fen sites as opposed to between peat types and is probably related to spatial variation in bulk density, owing principally to mineral deposition at the peat surface.
2. Carbon stock ranges between 33 and 144 kt C and appears to be most dependent on peat depth and bulk density. Although depth and bulk density measurements can be problematic to obtain, regional estimates of carbon stock can vary substantially (by two thirds in this case) if unrepresentative measurements are used.
3. Recent carbon sequestration rates ranged between 112 and 125 g C m<sup>-2</sup> yr<sup>-1</sup> and was most dependent on peat carbon content, which appeared to be lower at tidally influenced sites, probably due to a higher rate of mineral deposition. Peat accretion was similar across all sites (~2.6 mm yr<sup>-1</sup>) and would not keep pace with sea-level rise. The effect of this on floodplain fen carbon storage is complex, but the wider literature suggests that peat carbon will most likely be lost if floodplain fens become permanently inundated (e.g. Henman & Poulter 2008).

## Chapter 6: A modelling study to explore the effects of sea-level rise on peat accretion

### 6.1 Introduction

This Chapter explores the effects of different components of sea-level rise (i.e. water depth and salinity) on peat accretion in floodplain fens. Previous modelling studies have explored accretion in other peatland types (e.g. Baird et al. 2009), but no studies focus specifically on the effect of sea-level rise on peat accretion in floodplain fens, with the most relevant studies conducted in other types of lowland wetland (Larsen et al. 2007; Kirwan et al. 2016). We use peat accretion in this Chapter to refer to the gradual increase in peat height (m) and peat accumulation to refer to the gradual increase in peat carbon stock ( $\text{kg C m}^{-2}$ ) at each time step of the model (Cahoon et al. 2003; Larsen et al. 2007; Whittle & Gallego-Sala 2016). Throughout this Chapter, sea-level rise refers to relative rates (i.e. corrected for isostatic rebound).

It is well established that peatland development is a consequence of rate of production exceeding decomposition, with the theoretical basis for the peat accretion process given by Clymo (1984). Central to his theory is the addition of litter to the wetland surface, which is processed to form peat. Peat formed from litter at the surface is captured for long-term carbon storage. All peat is subject to some degree of decomposition, with permanently submerged peat decaying at a much lower rate than seasonally exposed peat at the wetland surface. In essence - the peat stock will continue to grow providing rate of input of fresh litter at the wetland surface exceeds rate of decay. This theory of peatland development is based in an ombrotrophic environment dominated by *Sphagnum*. Floodplain fens differ from bogs as they have a higher above-ground biomass that is more herbaceous in composition, and hydrology is influenced by tidal range and seasonal fluctuations in water level (van Diggelen et al. 2006). Therefore, the theoretical basis posited by Clymo needs to be modified to account for these processes.

Peatland carbon and water dynamics are closely linked, with hydrological metrics (such as water table depth) powerful predictors of ecological processes that regulate carbon flux to, from and within peatlands (Yu 2006). There are three hydrological metrics to consider for floodplain fens: mean water depth, seasonal range and tidal range – the latter only applicable to sites vulnerable to sea-level rise. An increase in

salinity will also result from sea-level rise and it has been shown that in the Broads, saline water is delivered to the fen via overtopping of rivers, and through groundwater upwelling as sea water is drawn in from the coast (Simpson et al. 2011). Overtopping of rivers transports suspended sediment to the fen, which may be deposited when the floodwater recedes and will therefore contribute to wetland height (Chmura et al. 2003). The extent of the mineral deposit is related primarily to suspended sediment concentration, depth of floodwater and vegetation cover (which can aid the interception of mineral particles) (Kirwan et al. 2016). Mineral deposition is an important factor to consider, as the results of Chapter 5 indicated that carbon sequestration was lower at tidally influenced sites due to lower organic matter content in surface peat. This is supported by other wetland accretion studies, that have suggested sea-level rise may increase the suspended sediment concentration of floodwaters, thereby increasing the relative contribution of mineral sediment to wetland height and reducing rates of carbon sequestration (Day et al. 1999; Kirwan et al. 2016). This issue has gained importance in saltmarsh literature over the last decade (Neubauer et al. 2013), yet few studies have explored the importance of the relative contribution of mineral deposition on peat height and carbon sequestration in lowland wetlands (Chmura et al. 2003).

As shown in Chapter 5, *Phragmites australis* (Cav.) Trin. Ex Steud dominates above-ground vegetation in the Broads and is ubiquitous in wetlands throughout the world (e.g. Minchinton & Bertness 2003). Therefore, processes related to *P. australis* are the focus of this Chapter. Previous authors have studied the effect of sea-level rise on both production and decomposition of *P. australis* for a range of purposes. These include understanding nutrient cycling amongst *P. australis* organs (Eid et al. 2010), understanding dynamics more generally (Asaeda et al. 2002) and understanding how *P. australis* stocks respond to differing salinity and inundation frequency (Soetaert et al. 2004). Findings from such studies can be used to help parameterise plant growth in our model of carbon storage in floodplain fens. For example, production has been shown to increase between 0 and 5 ppt, but decrease at higher salinities (Pagter et al. 2009; Qi et al. 2016). It is also important to consider the effects of allocation of assimilate to peat accretion, as some studies have shown that the allocation of carbon assimilate to above- and below-ground organs is affected by saline influence and water level (Rolletschek et al. 1999; Soetaert et al. 2004).

Decomposition is affected by tidal range, mean water level and salinity (Wichern et al. 2006; Limpens et al. 2008; Brouns et al. 2014). It is not possible to observe the effect of diurnal (such as tides) or seasonal fluctuations in water level for models run on an

annual time step. Instead, fluctuations over the year can be integrated to give a cumulated water depth, which refers to mean water depth above the peat surface. Decomposition will be highest when mean water depth is below the peat surface, and slower when mean water depth is above the peat surface, since anoxic conditions retard decay rate (Gorham 1991; Laiho 2006). Decomposition is also dependent on the supply of fresh litter, since microbes initially sequester nitrogen from plant litter (Berg & McClaugherty 2008) and peat becomes enriched with fibrous compounds (Hilasvuori et al. 2013). Consequently, rate of decay is likely to be substantially reduced when mean water depth reaches a level detrimental to above-ground production (and hence a reduced supply of fresh litter), which has been shown by other *P. australis* studies to occur when water depth is  $\pm 0.8$  m from the peat surface (Coops et al. 1996).

Organic matter consists of a labile (it does decay) and refractory (it does not decay) components (Dinka et al. 2004). Previous research has suggested that the accumulation of labile organic matter tends to equilibrate through time, as any labile carbon deposited is eventually decayed (Kirwan & Mudd 2012). Therefore, the labile component contributes to carbon storage, but does not contribute to the accretion of organic matter (Mudd et al. 2009).

This study uses an unpublished model by Belyea (2016) that focuses on the link between relative sea-level rise (water level and salinity) and two key ecological processes that are important for peatland development (rate of production and rate of decay in this case), applied to floodplain fens only. Relative stress tolerance curves (Qi et al. 2016) are used to represent the response of production and decomposition to varying salinity and water level. The model is parameterised by a combination of published and field derived values presented in earlier Chapters. The overall aim of this Chapter is to explore the effects of an increase in water level and salinity as a result of sea-level rise on peat accretion in floodplain fens. Ultimately, the research questions of this Chapter are:

**Research question 6.1:** How is mineral sedimentation rate affected by a change in suspended sediment concentration and cumulated water depth?

**Research question 6.2:** To what extent is the mass flux of vegetation to peat dependent on below-ground allocation, salinity and cumulated water depth?

**Research question 6.3:** How are the relative contributions of the labile and refractory components to organic matter influenced by salinity and water level? How many years does it take for the labile component to approach steady state?

**Research question 6.4:** Are the relative contributions of the mineral and organic components to vertical accretion affected by salinity and cumulated water depth?

**Research question 6.5:** What are the key controlling factors that will determine whether vertical accretion in floodplain fens can keep pace with relative sea-level rise (RSLR)?

## 6.2 Methodology

### 6.2.1 Model description

The unpublished model by Belyea (2016) simulates total peat mass and the height of the floodplain fen. An analytical approach is used, whereby a series of differential equations are solved analytically as opposed to numerically to calculate a total peat mass or peat height. In floodplain fens, water level relative to the peat surface,  $Z$  (m), fluctuates around the mean water depth,  $W_{mean}$  (m), due to tidal range ( $R_{tide}$ , in this case refers to a  $\frac{1}{2}$  day period) and seasonal range ( $R_{yr}$ , over 365 days). A cosine function can be used to simulate such fluctuations:

$$Z = W_{mean} + \frac{R_{yr}}{2} \cos\left(2\pi \frac{d}{365}\right) + \frac{R_{tide}}{2} \cos\left(2\pi \frac{d}{0.5}\right) \quad \text{Equation 6.1}$$

where  $d$  is day of year. To avoid the need to alter  $W_{mean}$  (m),  $R_{tide}$  and  $R_{yr}$  independently for each simulation, cumulated water depth,  $W$  (m) is calculated by integrating the depth of floodwaters over one year. Overbank flooding events transport suspended sediment to the fen. Sediment may be deposited onto the peat surface via settlement or trapping by vegetation. The rate at which mineral material is deposited (i.e. sedimentation rate),  $dP_{min}/dt$  ( $\text{kg m}^{-2} \text{ yr}^{-1}$ ), is the product of cumulated depth of floodwaters,  $W$  (m), total suspended sediment concentration,  $\eta$  ( $\text{kg m}^{-3}$ ), and an efficiency factor,  $\nu$  ( $\text{yr}^{-1}$ ):

$$\frac{dP_{min}}{dt} = \eta \nu W \quad \text{Equation 6.2}$$

When sedimentation rate is integrated over time, the mass of mineral sediment  $P_{min}$  ( $\text{kg m}^{-2}$ ) accumulated after time  $T$  (y) can be given by:

$$P_{min} = \eta \nu W T \quad \text{Equation 6.3}$$

As outlined in the introduction to this Chapter, growth of *P. australis* is influenced by inundation (in this case, cumulated water depth) and salinity (Farquhar & Sharkey 1982; Coops et al. 1996; Armstrong & Armstrong 2001; Mauchamp & Mesleard 2001; Engloner 2009; Pagter et al. 2009; Gorai et al. 2010). As in Qi et al. (2016), stress tolerance curves are used to model relative net growth in response to salinity stress,  $\varepsilon_{S, g}$ , and water stress,  $\varepsilon_{W, g}$ :



$$\varepsilon_{S,g} = e^{\left[-0.5(s-m_{S,g})^2/r_{S,g}\right]} \quad \text{Equation 6.4}$$

$$\varepsilon_{W,g} = e^{\left[-0.5(w-m_{W,g})^2/r_{W,g}\right]} \quad \text{Equation 6.5}$$

where  $m_{S,g}$  and  $m_{W,g}$  are the values of salinity and cumulated water depth, respectively, for which plant performance is maximum.  $r_{S,g}$  and  $r_{W,g}$  represent the tolerance range of *P. australis* to these stressors (figure 6.1). Note we ignore effects of salinity and water depth on competitive ability (cf. Qi et al., 2016). Net growth,  $G$  ( $\text{kg m}^{-2} \text{y}^{-1}$ ), is calculated by scaling maximum growth rate,  $G_{max}$  ( $\text{kg m}^{-2} \text{y}^{-1}$ ), in response to these two stressors:

$$G = \varepsilon_{S,g}\varepsilon_{W,g}G_{max} \quad \text{Equation 6.6}$$

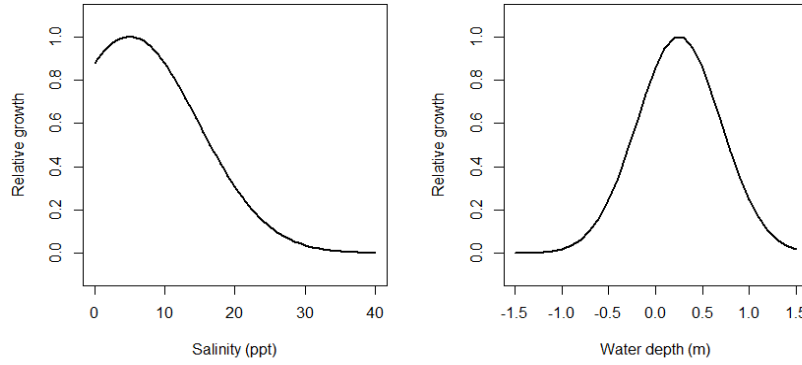


Figure 6.1: Relationship between relative net growth and salinity and water depth.

Evidence for an effect of water depth or salinity on the allocation of assimilates to above- and below-ground organs is ambiguous (e.g. Bazzaz et al. 1987; Lissner et al. 1999; Yang et al. 2014). Accordingly, the net rate of allocation of new assimilates to below-ground organs (i.e. translocation minus remobilisation) is assumed to be a constant proportion  $\beta$ , of new growth. Below-ground biomass persists for many years: on an annual basis, a proportion,  $\sigma$ , is lost to maintenance respiration, and a small proportion,  $\mu_{bg}$ , dies and becomes part of the peat pool. Hence, the dynamics of below-ground biomass are given by:

$$\frac{dB_{bg}}{dt} = \beta G_{max}\varepsilon_{S,g}\varepsilon_{W,g} - (\sigma + \mu_{bg})B_{bg} \quad \text{Equation 6.7}$$

and steady-state below-ground biomass is given by:

$$B_{bg}^* = \frac{\beta G_{max} \varepsilon_{s,g} \varepsilon_{w,g}}{(\sigma + \mu_{bg})} \quad \text{Equation 6.8}$$

Above-ground biomass turns over completely each year where a proportion of assimilates allocated to aboveground organs is used for maintenance respiration ( $\sigma$ ), a proportion enters the peat pool as litterfall ( $\mu_{ag}$ ) and the rest (i.e.  $1 - \sigma - \mu_{ag}$ ) remains above-ground as standing dead. A proportion of the standing dead pool collapses to the peat surface each year ( $\delta$ ) and a proportion decays in situ (i.e. air decay,  $\alpha_{sd}$ ). The dynamics of the standing dead pool are given by:

$$\frac{dD_{ag}}{dt} = (1 - \sigma - \mu_{ag})(1 - \beta)G_{max} \varepsilon_{s,g} \varepsilon_{w,g} - (\delta + \alpha_{sd})D_{ag} \quad \text{Equation 6.9}$$

and steady-state standing dead mass is given by:

$$D_{ag}^* = \frac{(1 - \sigma - \mu_{ag})(1 - \beta)G_{max} \varepsilon_{s,g} \varepsilon_{w,g}}{(\delta + \alpha_{sd})} \quad \text{Equation 6.10}$$

Inputs to the peat in the near-surface rooting zone are: organic matter from direct litterfall,  $\mu_{ag}(1 - \beta)G$ , collapse of standing dead,  $\delta D_{ag}$ , and the death of below-ground organs,  $\mu_{bg}B_{bg}$ . The mass flux from vegetation to peat  $F$  [ $\text{kg m}^{-2} \text{y}^{-1}$ ], is given by:

$$F = \mu_{ag}(1 - \beta)\varepsilon_{s,g}\varepsilon_{w,g}G_{max} + \delta D_{ag} + \mu_{bg}B_{bg} \quad \text{Equation 6.11}$$

and steady-state mass flux is given by:

$$F^* = \left[ \mu_{ag}(1 - \beta) + \frac{\delta(1 - \sigma - \mu_{ag})(1 - \beta)}{(\delta + \alpha_{sd})} + \frac{\mu_{bg}\beta}{(\sigma + \mu_{bg})} \right] \varepsilon_{s,g} \varepsilon_{w,g} G_{max} \quad \text{Equation 6.12}$$

Note that  $F^*$  simplifies to

$$F^* = \kappa \varepsilon_{s,g} \varepsilon_{w,g} G_{max} \quad \text{Equation 6.13}$$

where  $\kappa$  is the proportion of plant growth that enters the peat stock, determined by parameters relating to above-ground, below-ground and standing dead compartments:

$$\kappa = \mu_{ag}(1 - \beta) + \frac{\delta(1 - \sigma - \mu_{ag})(1 - \beta)}{(\delta + \alpha_{sd})} + \frac{\mu_{bg}\beta}{(\sigma + \mu_{bg})} \quad \text{Equation 6.14}$$

These new organic inputs are comprised of several portions: a portion lost almost immediately by physical leaching,  $\chi_{sol}$  (-), a refractory portion that does not decay (equivalent to the proportion of acid unhydrolysable residue, about 9.5% in *P. australis* leaves and culms; Dinka et al. 2004),  $\chi_{ref}$  [-], and finally, a labile portion,  $\chi_{lab}$  (-) which is equal to:  $1 - \chi_{sol} - \chi_{ref}$ . This final portion undergoes microbial decomposition at a maximum rate determined by the coefficient  $\alpha_{lab}$  ( $y^{-1}$ ). The decay rate coefficient is modified by stress functions for cumulated water depth,  $W$  (m) and salinity,  $S$  (ppt) (Dinka et al. 2004; Bedford 2005; Quintino et al. 2009; Voellm & Tanneberger 2014):

$$\varepsilon_{W,d} = e^{[-0.5(W-m_{W,d})^2/r_{W,d}]} \quad \text{Equation 6.15}$$

$$\varepsilon_{S,d} = e^{[-0.5(S-m_{S,d})^2/r_{S,d}]} \quad \text{Equation 6.16}$$

where  $m_{W,d}$  and  $m_{S,d}$  are the values of water depth and salinity, respectively, for which the decay rate coefficient is maximum.  $r_{W,d}$  and  $r_{S,d}$  represent the tolerance range of *P. australis* to these stressors (figure 6.2).

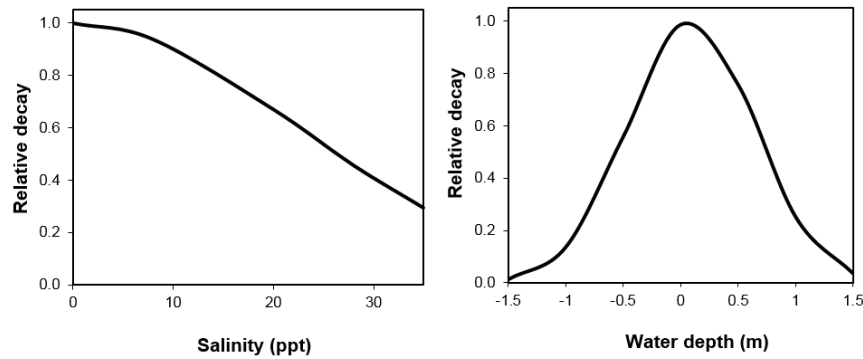


Figure 6.2: Relationship between relative decay and salinity and water depth.

Hence the labile,  $P_{lab}$  ( $kg\ m^{-2}$ ) and refractory components of organic matter,  $P_{ref}$  ( $kg\ m^{-2}$ ), accumulate at rates given by:

$$\frac{dP_{lab}}{dt} = (1 - \chi_{sol} - \chi_{ref})F - \varepsilon_{W,d}\varepsilon_{S,d}\alpha_{lab}P_{lab} \quad \text{Equation 6.17}$$

$$\frac{dP_{ref}}{dt} = \chi_{ref}F \quad \text{Equation 6.18}$$

Organic matter accumulated at time,  $T$ , is given by

$$P_{org} = P_{lab} + P_{ref} = \frac{(1-\chi_{sol}-\chi_{ref})F}{\varepsilon_{W,d}\varepsilon_{S,d}\alpha_{lab}}(1 - e^{-\varepsilon_{W,d}\varepsilon_{S,d}\alpha_{lab}T}) + \chi_{ref}FT \quad \text{Equation 6.19}$$

Eventually, the labile component approaches a steady state,  $P_{lab}^*$  ( $\text{kg m}^{-2}$ ). When steady state is reached, the rate of organic matter sequestration is driven almost entirely by the refractory component:

$$P_{lab}^* = \frac{(1-\chi_{sol}-\chi_{ref})F^*}{\varepsilon_{W,d}\varepsilon_{S,d}\alpha_{lab}} \quad \text{Equation 6.20}$$

This study is concerned with peat height in addition to peat mass. Both organic matter accumulation and mineral sedimentation contribute to vertical accretion,  $dH/dt$  ( $\text{m y}^{-1}$ ), according to the relevant bulk densities,  $\rho_{org}$  ( $\text{kg m}^{-3}$ ) and  $\rho_{min}$  ( $\text{kg m}^{-3}$ ) (Morris et al. 2016):

$$\frac{dH}{dt} = \frac{dP_{org}/dt}{\rho_{org}} + \frac{dP_{min}/dt}{\rho_{min}} \quad \text{Equation 6.21}$$

Hence, the height of the wetland surface,  $H$  (m), is given by:

$$H = \frac{P_{lab}+P_{ref}}{\rho_{org}} + \frac{P_{min}}{\rho_{min}} \quad \text{Equation 6.22}$$

### 6.2.2 Parameter values for numerical experiments

Salinity was varied between 0 and 35 ppt, representing the full gradient between freshwater and seawater. Cumulated water depth,  $W$  (m), accounts for variation in tidal range, seasonal range and mean water level.  $W$  was varied between 0 and 1, representing a range in hydrological regimes. Note it is assumed that seasonal range is fixed at 1 m. The effect of below-ground allocation,  $\beta$  (-), on peat accumulation is also explored for varying degrees of salinity and  $W$ . This is important to include as previous studies have shown that sea-level rise is likely to result in a shift in allocation of assimilates from above-to below-ground organs (Rolletschek et al. 1999; Soetaert et al. 2004), which will have implications on rate of mass flux from vegetation to peat. When  $\beta = 1$ , all available assimilates are allocated to below-ground organs. Conversely, when  $\beta = 0$ , all assimilates are allocated to above-ground. Thus,  $\beta$  is varied between 0 and 1 in increments of 0.2 for the purposes of this model.

Salinity,  $W$  and  $\beta$  were altered in the model; otherwise a consistent set of default parameters was used (table 6.1). The advantage of an analytical modelling approach is that controls on the dynamics can be explored much more readily than a numerical model. The disadvantage of analytical models is that they have to be highly simplified in order to be solved, and this needs to be considered when applying the results to real peatlands.

Table 6.1: Glossary of symbols used and parameter default values. The appropriate chapter number notes values derived from this study. Derived variables are those calculated based on the calculation of a combination of parameter values.

Parameter	Explanation	Units	Default	Source
$\eta$	total suspended sediment concentration	$\text{kg m}^{-3}$	0.01	Kirwan et al. (2016)
$G_{\max}$	maximum plant growth	$\text{kg m}^{-2} \text{y}^{-1}$	1.5	Windham (2001), Soetaert et al. (2004), Eid et al. (2010)
$m_{S,g}$	salinity at maximum plant growth	ppt	5	Engloner (2009)
$r_{S,g}$	scalar for salinity tolerance of plant growth	$\text{ppt}^2$	95	Analytically solved (figure 6.1)
$m_{W,g}$	water depth at maximum plant growth	m	0.25	Engloner (2009)
$r_{W,g}$	scalar for water depth tolerance of plant growth	$\text{m}^2$	0.2	Analytically solved (figure 6.2)
$\beta$	net allocation of assimilates belowground	-	0.3	Rolletschek & Hartzendorf (2000), Soetaert et al. (2004)
$\sigma$	maintenance respiration coefficient	$\text{y}^{-1}$	0.3	Hocking et al. (1983)
$\mu_{ag}$	aboveground litterfall proportion	-	0.4	Hocking et al. (1983)
$\mu_{bg}$	belowground mortality coefficient	$\text{y}^{-1}$	0.03	Hocking et al. (1983)
$\delta$	standing dead collapse coefficient	$\text{y}^{-1}$	0.9	Asaeda & Karunaratne (2000)
$\alpha_{sd}$	decay coefficient for standing dead	$\text{y}^{-1}$	0.01	Chapter 4
$\chi_{sol}$	soluble portion of plant remains	-	0.1	Chapter 4 (refers to mass loss after month 1)
$\chi_{ref}$	refractory portion of plant remains	-	0.1	Clymo (1984)
$\alpha_{lab}$	decay coefficient for labile organic matter	$\text{y}^{-1}$	0.04	Chapter 4 (refers to decay rate coefficient of leaves)
$m_{S,d}$	salinity at maximum peat decay	ppt	0.001	Quintino et al. (2009)
$r_{S,d}$	scalar for salinity tolerance of peat decay	$\text{ppt}^2$	500	Analytically solved (figure 6.2)
$m_{W,d}$	water depth at maximum peat decay	m	0.09	Dinka et al. (2004), Bedford (2005), Voellm & Tanneberger (2014)
$r_{W,d}$	scalar for water depth tolerance of peat decay	$\text{m}^2$	0.3	Analytically solved (figure 6.2)

$\rho_{\text{org}}$	self-packing bulk density of organic matter	$\text{kg m}^{-3}$	85	Chapter 5 (refers to Strumpshaw bulk density)
$\rho_{\text{min}}$	self-packing bulk density of mineral matter	$\text{kg m}^{-3}$	1995	Mudd et al. (2009)

---

**Derived variables**


---

$\psi$	efficiency of sediment settling and trapping	$\text{y}^{-1}$
$W$	cumulative floodwater depth for one year	$\text{m}$
$\varepsilon_{\text{S,g}}$	scalar for salinity stress on plant growth	-
$\varepsilon_{\text{W,g}}$	scalar for water depth stress on plant growth	-
$\varepsilon_{\text{S,d}}$	scalar for salinity stress on peat decay	-
$\varepsilon_{\text{W,d}}$	scalar for water depth stress on peat decay	-
$G$	plant growth	$\text{kg m}^{-2} \text{y}^{-1}$
$\kappa$	proportion of plant growth entering peat	-
$F$	flux of organic matter from vegetation to peat	$\text{kg m}^{-2} \text{y}^{-1}$
$\chi_{\text{lab}}$	labile portion of plant remains	-
$dP_{\text{x}}/dt$	rate of accumulation of labile (lab), refractory (ref) or total (org) organic matter, or mineral (min) matter	$\text{kg m}^{-2} \text{y}^{-1}$
$dH/dt$	rate of vertical accretion	$\text{m y}^{-1}$

---

## 6.3 Results

### 6.3.1 Mineral sedimentation rate

Mineral sedimentation rate increased with both cumulated water depth,  $W$ , and suspended sediment concentration,  $\eta$  (figure 6.3). Varying the efficiency factor was not found to effect mineral sedimentation rate (not shown).

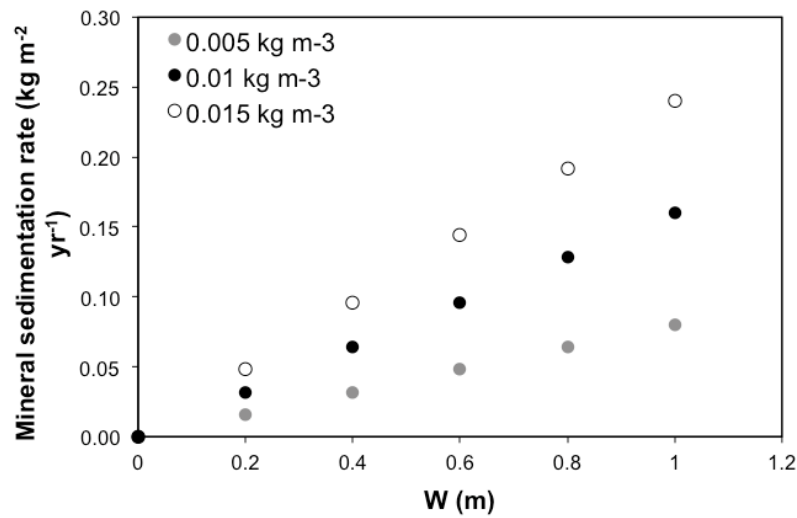


Figure 6.3: Change in mineral sedimentation rate,  $dP_{\min}/dt$  ( $\text{kg m}^{-2} \text{ yr}^{-1}$ ), when suspended sediment concentration,  $\eta$  ( $\text{kg m}^{-3}$ ), and cumulated water depth,  $W$  (m), are varied. Different values for  $\eta$  are indicated by coloured points (see legend).

### 6.3.2 Mass flux from vegetation to peat

$F^*$  decreases substantially when salinity  $> 15$  ppt, regardless of  $W$  (figure 6.4). At 15 ppt, growth is reduced to 60% of maximal production. When salinity is  $< 15$  ppt,  $F^*$  is highest at low  $W$  (0.2 to 0.4 m). When  $F^*$  is maximum (salinity = 5 ppt and  $W = 0.2$  m), the steady state stock for  $B_{bg}$  was  $1.5 \text{ kg C m}^{-2}$ ,  $D_{ag}$  was  $0.4 \text{ kg C m}^{-2}$  and  $P_{lab}$  was substantially larger at  $16 \text{ kg C m}^{-2}$ . In this simulation, 30% of assimilates ( $\beta$ ) were allocated below-ground and 40% of plant growth entering the peat pool ( $\kappa$ ).



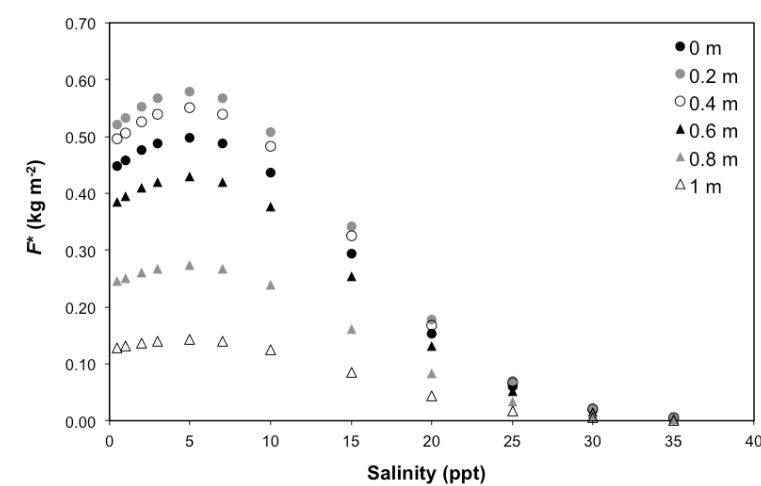


Figure 6.4: Change in the flux from vegetation to peat at steady state,  $F^*$  ( $\text{kg m}^{-2}$ ), when salinity (ppt) and cumulated water depth,  $W$  (m), are varied. Coloured points indicate differed values for  $W$  (see legend).

Mass flux from vegetation to peat,  $F^*$ , decreased as net allocation of assimilates to below-ground organs,  $\beta$ , increased (figure 6.5). An increase in salinity coupled with an increase in  $\beta$  reduced  $F^*$  to a greater extent than an increase in  $W$ .  $F^*$  was most sensitive to a change in allocation when salinity was between 2 and 5 ppt, and when  $W$  was between 0 and 0.6 m. The proportion of flux coming from below-ground material was 0.03, 0.08, 0.2 and 0.3 and 1 for allocations of 0.2, 0.4, 0.6 and 0.8 respectively.

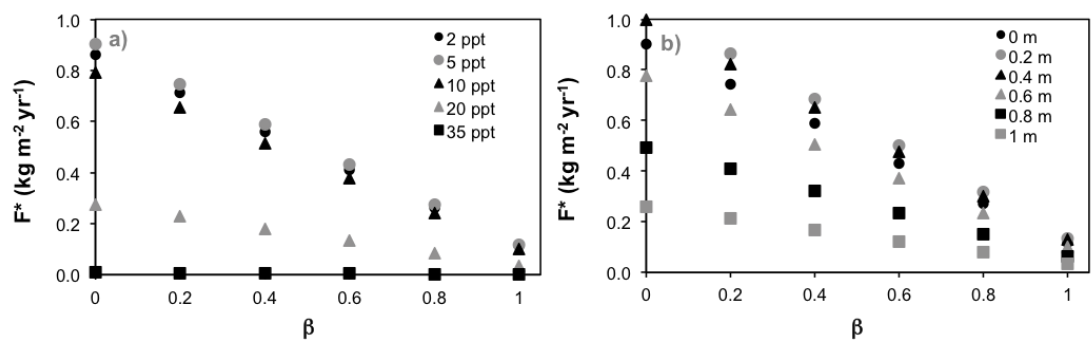


Figure 6.5: The relationship between flux from vegetation to peat at steady state,  $F^*$  ( $\text{kg m}^{-2}$ ) and allocation of net assimilates to below-ground organs,  $\beta$  (-), when (a) salinity (ppt) and (b) cumulated water depth,  $W$  (m), also varied. Points indicate varying salinity (ppt) and  $W$  (m) (see legend on each graph).

### 6.3.3 Labile and refractory components of decay

The labile component appeared to reach steady state after 200 years for all simulations apart from when salinity was 20 ppt and  $W$  was 0.8 m, where steady state was reached after 1000 years (figure 6.6). Peat organic mass will not reach a steady state as the refractory component does not decay (i.e. accumulates each year). The optimal conditions for the growth of peat organic mass is when salinity and  $W$  is low. Increasing  $W$  to 0.8 m appears to increase the period required for the refractory component to contribute primarily to the peat stock – which is further exacerbated by an increase in salinity.

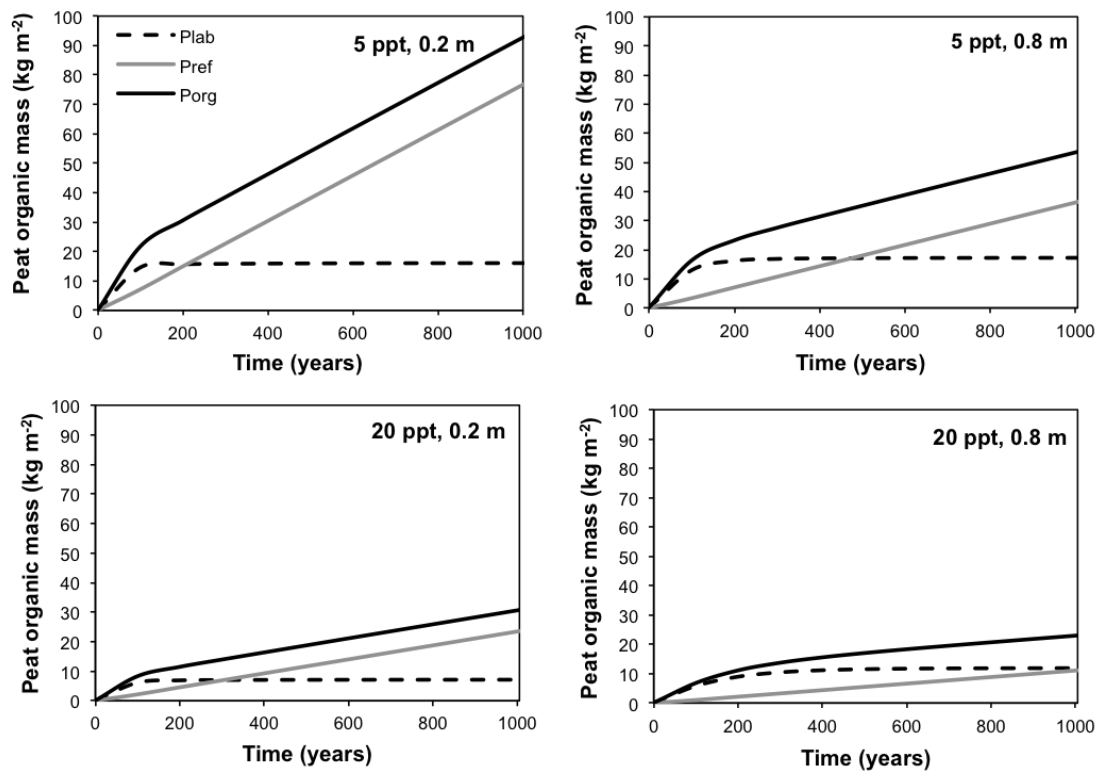


Figure 6.6: Peat organic carbon (kg m<sup>-2</sup>) over time:  $P_{org}$  is total organic content of the peat store,  $P_{lab}$  is the labile component and  $P_{ref}$  is the refractory component. Relative contributions are compared when salinity is 5 and 20 ppt, and when  $W$  is 0.2 and 0.8 m (see individual chart titles).

As indicated by figure 6.7, at steady state, peat mass is reduced when salinity exceeds 15 ppt regardless of  $W$ . Some degree of submergence increases the peat stock, but otherwise the size of the organic matter stock decreases with increasing  $W$ . For this simulation, below-ground allocation was fixed at 0.3, suggesting that around

6% of mass flux is coming from below-ground material (section 6.3.2). Decomposition was 43% of the maximum rate of decay when water level was 0.8 m, and production was 47% of maximum growth, indicating that rate of decomposition is close to exceeding rate of production.

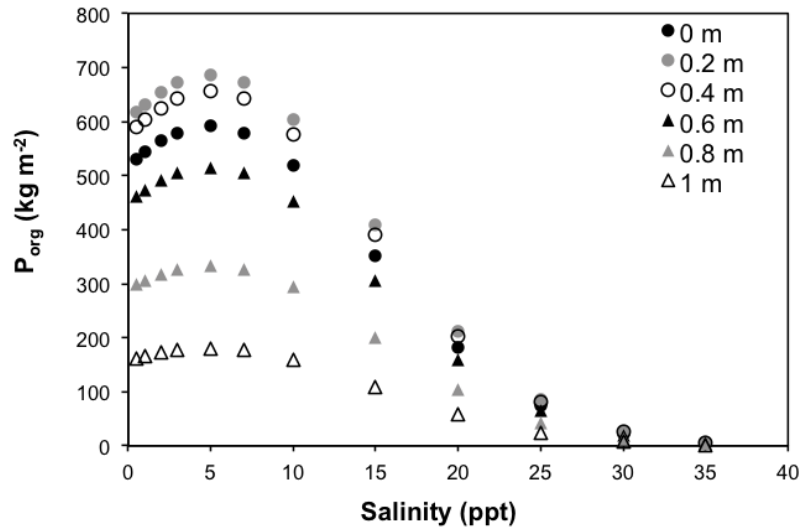


Figure 6.7: Change in the organic peat carbon store,  $P_{org}$  ( $\text{kg m}^{-2}$ ), after 9000 years.

#### 6.3.4 Relative contributions of mineral and organic matter to vertical accretion

Peat height is greatest when salinity is  $\leq 10$  ppt and when  $W$  is  $\leq 0.5$  m (figure 6.8). When  $W$  reaches 0.8 m, peat accretion reduces noticeably regardless of salinity. Ultimately, peat accretion will be the most compromised when salinity and water level are high.

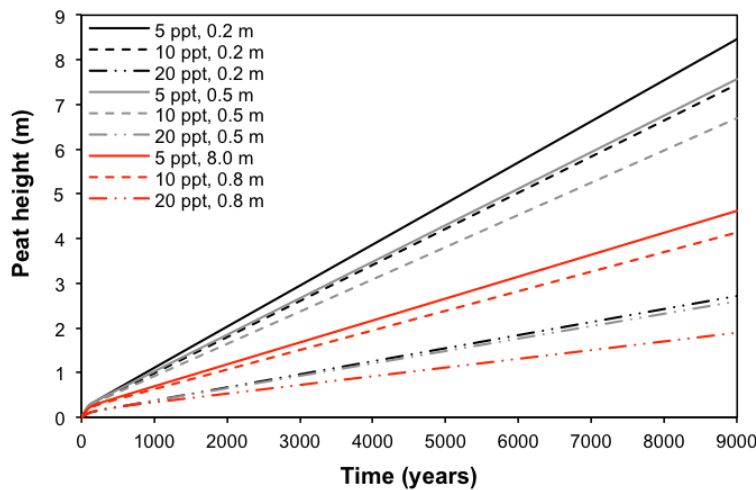


Figure 6.8: Change in height of a floodplain fen ( $H$ , m) under combinations of varying salinities (ppt) and cumulated water table depths ( $W$ , m). Colour of line indicates  $W$  and dashing of line indicates salinity.

Proportional contribution to peat height of the organic component is substantially greater than the mineral component when  $W$  is below 0.5 m (figure 6.9). The mineral component contributes at least 15% to peat height when  $W = 0.8$  m, doubling to 30% when salinity reaches 20 ppt. For an increase in salinity, mineral deposition is further exacerbated by an increase in  $W$ .

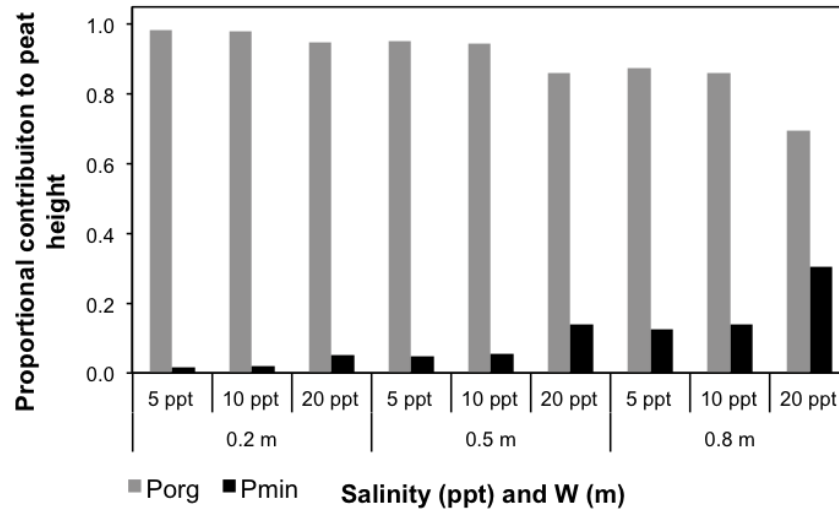


Figure 6.9: Proportional contribution of organic ( $P_{org} / \rho_{org}$ ) and mineral components ( $P_{min} / \rho_{min}$ ) to the peat height ( $H$ , m) over time for varying salinity (ppt) and cumulated water table depths,  $W$  (m).

### 6.3.5 Projected relative sea-level rise

The rate of increase in peat height has a negative relationship with salinity (figure 6.10). Regardless of salinity and  $W$ , peat accretion will not be able to keep pace with projected sea-level rise, even under the most conservative scenario. When salinity reaches 20 ppt and  $W \geq 0.8$  m, a small net reduction in peat accretion is observed as rate of decay exceeds rate of production as a consequence of salinity ( $\epsilon_{s,g} = 0.3$ ,  $\epsilon_{s,d} = 0.7$ ), although decomposition is close to offsetting production as a result of water level also ( $\epsilon_{w,g} = 0.5$ ,  $\epsilon_{w,d} = 0.4$ ).

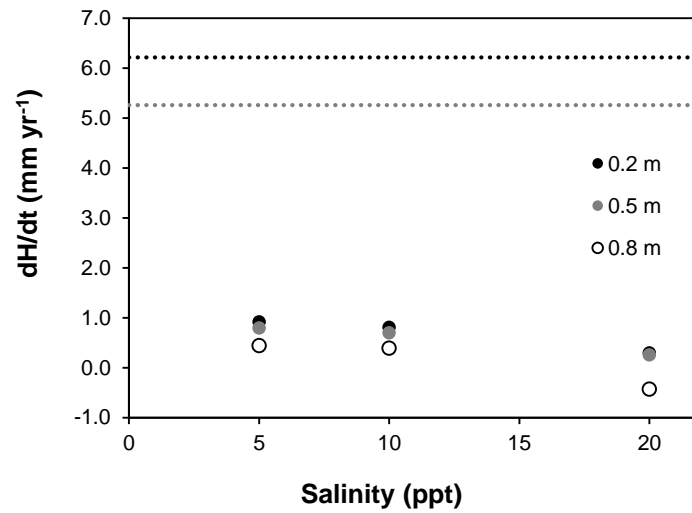


Figure 6.10: Rate of change in peat height ( $dH/dt$ , mm yr<sup>-1</sup>) under varying salinity, ppt, and cumulated water depth,  $W$  (m). The black dotted line indicates the projected rate of relative sea-level rise for RCP 6.0 and the grey dotted line is for RCP 2.5 (Church et al. 2013). Rates of sea-level rise are corrected for isotactic rebound of 0.05 mm yr<sup>-1</sup> in East Anglia (Bradley et al. 2009).

## 6.4 Discussion

A simple modelling approach was used to address the overarching question: what are the key controlling factors determining the growth of floodplain fens? By sequentially changing salinity and cumulative water level in simple analytical model by Belyea (2016, unpublished), it appears that rate of peat accretion depends primarily on cumulated water depth,  $W$ , remaining below 0.5 m, and salinity below 15 ppt.

In the model, relative stress tolerance curves (Qi et al. 2016) were the critical determinant of the response of *P. australis* to external stress. The results suggest that mass flux from vegetation to peat will decrease with increasing sea-level rise (i.e. salinity and water depth). Salinity in excess of 15 ppt was the primary reason for the reduction in mass flux to the peat, as growth was reduced to 60% of  $G_{\max}$ , whereas  $W$  needed to be 0.8 m or higher to induce a similar degree of stress on the growth of *P. australis*. Saltmarshes of similar elevation to the Broads (i.e. < 5 m above sea-level) frequently experience salinities in excess of 15 ppt (Bartlett et al. 1987; Craft et al. 2009), although it is unlikely that study sites described in this thesis will exceed this level owing to the connection to the sea via the river network as opposed to inundation from the sea directly. The work of Hiscock et al., (1996) indicates that an increase in saline incursion via the chalk aquifer in the Broads is also unlikely due to low salinities even at depths of 65 m (0.1 ppt). The current salinity of the Broads (~0.2 ppt, Chapter 3) means that productivity is almost maximal (figure 6.1), therefore any increase in salinity past 5 ppt would result in a decrease in production in comparison to the current situation.

The effect of sea-level rise on mass flux is amplified by changes in allocation of assimilate as, for a given degree of sea-level rise, mass flux to the peat will always be highest when the majority of assimilates are allocated above-ground (although obviously some needs to be allocated below-ground to maintain growth) – illustrating the importance of above-ground production to floodplain fen development (Vitt 1990). There are many environmental factors that might affect proportional allocation in *P. australis*, such as nutrient enrichment, salinity and waterlogging (Hellings & Gallagher 1992; Tylova-Munzarova et al. 2005). The magnitude and the direction of the response of allocation to an environmental stressor is generally equivocal in the literature, with some research reporting no change in proportional allocation as a result of stress (Lissner et al. 1999; Mauchamp & Mesleard 2001). Other evidence suggests that proportional allocation will change with increasing saline influence, due

primarily to an increase in the supply of carbon to below-ground material to support the lignification of roots – both to prevent the uptake of phytotoxins and to regulate the diffusion of oxygen to the rhizosphere (Armstrong et al. 1996). Whilst the lignification of roots would deprive other tissues of assimilate, an increase in allocation under these circumstances would not result in an increase in below-ground production. This is perhaps the reason why some *P. australis* studies that use above- to below-ground production quotients report that proportional allocation does not change under stressful conditions.

Peat accretion can only occur when the refractory component contributes more to total carbon than the labile component, which occurs when the labile peat reaches steady state. The results indicate that the labile component reached steady state the quickest when salinity and water level were low, suggesting that peat is accreting each year. An increase in sea-level rise will increase the time taken for the labile component to reach steady state, indicating that peat accretion will be reduced. This finding is supported by other studies that have shown the detrimental effects of sea-level rise on peatland development (e.g. Whittle & Gallego-sala 2016). Note that although not modelled here, refractory peat will be subject to a small degree of decomposition (Robinson & Moore 1999) – therefore this component is perhaps slightly overestimated. Nevertheless, the modelled mass of organic carbon accumulated after 9000 years ( $620 \text{ kg m}^{-2}$ ) is in good agreement with peat stocks estimated from long cores in Chapter 5 ( $550 \text{ kg m}^{-2}$ ) – therefore the model is thought to give a reliable insight into the effects of sea-level rise on peat organic mass.

The results in this Chapter indicate that vertical accretion of floodplain fens will not be able to keep pace with sea-level rise. Results derived from radiometric dating in Chapter 5 were compared to modelled values in the first 200 years of the 9000-year simulation because radiometric dated cores were taken at the peatland surface, and therefore consist primarily of newly formed peat. Results from Chapter 4 were in good agreement with modelled values for peat accretion and peat organic matter accumulation ( $2 \text{ mm yr}^{-1}$  and  $150 \text{ g m}^{-2} \text{ yr}^{-1}$ ). The model indicated that the effect of sea-level rise on peat accretion is likely to be severe, as a salinity of 20 ppt and *W* of 0.8 m would lead to rate of decomposition exceeding rate of production, and the peatland would no longer continue to develop. Similar conclusions have been drawn from other wetland elevation studies (Cahoon 2006), however, an apparent lack of surface elevation data, especially for lowland peatlands (Chmura et al. 2003), makes it difficult to understand the magnitude of this effect on the global carbon cycle. There will certainly be implications for site-level and regional conservation management, as

the model has provided preliminary evidence to suggest that salinity and water depth should be kept relatively low, even if this requires some degree of artificial management.

Carbon dynamics are also sensitive to inorganic sediment supply. The dependence of mineral sedimentation rate on cumulated water table depth suggests that sedimentation rate will increase with sea-level rise – a finding supported by previous lowland wetland studies (Kirwan & Mudd 2012). The model indicated that mineral deposition will be important for floodplain fen development. The lower carbon content of inorganic material (Chapter 5) indicates that a higher mineral sedimentation rate could reduce the size of the carbon store. Mineral sedimentation rate is dependent on supply, and since suspended sediment concentration in floodwater decreases rapidly as a function of distance from sea (Chmura et al. 2003), study sites closer to the river and/or the river mouth will be most vulnerable to sediment deposition. Mineral sedimentation rate calculated by the model was in good agreement with data derived from radiometric dating in Chapter 5, as cumulated water depth at Strumpshaw was calculated to be 0.2 m with a mineral sedimentation rate of  $0.03 \text{ kg m}^{-2} \text{ yr}^{-1}$ . This is at the lower end of estimates for other freshwater marshes (DeLaune et al. 2013), perhaps because suspended sediment concentrations are generally lower at floodplain fens due to their position at the terrestrial/open water interface (Diack et al. 2011). Due to the high bulk density of inorganic sediment, compaction from mineral deposition plays a significant role in determining the elevation of wetland surfaces (Cahoon 2006), particularly because porosity (i.e. compressible space) of peat is around 95% (Saltmarsh et al. 2006; Stanley 2015). The effect of compaction was evident in Chapter 5, where bulk density of Strumpshaw increased from  $0.85 \text{ g cm}^{-3}$  to  $1.2 \text{ g cm}^{-3}$  directly below the clay pan. Since compaction is not accounted for in the model, peat height could be overestimated. However, this is only likely to apply when salinity is 15 ppt or higher, as the relative contribution of the mineral component to peat height is negligible below this level (figure 6.9).



## 6.5 Conclusions and future research

This simple analytical modelling approach sought to understand the main controlling factors on peat growth in floodplain fens, and is believed to be a reasonable representation of the physical environment since model output was in good agreement with field data presented earlier in the thesis. The model by Belyea (2016, unpublished) suggested that peat accretion and peat organic mass will decrease as a result of sea-level rise – owing primarily to salinity but also to higher water depths. Previous Chapters in this thesis have discussed the delicate balance between sea-level rise, cutting regime and nutrient status etc. on the maintenance of above-ground productivity, and these findings become more relevant in the light of the findings in this Chapter. There are practical implications of these results, since the Broads, UK provide reed for commercial use and are important habitats for rare flora and fauna - all of which require specific management strategies that may or may not be in line with the maintenance of high above-ground production.

Peatlands store several hundred Gt of carbon in the form of organic matter (Yu et al. 2001), and it is currently unclear how stable the peatland carbon store will be under a changing climate (Charman et al. 2013). The effect of climate change on ombrotrophic peatlands has been high on the research agenda over the past two decades, focusing on climate parameters such as rainfall and temperature (Waddington et al. 2015). Despite 20 of the 600 Gt of carbon stored in peatlands being at less than 5 m elevation (Whittle & Gallego-Sala 2016), little attention has been paid to the effect of sea-level rise. With some degree of sea-level rise over the coming century now certain (Church et al. 2013), our work has highlighted some important directions for future research. Firstly, in-line with conclusions drawn from salt-marsh studies (Kirwan et al. 2016), the contribution of mineral deposition on vertical accretion has been shown in this Chapter to be important for floodplain fens. Modelled results are only theoretical, and a comprehensive field study would be important in determining the relative importance of mineral deposition on peat accretion and carbon sequestration. Secondly, an increase in allocation to below-ground material has been shown in this Chapter to further exacerbate the effects of sea-level rise on peat accretion. However, there is no consensus in the literature as to the certainty of this occurring in the field, therefore it would be highly beneficial for a future study to investigate the controls on the allocation of assimilate in floodplain fens.

## Chapter 7: Summary and Further Research

This research into carbon storage in floodplain fens along a gradient of saline influence has quantified rate of inputs to and rate of outputs from the peat carbon store and investigated differences in carbon sequestration and peat accretion. Data obtained from this work was used to parameterise an analytical model to understand how carbon storage in floodplain fens might be affected by sea-level rise in the future. Previously, relatively few studies had been conducted in UK lowland fens due to the lesser areal extent in the UK compared to ombrotrophic bogs, leaving a knowledge gap in peatland carbon storage. The areal extent of floodplain fens worldwide remains unknown; therefore this knowledge gap also applies to global wetland research and has probably resulted in biased estimates of the role of peatlands in the global carbon cycle. The need to reduce GHG emissions is becoming increasingly important in order to minimise the increase in global average temperatures. Natural carbon sequestering ecosystems, such as peatlands, are being recognised in international policy for their role in curbing GHG emissions. Climate models have shown an increase in the frequency and intensity of storm surge events, in addition to projected sea-level rise, however, the impacts of this on floodplain fens are currently not well understood and there is a clear need to improve our knowledge. This Chapter provides a brief overview of all research objectives, synthesising empirical findings and suggesting where further work is warranted.

### 7.1 Overview of research aims and objectives

The research in **Chapter 3** was undertaken to establish whether there was a gradient of saline influence in the Broads, UK. The Broads was chosen because it accounts for the largest proportion of undrained floodplain fen in the UK (Giller & Wheeler 1986), and storm surges have been detected in Environment Agency water level data throughout the area. Both porewater and surface water samples were collected to determine whether there was any evidence for saline influence using principal components analysis, whilst water level and electrical conductivity time series data was used to investigate differences in hydrologic regime and to determine if storm surges had been detected at study sites.

***Research question 3.1: What is the main environmental influence on water chemistry variables in both porewater and surface water at six floodplain fens?***

Principal components analysis (PCA) indicated the sites chosen for this study were located along a gradient of saline influence - as originally hypothesised (H<sub>3.1.1</sub>) - due to significant loadings of ions associated with seawater (Cl<sup>-</sup> and Na<sup>+</sup>) onto PC1. It was confirmed by analysis of ionic ratios that the primary source of these ions for the most saline influence site (Strumpshaw) was not precipitation, suggesting a surface water source. PCA revealed that geological and nutrient influences are also important controls on water chemistry – although they explained less variation combined than saline influence alone. Nevertheless, geological influence is likely to be important for carbon cycling in the Broads in particular - since high concentrations of Ca<sup>2+</sup> in porewater has been shown by other authors to accelerate decomposition (Jenkins & Suberkropp 1995; Bragg et al. 2003) – and previous studies have found evidence for the upward movement of Ca<sup>2+</sup> rich porewater from the large chalk aquifer underlying East Anglia (Hiscock et al. 1996; Shand et al. 2007).

Although it is widely accepted that floodplain fens are reasonably mineral rich due to inputs of water and solutes from surface water (van Diggelen et al. 2006; Diack et al. 2011), the relative importance of geological and nutrient influences in comparison to saline influence in controlling biogeochemical processes - such as production and decomposition - is less well known. Thus, the results of PCA presented an opportunity for site scores associated with each of these influences to be included collectively in multivariate analysis in the proceeding Chapters. The standardisation of data prior to PCA meant that the relative importance of each influence could be examined. A caveat that was considered throughout this PhD thesis was that, although a significant gradient of saline influence was found, the current salinity at study sites (in ppt) was at the lower end of other wetland studies associated with sea-level rise (Bartlett et al. 1987; Craft et al. 2009). Consequently, the attribution of a significant effect of salinity was interpreted tentatively. Work in the Thurne catchment could have contributed to the present research, owing to the relatively high salinity (often in excess of 5 ppt) (Holman & White 2008; Simpson et al. 2011) in comparison to sites used in this study. However, extensive ochre deposits, the recent construction of drainage ditches (in 2012) and restricted access meant that the use of sites on the Thurne would have introduced impracticalities and additional variables into this research.

**Research question 3.2:** Are saline pulses following documented storm surge events evident in water level and electrical conductivity time series data at floodplain fen sites?

Documented storm surge events on 9<sup>th</sup> November 2007 and 3<sup>rd</sup> December 2012 were used to determine if an increase in EC or water level from tide-gauge data corresponded with peaks in EC and water level at study sites. The results indicated the importance of physical characteristics of the surge. As hypothesised (H<sub>3.2.2</sub>), water level at the most saline influenced site increased after both surges almost immediately, probably due to their location on the River Yare that is known to have a tidal influence. Less saline influenced sites were located further up the river network, and EC peaked several days after the event and for the December surge which was particularly high, these sites experienced a peak in water level which tended to reside for several days. Therefore, the gradient of saline influence determined in RQ 3.1 also related to some degree to susceptibility to inundation from storm surge events.

The extensive analysis of time series data indicated no overall trend for an increase in water level in line with sea-level rise between 2006 and 2014, however, trend analysis proved to be limited by substantial gaps in the data sets. To address this, position of water level across all sites was compared for 2012 – the year where EC and water level records were most complete. The results were included in multivariate analysis as a controlling factor in the proceeding Chapters.

The research in **Chapter 4** sought to determine the rate of inputs to, and outputs from, the peat carbon store. Above-ground production was the measured input, quantified by harvesting above-ground biomass (AGB) at all six study sites in both 2013 and 2014. AGB was subsequently divided by PAR so that controls on radiation use efficiency (RuE) could be examined. Below-ground production was measured using root in-growth cores buried for 12 months. Litterbags were buried at three sites representative of the gradient of saline influence from low to high (Woodbastwick, Wheatfen and Strumpshaw) to measure litter decomposition. Both these measured quantities were used to determine both above- and below-ground carbon accumulation potentials.

**Research question 4.1:** What factors influence above-ground carbon productivity and how do these controls vary among sites located on a gradient of saline influence?

As expected, N/C in leaves, water level and nutrient influence were important influences on RuE, however, saline influence was of minor importance and geological

influence was not significant, therefore  $H_{4.1.1}$  was only partially accepted. Growth of *P. australis* is reduced when salinity is in excess of 10 ppt (Mauchamp & Mesleard 2001), which is probably why it was of little significance in this study. Management factors (cutting and trampling in this case) have been shown by other studies to be important in *P. australis* dominated wetlands and were included in the analysis (Hocking et al. 1983). Indeed, cutting regime was found to be the most important control on RuE, reducing photosynthetic efficiency with increasing period since cutting. There was preliminary evidence to suggest that cutting over consecutive years has a detrimental effect on RuE, although this cannot be proved or disproved based on the results of this study. No other studies have shown the relative importance of cutting over water chemistry variables, and the findings here are applicable to conservation land managers who may have previously underestimated the magnitude of the effect of cutting on above-ground production.

**Research question 4.2:** What factors control below-ground carbon production and the quotient of above- to below-ground carbon production (AGCP/BGCP)? How do these controls vary between sites located on a gradient of saline influence?

The ingrowth core method was useful in giving an indication of the rate of fine root growth, revealing no significant difference between sites. This method excludes the growth of rhizomes; therefore it is not possible to determine whether rhizome growth is controlled by water chemistry and/or management factors. Cutting increased AGCP/BGCP despite the indication in RQ 4.1 that cutting reduced AGCP. It is likely that assimilate is actively translocated to above-ground organs with increased time since cutting. Cutting has never before been shown to be the most important factor in controlling allocation in comparison to water chemistry influences, therefore this finding builds on existing knowledge that reallocation of assimilate to above-ground organs occurs during periods of stress (Soetaert et al. 2004). Submergence was also an important control on AGCP/BGCP, which is in agreement with other studies that show the increased use of assimilates for lignification as opposed to growth to regulate diffusion of oxygen to the rhizosphere (Armstrong et al. 1996). It was expected that nutrient availability would be an important control and overall,  $H_{4.3.1}$  was rejected.

**Research question 4.3:** What are the controls on the carbon decay rate of *in situ* decomposition of *P. australis* leaves, stems and below-ground material?

Controls on microbial decomposition varied by tissue type and  $H_{4.3.1}$  was rejected, since it was expected that saline influence would be important for all tissue types.

Nutrient availability was important for decomposition of below-ground material, which is an agreement with other studies that show the importance of N and P for microbial activity (Berg & McClaugherty 2008; Ouyang et al. 2008). Decomposition of stems was principally controlled by salinity, but it is not clear why controlling factors differed for BG and stems since they had similar C/N. Decay rate of leaves was accelerated by an increase in geological influence. It was speculated in RQ 3.1 that geological influence would be particularly important for carbon cycling in the Broads, owing to  $\text{Ca}^{2+}$  stimulating the activity of pectin lyase, the enzyme commonly used by aquatic fungi to macerate leaves (Jenkins & Suberkropp 1995). This will be a particularly important consideration for policy makers, since  $\text{Ca}^{2+}$  was also present in reasonably high concentrations in surface water (Chapter 3, PC4), indicating that increased inundation will further accelerate the decomposition of leaves. Based on the results in this section, sea-level rise will accelerate the decomposition of stems and leaves, but there is little evidence in the wider literature to suggest that sea-level rise will increase nitrogen or SRP deposition, as these are more related to anthropogenic sources (Neal et al. 2010). Therefore, the Broads or other calcium rich lowland wetlands may become increasingly dependent on the maintenance of slow rates of decay of below-ground material for carbon sequestration.

**Research question 4.4:** Are differences in carbon decay rate due to changes in litter quality and/or microenvironment?

Transplanting litter from a relatively freshwater to a more saline influenced site allowed for the effects of microenvironment and litter quality on decomposition to be separated. The results indicated that in the short-term, an increase in saline influence may initially lead to faster decay rates, but longer-term changes in litter quality would partially offset these changes (as foliar C/N was higher at more saline influenced sites).  $H_{4.4.1}$  could only be partially accepted, since this result was only significant for leaves and stems. The overarching, practical finding from this section is that submergence reduced the rate of decomposition of the poorer quality litter transplanted to a more saline influenced site, indicating that peat accumulation could be sustained if - when sea-level rise becomes apparent - water levels are kept consistently above the peat surface, even if this requires artificially doing so.

**Research question 4.5:** Does carbon accumulation potential vary along the gradient of saline influence?

The results indicated that the most saline influenced site had the lowest potentials for both, and  $H_{4.5.1}$  was rejected. The relatively fast decay rates of AG tissues (i.e. leaves

and stems) means that AG accumulation potentials are dependent on a high rate of above-ground production. AGCP will probably reduce when salinity exceeds 10 ppt (e.g. Pagter et al. 2009) and the results of RQ 4.3 indicated that the controls on decomposition of leaves and stems will probably lead to an increase in decay rate as a result of sea-level rise, therefore BG carbon accumulation will become increasingly important. Indeed, this was reflected in the results of this research question, as BG carbon accumulation potential was sustained by low rates of decay of BG material as opposed to high rates of BG production.

The overall aim of **Chapter 5** was to understand the main control(s) on carbon density, and apply the results to calculate an accurate estimate of carbon stock for three floodplain fens representative of a gradient of saline influence in the Broads, UK. Peat types were identified according to the criteria of Lambert (1960) and were subsequently matched to a modified version of the Troels-Smith criteria so that results were applicable to the wider literature. Carbon sequestration and peat accretion rate were determined using results from radiometric dating.

**Research question 5.1:** Does carbon density and its components (bulk density and total carbon content) vary between different peat types found in three floodplain fen sites?

Carbon density differed between sites but not by peat type as expected, therefore  $H_{5.1.1}$  was rejected. The significant difference of carbon density between sites indicates spatial variation in carbon density, which is probably owing to spatial variation in bulk density. The results of this section indicated that mineral deposition is an important driver of spatial variation in bulk density, as sites located on the tidally influenced River Yare exhibited: (i) a reduced organic matter content of surface peat and (ii) a rapid increase in bulk density of surface peat with depth. Both of these observations have been suggested by other studies to be a common sign of compression from mineral deposition (Castañeda-Moya et al. 2010). The influence of mineral deposition for carbon storage in lowland wetlands is a relatively recent observation based on the results from salt marsh studies (Mudd et al. 2009; Neubauer et al. 2013). The spatial variation in carbon density was the key finding of this section, as this affected how carbon stocks should be calculated in RQ 5.2. However, the posited reason for the spatial variation forms the basis for further research of the effect of mineral deposition on carbon accumulation in floodplain fens.

**Research question 5.2:** What is the carbon stock for three sites varying in saline influence in a floodplain fen?

Carbon stock was calculated irrespective of peat type based on the results of RQ 5.1. The estimated carbon stock of Strumpshaw was almost five times that of Woodbastwick, owing primarily to peat depth, since Woodbastwick and Wheatfen had similar carbon densities. The implications of the findings of RQ 5.1 and 5.2 for regional carbon stock estimates were profound, as applying bulk density and peat depths determined in this study to the area of lowland fens given by Natural England (2010) (1000 km<sup>2</sup>) changed their carbon stock estimate by up to 60%. It is accepted that the detailed coring survey conducted over Lambert's career provided a unique opportunity to calculate site specific carbon stock in the Broads, and that obtaining site specific peat depth and bulk density measurements is methodologically intensive or even impossible in some instances. However, the results of this section will help future work understand the potential error in regional estimates of peat carbon stock.

**Research question 5.3:** What are recent carbon sequestration and peat accretion rates at three floodplain fen sites?

Unlike carbon density, recent carbon sequestration depends primarily on carbon content, which was lower at tidally influenced sites and is probably due to increased mineral deposition, supporting the findings of RQ 5.1. Bulk density might not have been important here as only the top 30 cm of peat were sampled for radiometric dating, whereas patterns of bulk density in the coring survey were apparent at greater depths. As expected, recent peat accretion was similar between study sites and H<sub>5.3.1</sub> was accepted. Accretion rate in the Broads is unlikely to keep pace with projected sea-level rise, and the implications for carbon sequestration and the persistence of floodplain fens remains unknown. To understand how sea-level rise will affect peat accretion, it would be necessary to isolate the key components of peatland development (i.e. production and decomposition) and determine how extreme instances of sea-level rise (such as high water level and salinity) might affect each of these processes. Carbon accumulation potentials calculated in RQ 4.5 addressed this to some degree, but did not account for other processes that have been shown throughout this thesis to be important considerations for carbon storage in floodplain fens, such as mineral deposition.



An unpublished model by Belyea (2016) was used in **Chapter 6** to explore the effects of different components of sea-level rise (water level and salinity) on peat accretion. The model was parameterised using field data obtained throughout this thesis and published values from the wider literature where appropriate. Five research questions were explored and discussed collectively in the Chapter; therefore conclusions will also be presented as a single synthesis. The research questions explored were:

**Research question 6.1:** How is mineral sedimentation rate affected by a change in suspended sediment concentration and cumulated water depth?

**Research question 6.2:** To what extent is the mass flux of vegetation to peat dependent on belowground allocation, salinity and cumulated water depth?

**Research question 6.3:** How are the relative contributions of the labile and refractory components to organic matter influenced by salinity and water level? How many years does it take for the labile component to approach steady state?

**Research question 6.4:** Are the relative contributions of the mineral and organic components to vertical accretion affected by salinity and cumulated water depth?

**Research question 6.5:** What are the key controlling factors that will determine whether vertical accretion in floodplain fens can keep pace with relative sea-level rise (RSLR)?

The analytical model proved to be an effective way of exploring controlling factors on peat accretion, especially with the inclusion of stress tolerance curves (Qi et al. 2016) which allowed the effects of salinity and water level to be included in the model simultaneously. Since salinity of study sites was relatively low in comparison to the wider literature, the model allowed the extrapolation of the effects of a higher degree of sea-level rise (i.e. salinity and water depth) on carbon storage. Data obtained from field and laboratory work in earlier Chapters was used in the model, such as rate of decomposition from Chapter 4 and peat bulk density from Chapter 5. Results from the coring survey and radiometric dating were successfully used to ‘reality check’ model output against what was observed in the field – therefore the model is considered to give a reliable insight into the effects of sea-level rise on carbon storage in floodplain fens.

A common theme running through this thesis is the importance of mineral deposition on peat accretion and carbon sequestration in floodplain fens. Previously, the relative

contributions of mineral and organic matter to vertical accretion had only been shown to be important for saltmarshes (Kirwan et al. 2016). Field and laboratory data from Chapter 5 indicated that the lower carbon sequestration rate at tidally influenced sites was probably due to a higher contribution of mineral matter to peat mass. Modelled output in Chapter 6 showed that mineral deposition would continue to increase when salinity and water level exceeds what is currently experienced at study sites. Collectively, the results suggest that an increase in the relative contribution of the mineral component as a result of sea-level rise is likely to reduce both carbon sequestration rate and vertical accretion in floodplain fens.

It has been shown in this research that carbon storage in floodplain fens is likely to reduce as a result of sea-level rise. Carbon accumulation potentials determined from field and laboratory data in Chapter 4 indicated that rate of decomposition was closer to exceeding rate of production at the most saline influenced site. This was later reflected in the results of the modelling study, which showed that carbon storage would decrease with increasing sea-level rise and in particular, vertical accretion would cease altogether under an extreme scenario, as rate of production no longer exceeds rate of decay. It was shown in Chapter 5 that carbon stocks in the Broads are of significance to UK peatland carbon estimates, and it can be extrapolated from the model that carbon storage here – and probably in floodplain fens worldwide – is at risk if sea-levels continue to rise in the future.

## **7.2 Directions for further research**

The three main research Chapters within this thesis have identified the possible effects of sea-level rise on carbon storage in floodplain fens and assessed the contribution of other controlling factors such as management regime and nutrient and geological influences, however, the research has also highlighted areas for future research.

## **The effect of cutting on rate of production**

This study has found the effect of cutting to be an important control on rate of above-ground production and AGCP/BGCP. The results of this thesis in general have indicated that the persistence of floodplain fens will partly depend upon a high rate of above-ground production. A large proportion of floodplain fens are managed to some degree, usually for either conservation purposes or commercial reed cutting, or are cleared periodically for agriculture (van Diggelen et al. 2006). All of these management practices will require a decision relating to frequency of cutting, and although affecting local processes, this decision has global implications on carbon sequestration in floodplain fens.

In order to understand if cutting in consecutive years is as detrimental as not cutting for three years or more, a comparison of rate of production under different cutting regimes could be measured. The effect of cutting on production in the following season remains equivocal in the wider literature, therefore an empirically based field study would be highly valuable. Other studies have shown the interaction between cutting and environmental factors such as salinity to have a negative effect (Asaeda et al. 2003), and the timing of cutting is also particularly important (Husák 1975) as cutting during the winter means that high water levels retard the growth of new shoots (Weisner & Granéli 1989). Few studies have addressed the effect of frequency of cutting on above-ground production whilst controlling for the aforementioned variables. A simple study could address this, as some sites in the Broads (such as Strumpshaw) are cut on a rotation, therefore above-ground biomass could be harvested in a single year and subsequently compared. The results of this further work will influence conservation management by helping to complete the picture of how different practices could help or hinder the possible effects of sea-level rise on above-ground production.

## **Controls on decomposition between litter types**

This thesis focused on the effect of hydrochemical variables and management regime on decomposition rate, using C/N as the only indication of litter quality. Saline influence was only significant for stems, and the reason for this remains unclear owing to the similar C/N between stems and below-ground material.

Previous *P. australis* studies related to decomposition have measured decay rate of leaves, stems and occasionally culms individually, but few have compared the controls on each litter type, focusing more on the effect of mesh size, or a particular

environmental or climatic perturbation such as water level or soil temperature on decomposition (Bedford 2005; Van Ryckegem et al. 2006). Other research carried out in the Broads indicated that differences in decomposition between tissue types was largely due to the presence of macro-fauna such as *Lymnaea* spp. and *Asellus*, which strip more complex tissues into smaller fragments, thereby increasing the surface area for microbial colonisation (Mason & Bryant 1975). C/N of litter gives a very broad indication of litter quality, and it is possible that stems have a higher proportion of fibrous structures that are not as readily broken down by microbes (Berg & McClaugherty 2008). Consequently, the apparent effect of salinity may well be the continuation of physical leaching, since NaCl decreases the surface tension of organic compounds, thereby increasing the solubility of phenols (Sahu et al. 2010). Although, it was not possible to confirm this based on the results of this study.

The mesh size chosen in this thesis precluded the inclusion of macro-fauna; therefore, a decomposition study where mesh size of litterbags is varied would help to understand the role of macro-fauna in decomposition. This work could be complemented by comprehensive characterisation of the relative proportions of fibrous structures in *P. australis* tissues.

### **Long-term implications of mineral deposition**

Field data from the present study alluded to the importance of considering the effect of increased mineral deposition on carbon sequestration and peat accretion rates in floodplain fens. The results of the analytical model suggested that the contribution of mineral deposition to peat height is minor in comparison to the contribution of organic matter. Nevertheless, mineral deposition at Wheatfen and Strumpshaw reduced carbon sequestration rate by approximately 10%. It is relatively unknown how suspended sediment concentration might vary with saline influence (Mudd et al. 2009) and if mineral deposition was to stay the same or even increase, then this could have substantial repercussions on long-term carbon accumulation rates (Chmura et al. 2003).

### 7.3 Conclusion

This thesis combined field, laboratory and modelling techniques to determine the effect of sea-level rise on carbon storage in floodplain fens, and has generated scope for additional research into how management practice could help offset the possible detrimental effects of sea-level rise.

Overall, this research has shown that despite the significant contribution of floodplain fens to the global peatland carbon store, sea-level rise is likely to reduce carbon sequestration rate in this important peatland type. The implications of this are profound, as data presented in this research suggests that floodplain fens represent a particularly dense carbon store of regional and global significance. With some degree of sea-level rise now certain due to historic anthropogenic greenhouse gas emissions, there is a very real chance that carbon stores in the Broads, and similar ecosystems in other parts of the world, will be lost. The ability of these ecosystems to retreat inland may be limited due to land-use change and - since it is well established that the formation of peat deposits can take several thousand years – these carbon deposits are not replaceable over decades or centuries. For example, in the Broads, saltmarshes might begin to form as the sea encroaches more permanently onto land. This newly developed environment might provide some of the ecosystem services delivered by floodplain fens; however, it is unlikely that the substantial above- and below-ground carbon pools supported by floodplain fens will be replicated by saltmarshes.

Once released from the terrestrial biosphere, carbon lost from floodplain fens will be a significant driver of positive climate feedbacks (including the acceleration of sea-level rise and permafrost thaw) – thus the net effect of a loss of these ecosystems on the global climate system is substantial and probably irreversible.

## Reference List

- Aerts, R. & De Caluwe, H., 1994. Nitrogen Use Efficiency of Carex Species in Relation to Nitrogen Supply. *Ecology*, 75(8), pp.2362–2372.
- Akumu, C.E. & McLaughlin, J.W., 2013. Regional variation in peatland carbon stock assessments, northern Ontario, Canada. *Geoderma*, 209, pp.161–167.
- Ali, A.A., Ghaleb, B., Garneau, M., Asnong, H. & Loisel, J., 2008. Recent peat accumulation rates in minerotrophic peatlands of the Bay James region, Eastern Canada, inferred by  $^{210}\text{Pb}$  and  $^{137}\text{Cs}$  radiometric techniques. *Applied Radiation and Isotopes*, 66(10), pp.1350–1358.
- Allen, D.J., Brewerton, L.J., Coleby, L.M., Gibbs, B.R., Lewis, M.A., MacDonald, A.M., Wagstaff, S.J. & Williams, A.T., 1997. *The physical properties of major aquifers in England and Wales*, British Geological Survey Technical Report WD/97/34.
- Álvarez-Iglesias, P., Quintana, B., Rubio, B. & Pérez-Arlucea, M., 2007. Sedimentation rates and trace metal input history in intertidal sediments from San Simón Bay (Ría de Vigo, NW Spain) derived from  $^{210}\text{Pb}$  and  $^{137}\text{Cs}$  chronology. *Journal of Environmental Radioactivity*, 98(3), pp.229–250.
- Ander, E., Shand, P. & Wood, S., 2006. *Baseline Report Series: 21. The Chalk and Crag of north Norfolk and the Waveney Catchment. Technical Report: CR/06/043N, NC/99/74/21*,
- Appleby, P.G., 2001. Chronostratigraphic techniques in recent sediments. In *Tracking environmental change using lake sediments*. Springer, pp. 171–203.
- Appleby, P.G., 2008. Three decades of dating recent sediments by fallout radionuclides: a review. *The Holocene*, 18(1), pp.83–93.
- Appleby, P.G. & Oldfield, F., 1978. The calculation of  $^{210}\text{Pb}$  dates assuming a constant rate of supply of unsupported  $^{210}\text{Pb}$  to the sediment. *Catena*, 5, pp.1–8.
- Arambarri, I., Garcia, R. & Millan, E., 2003. Assessment of tin and butyltin species in estuarine superficial sediments from Gipuzkoa, Spain. *Chemosphere*, 51(8), pp.643–649.
- Archer, D. & Brovkin, V., 2008. The millennial atmospheric lifetime of anthropogenic  $\text{CO}_2$ . *Climatic Change*, 90(3), pp.283–297.

- Armentano, T. V & Menges, E.S., 1986. Patterns of Change in the Carbon Balance of Organic Soil-Wetlands of the Temperate Zone. *Journal of Ecology*, 74(3), pp.755–774.
- Armstrong, J., Afreen-Zobayed, F., Blyth, S. & Armstrong, W., 1999. *Phragmites australis*: Effects of shoot submergence on seedling growth and survival and radial oxygen loss from roots. *Aquatic Botany*, 64(3-4), pp.275–289.
- Armstrong, J. & Armstrong, W., 2001. An overview of the effects of phytotoxins on *Phragmites australis* in relation to die-back. *Aquatic Botany*, 69(2-4), pp.251–268.
- Armstrong, J., Armstrong, W. & Van der Putten, W., 1996. *Phragmites* die-back: Bud and root death, blockages within the aeration and vascular systems and the possible role of phytotoxins. *New Phytologist*, 133(3), pp.399–414.
- Asaeda, T. & Karunaratne, S., 2000. Dynamic modeling of the growth of *Phragmites australis*: model description. *Aquatic Botany*, 67(4), pp.301–318.
- Asaeda, T., Manatunge, J., Fujino, T. & Sovira, D., 2003. Effects of salinity on the growth of *Phragmites australis*. *Wetlands Ecology and Management*, 11(3), pp.127 – 140.
- Asaeda, T., Nam, L.H., Hietz, P., Tanaka, N. & Karunaratne, S., 2002. Seasonal fluctuations in live and dead biomass of *Phragmites australis* as described by a growth and decomposition model: implications for duration of aerobic conditions for litter mineralization and sedimentation. *Aquatic Botany*, 73(3), pp.223–239.
- Asaeda, T., Rajapakse, L., Manatunge, J. & Sahara, N., 2006. The effect of summer harvesting of *Phragmites australis* on growth characteristics and rhizome resource storage. *Hydrobiologia*, 553(1), pp.327–335.
- BADC, 2016. NERC Data Discovery Service. *MIDAS Stations*. Available at: [www.badc.nerc.ac.uk/search/midas\\_stations/](http://www.badc.nerc.ac.uk/search/midas_stations/) [Accessed March 28, 2016].
- Bain, C., Joosten, H., Smith, P., Reed, M., Evans, C., Thompson, A., Coupar, A. & Coath, M., 2012. *Kyoto Protocol and National Accounting for Peatlands*, International Union for Conservation of Nature.
- Bain, C.G., Bonn, A., Stoneman, R., Chapman, S., Coupar, A., Evans, M., Gearey, B., Howat, M., Joosten, H., Keenleyside, C., Labadz, J., Lindsay, R., Littlewood, N.,

- Lunt, P., Miller, C., Moxey, A., Orr, H., Reed, M., Smith, P., Swales, V., Thompson, D.B., Thompson, P., Van de Noort, R., Wilson, J. & Worrall, F., 2011. *IUCN UK Commission of Inquiry on Peatlands*, ICUN UK Peatland Programme, Edinburgh.
- Baird, A.J., Belyea, L.R. & Morris, P.J., 2009. Upscaling of peatland-atmosphere fluxes of methane: Small-scale heterogeneity in process rates and the pitfalls of “bucket-and-slab” models. *Geophysical Monograph Series*, 184, pp.37–53.
- Baird, A.J., Morris, P.J. & Belyea, L.R., 2012. The DigiBog peatland development model 1: Rationale, conceptual model, and hydrological basis. *Ecohydrology*, 5(3), pp.242–255.
- Bakker, J.P., Olf, H., Willems, J.H. & Zobel, M., 1996. Why do we need permanent plots in the study of long- term vegetation dynamics? *Journal of Vegetation Science*, 7(2), pp.147–156.
- Baldwin, A.H. & Mendelssohn, I.A., 1998. Effects of salinity and water level on coastal marshes: An experimental test of disturbance as a catalyst for vegetation change. *Aquatic Botany*, 61(4), pp.255–268.
- Bao, K., Yu, X., Jia, L. & Wang, G., 2010. Recent Carbon Accumulation in Changbai Mountain Peatlands, Northeast China. *Mountain Research and Development*, 30(1), pp.33–41.
- Bartlett, K.B., Bartlett, D.S., Harriss, R.C. & Sebach, D.I., 1987. Methane emissions along a salt-marsh salinity gradient. *Biogeochemistry*, 4(3), pp.183–202.
- Basiliko, N., Blodau, C., Roehm, C., Bengtson, P. & Moore, T., 2007. Regulation of Decomposition and Methane Dynamics across Natural, Commercially Mined, and Restored Northern Peatlands. *Ecosystems*, 10(7), pp.1148–1165.
- Bates, D., Mächler, M., Bolker, B.M. & Walker, S.C., 2014. Fitting linear mixed-effects models using lme4. *Journal of Statistical Software*, 67(1), pp.1–48.
- Bates, D.M., 2010. *lme4: Mixed-effects modeling with R*, Springer.
- Bauer, I.E., Bhatti, J.S., Cash, K.J., Tarnocai, C. & Robinson, S.D., 2006. Developing statistical models to estimate the carbon density of organic soils. *Canadian Journal of Soil Science*, 86(Special Issue), pp.295–304.
- Bazzaz, F.A., Chiariello, N.R., Coley, P.D. & Pitelka, L.F., 1987. Allocating Resources



- to Reproduction and Defense. *BioScience*, 37(1), pp.58–67.
- Bedford, A.P., 2004. A modified litter bag design for use in lentic habitats. *Hydrobiologia*, 529(1), pp.187–193.
- Bedford, A.P., 2005. Decomposition of *Phragmites australis* litter in seasonally flooded and exposed areas of a managed reedbed. *Wetlands*, 25(3), pp.713–720.
- Beilman, D.W., Vitt, D.H., Bhatti, J.S. & Forest, S., 2008. Peat carbon stocks in the southern Mackenzie River Basin: Uncertainties revealed in a high-resolution case study. *Global Change Biology*, 14(6), pp.1221–1232.
- Belyea, L.R., 1996. Separating the effects of litter quality and microenvironment on decomposition rates in a patterned peatland. *Oikos*, pp.529–539.
- Belyea, L.R. & Baird, A.J., 2006. Beyond “The Limits to Peat Bog Growth”: Cross-Scale Feedback in Peatland Development. *Ecological Monographs*, 76(3), pp.299–322.
- Belyea, L.R., 2016. Floodplain Fen Analytical Model. *Unpublished*.
- Berendse, F. & Aerts, R., 1987. Nitrogen-Use-Efficiency: A Biologically Meaningful Definition? *Functional Ecology*, 1(3), pp.293–296.
- Berg, B. & McClaugherty, C., 2008. *Plant Litter* Second Edi., Springer.
- Bernal, B. & Mitsch, W.J., 2008. A comparison of soil carbon pools and profiles in wetlands in Costa Rica and Ohio. *Ecological Engineering*, 34(4), pp.311–323.
- Bernal, B. & Mitsch, W.J., 2012. Comparing carbon sequestration in temperate freshwater wetland communities. *Global Change Biology*, 18(5), pp.1636–1647.
- Berner, R., 2003. Fuels and Atmospheric Composition. *Nature*, 426, pp.323–326.
- Biasi, C., Rusalimova, O., Meyer, H., Kaiser, C., Wanek, W., Barsukov, P., Junger, H. & Richter, A., 2005. Temperature-dependent shift from labile to recalcitrant carbon sources of arctic heterotrophs. *Rapid Communications in Mass Spectrometry*, 19(11), pp.1401–1408.
- Billett, M.F., Palmer, S.M., Hope, D., Deacon, C., Storeton-West, R., Hargreaves, K.J., Flechard, C. & Fowler, D., 2004. Linking land-atmosphere-stream carbon fluxes in a lowland peatland system. *Global Biogeochemical Cycles*, 18(1), p.12.

- Birkett, J.W., Noreng, J.M.K. & Lester, J.N., 2002. Spatial distribution of mercury in the sediments and riparian environment of the River Yare, Norfolk, UK. *Environmental Pollution*, 116(1), pp.65–74.
- Bjørnstad, O.N., Ims, R. a. & Lambin, X., 1999. Spatial population dynamics: Analyzing patterns and processes of population synchrony. *Trends in Ecology and Evolution*, 14(11), pp.427–432.
- Blodau, C., 2002. Carbon cycling in peatlands A review of processes and controls. *Environmental Reviews*, 10(2), pp.111–134.
- Blodau, C., Basiliko, N. & Moore, T.R., 2004. Carbon turnover in peatland mesocosms exposed to different water table levels. *Biogeochemistry*, 67(3), pp.331–351.
- Boar, R., 1996. Temporal variations in the nitrogen content of *Phragmites australis* (Cav.) Trin. ex Steud. from a shallow fertile lake. *Aquatic Botany*, 55(3), pp.171–181.
- Bodensteiner, L.R. & Gabriel, A.O., 2003. Response of mid-water common reed stands to water level variations and winter conditions in Lake Poygan, Wisconsin, USA. *Aquatic Botany*, 76(1), pp.49–64.
- Bonn, A., Reed, M.S., Evans, C.D., Joosten, H., Bain, C., Farmer, J., Emmer, I., Couwenberg, J., Moxey, A., Artz, R., Tanneberger, F., von Unger, M., Smyth, M.A. & Birnie, D., 2014. Investing in nature: Developing ecosystem service markets for peatland restoration. *Ecosystem Services*, 9, pp.54–65.
- Bosello, F., Roson, R. & Tol, R.S.J., 2007. Economy-wide Estimates of the Implications of Climate Change: Sea Level Rise. *Environmental & Resource Economics*, 37, pp.549–571.
- Ter Braak, C.J.F. & Prentice, I.C., 1988. A theory of gradient analysis. *Advances in Ecological Research*, 18, pp.271–317.
- Ter Braak, C.J.F. & Verdonschot, P.F.M., 1995. Canonical correspondence analysis and related multivariate methods in aquatic ecology. *Aquatic Sciences*, 57(3), pp.255–289.
- Bradford, M.A., Tordoff, G.M., Eggers, T., Jones, T.H. & Newington, J.E., 2002. Microbiota, fauna, and mesh size interactions in litter decomposition. *Oikos*, 99(2), pp.317–323.

- Bradley, S.L., Milne, G.A., Teferle, F.N., Bingley, R.M. & Orliac, E.J., 2009. Glacial isostatic adjustment of the British Isles: new constraints from GPS measurements of crustal motion. *Geophysical Journal International*, 178(1), pp.14–22.
- Bragg, O., Lindsay, R., Risager, M., Silvius, M. & Zingstra, H., 2003. *Strategy and action plan for mire and peatland conservation in Central Europe*, Wetlands International Wageningen, NL.
- Bridgham, S.D., Megonigal, J.P., Keller, J.K., Bliss, N.B. & Trettin, C., 2006. The carbon balance of North American wetlands. *Wetlands*, 26(4), pp.889–916.
- Bridgham, S.D. & Richardson, C.J., 1993. Hydrology and nutrient gradients in North-Carolina peatlands. *Wetlands*, 13(3), pp.207–218.
- Bridgham, S.D., Richardson, C.J., Maltby, E. & Faulkner, S.P., 1991. Cellulose decay in natural and disturbed peatlands in North Carolina. *J. Environ. Qual.*, 20, pp.695–701.
- Bridgham, S.D., Updegraff, K. & Pastor, J., 1998. Carbon, nitrogen, and phosphorus mineralization in northern wetlands. *Ecology*, 79(5), pp.1545–1561.
- British Geological Survey, 2014. BGS Lexicon of Named Rock Units. Available at: <https://www.bgs.ac.uk/lexicon/lexicon.cfm?pub=NCG> [Accessed April 5, 2014].
- British Geological Survey, 2015. Sea level and coastal changes. *Discovering Geology*. Available at: <http://www.bgs.ac.uk/discoveringGeology/climateChange/general/coastal.html?src=topNav> [Accessed November 5, 2015].
- Brix, H., Sorrell, B.K. & Lorenzen, B., 2001. Are *Phragmites*-dominated wetlands a net source or net sink of greenhouse gases? *Aquatic Botany*, 69(2–4), pp.313–324.
- Broads Authority, 2013. *Broads Biodiversity and Water Strategy*, The Broads, UK.
- Broads Authority, 1997. *Fen Management Strategy*, Norwich, UK.
- Brouns, K., Verhoeven, J.T.A. & Hefting, M.M., 2014. Short period of oxygenation releases latch on peat decomposition. *Science of the Total Environment*, 481(1), pp.61–68.
- Buttery, A.B.R. & Lambert, J.M., 1965. Competition between *Glyceria Maxima* and

- Phragmites Communis* in the Region of Surlingham Broad : I . The Competition Mechanism. *Journal of Ecology*, 53(1), pp.163–181.
- Cahoon, D., 2006. A review of major storm impacts on coastal wetland elevations. *Estuaries and Coasts*, 29(6A), pp.889 – 898.
- Cahoon, D.R., Hensel, P., Rybczyk, J., McKee, K.L., Proffitt, C.E. & Perez, B.C., 2003. Mass tree mortality leads to mangrove peat collapse at Bay Islands, Honduras after Hurricane Mitch. *Journal of Ecology*, 91(6), pp.1093–1105.
- Callaway, J.C., DeLaune, R.D. & Patrick, W.H., 1996. Chernobyl <sup>137</sup>Cs used to determine sediment accretion rates at selected northern European coastal wetlands. *Limnology and Oceanography*, 41(3), pp.444–450.
- Campolo, M., Andreussi, P. & Soldati, A., 1999. River flood forecasting with a neural network model. *Water Resources Research*, 35(4), pp.1191–1197.
- Castañeda-Moya, E., Twilley, R.R., Rivera-Monroy, V.H., Zhang, K., Davis, S.E. & Ross, M., 2010. Sediment and Nutrient Deposition Associated with Hurricane Wilma in Mangroves of the Florida Coastal Everglades. *Estuaries and Coasts*, 33(1), pp.45–58.
- CEH, 2010. The Centre for Ecology and Hydrology: UK Environmental Change Network. Available at: <http://www.ecn.ac.uk/sites/site/rivers/bure> [Accessed August 8, 2015].
- Chaloupka, M., 2001. Historical trends, seasonality and spatial synchrony in green sea turtle egg production. *Biological Conservation*, 101(3), pp.263–279.
- Chambers, F.M., Beilman, D.W. & Yu, Z., 2010. Methods for determining peat humification and for quantifying peat bulk density, organic matter and carbon content for palaeostudies of climate and peatland carbon dynamics. *Mires and Peat*, 7(10), pp.1 – 10.
- Chambers, L.G., Davis, S.E., Troxler, T., Boyer, J.N., Downey-Wall, A. & Scinto, L.J., 2014. Biogeochemical effects of simulated sea level rise on carbon loss in an Everglades mangrove peat soil. *Hydrobiologia*, 726, pp.195 – 211.
- Chambers, R.M., Osgood, D.T., Bart, D.J. & Montalto, F., 2003. *Phragmites australis* invasion and expansion in tidal wetlands: interactions among salinity, sulfide, and hydrology. *Estuaries*, 26(2), pp.398–406.

- Charman, D.J., Beilman, D.W., Blaauw, M., Booth, R.K., Brewer, S., Chambers, F.M., Christen, J.A., Gallego-Sala, A., Harrison, S.P., Hughes, P.D.M., Jackson, S.T., Korhola, A., Mauquoy, D., Mitchell, F.J.G., Prentice, I.C., van der Linden, M., De Vleeschouwer, F., Yu, Z.C., Alm, J., Bauer, I.E., Corish, Y.M.C., Garneau, M., Hohl, V., Huang, Y., Karofeld, E., Le Roux, G., Loisel, J., Moschen, R., Nichols, J.E., Nieminen, T.M., MacDonald, G.M., Phadtare, N.R., Rausch, N., Sillasoo, Ü., Swindles, G.T., Tuittila, E.-S., Ukonmaanaho, L., Väliranta, M., van Bellen, S., van Geel, B., Vitt, D.H. & Zhao, Y., 2013. Climate-related changes in peatland carbon accumulation during the last millennium. *Biogeosciences*, 10(2), pp.929–944.
- Chaudhari, P.R., Ahire, D. V, Ahire, V.D., Chkravarty, M. & Maity, S., 2013. Soil Bulk Density as related to Soil Texture, Organic Matter Content and available total Nutrients of Coimbatore Soil. *International Journal of Scientific and Resaerch Publications*, 3(2), pp.1–8.
- Chimner, R. a & Karberg, J.M., 2008. Long-term carbon accumulation in two tropical mountain peatlands, Andes Mountains, Ecuador. *Mires and Peat*, 3, pp.1 – 10.
- Chimner, R., Cooper, D. & Patron, W., 2002. Modeling carbon accumulation in Rocky Mountain fens. *Wetlands*, 22(1), pp.100 – 110.
- Chini, N., Stansby, P., Leake, J., Wolf, J., Roberts-Jones, J. & Lowe, J., 2010. The impact of sea level rise and climate change on inshore wave climate: A case study for East Anglia (UK). *Coastal Engineering*, 57(11-12), pp.973–984.
- Chmura, G.L., Anisfeld, S.C., Cahoon, D.R. & Lynch, J.C., 2003. Global carbon sequestration in tidal, saline wetland soils. *Global Biogeochemical Cycles*, 17(4), p.12.
- Choi, Y. & Wang, Y., 2004. Dynamics of carbon sequestration in a coastal wetland using radiocarbon measurements. *Global Biogeochemical Cycles*, 18, pp.1 – 12.
- Church, J.A., Clark, P.U., Cazenave, A., Gregory, J.M., Jevrejeva, S., Levermann, A., Merrifield, M. a., Milne, G. a., Nerem, R., Nunn, P.D., Payne, A.J., Pfeffer, W.T., Stammer, D. & Unnikrishnan, A.S., 2013. *Sea Level Change. In: Climate Change 2013: The Physical Science Basis. Contribution of Working Group I to the Fifth Assessment Report of the Intergovernmental Panel on Climate Change* T. F. Stocker, D. Qin, G.-K. Plattner, M. Tignor, S. K. Allen, J. Boschung, A. Nauels, Y. Xia, V. Bex, & P. M. Midgley, eds., Cambridge, UK and New York, NY, USA:

Cambridge University Press.

Ciais, P., Sabine, C., Bala, G., Bopp, L., Brovkin, V., Canadell, J., Chhabra, A., DeFries, R., Galloway, J., Heimann, M., Jones, C., Le Quéré, C., Myneni, R.B., Piao, S. & Thornton, P., 2013. *Carbon and Other Biogeochemical Cycles*. In *Climate Change 2013: The Physical Science Basis. Contribution of Working Group I to the Fifth Assessment Report of the Intergovernmental Panel on Climate Change* T. F. Stocker, D. Qin, G. K. Plattner, M. Tignor, S. K. Allen, J. Boschung, A. Nauels, Y. Xia, V. Bex, & P. M. Midgley, eds., Cambridge, UK and New York, NY, USA: Cambridge University Press.

Ciais, P., Sabine, C., Bala, G., Bopp, L., Brovkin, V., Canadell, J., Chhabra, A., DeFries, R., Galloway, J., Heimann, M., Jones, C., Quéré, C. Le, Myneni, R.B., Piao, S., Thornton, P., France, P.C., Willem, J., Friedlingstein, P. & Munhoven, G., 2013. *Carbon and Other Biogeochemical Cycles*. In *Climate Change 2013: The Physical Science Basis. Contribution of Working Group I to the Fifth Assessment Report of the Intergovernmental Panel on Climate Change*. T. F. Stocker, D. Qin, G.-K. Plattner, M. Tignor, S. K. Allen, J. Boschung, A. Nauels, Y. Xia, V. Bex, & P. M. Midgley, eds., UK and New York, NY, USA.

Cleveland, R., Cleveland, W., McRae, J. & Terpenning, I., 1990. STL: A seasonal-trend decomposition procedure based on loess. *Journal of Official Statistics*, 6(1), pp.3–73.

Clevering, O.A., 1998. An investigation into the effects of nitrogen on growth and morphology of stable and die-back populations of *Phragmites australis*. *Aquatic Botany*, 60(1), pp.11–25.

Clevering, O.A. & Lissner, J., 1999. Taxonomy, chromosome numbers, clonal diversity and population dynamics of *Phragmites australis*. *Aquatic Botany*, 64(3), pp.185–208.

Clymo, R.S., 1984. The Limits to Peat Bog Growth. *Philosophical Transactions of the Royal Society of London. Series B, Biological Sciences*, 303(1117), pp.605–654.

Clymo, R.S., Turunen, J. & Tolonen, K., 1998. Carbon Accumulation in Peatland. *Oikos*, 81(2), pp.368–388.

Committee on Climate Change, 2015. *Aggregate Assessment of Climate Change Impacts on the Goods and Benefits Provided By the UK's Natural Assets*,

AECOM, University of Exeter and University of York, London, UK.

- Connolly, C.T., Sobczak, W. V. & Findlay, S.E.G., 2014. Salinity effects on *Phragmites* decomposition dynamics among the hudson river's freshwater tidal wetlands. *Wetlands*, 34(3), pp.575–582.
- Conrad, R., 1996. Soil microorganisms as controllers of atmospheric trace gases (H<sub>2</sub>, CO, CH<sub>4</sub>, OCS, N<sub>2</sub>O, and NO). *Microbiological Reviews*, 60(4), pp.609 – 640.
- Cooper, W., Townend, I. & Balson, P., 2008. *A synthesis of current knowledge on the genesis of the Great Yarmouth and Norfolk Bank Systems*, London, UK.
- Coops, H., van den Brink, F.W.B. & van der Velde, G., 1996. Growth and morphological responses of four helophyte species in an experimental water-depth gradient. *Aquatic Botany*, 54(1), pp.11–24.
- Coops, H. & van der Velde, G., 1996. Effects of waves on helophyte stands: mechanical characteristics of stems of *Phragmites australis* and *Scirpus lacustris*. *Aquatic Botany*, 53(3-4), pp.175–185.
- Council Directive, 1992. *The conservation of natural habitats and of wild fauna and flora. Council Directive 92/43/EEC*,
- Couwenberg, J., Thiele, A., Tanneberger, F., Augustin, J., Barisch, S., Dubovik, D., Liashchynskaya, N., Michaelis, D., Minke, M., Skuratovich, A. & Joosten, H., 2011. Assessing greenhouse gas emissions from peatlands using vegetation as a proxy. *Hydrobiologia*, 674(1), pp.67–89.
- Cowie, N.R., Sutherland, W.J., Dithlago, M.K.M. & James, R., 1992. The Effects of Conservation Management of Reed Beds . II . The Flora and Litter Disappearance. *Journal of Applied Ecology*, 29(2), pp.277–284.
- Cowles, H.C., 1899. The Ecological Relations of the Vegetation on the Sand Dunes of Lake Michigan. *Botanical Gazette*, 27(3), pp.167–202.
- Craft, C., Clough, J., Ehman, J., Joye, S., Park, R., Pennings, S., Guo, H.Y. & Machmuller, M., 2009. Forecasting the effects of accelerated sea-level rise on tidal marsh ecosystem services. *Frontiers in Ecology and the Environment*, 7(2), pp.73–78.
- Cundy, A.B., Croudace, I.W., Cearreta, A., Irabien, M., amp, x & A, J., 2003. Reconstructing historical trends in metal input in heavily-disturbed, contaminated

- estuaries: studies from Bilbao, Southampton Water and Sicily. *Applied Geochemistry*, 18(2), pp.311–325.
- Dawson, A., 1984. Quaternary sea-level changes in western Scotland. *Quaternary science reviews*, 3(4), pp.345 – 268.
- Day, J.W., Rybczyk, J., Scarton, F., Rismondo, A., Are, D. & Cecconi, G., 1999. Soil accretionary dynamics, sea-level rise and the survival of wetlands in Venice Lagoon: A field and modelling approach. *Estuarine Coastal and Shelf Science*, 49, pp.607–628.
- Debernard, J.B. & Røed, L.P., 2008. Future wind, wave and storm surge climate in the Northern Seas: a revisit. *Tellus A*, 60(3), pp.427–438.
- Defra, 2011. *Developing Tools to Evaluate the Consequences for Biodiversity of Options for Coastal Zone Adaptation to Climate Change (CR0422)*,
- Defra, 2016. United Kingdom Eutrophying and Acidifying Network. Available at: [www.uk-air.defra.gov.uk/networks/network-info?view=ukeep](http://www.uk-air.defra.gov.uk/networks/network-info?view=ukeep) [Accessed September 1, 2015].
- DeLaune, R.D., Kongchum, M., White, J.R. & Jugsujinda, A., 2013. Freshwater diversions as an ecosystem management tool for maintaining soil organic matter accretion in coastal marshes. *Catena*, 107, pp.139–144.
- Diack, I., Droy, N., Hamill, B., Jones, P., Schutten, J., Skinner, A. & Street, M., 2011. The Fen Management Handbook. *Scottish Natural Heritage*.
- van Diggelen, R., Middleton, B., Bakker, J., Grootjans, A. & Wassen, M., 2006. Fens and floodplains of the temperate zone: Present status, threats, conservation and restoration. *Applied Vegetation Science*, 9(2), pp.157–162.
- Digimap, 2015. Digimap Roam. Available at: <http://digimap.edina.ac.uk/> [Accessed October 15, 2015].
- Dinka, M., Ágoston- Szabó, E. & Tóth, I., 2004. Changes in nutrient and fibre content of decomposing *Phragmites australis* litter. *International Review of Hydrobiology*, 89(5- 6), pp.519–535.
- van Dokkum, H.P., Slijkerman, D.M.E., Rossi, L. & Costantini, M.L., 2002. Variation in the decomposition of *Phragmites australis* litter in a monomictic lake: the role of gammarids. *Ecology*, 482(1-3), pp.69–77.



- Dray, S. & Dufour, A.B., 2007. The ade4 package: implementing the duality diagram for ecologists. *Journal of Statistical Software*, 22(4), pp.1–20.
- Dunn, C. & Freeman, C., 2011. Peatlands: our greatest source of carbon credits? *Carbon Management*, 2(3), pp.289–301.
- Dykyjova, D., 1971. Production, vertical structure and light profiles in littoral stands of reed-bed species. *Hydrobiologia*, 12, pp.361 – 376.
- Dytham, C., 2011. Choosing and Using Statistics: A Biologist's Guide. In Oxford: Wiley-Blackwell, pp. 32 – 49.
- Eickenscheidt, T., Heinichen, J. & Drösler, M., 2015. The greenhouse gas balance of a drained fen peatland is mainly controlled by land-use rather than soil organic carbon content. *Biogeosciences*, 12(17), pp.5161–5184.
- Eid, E.M., Shaltout, K.H., Al-Sodany, Y.M., Soetaert, K. & Jensen, K., 2010. Modeling growth, carbon allocation and nutrient budgets of *Phragmites australis* in lake burullus, Egypt. *Wetlands*, 30(2), pp.240–251.
- Ellis, E.A., 1965. *The Broads*, London: Collins.
- Engloner, A.I., 2009. Structure, growth dynamics and biomass of reed (*Phragmites australis*) - A review. *Flora: Morphology, Distribution, Functional Ecology of Plants*, 204(5), pp.331–346.
- Environment Agency, 2003. *A Guide to Monitoring Water Levels and Flows at Wetland Sites*, Bristol.
- Environment Agency, 2009. *Broadland Rivers Catchment Flood Management Plan, Managing Flood Risk*, Peterborough.
- Evans, J.R., 1989. Photosynthesis and nitrogen relationships in leaves of C<sub>3</sub> plants. *Oecologia*, 78, pp.9–19.
- Farquhar, G.D. & Sharkey, T.D., 1982. Stomatal Conductance and Photosynthesis. *Annual Review of Plant Physiology*, 33(1), pp.317–345.
- Feast, N.A., Hiscock, K.M., Dennis, P.F. & Andrews, J.N., 1998. Nitrogen isotope hydrochemistry and denitrification within the Chalk aquifer system of north Norfolk, UK. *Journal of Hydrology*, 211(1), pp.233–252.
- Fenner, N. & Freeman, C., 2011. Drought-induced carbon loss in peatlands. *Nature*

*Geoscience*, 4(12), pp.895–900.

Ferry, J.G., 2010. How to Make a Living by Exhaling Methane S. Gottesman & C. S. Harwood, eds. *Annual Review of Microbiology*, 64, pp.453–473.

Fiałkiewicz-Kozieł, B., Smieja-Król, B., Piotrowska, N., Sikorski, J. & Gałka, M., 2014. Carbon accumulation rates in two poor fens with different water regimes: Influence of anthropogenic impact and environmental change. *The Holocene*, 24(11), pp.1539 – 1549.

Field, A., 2013. *Discovering statistics using IBM SPSS statistics*, Sage.

Field, A., Miles, J. & Field, Z., 2012. *Discovering Statistics Using R*, London, UK: SAGE Publications Ltd.

Field, C., 1983. Allocating Leaf Nitrogen for the Maximization of Carbon Gain: Leaf Age as a Control on the Allocation Program. *Oecologia*, 56(2/3), pp.341–347.

Findlay, S.E.G., Dye, S. & Kuehn, K.A., 2002. Microbial growth and nitrogen retention in litter of *Phragmites australis* compared to *Typha angustifolia*. *Wetlands*, 22(3), pp.616–625.

Fontaine, S., Mariotti, A. & Abbadie, L., 2003. The priming effect of organic matter: A question of microbial competition? *Soil Biology and Biochemistry*, 35(6), pp.837–843.

Ford, J.D., Cameron, L., Rubis, J., Maillet, M., Nakashima, D., Willox, A.C. & Pearce, T., 2016. Including indigenous knowledge and experience in IPCC assessment reports. *Nature Climate Change*, 6(4), pp.349–353.

Forster, P., Ramaswamy, V., Artaxo, P., Berntsen, T., Betts, R., Fahey, D.W., Haywood, J., Lean, J., Lowe, D.C., Myhre, G., Nganga, J., Prinn, R., Raga, G., Schulz, M. & Dorland, R. Van, 2007. Changes in Atmospheric Constituents and Radiative forcing. In: *Climate Change 2007: The Physical Science Basis. Contribution of Working Group I to the Fourth Assessment Report of the Intergovernmental Panel on Climate Change*. In S. Solomon, D. Qin, M. Manning, Z. Chen, M. Marquis, K. B. Averyt, M. Tignor, & H. L. Miller, eds. Cambridge, United Kingdom and New York, NY, USA: Cambridge University Press.

Fox, S., Stieve, E. & Valiela, I., 2008. Macrophyte abundance in Waquoit Bay: Effects

- of land-derived nitrogen loads on seasonal and multi-year biomass patterns. *Estuaries and Coasts*, 31, pp.532 – 541.
- Freeman, C., Evans, C.D., Monteith, D.T., Reynolds, B. & Fenner, N., 2001. Export of organic carbon from peat soils. *Nature*, 412, p.785.
- Frey, K.E. & Smith, L.C., 2005. Amplified carbon release from vast West Siberian peatlands by 2100. *Geophysical Research Letters*, 32(9).
- Frolking, S., Roulet, N.T., Moore, T.R., Lafleur, P.M., Bubier, J.L. & Crill, P.M., 2002. Modeling seasonal to annual carbon balance of Mer Bleue Bog, Ontario, Canada. *Global Biogeochemical Cycles*, 16(3), pp.4–21.
- Frolking, S., Roulet, N.T., Moore, T.R., Richard, P.J.H., Lavoie, M. & Muller, S.D., 2001. Modeling northern peatland decomposition and peat accumulation. *Ecosystems*, 4(5), pp.479–498.
- Fukami, T. & Wardle, D.A., 2005. Long-term ecological dynamics: reciprocal insights from natural and anthropogenic gradients. *Proceedings of the Royal Society B: Biological Sciences*, 272(1577), pp.2105–2115.
- Garcia-Palacios, P., Mckie, B.G., Handa, I.T., Frainer, A. & Hattenschwiler, S., 2016. The importance of litter traits and decomposers for litter decomposition: A comparison of aquatic and terrestrial ecosystems within and across biomes. *Functional Ecology*, 30(5), pp.819–829.
- Garneau, M., Bellen, S., Magnan, G., Beaulieu-Audy, V., Lamarre, A. & Asnong, H., 2014. Holocene carbon dynamics of boreal and subarctic peatlands from Québec, Canada. *The Holocene*, 24(9), pp.1043 – 1053.
- Gessner, M.O., 2000. Breakdown and nutrient dynamics of submerged *Phragmites* shoots in the littoral zone of a temperate hardwater lake. *Aquatic Botany*, 66(1), pp.9–20.
- Gessner, M.O., 2001. Mass loss, fungal colonisation and nutrient dynamics of *Phragmites australis* leaves during senescence and early aerial decay. *Aquatic Botany*, 69(2-4), pp.325–339.
- Giardina, C.P. & Ryan, M.G., 2002. Total Belowground Carbon Allocation in a Fast-growing *Eucalyptus* Plantation Estimated Using a Carbon Balance Approach. *Ecosystems*, 5(5), pp.487–499.

- Gilbert, B. & Lechowicz, M.J., 2004. Neutrality, niches, and dispersal in a temperate forest understory. *Proceedings of the National Academy of Sciences of the United States of America*, 101(20), pp.7651–7656.
- Gilbert, G., Tyler, G., Dunn, C., Ratcliffe, N. & Smith, K., 2007. The influence of habitat management on the breeding success of the Great Bittern *Botaurus stellaris* in Britain. *Ibis*, 149(1), pp.53–66.
- Giller, K.E. & Wheeler, B.D., 1986. Past Peat Cutting and Present Vegetation Patterns in an Undrained Fen in the Norfolk Broadland. *Journal of Ecology*, 74(1), pp.219–247.
- Giller, K.E. & Wheeler, B.D., 1986. Peat and peat water chemistry of a flood- plain fen in Broadland, Norfolk, UK. *Freshwater Biology*, 16(1), pp.99–114.
- Gillingham, P., 2015. *Implications of Climate Change for SSSIs and other Protected Areas*, Biodiversity Report Card paper 4, Natural England.
- Glaser, P.H., 1987. The Ecology of Patterened Boreal Peatlands of Northern Minnesota: A Community Profile. *US Fish Wildlife Service Report*, 85(7.14), p.98.
- Global Climate Observing System, 2010. *Implementation plan for the global observing system for climate in support of the UNFCCC*,
- Godwin, H., 1945. Coastal peat beds of the North Sea region, as indices of land and sea level changes. *New Phytologist*, 44(1), pp.29–69.
- Godwin, H. & Tallantire, P.A., 1951. Studies in the Post-Glacial History of British Vegetation: XII. Hockham Mere, Norfolk. *The Journal of Ecology*, pp.285–307.
- Gonzalez-Alcaraz, M.N., Egea, C., Jimenez-Carceles, F.J., Parraga, I., Maria-Cervantes, A., Delgado, M.J. & Alvarez-Rogel, J., 2012. Storage of organic carbon, nitrogen and phosphorus in the soil-plant system of *Phragmites australis* stands from a eutrophicated Mediterranean salt marsh. *Geoderma*, 185, pp.61–72.
- González, G. & Seastedt, T.R., 2001. Soil fauna and plant litter decomposition in tropical and subalpine forests. *Ecology*, 82(4), pp.955–964.
- Gorai, M., Ennajeh, M., Khemira, H. & Neffati, M., 2010. Combined effect of NaCl-salinity and hypoxia on growth, photosynthesis, water relations and solute

- accumulation in *Phragmites australis* plants. *Flora: Morphology, Distribution, Functional Ecology of Plants*, 205(7), pp.462–470.
- Gorham, E., 1991. Northern peatlands - role in the carbon-cycle and probable response to climatic warming. *Ecological Applications*, 1(2), pp.182–195.
- Grung, B. & Manne, R., 1998. Missing values in principal component analysis. *Chemometrics and Intelligent Laboratory Systems*, 42(1), pp.125–139.
- Hanganu, J., Mihail, G. & Coops, H., 1999. Responses of ecotypes of *Phragmites australis* to increased seawater influence: A field study in the Danube Delta, Romania. *Aquatic Botany*, 64(3-4), pp.351–358.
- Harden, J.W., Sundquist, E.T., Stallard, R.F., Mark, R.K., Harden, J.W., Sundquist, E.T., Stallard, R.F. & Mark, R.K., 1992. Dynamics of Soil Carbon During Deglaciation of the Laurentide Ice Sheet. *American Association for the Advancement of Science*, 258(5090), pp.1921–1924.
- Haslam, S.M., 1965. Ecological Studies in the Breck Fens I. Vegetation in Relation to Habitat. *Journal of Ecology*, pp.599 – 619.
- Hayball, N. & Pearce, M., 2004. Influences of simulated grazing and water-depth on the growth of juvenile *Bolboschoenus caldwellii*, *Phragmites australis* and *Schoenoplectus validus* plants. *Aquatic Botany*, 78(3), pp.233–242.
- Hellings, S.E. & Gallagher, J.L., 1992. The effects of salinity and flooding on *Phragmites australis*. *Journal of Applied Ecology*, 29(1), pp.41–49.
- Helton, A., Bernhardt, E. & Fedders, A., 2014. Biogeochemical regime shifts in coastal landscapes: the contrasting effects of saltwater incursion and agricultural pollution on greenhouse gas emissions from a freshwater wetland. *Biogeochemistry*, 120(1-3), pp.133–147.
- Hemond, H.F., 1980. Biogeochemistry of Thoreau's Bog, Concord, Massachusetts. *Ecological Monographs*, 50(4), pp.507–526.
- Henman, J. & Poulter, B., 2008. Inundation of freshwater peatlands by sea level rise: Uncertainty and potential carbon cycle feedbacks. *Journal of Geophysical Research*, 113, pp.1 – 11.
- Heyman, R., Lorber, M., Eddy, J. & West, T., 2000. Behavioural Observation and Coding. In H. Reis & C. Judd, eds. *Handbook of Research Methods in Social and*

*Personality Psychology*. Cambridge, UK: Cambridge University Press, pp. 364 – 365.

Hieber, M. & Gessner, M., 2002. Contribution of Stream Detritivores, Fungi, and Bacteria to Leaf Breakdown Based on Biomass Estimates. *Ecology*, 83(4), pp.1026–1038.

Hietz, P., 1992. Decomposition and nutrient dynamics of reed (*Phragmites australis* (Cav.) Trin. ex Steud.) litter in Lake Neusiedl, Austria. *Aquatic Botany*, 43(3), pp.211–230.

Hilasvuori, E., Akujarvi, A., Fritze, H., Karhu, K., Laiho, R., Makiranta, P., Oinonen, M., Palonen, V., Vanhala, P. & Liski, J., 2013. Temperature sensitivity of decomposition in a peat profile. *Soil Biology and Biochemistry*, 67, pp.47–54.

Hilbert, D.W., Roulet, N. & Moore, T., 2000. Modelling and analysis of peatlands as dynamical systems. *Journal of Ecology*, 88(2), pp.230–242.

Hilker, T., Coops, N.C., Wulder, M.A., Black, T.A. & Guy, R.D., 2008. The use of remote sensing in light use efficiency based models of gross primary production: A review of current status and future requirements. *Science of The Total Environment*, 404(2-3), pp.411–423.

Hiscock, K.M., Dennis, P.F., Saynor, P.R. & Thomas, M.O., 1996. Hydrochemical and stable isotope evidence for the extent and nature of the effective Chalk aquifer of north Norfolk, UK. *Journal of Hydrology*, 180(1), pp.79–107.

Hobbie, S.E., 1996. Temperature and plant species control over litter decomposition in Alaska Tundra. *Ecological Monographs*, 66(4), pp.502–522.

Hocking, P.J., 1989. Seasonal dynamics of production, and nutrient accumulation and cycling by *Phragmites australis* (Cav.) Trin. ex Steudel in a nutrient-enriched swamp in Inland Australia. I. Whole Plants. *Marine and Freshwater Research*, 40(5), pp.421–444.

Hocking, P.J., Finlayson, C.M. & Chick, a J., 1983. The biology of Australian weeds. 12. *Phragmites australis* (Cav.) Trin. ex Steud. *Journal of the Australian Institute of Agricultural Science* 49:, 49, pp.123–132.

Holman, I.P. & Hiscock, K.M., 1998. Land drainage and saline intrusion in the coastal marshes of northeast Norfolk. *Quarterly Journal of Engineering Geology*, 31,

pp.47–62.

- Holman, I.P., Hiscock, K.M. & Chroston, P.N., 1999. Crag aquifer characteristics and water balance for the Thurne catchment, northeast Norfolk. *Quarterly Journal of Engineering Geology*, 32, pp.365–380.
- Holman, I.P. & White, S., 2008. *Synthesis of the Upper Thurne Research and Recommendations for Management*,
- Hootsmans, M. & Wiegman, F., 1998. Four helophyte species growing under salt stress: their salt of life? *Aquatic Botany*, 62(2), pp.81–94.
- Hudon, C., Gagnon, P. & Jean, M., 2005. Hydrological factors controlling the spread of common reed (*Phragmites australis*) in the St. Lawrence River (Québec, Canada). *Écoscience*, 12(3), pp.347–357.
- Hughes, P.D.M., Roland, T.P. & Mauquoy D, D., 2014. Peatlands and carbon credits: natural and anthropogenic threats to the carbon stock. *Carbon Management*, 5(3), pp.259–263.
- Hung, L., Asaeda, T., Fujino, T. & Mnaya, B., 2007. Inhibition of *Zizania latifolia* growth by *Phragmites australis*: an experimental study. *Wetlands Ecology and Management*, 15(2), pp.105–111.
- Husák, Š., 1975. Control of reed and reed mace stands by cutting. In *Pond littoral Ecosystems*. Heidelberg, Berlin: Springer, pp. 404 – 408.
- Hyndman, R. & Athanasopoulos, G., 2014. Time Series Decomposition. In *Forecasting: principles and practice*. Otexts, pp. 148 – 149.
- Ingram, H., Barclay, A., Coupar, A.M., Glover, J.G., Lynch, B.M. & Sprent, J.I., 1980. *Phragmites* performance in reed beds in the Tay Estuary. *Proceedings of the Royal Society of Edinburgh*, 78(3 - 4), pp.89 – 107.
- Ingram, R. & Otte, L., 1981. Peat - Potential Energy Bridge for North Carolina. *AAPG Bulletin*.
- Jaenicke, J., Rieley, J.O., Mott, C., Kimman, P. & Siegert, F., 2008. Determination of the amount of carbon stored in Indonesian peatlands. *Geoderma*, 147(3-4), pp.151–158.
- Janssen, B.H., 1996. Nitrogen mineralization in relation to C:N ratio and

- decomposability of organic materials. *Plant and Soil*, 181(1), pp.39–45.
- Jenkins, C.. & Suberkropp, K., 1995. The influence of water chemistry on the enzymatic degradation of leaves in streams. *Freshwater Biology*, 33(2), pp.245–253.
- Jennings, J.N., 1955. Further pollen data from the Norfolk Broads. *New Phytologist*, 54(2), pp.199–207.
- Jennings, J.N. & Lambert, J.M., 1951. Alluvial Stratigraphy and Vegetational Succession in the Region of the Bure Valley Broads: I. Surface Features and General Stratigraphy. *Journal of Ecology*, 39(1), pp.106–148.
- Jenny, H., 1941. *Factors of soil formation*, McGraw-Hill Book Company New York, NY.
- Jenny, H., Gessel, S. & Bingham, F., 1949. Comparative study of decomposition rates of organic matter in temperate and tropical regions. *Soil Science*, 68, pp.419 – 432.
- Joint Nature Conservation Committee, 2014. Designated and Proposed Ramsar sites in the UK and Overseas Territories & Crown Dependencies. Available at: <http://jncc.defra.gov.uk/page-1389> [Accessed February 2, 2015].
- Joosten, H., 2009. *The Global CO<sub>2</sub> Picture: Peatland status and emissions in all countries of the world*, Wetlands International.
- Kandel, T.P., Elsgaard, L. & Lærke, P.E., 2013. Measurement and modelling of CO<sub>2</sub> flux from a drained fen peatland cultivated with reed canary grass and spring barley. *GCB Bioenergy*, 5, pp.548–561.
- Karl, T. & Trenberth, K., 2003. Modern Global Climate Change. *Science*, 302, p.1719.
- Kendon, M. & McCarthy, M., 2015. The UK's wet and stormy winter of 2013/2014. *Weather*, 70(2), pp.40 – 47.
- Keough, J., Thompson, T., Guntenspergen, G. & DA Wilcox, 1999. Hydrogeomorphic factors and ecosystem responses in coastal wetlands of the Great Lakes. *Wetlands*, 19(4), pp.821 – 834.
- Kershaw, A.P., 1997. A modification of the Troels-Smith system of sediment description and portrayal. *Quaternary Australasia*, 15(2), pp.63–68.



- Kettunen, A., 2002. *Connecting methane fluxes to vegetation cover and water table fluctuations at microsite level: A modeling study*. Systems Analysis Laboratory Research Reports E10, Peatland Ecology and Forestry, Department of Forest Ecology, Finland.
- Kettunen, A., Kaitala, V., Alm, J., Silvola, J., Nykanen, H. & Martikainen, P.J., 1996. Cross-correlation analysis of the dynamics of methane emissions from a boreal peatland. *Global Biogeochemical Cycles*, 10(3), pp.457–471.
- Killham, K., 1994. *Soil ecology*, Cambridge University Press.
- Kirwan, M.L. & Mudd, S.M., 2012. Response of salt-marsh carbon accumulation to climate change. *Nature*, 489, pp.550 – 554.
- Kirwan, M.L., Temmerman, S., Skeehean, E.E., Guntenspergen, G.R. & Fagherazzi, S., 2016. Overestimation of marsh vulnerability to sea level rise. *Nature Climate Change*, 6(3), pp.253–260.
- Koch, M. & Jurasinski, G., 2015. Four decades of vegetation development in a percolation mire complex following intensive drainage and abandonment. *Plant Ecology & Diversity*, 8(1), pp.1–12.
- Komínková, D., Kuehn, K. a., Büsing, N., Steiner, D. & Gessner, M.O., 2000. Microbial biomass, growth, and respiration associated with submerged litter of *Phragmites australis* decomposing in a littoral reed stand of a large lake. *Aquatic Microbial Ecology*, 22(3), pp.271–282.
- Kuehn, K., Lemke, M., Suberkropp, K. & Wetzel, R., 2000. Microbial biomass and production associated with decaying leaf litter of the emergent macrophyte *Juncas effusus*. *Limnology and Oceanography*, 45(4), pp.862–870.
- Kuehn, K.A., Steiner, D. & Gessner, M.O., 2004. Diel mineralization patterns of standing-dead plant litter: Implications for CO<sub>2</sub> flux from wetlands. *Ecology*, 85(9), pp.2504–2518.
- van Kuijk, M., Anten, N.P.R., Oomen, R.J., van Bentum, D.W. & Werger, M.J.A., 2008. The limited importance of size-asymmetric light competition and growth of pioneer species in early secondary forest succession in Vietnam. *Oecologia*, 157(1), pp.1–12.
- Laanbroek, H.J. & Pfennig, N., 1981. Oxidation of short-chain fatty acids by sulfate-

- reducing bacteria in freshwater and in marine sediments. *Archives of Microbiology*, 128(3), pp.330–335.
- Lähteenoja, O., Ruokolainen, K., Schulman, L. & Alvarez, J., 2009. Amazonian floodplains harbour minerotrophic and ombrotrophic peatlands. *Catena*, 79(2), pp.140–145.
- Laiho, R., 2006. Decomposition in peatlands: Reconciling seemingly contrasting results on the impacts of lowered water levels. *Soil Biology and Biochemistry*, 38(8), pp.2011–2024.
- Lambert, J.M., 1951. Alluvial Stratigraphy and Vegetational Succession in the Region of the Bure Valley Broads: III. Classification, Status and Distribution of Communities. *Journal of Ecology*, 39(1), pp.149–170.
- Lambert, J.M., 1960. *The Making of the Broads: A Reconsideration of Their Origin in the Light of New Evidence.*, Royal Geographical Society and John Murray.
- Lamers, L.P.M., Ten Dolle, G.E., Van Den Berg, S.T.G., Van Delft, S.P.J. & Roelofs, J.G.M., 2001. Differential responses of freshwater wetland soils to sulphate pollution. *Biogeochemistry*, 55(1), pp.87–102.
- Lamers, L.P.M., Vile, M.A., Grootjans, A.P., Acreman, M.C., van Diggelen, R., Evans, M.G., Richardson, C.J., Rochefort, L., Kooijman, A.M. & Roelofs, J.G.M., 2015. Ecological restoration of rich fens in Europe and North America: from trial and error to an evidence- based approach. *Biological Reviews*, 90, pp.182 – 203.
- Lara, R.J. & Cohen, M.C.L., 2006. Sediment porewater salinity, inundation frequency and mangrove vegetation height in Bragança, North Brazil: an ecohydrology-based empirical model. *Wetlands Ecology and Management*, 14(4), pp.349–358.
- Larsen, L.G., Harvey, J.W. & Crimaldi, J.P., 2007. A delicate balance: Ecohydrological feedbacks governing landscape morphology in a lotic peatland. *Ecological Monographs*, 77(4), pp.591–614.
- Laws, E.A. & Archie, J.W., 1981. Appropriate use of regression analysis in marine biology. *Marine Biology*, 65(1), pp.13 – 16.
- Limpens, J., Berendse, F., Blodau, C., Canadell, J.G., Freeman, C., Holden, J., Roulet, N., Rydin, H. & Schaepman-Strub, G., 2008. Peatlands and the carbon cycle: from local processes to global implications - a synthesis. *Biogeosciences*

*Discussions*, 5, pp.1475 – 1491.

- Lindo, Z. & Winchester, N.N., 2009. Spatial and environmental factors contributing to patterns in arboreal and terrestrial oribatid mite diversity across spatial scales. *Oecologia*, 160, pp.817–825.
- Lindsay, R., 2010. *Peatbogs and carbon: a critical synthesis to inform policy development in oceanic peat bog conservation and restoration in the context of climate change*, University of East London Environmental Research Group and RSPB Scotland.
- Lissner, J. & Schierup, H.-H., 1997. Effects of salinity on the growth of *Phragmites australis*. *Aquatic Botany*, 55(4), pp.247–260.
- Lissner, J., Schierup, H.H., Comín, F. a. & Astorga, V., 1999. Effect of climate on the salt tolerance of two *Phragmites australis* populations. I. Growth, inorganic solutes, nitrogen relations and osmoregulation. *Aquatic Botany*, 64(3-4), pp.317–333.
- Loeb, R., Lamers, L.P.M. & Roelofs, J.G.M., 2008. Prediction of phosphorus mobilisation in inundated floodplain soils. *Environmental Pollution*, 156(2), pp.325–331.
- Loisel, J., Yu, Z., Beilman, D.W., Camill, P., Alm, J., Amesbury, M.J., Anderson, D., Andersson, S., Bochicchio, C. & Barber, K., 2014. A database and synthesis of northern peatland soil properties and Holocene carbon and nitrogen accumulation. *The Holocene*, 24(9), pp.1028 – 1042.
- Madgwick, F.J., 1999. Restoring nutrient-enriched shallow lakes: integration of theory and practice in the Norfolk Broads, UK. In *Shallow Lakes' 98*. Springer, pp. 1–12.
- Malik, K., Bhatti, N. & Kauser, F., 1979. Effect of soil salinity on decomposition and humification of organic matter by some cellulolytic fungi. *Mycologia*, 71(4), pp.811–820.
- Malmer, N., Albinsson, C., Svensson, B.M. & Wallén, B., 2003. Interferences between Sphagnum and vascular plants: effects on plant community structure and peat formation. *Oikos*, 100(3), pp.469–482.
- Maltby, E. & Immirzi, P., 1993. Carbon dynamics in peatlands and other wetland soils regional and global perspectives. *Chemosphere*, 27(6), pp.999–1023.

- Manzoni, S., Piñeiro, G., Jackson, R.B., Jobbágy, E.G., Kim, J.H. & Porporato, A., 2012. Analytical models of soil and litter decomposition: solutions for mass loss and time-dependent decay rates. *Soil Biology and Biochemistry*, 50, pp.66–76.
- Manzoni, S., Trofymow, J.A., Jackson, R.B. & Porporato, A., 2010. Stoichiometric controls on carbon, nitrogen, and phosphorus dynamics in decomposing litter. *Ecological Monographs*, 80(1), pp.89–106.
- Marcovaldi, M. & Chaloupka, M., 2007. Conservation status of the loggerhead sea turtle in Brazil: an encouraging outlook. *Endangered Species Research*, 3(October), pp.133–143.
- Maria do Rosário, G.O., Van Noordwijk, M., Gaze, S.R., Brouwer, G., Bona, S., Mosca, G. & Hairiah, K., 2000. Auger sampling, ingrowth cores and pinboard methods. In *Root methods*. Springer, pp. 175–210.
- Mars, H. De, Wassen, M.J. & Venterink, H.O., 1997. Flooding and groundwater dynamics in fens in eastern Poland. *Journal of Vegetation Science*, 8(3), pp.319–328.
- Marsh, H.W., 1998. Pairwise deletion for missing data in structural equation models: Nonpositive definite matrices, parameter estimates, goodness of fit, and adjusted sample sizes. *Structural Equation Modeling: A Multidisciplinary Journal*, 5(1), pp.22–36.
- Mason, C.F. & Bryant, R.J., 1975. Production, Nutrient Content and Decomposition of *Phragmites communis* Trin. and *Typha Angustifolia* L. *The Journal of Ecology*, pp.71–95.
- Mauchamp, A. & Mesleard, F., 2001. Salt tolerance in *Phragmites australis* populations from coastal Mediterranean marshes. *Aquatic Botany*, 70(1), pp.39–52.
- McGarrigle, P., Bradshaw, E., Bradley, L., Hargreaves, G., Macleod, L., Hibbert, A., Downer, R., Horsburgh, K., Williams, J. & Rickards, L., 2014. *UK Coastal Monitoring and Forecasting: 2014 Annual Report for the UK National Tide Gauge Network UK Coastal Monitoring and Forecasting*,
- McLatchey, G. & Reddy, K., 1998. Regulation of organic matter decomposition and nutrient release in a wetland soil. *Journal of Environmental Quality*, 27(5), pp.1268–1274.

- McLeod, E., Poulter, B., Hinkel, J., Reyes, E. & Salm, R., 2010. Sea-level rise impact models and environmental conservation: A review of models and their applications. *Ocean & Coastal Management*, 53(9), pp.507–517.
- Medlyn, B.E., 1998. Physiological basis of the light use efficiency model. *Tree physiology*, 18(3), pp.167–176.
- Mendelssohn, I.A., Sorrell, B.K., Brix, H., Schierup, H.-H.H., Lorenzen, B. & Maltby, E., 1999. Controls on soil cellulose decomposition along a salinity gradient in a *Phragmites australis* wetland in Denmark. *Aquatic Botany*, 64(3), pp.381–398.
- Met Office, 2011. Storm Surge of November 2007. Available at: <http://www.metoffice.gov.uk/about-us/who/how/case-studies/floods-2007>.
- Meyerson, L., Saltonstall, K., Windham, L., Kiviat, E. & Findlay, S., 2000. A comparison of *Phragmites australis* in freshwater and brackish marsh environments in North America. *Wetlands Ecology and Management*, 8, pp.89 – 103.
- Minchinton, T.E. & Bertness, M.D., 2003. Disturbance-mediated competition and the spread of *Phragmites australis* in a coastal marsh. *Ecological Applications*, 13(5), pp.1400–1416.
- Mitch, W.J. & Gosselink, J.G., 2000. *Wetlands: Third Edition*, John Wiley & Sons Inc, NY, USA.
- Mitchell, E.A.D. & Gilbert, D., 2004. Vertical Micro-Distribution and Response to Nitrogen Deposition of Testate Amoebae in *Sphagnum*. *The Journal of Eukaryotic Microbiology*, 51(4), pp.480–490.
- Mitsch, W. & Gosselink, J., 2000. *Wetlands* 3rd ed., New York, USA: John Wiley & Sons Inc.
- Mollema, P.N., Antonellini, M., Dinelli, E., Gabbianelli, G., Greggio, N. & Stuyfzand, P.J., 2013. Hydrochemical and physical processes influencing salinization and freshening in Mediterranean low-lying coastal environments. *Applied Geochemistry*, 34, pp.207 – 221.
- Möller, D., 1990. The Na/Cl ratio in rainwater and the seasalt chloride cycle. *Tellus*, 42(B), pp.254 – 262.
- Mondal, N.C., Singh, V.P., Singh, V.S. & Saxena, V.K., 2010. Determining the

- interaction between groundwater and saline water through groundwater major ions chemistry. *Journal of Hydrology*, 388(1–2), pp.100–111.
- Montero, E., Cabot, C., Poschenrieder, C.H. & Barcelo, J., 1998. Relative importance of osmotic-stress and ion-specific effects on ABA-mediated inhibition of leaf expansion growth in *Phaseolus vulgaris*. *Plant, Cell and Environment*, 21(1), pp.54–62.
- Moore, G.E., Burdick, D.M., Peter, C.R. & Keirstead, R., 2012. Belowground Biomass of *Phragmites australis* in Coastal Marshes. *Northeast Naturalist*, 19(4), pp.611–626.
- Moore, T.R., Bubier, J.L. & Bledzki, L., 2007. Litter decomposition in temperate peatland ecosystems: the effect of substrate and site. *Ecosystems*, 10(6), pp.949–963.
- Moore, T.R., Trofymow, J.A., Prescott, C.E. & Titus, B.D., 2011. Nature and nurture in the dynamics of C, N and P during litter decomposition in Canadian forests. *Plant and Soil*, 339(1), pp.163–175.
- Morecroft, M.D. & Speakman, L., 2015. *Biodiversity Climate Change Impacts Summary Report*, Living with Environmental Change.
- Morris, J.T., Sundareshwar, P. V., Nietch, C.T., Kjerfve, B. & Cahoon, D.R., 2002. Responses of Coastal Wetlands to Rising Sea Level. *Ecology*, 83(10), pp.2869 – 2877.
- Morris, P.J., Baird, A.J. & Belyea, L.R., 2012. The DigiBog peatland development model 2: ecohydrological simulations in 2D. *Ecohydrology*, 5(3), pp.256–268.
- Morris, P.J., Belyea, L.R. & Baird, A.J., 2011. Ecohydrological feedbacks in peatland development: a theoretical modelling study. *Journal of Ecology*, 99(5), pp.1190–1201.
- Morris, P.J. & Waddington, J.M., 2011. Groundwater residence time distributions in peatlands: Implications for peat decomposition and accumulation. *Water Resources Research*, 47(2).
- El Moujabber, M., Samra, B.B., Darwish, T. & Atallah, T., 2006. Comparison of different indicators for groundwater contamination by seawater intrusion on the Lebanese coast. *Water resources management*, 20(2), pp.161–180.

- Mudd, S.M., Howell, S.M. & Morris, J.T., 2009. Impact of dynamic feedbacks between sedimentation, sea-level rise, and biomass production on near-surface marsh stratigraphy and carbon accumulation. *Estuarine, Coastal and Shelf Science*, 82(3), pp.377–389.
- Munns, R., 2002. Comparative physiology of salt and water stress. *Plant, Cell & Environment*, 25(2), pp.239–250.
- Nakagawa, S. & Cuthill, I.C., 2007. Effect size, confidence interval and statistical significance: a practical guide for biologists. *Biological Reviews*, 82(4), pp.591–605.
- Nash, J.E. & Sutcliffe, J. V., 1970. River flow forecasting through conceptual models part I - A discussion of principles. *Journal of Hydrology*, 10(3), pp.282–290.
- Natural England, 2006. *Coastal squeeze, saltmarsh loss and Special Protection Areas*, English Nature Research Reports, Royal Haskining, London, UK.
- Natural England, 2010. *England's peatlands: carbon storage and greenhouse gases*, Natural England Report NE257.
- Natural England and RSPB, 2014. Chapter 12: Lowland fens. In *Climate Change Adaption Manual*. pp. 103–110.
- Neal, C., Jarvie, H., Williams, R., Neal, M., Wickham, H. & Hill, L., 2002. Phosphorus-calcium carbonate saturation relationships in a lowland chalk river impacted by sewage inputs and phosphorus remediation: an assessment of. *the Science of the Total Environment*, pp.295 – 310.
- Neal, C. & Kirchner, J., 2000. Sodium and chloride levels in rainfall, mist, streamwater and groundwater at the Plynlimon catchments, mid-Wales: inferences on hydrological and chemical controls. *Hydrology and Earth System Sciences*, 4(2), pp.295 – 310.
- Neal, C., Martin, E., Neal, M., Hallett, J., Wickham, H., Harman, S., Armstrong, L., Bowes, M., Wade, A. & Keay, D., 2010. Sewage effluent clean-up reduces phosphorus but not phytoplankton in lowland chalk stream (River Kennet, UK) impacted by water mixing from adjacent canal. *Science of The Total Environment*, 408, pp.5306 – 5316.
- Nelson, P.N., Ladd, J.N. & Oades, J.M., 1996. Decomposition of <sup>14</sup>C-labelled plant

- material in a salt-affected soil. *Soil Biology and Biochemistry*, 28(4-5), pp.433–441.
- Neubauer, S.C., 2008. Contributions of mineral and organic components to tidal freshwater marsh accretion. *Estuarine, Coastal and Shelf Science*, 78(1), pp.78–88.
- Neubauer, S.C., Franklin, R.B. & Berrier, D.J., 2013. Saltwater intrusion into tidal freshwater marshes alters the biogeochemical processing of organic carbon. *Biogeosciences*, 10(12).
- Nicholls, R.J., 2004. Coastal flooding and wetland loss in the 21st century: Changes under the SRES climate and socio-economic scenarios. *Global Environmental Change*, 14(1), pp.69–86.
- Nicholls, R.J. & Cazenave, A., 2010. Sea Level Rise and Its Impact on Coastal Zones. *Science*, 328, pp.1517–1520.
- NOAA, 2016. Global Greenhouse Gas Reference Network. *Earth System Research Laboratory, Global Monitoring Division*. Available at: <http://www.esrl.noaa.gov/gmd/ccgg/trends/> [Accessed March 25, 2016].
- Nykänen, H., Heikkinen, J.E.P., Pirinen, L., Tiilikainen, K. & Martikainen, P.J., 2003. Annual CO<sub>2</sub> exchange and CH<sub>4</sub> fluxes on a subarctic palsamire during climatically different years. *Global Biogeochem. Cycles*, 17(1), p.1018.
- Oksanen, J., Blanchet, F.G., Kindt, R., Minchin, P.R., Simpson, G.L., Solymos, P., Stevens, H. & Wagner, H., 2015. *Vegan: Community Ecology Package*.
- Olefeldt, D., Roulet, N., Giesler, R. & Persson, A., 2012. Total waterborne carbon export and DOC composition from ten nested subarctic peatland catchments—importance of peatland cover, groundwater influence, and inter-annual variability of precipitation patterns. *Hydrological Processes*, 27, pp.2280 – 2294.
- Olson, J.S., 1963. Energy storage and the balance of producers and decomposers in ecological systems. *Ecology*, 44(2), pp.322–331.
- Ostendorp, W., 1989. “Die-back” of reeds in Europe—a critical review of literature. *Aquatic Botany*, 35(1), pp.5–26.
- Outram, F.N. & Hiscock, K.M., 2012. Indirect Nitrous Oxide Emissions from Surface Water Bodies in a Lowland Arable Catchment: A Significant Contribution to



- Agricultural Greenhouse Gas Budgets? *Environmental Science & Technology*, 46(15), pp.8156–8163.
- Ouyang, X., Zhou, G., Huang, Z., Zhou, C., Li, J., Shi, J. & Zhang, D., 2008. Effect of N and P addition on soil organic C potential mineralization in forest soils in South China. *Journal of Environmental Sciences*, 20(9), pp.1082–1089.
- Page, S.E., Rieley, J.O. & Banks, C.J., 2011. Global and regional importance of the tropical peatland carbon pool. *Global Change Biology*, 17, pp.798–818.
- Pagter, M., Bragato, C. & Brix, H., 2005. Tolerance and physiological responses of *Phragmites australis* to water deficit. *Aquatic Botany*, 81(4), pp.285–299.
- Pagter, M., Bragato, C., Malagoli, M. & Brix, H., 2009. Osmotic and ionic effects of NaCl and Na<sub>2</sub>SO<sub>4</sub> salinity on *Phragmites australis*. *Aquatic Botany*, 90(1), pp.43–51.
- Paradis, E., Baillie, S.R., Sutherland, W.J. & Gregory, R.D., 1999. Dispersal and spatial scale affect synchrony in spatial population dynamics. *Ecology Letters*, 2, pp.114–120.
- Pendea, I.F. & Chmura, G.L., 2012. A high-resolution record of carbon accumulation rates during boreal peatland initiation. *Biogeosciences*, 9, pp.2711 – 2717.
- Petrokofsky, G., Kanamaru, H., Achard, F., Goetz, S.J., Joosten, H., Holmgren, P., Lehtonen, A., Menton, M.C., Pullin, A.S. & Wattenbach, M., 2012. Comparison of methods for measuring and assessing carbon stocks and carbon stock changes in terrestrial carbon pools. How do the accuracy and precision of current methods compare? A systematic review protocol. *Environmental Evidence*, 1(6), pp.1 – 21.
- Philipona, R., Du, B., Marty, C., Ohmura, A. & Wild, M., 2004. Radiative forcing - measured at Earth's surface - corroborate the increasing greenhouse effect. *Geophysical Research Letters*, 31(3), pp.1 – 4.
- Piao, S., Friedlingstein, P., Ciais, P., Viovy, N. & Demarty, J., 2007. Growing season extension and its impact on terrestrial carbon cycle in the Northern Hemisphere over the past 2 decades. *Global Biogeochemical Cycles*, 21(3), p.n/a–n/a.
- Pickett, S.T.A., 1989. Space-for-time substitution as an alternative to long-term studies. *Long-Term Studies in Ecology*, pp.110–135.

- Pinna, M., Fonnesu, A., Sangiorgio, F. & Basset, A., 2004. Influence of summer drought on spatial patterns of resource availability and detritus processing in Mediterranean stream sub-basins (Sardinia, Italy). *International Review of Hydrobiology*, 89(5-6), pp.484–499.
- Poulter, B., Christensen, N.L. & Halpin, P.N., 2006. Carbon emissions from a temperate peat fire and its relevance to interannual variability of trace atmospheric greenhouse gases. *Journal of Geophysical Research*, 111, pp.1 – 11.
- Pouyat, R. V & Carreiro, M.M., 2003. Controls on mass loss and nitrogen dynamics of oak leaf litter along an urban-rural land-use gradient. *Oecologia*, 135(2), pp.288–298.
- Prescott, C.E., 2005. Do rates of litter decomposition tell us anything we really need to know? *Forest Ecology and Management*, 220(1), pp.66–74.
- Qi, M., Sun, T., Zhan, M. & Xue, S.F., 2016. Simulating Dynamic Vegetation Changes in a Tidal Restriction Area with Relative Stress Tolerance Curves. *Wetlands*, 36(Suppl 1), pp.31–43.
- Quintino, V., Sangiorgio, F., Ricardo, F., Mamede, R., Pires, A., Freitas, R., Rodrigues, A.M. & Basset, A., 2009. *In situ* experimental study of reed leaf decomposition along a full salinity gradient. *Estuarine, Coastal and Shelf Science*, 85(3), pp.497–506.
- R Core Development Team, 2014. R: A language and environment for statistical computing. R Foundation for Statistical Computing.
- Reddy, K.R., Delaune, R.D., DeBusk, W.F., Koch, M.S., Delaune, R.D. & Koch, M.S., 1993. Long-Term Nutrient Accumulation Rates in the Everglades. *Soil Science Society of America Journal*, 57(4), p.1147.
- Reichstein, M., Bahn, M., Ciais, P., Frank, D., Mahecha, M.D., Seneviratne, S.I., Zscheischler, J., Beer, C., Buchmann, N., Frank, D.C., Papale, D., Rammig, A., Smith, P., Thonicke, K., Velde, M. van der, Vicca, S., Walz, A. & Wattenbach, M., 2013. Climate extremes and the carbon cycle. *Nature*, 500(7462), pp.287–295.
- Reid, M.K. & Spencer, K.L., 2009. Use of principal components analysis (PCA) on estuarine sediment datasets: the effect of data pre-treatment. *Environmental Pollution*, 157(8), pp.2275–2281.

- Reynolds, B.C., Hamel, J., Isbanioly, J., Klausman, L. & Moorhead, K.K., 2007. From forest to fen: Microarthropod abundance and litter decomposition in a southern Appalachian floodplain/fen complex. *Pedobiologia*, 51(4), pp.273–280.
- Rice, D., Rooth, J. & Stevenson, J.C., 2000. Colonization and expansion of *Phragmites australis* in upper Chesapeake Bay tidal marshes. *Wetlands*, 20(2), pp.280–299.
- Richert, M., Saarnio, S., Juutinen, S., Silvola, J., Augustin, J. & Merbach, W., 2000. Distribution of assimilated carbon in the system *Phragmites australis* - waterlogged peat soil after carbon-14 pulse labelling. *Biology and Fertility of Soils*, 32, pp.1–7.
- Ricker, W.E., 1973. Linear Regressions in Fishery Research. *Journal of the Fisheries Board of Canada*, 30(3), pp.409 – 434.
- Rickey, M. a & Anderson, R.C., 2004. Effects of nitrogen addition on the invasive grass *Phragmites australis* and a native competitor *Spartina pectinata*. *Journal of Applied Ecology*, 41(5), pp.888–896.
- Riet, B.P., Hefting, M.M. & Verhoeven, J.T.A., 2013. Rewetting Drained Peat Meadows: Risks and Benefits in Terms of Nutrient Release and Greenhouse Gas Exchange. *Water, Air, & Soil Pollution*, 224(4), pp.1–12.
- Rietz, D.N. & Haynes, R.J., 2003. Effects of irrigation-induced salinity and sodicity on soil microbial activity. *Soil Biology and Biochemistry*, 35(6), pp.845–854.
- Robinson, S.D. & Moore, T.R., 1999. Carbon and peat accumulation over the past 1200 years in a landscape with discontinuous permafrost, northwestern Canada. *Global Biogeochemical Cycles*, 13(2), pp.591–601.
- Rolletschek, H. & Hartzendorf, T., 2000. Effects of salinity and convective rhizome ventilation on amino acid and carbohydrate patterns of *Phragmites australis* populations in the Neusiedler See region of Austria and Hungary. *New Phytologist*, 146(1), pp.95–105.
- Rolletschek, H., Rolletschek, A., Köhl, H. & Köhl, J.G., 1999. Clone specific differences in a *Phragmites australis* stand II. Seasonal development of morphological and physiological characteristics at the natural site and after transplantation. *Aquatic Botany*, 64(3-4), pp.247–260.

- Romero, J.A., Brix, H. & Comín, F.A., 1999. Interactive effects of N and P on growth, nutrient allocation and NH<sub>4</sub> uptake kinetics by *Phragmites australis*. *Aquatic Botany*, 64(3), pp.369–380.
- Le Roux, G. & Marshall, W.A., 2011. Constructing recent peat accumulation chronologies using atmospheric fall-out radionuclides. *Mires and Peat*, 7(1), p.e14.
- Rovira, P. & Rovira, R., 2010. Fitting litter decomposition datasets to mathematical curves: Towards a generalised exponential approach. *Geoderma*, 155(3-4), pp.329–343.
- Russell, I.A. & Kraaij, T., 2008. Effects of cutting *Phragmites australis* along an inundation gradient, with implications for managing reed encroachment in a South African estuarine lake system. *Wetlands Ecology and Management*, 16(5), pp.383–393.
- Van Ryckegem, G., Van Driessche, G., Van Beeumen, J.J. & Verbeken, A., 2006. The estimated impact of fungi on nutrient dynamics during decomposition of *Phragmites australis* leaf sheaths and stems. *Microbial Ecology*, 52(3), pp.564–574.
- Rydin, H. & Jeglum, J., 2013. *The Biology of Peatlands*, Oxford, UK: Oxford University Press.
- Sahu, K., McNeill, V.F. & Eisenthal, K.B., 2010. Effect of salt on the adsorption affinity of an aromatic carbonyl molecule to the air-aqueous interface: Insight for aqueous environmental interfaces. *Journal of Physical Chemistry C*, 114, pp.18258–18262.
- Saiz-Jimenez, C., 1996. The chemical structure of humic substances: recent advances. In: Humic Substances in Terrestrial Ecosystems. In A. Piccolo, ed. Elsevier, Amsterdam: Elsevier, Amsterdam, pp. 1 – 45.
- Saleque, M. & Kirk, G., 1995. Root-induced solubilization of phosphate in the rhizosphere of lowland rice. *New Phytologist*, 129(2), pp.325–336.
- Saltmarsh, A., Mauchamp, A. & Rambal, S., 2006. Contrasted effects of water limitation on leaf functions and growth of two emergent co-occurring plant species, *Cladium mariscus* and *Phragmites australis*. *Aquatic Botany*, 84(3), pp.191–198.

- Sangiorgio, F., Basset, A., Pinna, M., Sabetta, L., Abbiati, M., Ponti, M., Monocci, M., Orfanidis, S., Nicolaidou, A., Mocheva, S., Trayanova, A., Georgescu, L., Dragan, S., Beqiraj, S., Koutsoubas, D., Evagelopoulos, A. & Reizopoulou, S., 2008. Environmental factors affecting *Phragmites australis* litter decomposition in Mediterranean and Black Sea transitional waters. *Aquatic Conservation: Marine and Freshwater Ecosystems*, 19, pp.671–675.
- Sardinha, M., Müller, T., Schmeisky, H. & Joergensen, R.G., 2003. Microbial performance in soils along a salinity gradient under acidic conditions. *Applied Soil Ecology*, 23(3), pp.237–244.
- Scarton, F., Day, J.W. & Rismondo, A., 2002. Primary Production and Decomposition of *Sarcocornia fruticosa* (L.) Scott and *Phragmites australis* Trin. Ex Steudel in the Po Delta, Italy. *Estuaries*, 25(3), pp.325–336.
- Schimel, D., 1995. Terrestrial ecosystems and the carbon cycle. *Global change biology*, 1(1), pp.77 – 91.
- Seer, F.K. & Schrautzer, J., 2014. Status, future prospects, and management recommendations for alkaline fens in an agricultural landscape: A comprehensive survey. *Journal for Nature Conservation*, 22(4), pp.358–368.
- Self, M., 2005. A review of management for fish and bitterns, *Botaurus stellaris*, in wetland reserves. *Fisheries Management and Ecology*, 12(6), pp.387–394.
- Shamsudduha, M., Chandler, R., Taylor, R. & Ahmed, K., 2009. Recent trends in groundwater levels in a highly seasonal hydrological system: the Ganges-Brahmaputra-Meghna Delta. *Hydrology and Earth System Sciences*, 13, pp.2373–2385.
- Shand, P., Edmunds, W.M., Lawrence, A.R., Smedley, P. & Burke, S., 2007. *The natural (baseline) quality of groundwater in England and Wales*, British Geological Survey Research Report No. RR/07/06.
- Shennan, I. & Horton, B., 2002. Holocene land- and sea-level changes in Great Britain. *Journal of Quaternary Science*, 17(5-6), pp.511–526.
- Shennan, I., Lambeck, K., Horton, B., Innes, J., Lloyd, J., McArthur, J., Purcell, T. & Rutherford, M., 2000. Late Devensian and Holocene records of relative sea-level changes in northwest Scotland and their implications for glacio-hydro-isostatic modelling. *Quaternary Science Reviews*, 19(11), pp.1103–1135.

- Sheppard, L.J., Leith, I.D., Leeson, S.R., Van Dijk, N., Field, C. & Levy, P., 2013. Fate of N in a peatland, Whim bog: Immobilisation in the vegetation and peat, leakage into pore water and losses as N<sub>2</sub>O depend on the form of N. *Biogeosciences*, 10(1), pp.149–160.
- Shi, R. & Yu, K., 2014. Impact of exposure of crude oil and dispersant (COREXIT® EC 9500A) on denitrification and organic matter mineralization in a Louisiana salt marsh sediment. *Chemosphere*, 108(0), pp.300–305.
- Sibley, A. & Titley, H., 2015. Coastal flooding in England and Wales from Atlantic and North Sea storms during the 2013/2014 winter. *Weather*, 70(2), pp.62 – 70.
- Simpson, T., Holman, I.P. & Rushton, K., 2011. Drainage ditch-aquifer interaction with special reference to surface water salinity in the Thurne catchment, Norfolk, UK. *Water and Environment Journal*, 25(1), pp.116–128.
- Sissons, J., 1966. Relative sea-level changes between 10,300 and 8,300 BP in part of the Carse of Stirling. *Transactions of the Institute of British Geographers*, pp.19 – 29.
- Sjors, H., 1991. Phyto- and Necromass above and below Ground in a Fen. *Holarctic Ecology*, 14(3), pp.208–218.
- Sjörs, H., 1980. Peat on earth: Multiple use or conservation? *Ambio*, pp.303–308.
- Slingo, J., Belcher, S., Scaife, A., McCarthy, M., Saulter, A., McBeath, K., Jenkins, A., Huntingford, C., Marsh, T., Hannaford, J. & Parry, S., 2014. *The Recent Storms and Floods in the UK*, Met Office, Exeter, UK.
- Smemo, K.A. & Yavitt, J.B., 2007. Evidence for anaerobic CH<sub>4</sub> oxidation in freshwater peatlands. *Geomicrobiology Journal*, 24(7-8), pp.583–597.
- Soetaert, K., 2015. Nonlinear Root Finding, Equilibrium and Steady-State Analysis of Ordinary Differential Equations. , p.62.
- Soetaert, K. & Herman, P.M.J., 2008. *A practical guide to ecological modelling: using R as a simulation platform*, Springer.
- Soetaert, K., Hoffmann, M., Meire, P., Starink, M., Oevelen, D. van, Regenmortel, S. Van & Cox, T., 2004. Modeling growth and carbon allocation in two reed beds (*Phragmites australis*) in the Scheldt estuary. *Aquatic Botany*, 79(3), pp.211–234.

- Song, L. & Atkinson, T.C., 1985. Dissolved iron in chalk groundwaters from Norfolk, England. *Quarterly Journal of Engineering Geology and Hydrogeology*, 18(3), pp.261–274.
- Sparling, G. & West, A., 1989. Importance of soil water content when estimating soil microbial C, N and P by the fumigation-extraction methods. *Soil Biology and Biochemistry*, 21(2), pp.245–253.
- Stanley, K.M., 2015. *The impacts of nutrient loading on greenhouse gas exchange in floodplain fens*. London: PhD Thesis, Queen Mary University of London.
- Steinmann, P. & Shotyk, W., 1997. Chemical composition, pH, and redox state of sulfur and iron in complete vertical porewater profiles from two *Sphagnum* peat bogs, Jura Mountains, Switzerland. *Geochimica Et Cosmochimica Acta*, 61(6), pp.1143–1163.
- Sterl, A., Van Den Brink, H., De Vries, H., Haarsma, R. & Van Meijgaard, E., 2009. An ensemble study of extreme storm surge related water levels in the North Sea in a changing climate. *Ocean Science*, 5(3), pp.369–378.
- Stocker, T.F., D. Qin, G.-K., Plattner, L.V., Alexander, S.K., Allen, N.L., Bindoff, F.-M., Bréon, J. a., Church, U., Cubasch, S., Emori, P., Forster, P., Friedlingstein, N., Gillett, J.M., Gregory, D.L., Hartmann, E., Jansen, B., Kirtman, R., Knutti, K., Krishna Kumar, P., Lemke, J., Marotzke, V., Masson-Delmotte, G. a., Meehl, I.I., Mokhov, S., Piao, V., Ramaswamy, D., Randall, M., Rhein, M., Rojas, C., Sabine, D., Shindell, L.D., Talley, D.G. & Xie, V. and S.-P., 2013. *Technical Summary. In: Climate Change 2013: The Physical Science Basis. Contribution of Working Group I to the Fifth Assessment Report of the Intergovernmental Panel on Climate Change* T. F. Stocker, D. Qin, G.-K. Plattner, M. Tignor, S. K. Allen, J. Boschung, A. Nauels, Y. Xia, V. Bex, & P. M. Midgley, eds., Cambridge, United Kingdom and New York, NY, USA: Cambridge University Press.
- Strakova, P., Penttilä, T., Laine, J. & Laiho, R., 2012. Disentangling direct and indirect effects of water table drawdown on above- and belowground plant litter decomposition: Consequences for accumulation of organic matter in boreal peatlands. *Global Change Biology*, 18(1), pp.322–335.
- Surridge, B.W.J., 2004. *Biogeochemical and hydrological controls on phosphorus transport in a floodplain fen*: PhD Thesis, University of Sheffield.

- Surridge, B.W.J., Heathwaite, a. L. & Baird, A.J., 2012. Phosphorus mobilisation and transport within a long-restored floodplain wetland. *Ecological Engineering*, 44, pp.348–359.
- Tanaka, Y., 1991. Microbial decomposition of reed (*Phragmites communis*) leaves in a saline lake. *Hydrobiologia*, 220, pp.119 – 129.
- Tanneberger, F., Tegetmeyer, C., Dylawski, M., Flade, M. & Joosten, H., 2009. Commercially cut reed as a new and sustainable habitat for the globally threatened Aquatic Warbler. *Biodiversity and Conservation*, 18(6), pp.1475–1489.
- Tao, R. & Yu, K., 2013. Nitrate addition has minimal effect on anaerobic biodegradation of benzene in coastal saline (salt), brackish and freshwater marsh sediments. *Wetlands*, 33(4), pp.759–767.
- Tarnocai, C., Canadell, J.G., Schuur, E. a G., Kuhry, P., Mazhitova, G. & Zimov, S., 2009. Soil organic carbon pools in the northern circumpolar permafrost region. *Global Biogeochemical Cycles*, 23(2), pp.1–11.
- Taverniers, I., De Loose, M. & Van Bockstaele, E., 2004. Trends in quality in the analytical laboratory. II. Analytical method validation and quality assurance. *Trends in Analytical Chemistry*, 23(8), pp.535–552.
- Taylor, R., 1990. Interpretation of the correlation coefficient: a basic review. *Journal of Diagnostic Medical Sonography*, 6(1), pp.35–39.
- Thimonier, A., Schmitt, M., Waldner, P. & Schleppi, P., 2008. Seasonality of the Na/Cl ratio in precipitation and implications of canopy leaching in validating chemical analyses of throughfall samples. *Atmospheric Environment*, 42, pp.9106 – 9117.
- Thormann, M. & Bayley, E., 1997. Aboveground plant production and nutrient content of the vegetation in six peatlands in Alberta, Canada. *Plant Ecology*, 131(1), pp.1–16.
- Thormann, M., Szumigalski, A. & Bayley, S., 1999. Aboveground peat and carbon accumulation potentials along a bog-fen-marsh wetland gradient in southern boreal Alberta, Canada. *Wetlands*, 19(2), pp.305–317.
- Thormann, M.N. & Bayley, S.E., 1997. Decomposition along a moderate-rich fen-marsh peatland gradient in boreal Alberta, Canada. *Wetlands*, 17(1), pp.123–



- Thormann, M.N., Bayley, S.E. & Currah, R.S., 2001. Comparison of decomposition of belowground and aboveground plant litters in peatlands of boreal Alberta, Canada. *Canadian Journal of Botany*, 79(1), pp.9–22.
- Todolí, J.L., Gras, L., Hernandis, V. & Mora, J., 2002. Elemental matrix effects in ICP-AES. *Journal of Analytical Atomic Spectrometry*, 17(2), pp.142–169.
- Tooley, M., 1974. Sea-level changes during the last 9000 years in north-west England. *Geographical Journal*, pp.18 – 42.
- Travis, S.E. & Hester, M.W., 2005. A space- for- time substitution reveals the long-term decline in genotypic diversity of a widespread salt marsh plant, *Spartina alterniflora*, over a span of 1500 years. *Journal of Ecology*, 93(2), pp.417–430.
- Troels-Smith, J., 1955. Characterization of unconsolidated sediments. *Geological Survey of Denmark: iv*, 3(10), p.73.
- Turetsky, M.R., Manning, S.W. & Wieder, R.K., 2004. Dating recent peat deposits. *Wetlands*, 24(2), pp.324–356.
- Turtola, E. & Yli-Halla, M., 1999. Fate of phosphorus applied in slurry and mineral fertilizer: accumulation in soil and release into surface runoff water. *Nutrient Cycling in Agroecosystems*, 55(2), pp.165–174.
- Turunen, J., Roulet, N.T., Moore, T.R. & Richard, P.J.H., 2004. Nitrogen deposition and increased carbon accumulation in ombrotrophic peatlands in eastern Canada. *Global Biogeochemical Cycles*, 18(3), pp.1–12.
- Turunen, J., Tomppo, E., Tolonen, K. & Reinikainen, A., 2002. Estimating carbon accumulation rates of undrained mires in Finland—application to boreal and subarctic regions. *The Holocene*, 12(1), pp.69 – 80.
- Tylova-Munzarova, E., Lorenzen, B., Brix, H. & Votrubova, O., 2005. The effects of  $\text{NH}_4^+$  and  $\text{NO}_3^-$  on growth, resource allocation and nitrogen uptake kinetics of *Phragmites australis* and *Glyceria maxima*. *Aquatic Botany*, 81(4), pp.326–342.
- USEPA, 2008. *Methods for Evaluating Wetland Condition: Wetland Hydrology*, Washington, DC: Office of Water, U.S. Environmental Protection Agency.
- Van Veen, J.A., Merckx, R. & Van de Geijn, S.C., 1989. Plant-and soil related controls

- of the flow of carbon from roots through the soil microbial biomass. *Plant and Soil*, 115, pp.179 – 188.
- Venterink, H., Wassen, M., Belgers, J.D. & Verhoeven, J.T., 2001. Control of environmental variables on species density in fens and meadows: importance of direct effects and effects through community biomass. *Journal of Ecology*, 89, pp.1033 – 1040.
- Vermaire, J.C., Pisaric, M.F.J., Thienpont, J.R., Courtney Mustaphi, C.J., Kokelj, S. V. & Smol, J.P., 2013. Arctic climate warming and sea ice declines lead to increased storm surge activity. *Geophysical Research Letters*, 40, pp.1386–1390.
- Vitt, D., 1990. Growth and production dynamics of boreal mosses over climatic, chemical and topographical gradients. *Botanical journal of the Linnean Society*, 104(1-3), p.35.–59.
- Vitt, D.H. & Chee, W., 1990. The relationships of vegetation to surface water chemistry and peat chemistry in fens of Alberta, Canada. *Vegetatio*, 89(2), pp.87–106.
- Voellm, C. & Tanneberger, F., 2014. Shallow inundation favours decomposition of *Phragmites australis* leaves in a near-natural temperate fen. *Mires and Peat*, 14(6), pp.1–9.
- Waddington, J.M., Morris, P.J., Kettridge, N., Granath, G., Thompson, D.K. & Moore, P.A., 2015. Hydrological feedbacks in northern peatlands. *Ecohydrology*, 8(1), pp.113–127.
- Wang, M., Moore, T.R., Talbot, J. & Richard, P.J.H., 2014. The cascade of C:N:P stoichiometry in an ombrotrophic peatland: from plants to peat. *Environmental Research Letters*, 9(2), p.024003.
- Wang, T. & Peverly, J., 1999. Iron oxidation states on root surfaces of a wetland plant (*Phragmites australis*). *Soil Science Society of America Journal*, 63(1), pp.247 – 252.
- Warren, R.S., Fell, P.E., Grimsby, J.L., Buck, E.L., Rilling, G.C. & Fertik, R. a., 2001. Rates, Patterns, and Impacts of *Phragmites australis* Expansion and Effects of Experimental *Phragmites* Control on Vegetation, Macroinvertebrates, and Fish within Tidelands of the Lower Connecticut River. *Estuaries*, 24(1), p.90.

- Wassen, M.J., Barendregt, A., Bootsma, M.C. & Schot, P.P., 1988. Groundwater Chemistry and Vegetation of Gradients from Rich Fen to Poor Fen in the Naardermeer (The Netherlands). *Vegetatio*, 79(3), pp.117–132.
- Wassen, M.J. & Joosten, J.H.J., 1996. In search of a hydrological explanation for vegetation changes along a fen gradient in the Biebrza Upper Basin (Poland). *Vegetatio*, 124(2), pp.191–209.
- Webster, J. & Benfield, E., 1986. Vascular Plant Breakdown in Freshwater Ecosystems. *Annual Review of Ecology and Systematics*, 17, pp.567–594.
- Weisner, S.E.B. & Granéli, W., 1989. Influence of substrate conditions on the growth of *Phragmites australis* after a reduction in oxygen transport to below-ground parts. *Aquatic botany*, 35(1), pp.71 – 80.
- Weissert, L.F. & Disney, M., 2013. Carbon storage in peatlands: A case study on the Isle of Man. *Geoderma*, 204–205, pp.111–119.
- Weston, N.B., Vile, M.A., Neubauer, S.C. & Velinsky, D.J., 2011. Accelerated microbial organic matter mineralization following salt-water intrusion into tidal freshwater marsh soils. *Biogeochemistry*, 102(1-3), pp.135–151.
- Wheeler, B.D. & Giller, K.E., 1982. Species Richness of Herbaceous Fen Vegetation in Broadland , Norfolk in Relation to the Quantity of Above-Ground Plant Material P. *Journal of Ecology*, 70(1), pp.179–200.
- Wheeler, B.D. & Shaw, S.C., 2000. *A wetland framework for impact assessmentsnet at Statutory sites in eastern England. R & D Technical Report W6-068 / TR2*, Environment Agency and The Wetlands Research Group, University of Sheffield.
- Whittaker, R.H., 1970. Communities and ecosystems. *Communities and Ecosystems*.
- Whittle, A. & Gallego-Sala, A. V, 2016. Vulnerability of the peatland carbon sink to sea-level rise. *Scientific Reports*, 6(28758), pp.1–11.
- Wichern, J., Wichern, F. & Joergensen, R.G., 2006. Impact of salinity on soil microbial communities and the decomposition of maize in acidic soils. *Geoderma*, 137(1-2), pp.100–108.
- Wider, R.K. & Lang, G.E., 1982. A Critique of the Analytical Methods Used in Examining Decomposition Data Obtained From Litter Bags. *Ecology*, 63(6), pp.1636–1642.

- Wiegert, R. & Evans, F., 1964. Primary production and the disappearance of dead vegetation on an old field in southeastern Michigan. *Ecology*, 45(1), pp.49–63.
- Wind-Mulder, H.L., Rochefort, L. & Vitt, D.H., 1996. Water and peat chemistry comparisons of natural and post-harvested peatlands across Canada and their relevance to peatland restoration. *Ecological Engineering*, 7(3), pp.161–181.
- Windham, L., 2001. Comparison of biomass production and decomposition between *Phragmites australis* (common reed) and *Spartina patens* (salt hay grass) in brackish tidal marshes on New Jersey, USA. *Wetlands*, 21(2), pp.179–188.
- Winter, B., 2013. *Linear models and linear mixed effects models in R with linguistic applications*, University of California.
- Worrall, F., Chapman, P., Holden, J., Evans, C., Artz, R., Smith, P. & Grayson, R., 2011. *A review of current evidence on carbon fluxes and greenhouse gas emissions from UK peatlands*, JNCC Report, No. 442, Peterborough, UK.
- Woth, K., Weisse, R. & Storch, H. Von, 2006. Climate change and North Sea storm surge extremes: an ensemble study of storm surge extremes expected in a changed climate projected by four different regional climate models. *Ocean Dynamics*, 56, pp.3 – 15.
- Yang, S., Shih, S., Hwang, G., Adams, J., Leeds-Harrison, P.B. & Chen, C., 2013. The salinity gradient influences on the inundation tolerance thresholds of mangrove forests. *Ecological Engineering*, 51, pp.59–65.
- Yang, Z., Xie, T. & Liu, Q., 2014. Physiological responses of *Phragmites australis* to the combined effects of water and salinity stress. *Ecohydrology*, 7(2), pp.420–426.
- Yidana, S.M., Ophori, D. & Banoeng-Yakubo, B., 2008. A multivariate statistical analysis of surface water chemistry data—The Ankobra Basin, Ghana. *Journal of Environmental Management*, 86(1), pp.80–87.
- Yu, Z., 2006. Holocene carbon accumulation of fen peatlands in boreal western Canada: a complex ecosystem response to climate variation and disturbance. *Ecosystems*, 9(8), pp.1278 – 1288.
- Yu, Z., Campbell, I.D., Vitt, D.H. & Apps, M.J., 2001. Modelling long-term peatland dynamics. I. Concepts, review, and proposed design. *Ecological Modelling*,

145(2-3), pp.197–210.

Yu, Z., Loisel, J., Brosseau, D.P., Beilman, D.W. & Hunt, S.J., 2010. Global peatland dynamics since the Last Glacial Maximum. *Geophysical Research Letters*, 37, pp.1 – 5.

Yu, Z., Vitt, D.H., Campbell, I.D. & Apps, M.J., 2003. Understanding Holocene peat accumulation pattern of continental fens in western Canada. *Canadian Journal of Botany*, 81(3), pp.267–282.

Yu, Z.C., 2012. Northern peatland carbon stocks and dynamics: a review. *Biogeosciences*, 9(10), pp.4071–4085.

Zauft, M., Fell, H., Glasser, F., Rosskopf, N. & Zeitz, J., 2010. Carbon storage in the peatlands of Mecklenburg-Western Pomerania, north-east Germany. *Mires and Peat*, 6, pp.1–12.

Zhang, L., Song, C., Wang, D., Wang, Y. & Xu, X., 2007. The variation of methane emission from freshwater marshes and response to the exogenous N in Sanjiang Plain Northeast China. *Atmospheric Environment*, 41(19), pp.4063–4072.

Zhang, X., Song, C., Mao, R., Yang, G., Tao, B., Shi, F., Zhu, X. & Hou, A., 2014. Litter mass loss and nutrient dynamics of four emergent macrophytes during aerial decomposition in freshwater marshes of the Sanjiang plain, Northeast China. *Plant and Soil*, 385, pp.139–147.

Zhao, Y., Xia, X. & Yang, Z., 2013. Growth and nutrient accumulation of *Phragmites australis* in relation to water level variation and nutrient loadings in a shallow lake. *Journal of Environmental Sciences*, 25(1), pp.16–25.

**Appendix 1: Field data used to calculate above-ground carbon mass.**

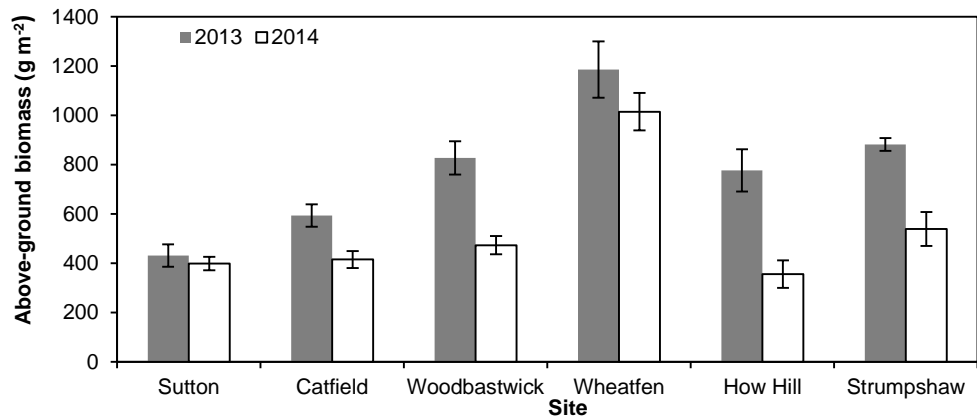


Figure 1: Above-ground biomass for each study site in both 2013 and 2014. Bars indicate mean values and errors are  $\pm 1$  SE.

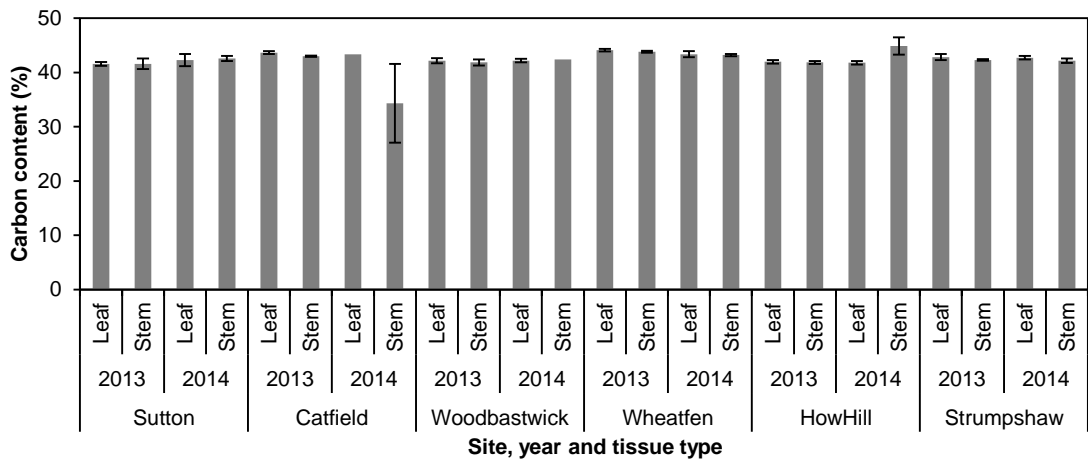


Figure 2: Comparison of carbon content between site, year and leaves and stems of *Phragmites australis*. A three-way ANOVA showed no significant differences. Bars indicate mean and errors are  $\pm 1$  SE.

## Appendix 2: Scatterplots to show goodness of fit of multiple regression models.

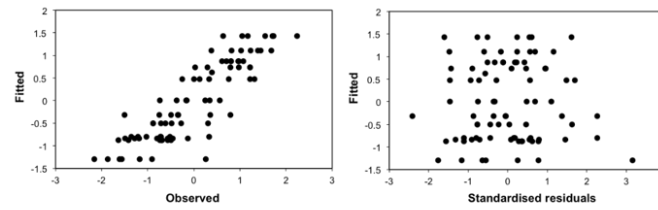


Figure 1: Dependent variable is RuE

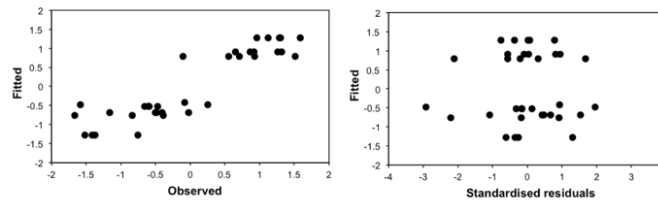


Figure 2: Dependent variable is AGCP/BGCP

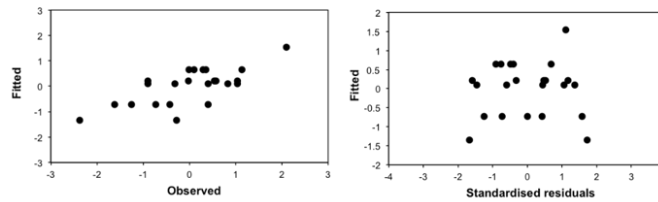


Figure 3: Dependent variable is mass loss of leaves after month 1.

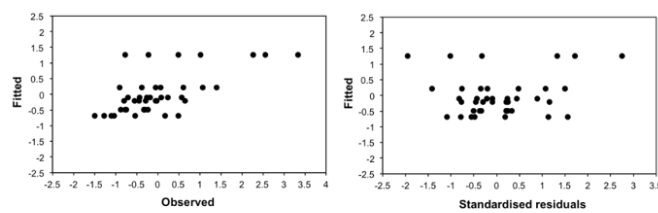


Figure 4: Dependent variable is mass loss of BG material after month 1.

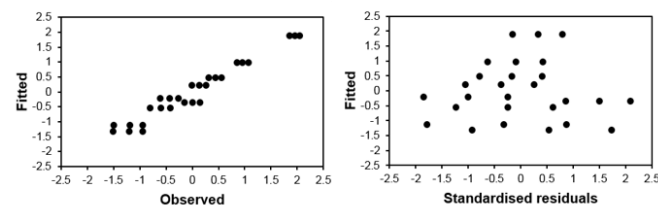


Figure 5: Dependent variable is the decay rate coefficient (k) for leaves after 1 month.

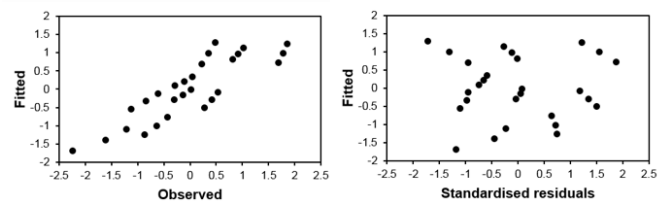


Figure 6: Dependent variable is the decay rate coefficient (k) for stems after 12 months.

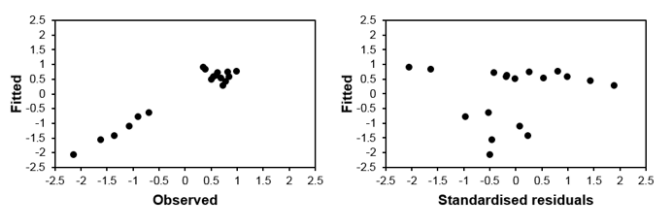


Figure 7: Dependent variable is the decay rate coefficient (k) for BG material after 12 months.

### Appendix 3: Parameter estimates fitted to each core using the Ricker function.

n.s. indicates a non-significant result

Parameter	Site	Core	Value	SE	p-value
$\alpha$	Strumpshaw	1	4822	6590	ns
$\alpha$	Strumpshaw	2	6382	2809	< 0.05
$\alpha$	Strumpshaw	3	4970	2643	ns
$\alpha$	Strumpshaw	4	8372	2976	< 0.05
$\alpha$	Strumpshaw	5	9365	4079	< 0.05
$\alpha$	Strumpshaw	6	3564	2518	ns
$\alpha$	Wheatfen	1	3820	2703	ns
$\alpha$	Wheatfen	2	5783	2353	< 0.05
$\alpha$	Wheatfen	3	20479	6954	< 0.05
$\alpha$	Wheatfen	4	7499	2894	< 0.05
$\alpha$	Catfield	1	4065	2599	ns
$\alpha$	Catfield	2	3860	2541	ns
$\alpha$	Catfield	3	2770	2203	ns
$\alpha$	Catfield	4	4902	2736	ns
$\alpha$	Catfield	5	2255	2232	ns
$\alpha$	Sutton	1	4180	2396	ns
$\alpha$	Sutton	2	10794	3038	< 0.05
$\alpha$	Sutton	3	6237	2839	< 0.05
$\alpha$	Sutton	4	7157	2832	< 0.05
$\alpha$	Sutton	5	8285	2839	< 0.05
$\alpha$	Sutton	6	6116	2749	< 0.05
$\alpha$	Sutton	7	8060	2933	< 0.05
$\alpha$	How Hill	1	3088	2352	ns
$\alpha$	How Hill	2	2192	2074	ns
$\alpha$	How Hill	3	2071	2069	ns
$\alpha$	How Hill	4	8328	3100	< 0.05
$\alpha$	How Hill	5	3270	2250	ns
$\alpha$	How Hill	6	4849	2799	ns
$\alpha$	Woodbastwick	1	6788	3589	ns
$\alpha$	Woodbastwick	2	12839	4283	< 0.05
$\alpha$	Woodbastwick	3	5773	2756	< 0.05
$\alpha$	Woodbastwick	4	5896	2675	< 0.05
$\alpha$	Woodbastwick	5	3631	2395	ns
$\alpha$	Woodbastwick	6	11245	3134	< 0.05
$b$	Strumpshaw	1	3.6	2.0	ns
$b$	Strumpshaw	2	3.9	0.68	< 0.0001
$b$	Strumpshaw	3	3.5	0.83	< 0.001
$b$	Strumpshaw	4	4.4	0.56	< 0.0001
$b$	Strumpshaw	5	4.7	0.68	< 0.0001
$b$	Strumpshaw	6	3.2	1.1	< 0.05
$b$	Wheatfen	1	2.0	1.6	ns
$b$	Wheatfen	2	3.3	0.70	< 0.0001
$b$	Wheatfen	3	3.9	0.25	< 0.0001

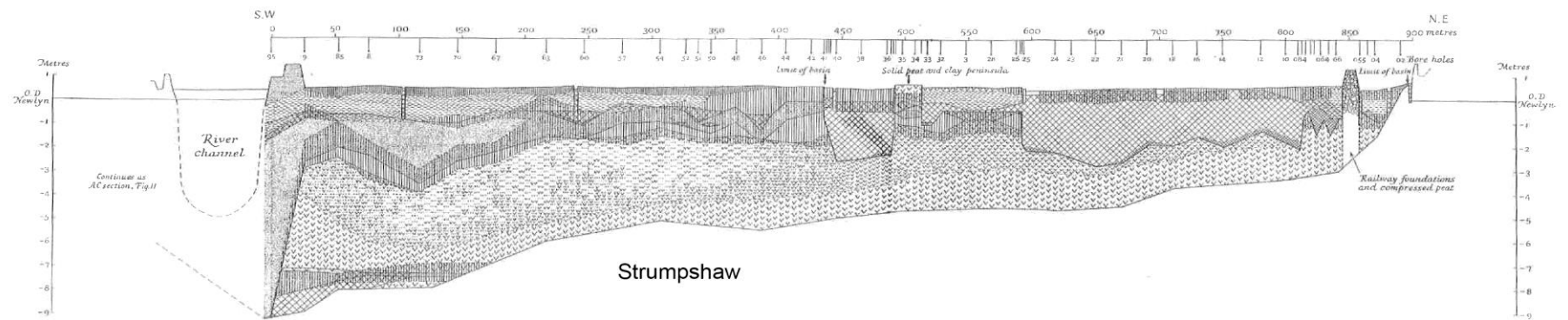
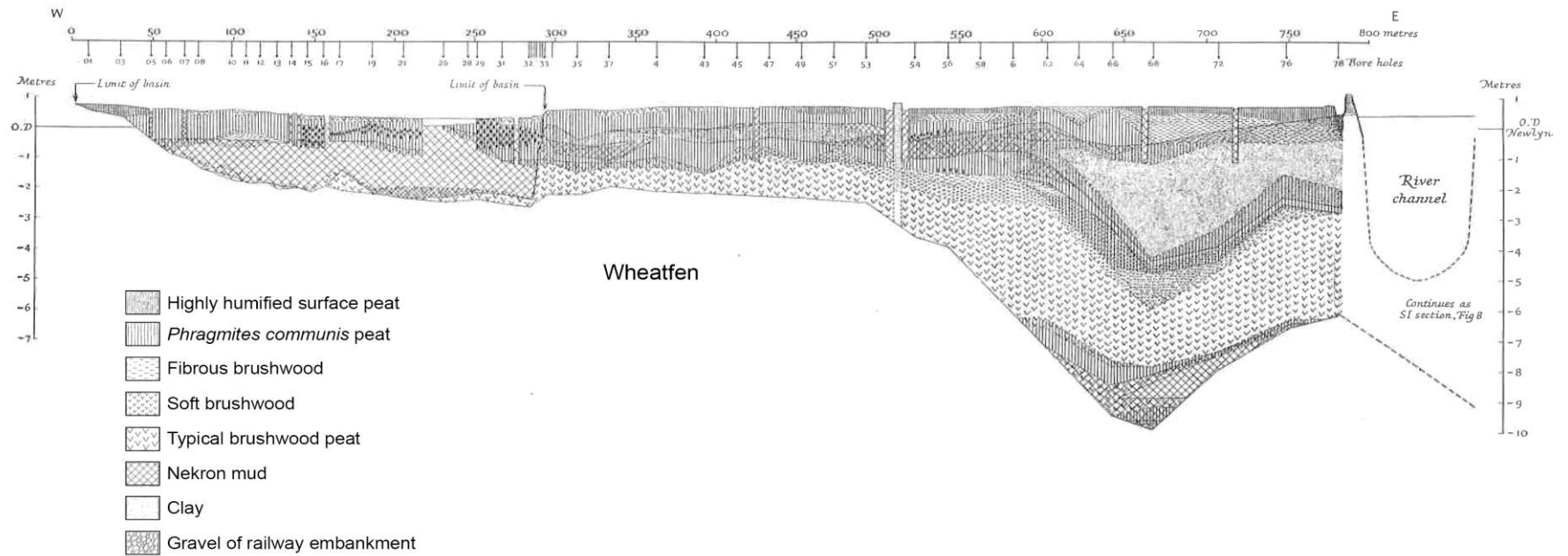


b	Wheatfen	4	4.1	0.60	< 0.0001
b	Catfield	1	3.4	1.0	< 0.05
b	Catfield	2	3.3	1.0	< 0.05
b	Catfield	3	2.5	1.3	ns
b	Catfield	4	3.7	0.87	< 0.0001
b	Catfield	5	2.6	1.6	ns
b	Sutton	1	2.9	0.93	< 0.05
b	Sutton	2	4.6	0.45	< 0.0001
b	Sutton	3	4.0	0.71	< 0.0001
b	Sutton	4	4.0	0.61	< 0.0001
b	Sutton	5	4.0	0.53	< 0.0001
b	Sutton	6	3.8	0.70	< 0.0001
b	Sutton	7	4.2	0.57	< 0.0001
b	How Hill	1	2.8	1.2	< 0.05
b	How Hill	2	2.2	1.6	ns
b	How Hill	3	2.2	1.7	ns
b	How Hill	4	4.8	0.62	< 0.0001
b	How Hill	5	2.6	1.1	< 0.05
b	How Hill	6	3.9	0.90	< 0.05
b	Woodbastwick	1	3.9	0.86	< 0.0001
b	Woodbastwick	2	5.0	0.52	< 0.0001
b	Woodbastwick	3	3.8	0.74	< 0.0001
b	Woodbastwick	4	3.6	0.71	< 0.0001
b	Woodbastwick	5	2.9	1.1	< 0.05
b	Woodbastwick	6	4.9	0.47	< 0.0001
c	Strumpshaw	1	-202	279	ns
c	Strumpshaw	2	-256	170	ns
c	Strumpshaw	3	-216	167	ns
c	Strumpshaw	4	-313	173	ns
c	Strumpshaw	5	-371	191	ns
c	Strumpshaw	6	-142	164	ns
c	Wheatfen	1	-218	174	ns
c	Wheatfen	2	-275	131	< 0.05
c	Wheatfen	3	-1474	640	< 0.05
c	Wheatfen	4	-321	172	ns
c	Catfield	1	-188	166	ns
c	Catfield	2	-182	165	ns
c	Catfield	3	-157	156	ns
c	Catfield	4	-228	169	ns
c	Catfield	5	-117	157	ns
c	Sutton	1	-210	161	ns
c	Sutton	2	-424	173	< 0.05
c	Sutton	3	-247	171	ns
c	Sutton	4	-298	171	ns
c	Sutton	5	-358	171	< 0.05
c	Sutton	6	-264	169	ns
c	Sutton	7	-341	172	ns
c	How Hill	1	-153	160	ns
c	How Hill	2	-125	153	ns

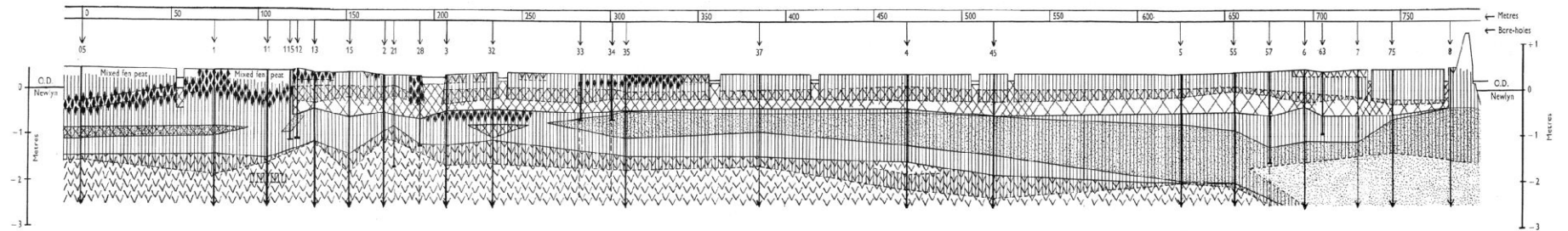
c	How Hill	3	-115	152	ns
c	How Hill	4	-322	174	ns
c	How Hill	5	-167	157	ns
c	How Hill	6	-203	170	ns
c	Woodbastwick	1	-275	182	ns
c	Woodbastwick	2	-502	193	< 0.05
c	Woodbastwick	3	-262	169	ns
c	Woodbastwick	4	-258	168	ns
c	Woodbastwick	5	-180	161	ns
c	Woodbastwick	6	-418	174	< 0.05


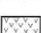
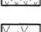
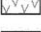

---

## **Appendix 4: Lambert Transect Maps**



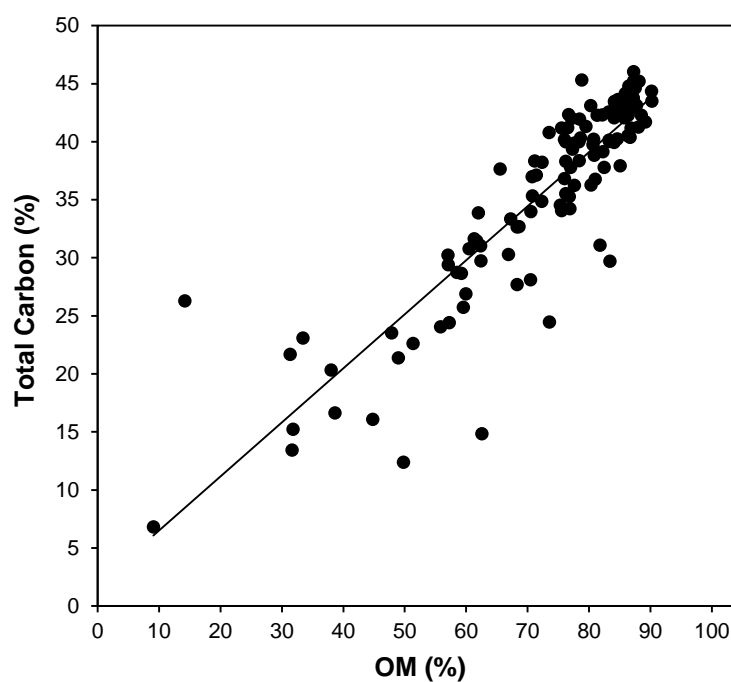
## Woodbastick



-  Highly humified surface peat
-  *Phragmites communis* peat
-  Fibrous brushwood
-  Soft brushwood
-  Typical brushwood peat
-  Nekron mud
-  Clay
-  Gravel of railway embankment

## Appendix 5: The relationship between organic matter and total carbon for cores used in radiometric dating.

Solid line indicates a significant linear regression result ( $F_{1, 118} = 498$ ,  $p < 0.0001$ ) and an  $r^2$  value of 0.81 was achieved. Organic matter was derived from loss on ignition, total carbon was derived from elemental analysis.



## Appendix 6: Summary statistics for the mixed-effects linear model.

Site, depth (d), peat type (Pt) and their interaction are independent variables.

Table 1: Dependent variable is carbon content (C).

Equation:	$C = b_0 + b_1.P_{BF} + b_2.P_{BS} + b_3.P_{HHS} + b_4.P_{PC} + b_5.Site-Wheatfen + b_6.Site-Woodbastwick + b_7.d + b_8.(P_{HHS}.Site-Wheatfen) + b_9.(P_{PC}.Site-Wheatfen) + b_{10}.(P_{PC}.Site-Woodbastwick) + b_{11}.(P_{BF}.d) + b_{12}.(P_{BS}.d) + b_{13}.(P_{HHS}.d) + b_{14}.(P_{PC}.d) + b_{15}.(Site-Wheatfen.d) + b_{16}.(Site-Woodbastwick.d) + b_{17}.(P_{PC}.Site-Wheatfen.d) + b_{18}.(P_{PC}.Site-Woodbastwick.d)$			
Random effects:	(1 + site core)			
	Intercept	Wheatfen	Woodbastwick	Residual
SE	0.35	0.57	0.48	0.75
Core	(Intercept)	Wheatfen	Woodbastwick	
1	-0.19	0.18	0.31	
2	0.91	-0.84	-1.5	
3	0.057	-0.052	-0.091	
4	-0.35	0.32	0.57	
5	-0.42	0.39	0.68	
Fixed effect	Estimate	SE	t-test	
	(Intercept)	0.66	0.69	0.95
P <sub>t</sub>	BF	4.5	1.7	2.7
P <sub>t</sub>	BS	5.7	5.9	0.97
P <sub>t</sub>	HHS	-0.77	1.2	-0.62
P <sub>t</sub>	PC	-0.97	0.71	-1.4
Site	Wheatfen	-1.6	1.0	-1.5
Site	Woodbastwick	0.10	1.2	0.09
d	Depth	-0.0014	0.0017	-0.83
P <sub>t</sub> .Site	HHS.Wh	0.85	1.6	0.54
P <sub>t</sub> .Site	PC.Wh	1.1	1.1	1.0
P <sub>t</sub> .Site	PC.Wo	0.92	1.2	0.77
P <sub>t</sub> .d	BF.d	-0.019	0.0058	-3.3
P <sub>t</sub> .d	BS.d	-0.020	0.022	-0.90
P <sub>t</sub> .d	HHS.d	-0.010	0.0050	-2.0
P <sub>t</sub> .d	PC.d	-0.00061	0.0032	-0.19
Site.d	Wh.d	0.0067	0.0033	2.1
Site.d	Wo.d	-0.00091	0.0030	-0.30
P <sub>t</sub> .Site.d	PC.Wh.d	0.0033	0.0056	0.59
P <sub>t</sub> .Site.d	PC.Wo.d	-0.00046	0.0056	-0.081

Table 1: Dependent variable is carbon density (pbd).

Equation:	$\rho_{bd} = b_0 + b_1.P_{BF} + b_2.P_{BS} + b_3.P_{HHS} + b_4.P_{PC} + b_5.Site-Wheatfen + b_6.Site-Woodbastwick + b_7.d + b_8.(P_{HHS}.Site-Wheatfen) + b_9.(P_{PC}.Site-Wheatfen) + b_{10}.(P_{PC}.Site-Woodbastwick) + b_{11}.(P_{BF}.d) + b_{12}.(P_{BS}.d) + b_{13}.(P_{HHS}.d) + b_{14}.(P_{PC}.d) + b_{15}.(Site-Wheatfen.d) + b_{16}.(Site-Woodbastwick.d) + b_{17}.(P_{PC}.Site-Wheatfen.d) + b_{18}.(P_{PC}.Site-Woodbastwick.d)$			
Random effects:	(1 + site core)			
	Intercept	Wheatfen	Woodbastwick	Residual
SE	0.60	0.56	0.97	0.79
Core	(Intercept)	Wheatfen	Woodbastwick	
1	0.29	0.37	-0.032	
2	0.21	-0.013	-0.058	
3	-0.33	0.56	0.54	
4	-0.22	-0.39	-0.011	
5	0.049	-0.52	-0.44	
Fixed effect		Estimate	SE	t-test
	(Intercept)	-0.67	0.62	-1.1
P <sub>t</sub>	BF	-2.1	1.8	-1.2
P <sub>t</sub>	BS	-5.6	5.7	-1.0
P <sub>t</sub>	HHS	1.5	1.2	1.2
P <sub>t</sub>	PC	0.49	0.67	0.74
Site	Wheatfen	0.30	1.0	0.29
Site	Woodbastwick	-1.2	1.1	-1.1
d	Depth	0.0030	0.0016	1.9
P <sub>t</sub> .Site	HHS.Wh	-0.92	1.5	-0.59
P <sub>t</sub> .Site	PC.Wh	0.37	1.1	0.35
P <sub>t</sub> .Site	PC.Wo	0.87	1.2	0.73
P <sub>t</sub> .d	BF.d	0.0080	0.0064	1.3
P <sub>t</sub> .d	BS.d	0.021	0.021	0.99
P <sub>t</sub> .d	HHS.d	0.00030	0.0054	0.06
P <sub>t</sub> .d	PC.d	0.0047	0.0030	1.6
Site.d	Wh.d	-0.0027	0.0033	-0.84
Site.d	Wo.d	0.0016	0.0030	0.55
P <sub>t</sub> .Site.d	PC.Wh.d	-0.013	0.0055	-2.46
P <sub>t</sub> .Site.d	PC.Wo.d	-0.015	0.0055	-2.73



Table 1: Dependent variable is carbon density (pcd).

Equation:	$\rho_{cd} = b_0 + b_1.P_{BF} + b_2.P_{BS} + b_3.P_{HHS} + b_4.P_{PC} + b_5.Site-Wheatfen + b_6.Site-Woodbastwick + b_7.d + b_8.(P_{HHS}.Site-Wheatfen) + b_9.(P_{PC}.Site-Wheatfen) + b_{10}.(P_{PC}.Site-Woodbastwick) + b_{11}.(P_{BF}.d) + b_{12}.(P_{BS}.d) + b_{13}.(P_{HHS}.d) + b_{14}.(P_{PC}.d) + b_{15}.(Site-Wheatfen.d) + b_{16}.(Site-Woodbastwick.d) + b_{17}.(P_{PC}.Site-Wheatfen.d) + b_{18}.(P_{PC}.Site-Woodbastwick.d)$			
Random effects:	(1 + site core)			
	Intercept	Wheatfen	Woodbastwick	Residual
SE	0.6	0.66	0.86	0.87
Core	(Intercept)	Wheatfen	Woodbastwick	
1	-0.08	0.31	0.22	
2	0.88	-0.86	-1.2	
3	-0.44	0.58	0.69	
4	-0.35	0.13	0.39	
5	-0.02	-0.16	-0.057	
Fixed effect	Estimate	SE	t-test	
	(Intercept)	-0.26	0.76	-0.34
P <sub>t</sub>	BF	2.5	1.9	1.3
P <sub>t</sub>	BS	-3.6	6.5	-0.55
P <sub>t</sub>	HHS	0.73	1.4	0.54
P <sub>t</sub>	PC	-0.29	0.78	-0.37
Site	Wheatfen	-0.35	1.2	-0.31
Site	Woodbastwick	-0.8	1.3	-0.62
d	Depth	0.0022	0.0019	1.2
P <sub>t</sub> .Site	HHS.Wh	-0.4	1.7	-0.23
P <sub>t</sub> .Site	PC.Wh	0.98	1.2	0.81
P <sub>t</sub> .Site	PC.Wo	1.4	1.3	1.1
P <sub>t</sub> .d	BF.d	-0.012	0.0069	-1.7
P <sub>t</sub> .d	BS.d	0.015	0.024	0.64
P <sub>t</sub> .d	HHS.d	-0.0048	0.0058	-0.83
P <sub>t</sub> .d	PC.d	0.0052	0.0035	1.5
Site.d	Wh.d	0.00032	0.0037	0.09
Site.d	Wo.d	-0.0004	0.0033	-0.12
P <sub>t</sub> .Site.d	PC.Wh.d	-0.01	0.0062	-1.6
P <sub>t</sub> .Site.d	PC.Wo.d	-0.014	0.0062	-2.2

## Appendix 7: Raw data from radiometric dating

Table 1.  $^{210}\text{Pb}$  concentrations for the core taken from Wheatfen.

Depth	Dry Mass	Pb-210						Cum Unsupported	
		Total		Supported		Unsupp		Pb-210	
		Bq Kg <sup>-1</sup>	±	Bq Kg <sup>-1</sup>	±	Bq Kg <sup>-1</sup>	±	Bq m <sup>-2</sup>	±
cm	g cm <sup>-2</sup>								
0.5	0.0434	88.56	16.32	15.35	4.61	73.21	16.96	31.9	5.4
3.5	0.3243	138.89	15.66	24.74	4.57	114.15	16.31	290.8	38.3
5.5	0.5236	130.53	13.36	32.9	4.14	97.63	13.99	501.4	52.8
7.5	0.7284	102.93	14.1	37.63	4.46	65.3	14.79	666	60.7
8.5	0.8344	107.45	14.62	40.06	4.36	67.39	15.26	736.3	63.8
9.5	0.9404	88.05	12.75	36.59	3.73	51.46	13.28	798.9	65.7
10.5	1.0463	97.79	14.05	35.3	4.01	62.49	14.61	859.1	67.4
11.5	1.1523	87.48	13.67	36.82	4.08	50.66	14.27	918.9	69.2
12.5	1.2583	85.71	11.4	44.26	3.71	41.45	11.99	967.5	70.7
13.5	1.3624	57.75	10.83	51.82	3.85	5.93	11.49	986.5	71.8
14.5	1.4666	66.82	10.83	32.84	3.43	33.98	11.36	1003.3	72.8
15.5	1.5816	59.79	7.56	64.97	2.67	-5.18	8.02	1019.8	73.8
17.5	1.7855	37.59	7.48	36.55	2.48	1.04	7.88		
19.5	1.9735	29.91	6.51	38.7	2.27	-8.79	6.89		

Table 2. Artificial fallout radionuclide concentrations for the core taken from Wheatfen

Depth	Cs-137		Am-241	
cm	Bq Kg <sup>-1</sup>	±	Bq Kg <sup>-1</sup>	±
0.5	5.14	2.7	0	0
3.5	19.51	2.93	0	0
5.5	20.01	2.48	0	0
7.5	42.01	3.19	0	0
8.5	44.46	3.27	0	0
9.5	70.98	3.56	0	0
10.5	62.15	3.53	0	0
11.5	65.24	3.33	0	0
12.5	80.24	3.51	0	0
13.5	86.45	3.57	0	0
14.5	57.13	3.04	0	0
15.5	48.13	2.06	0	0
17.5	24.81	1.69	0	0
19.5	6.46	1.14	0	0

Table 3.  $^{210}\text{Pb}$  chronology for the core taken from Wheatfen

Depth	Drymass	Chronology			Sedimentation Rate		
		Date	Age				
cm	g cm <sup>-2</sup>	AD	yr	±	g cm <sup>-2</sup> yr <sup>-1</sup>	cm yr <sup>-1</sup>	± %
0	0	2014	0				
0.5	0.0434	2013	1	2	0.0514	0.554	23.8
3.5	0.3243	2005	9	2	0.0259	0.27	15.6
5.5	0.5236	1997	17	2	0.0236	0.233	15.9
7.5	0.7284	1989	25	3	0.0274	0.264	23.9
8.5	0.8344	1985	29	3	0.0233	0.219	24.1
9.5	0.9404	1981	33	3	0.0267	0.252	27.3
10.5	1.0463	1976	38	3	0.019	0.179	25.2
11.5	1.1523	1971	43	4	0.0197	0.186	30
12.5	1.2583	1965	49	4	0.0205	0.195	31
13.5	1.3624	1964	50	4	0.0929	0.892	32.6
14.5	1.4666	1961	53	5	0.0217	0.198	34.9

Table 4.  $^{210}\text{Pb}$  concentrations for the core taken from Woodbastwick.

Depth	Dry Mass	Pb-210						Cum Unsupported	
		Total		Supported		Unsupp		Pb-210	
		Bq Kg <sup>-1</sup>	±	Bq Kg <sup>-1</sup>	±	Bq Kg <sup>-1</sup>	±	Bq m <sup>-2</sup>	±
cm	g cm <sup>-2</sup>								
0.5	0.0639	179.63	18.6	26.43	4.08	153.2	19.04	104.7	10.1
3.5	0.3997	168.45	16.33	24.38	3.55	144.07	16.71	603.7	54.1
5.5	0.6048	149.41	19.18	23.89	5.17	125.52	19.86	879.7	69.2
7.5	0.8182	55.12	10.75	29.55	2.89	25.57	11.13	1013.7	79.4
8.5	0.9303	92.81	15.07	26.03	3.75	66.78	15.53	1061.9	81.1
9.5	1.0424	37	9.52	28.17	2.57	8.83	9.86	1094	82.7
11.5	1.2906	66.13	12.81	31.34	3.26	34.79	13.22	1141	86
12.5	1.418	53.55	9.68	23.7	2.72	29.85	10.05	1182	88.3
13.5	1.5388	48.13	8.56	23.73	2.28	24.4	8.86	1214.7	89.1
14.5	1.6389	65.14	11.12	17	2.86	48.14	11.48	1249.7	89.7
15.5	1.7336	42.09	9.15	24.37	2.49	17.72	9.48	1278.5	90.3
17.5	1.9458	45.38	9.4	19.88	2.42	25.5	9.71	1323.9	92
19.5	2.1571	31.16	8.28	20.72	2.31	10.44	8.6	1359.5	94.1
21.5	2.3712	22.23	7.39	19.65	1.95	2.58	7.64	1371.5	95.8
23.5	2.5687	24.58	7.11	19.07	1.96	5.51	7.38	1379.2	97

Table 5. Artificial fallout radionuclide concentrations for the core taken from Woodbastwick

Depth	Cs-137		Am-241	
cm	Bq Kg <sup>-1</sup>	±	Bq Kg <sup>-1</sup>	±
0.5	43.31	3.1	0	0
3.5	41.02	2.96	0	0
5.5	40.1	3.4	0	0
7.5	29.76	2	0	0
8.5	39.74	2.78	0	0
9.5	40.35	2.04	0	0
11.5	27.45	2.16	0	0
12.5	35.77	1.85	2	0.93
13.5	37.97	1.77	2.55	0.9
14.5	23.79	1.91	1.73	1.06
15.5	11.36	1.49	0	0
17.5	6.25	1.42	0	0
19.5	4.9	1.18	0	0
21.5	5.87	1.08	0	0
23.5	5.34	1.06	0	0

Table 6.  $^{210}\text{Pb}$  chronology for the core taken from Woodbastwick

Depth	Drymass	Chronology			Sedimentation Rate		
		Date	Age				
cm	g cm <sup>-2</sup>	AD	yr	±	g cm <sup>-2</sup> yr <sup>-1</sup>	cm yr <sup>-1</sup>	± %
0	0	2014	0				
0.5	0.0639	2012	2	2	0.0289	0.253	13.9
3.5	0.3997	1998	16	2	0.0199	0.184	13.9
5.5	0.6048	1986	28	3	0.016	0.153	18.1
7.5	0.8182	1979	35	3	0.0625	0.576	44.6
8.5	0.9303	1976	38	3	0.0217	0.193	25.5
9.5	1.0424	1975	39	4	0.0863	0.719	29.9
11.5	1.2906	1970	44	4	0.0345	0.276	39.2
12.5	1.418	1966	48	4	0.0359	0.29	35.3
13.5	1.5388	1963	51	4	0.0398	0.36	38.1
14.5	1.6389	1959	55	5	0.0179	0.184	27.3
15.5	1.7336	1956	58	5	0.0436	0.426	55.4
17.5	1.9458	1949	65	7	0.0248	0.234	43.2
19.5	2.1571	1943	71	9	0.0498	0.469	48.6

Table 7.  $^{210}\text{Pb}$  concentrations for the core taken from Strumpshaw.

Depth	Dry Mass	Pb-210						Cum Unsupported	
		Total		Supported		Unsupp		Pb-210	
		Bq Kg <sup>-1</sup>	±	Bq Kg <sup>-1</sup>	±	Bq Kg <sup>-1</sup>	±	Bq m <sup>-2</sup>	±
cm	g cm <sup>-2</sup>								
0.5	0.052	198.53	18.88	28.22	5.44	170.31	19.65	90.8	8.5
2.5	0.262	157.47	15.84	15.74	4.35	141.73	16.43	417.5	35.7
4.5	0.491	141.63	19.21	26.84	7.68	114.79	20.69	710.2	55.3
6.5	0.7105	104.89	15.1	14.41	4.63	90.48	15.79	934.4	71.2
8.5	0.928	79.36	11.12	33	3.74	46.36	11.73	1077.9	78.6
10.5	1.141	49.88	9.63	23.21	3.2	26.67	10.15	1153.7	82.4
12.5	1.3545	36.15	9.67	34.35	3.33	1.8	10.23	1173.4	85.2
13.5	1.4535	50.2	6.57	27.06	2.27	23.14	6.95	1181.7	86.1
14.5	1.5555	45.47	7.04	17.7	2.18	27.77	7.37	1207.6	86.4
15.5	1.658	55.86	10.74	28.01	3.6	27.85	11.33	1236.1	86.8
16.5	1.7645	25.24	8.31	18.45	2.7	6.79	8.74	1252	87.6
18.5	1.969	31	10.2	24.64	3.38	6.36	10.75	1265.4	89.2
19.5	2.0675	21.19	7.98	19.38	2.7	1.81	8.42	1269	90.1



Table 8. Artificial fallout radionuclide concentrations for the core taken from Strumpshaw

Depth	Cs-137		Am-241	
cm	Bq Kg <sup>-1</sup>	±	Bq Kg <sup>-1</sup>	±
0.5	7.86	2.91	0	0
2.5	19.46	2.65	0	0
4.5	29.07	3.78	0	0
6.5	45.12	3.57	0	0
8.5	42.04	2.53	0	0
10.5	20.52	1.85	0	0
12.5	33.3	2.44	0	0
13.5	37.17	1.65	0	0
14.5	32.04	1.72	0	0
15.5	35.35	2.53	0	0
16.5	26.38	1.94	0	0
18.5	26.32	2.25	0	0
19.5	14.02	1.7	0	0

Table 9.  $^{210}\text{Pb}$  chronology for the core taken from Strumpshaw

Depth	Drymass	Chronology			Sedimentation Rate		
		Date	Age				
cm	g cm <sup>-2</sup>	AD	yr	±	g cm <sup>-2</sup> yr <sup>-1</sup>	cm yr <sup>-1</sup>	± %
0	0	2014	0				
0.5	0.052	2012	2	2	0.0261	0.249	14.6
2.5	0.262	2004	10	2	0.0242	0.22	16
4.5	0.491	1994	20	3	0.0219	0.195	22.6
6.5	0.7105	1983	31	4	0.0201	0.184	25
8.5	0.928	1974	40	6	0.0295	0.274	34.2
10.5	1.141	1968	46	7	0.0425	0.399	46.7
12.5	1.3545	1967	47	8	0.1553	1.491	54.7
13.5	1.4535	1966	48	8	0.0452	0.45	41.7
14.5	1.5555	1963	51	9	0.0348	0.34	41.1
15.5	1.658	1960	54	10	0.0315	0.301	39.4